

AD-A079 633

HUGHES AIRCRAFT CO TUCSON AZ MISSILE DEVELOPMENT DIV
HIGH STRENGTH RAPID PAYOUT FIBER OPTIC CABLE ASSEMBLY.(U)
AUG 79 D S FOX, R A EISENTRAUT

F/G 20/6

DAAD07-78-C-2964

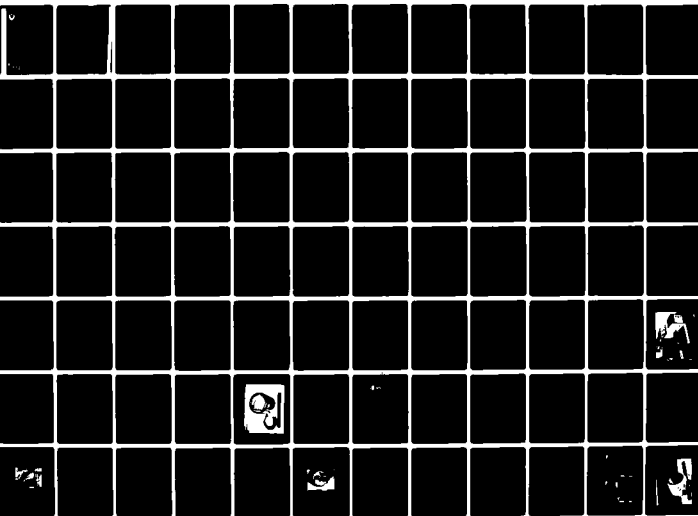
UNCLASSIFIED

FR7956-0003

CORADCOM-78-2964-1

NL

1 of 2
AD-A079633





(12)

LEVEL

RESEARCH AND DEVELOPMENT TECHNICAL REPORT
CORADCOM- CONTRACT NUMBER DAAB07-78-C-2964

HIGH STRENGTH RAPID PAYOUT FIBER OPTIC CABLE ASSEMBLY

D. S. Fox
R. A. Eisentraut
HUGHES AIRCRAFT COMPANY
Missile Development Division

August 1979

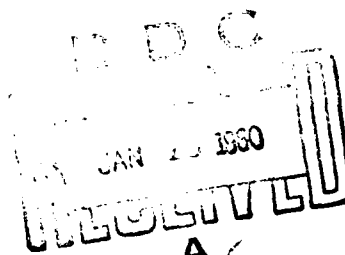
SEMI-ANNUAL REPORT FOR PERIOD
AUGUST 1978 - MAY 1979

DISTRIBUTION STATEMENT
Approved for public release;
distribution unlimited.

Prepared for:
CENCOMS

CORADCOM

US ARMY COMMUNICATIONS RESEARCH & DEVELOPMENT COMMAND
FORT MONMOUTH, NEW JERSEY 07703



DDC FILE COPY

ADA 079633

80 1 21 038

NOTICES

Disclaimers

The citation of trade names and names of manufacturers in this report is not to be construed as official Government indorsement or approval of commercial products or services referenced herein.

Disposition

Destroy this report when it is no longer needed. Do not return it to the originator.

HISA-FM-633-78

UNCLASSIFIED

SECURITY CLASSIFICATION OF THIS PAGE (When Data Entered)

REPORT DOCUMENTATION PAGE		READ INSTRUCTIONS BEFORE COMPLETING FORM
1. REPORT NUMBER 18 CORADCOM-78-2964-1 ✓	2. GOVT ACCESSION NO.	3. RECIPIENT'S CATALOG NUMBER
4. TITLE (and Subtitle) 6 High Strength Rapid Payout Fiber Optic Cable Assembly,		5. TYPE OF REPORT & PERIOD COVERED Semi-Annual, August 1978 through May 1979, inclusive
7. AUTHOR(s) 10 D. S. / Fox R. A. / Eisentraut		8. PERFORMING ORG. REPORT NUMBER 14 FR7956-0003 ✓
9. PERFORMING ORGANIZATION NAME AND ADDRESS Hughes Aircraft Company Missile Development Div., Tucson Operations Tucson, Arizona 85734		10. CONTRACT OR GRANT NUMBER(s) 15 DAAB07-78-C-2964
11. CONTROLLING OFFICE NAME AND ADDRESS U.S. Army Communications R&D Command Attn: DRDCO-COM-RM-1 Fort Monmouth, N.J. 07703		12. REPORT DATE 11 August 1979
14. MONITORING AGENCY NAME & ADDRESS (if different from Controlling Office)		13. NUMBER OF PAGES 167
16. DISTRIBUTION STATEMENT (of this Report) Approved for public release; distribution unlimited		15. SECURITY CLASS. (of this report) 12 170 / Unclassified
15a. DECLASSIFICATION/DOWNGRADING SCHEDULE		
17. DISTRIBUTION STATEMENT (of the abstract entered in Block 20, if different from Report)		
18. SUPPLEMENTARY NOTES None		
19. KEY WORDS (Continue on reverse side if necessary and identify by block number) Fiber Optics, Optical Communications, Cable Assemblies, Missile Guidance, Optical Waveguides		
20. ABSTRACT (Continue on reverse side if necessary and identify by block number) This report summarizes preliminary results obtained in the investigation of the feasibility of a fiber optic cable payout assembly capable of high speed payout with simultaneous optical transmission. The results of both cable design studies and payout assembly (dispenser) design studies are described. Experimental results for both optical attenuation and payout performance are provided.		

DD FORM 1 JAN 73 1473

EDITION OF 1 NOV 65 IS OBSOLETE

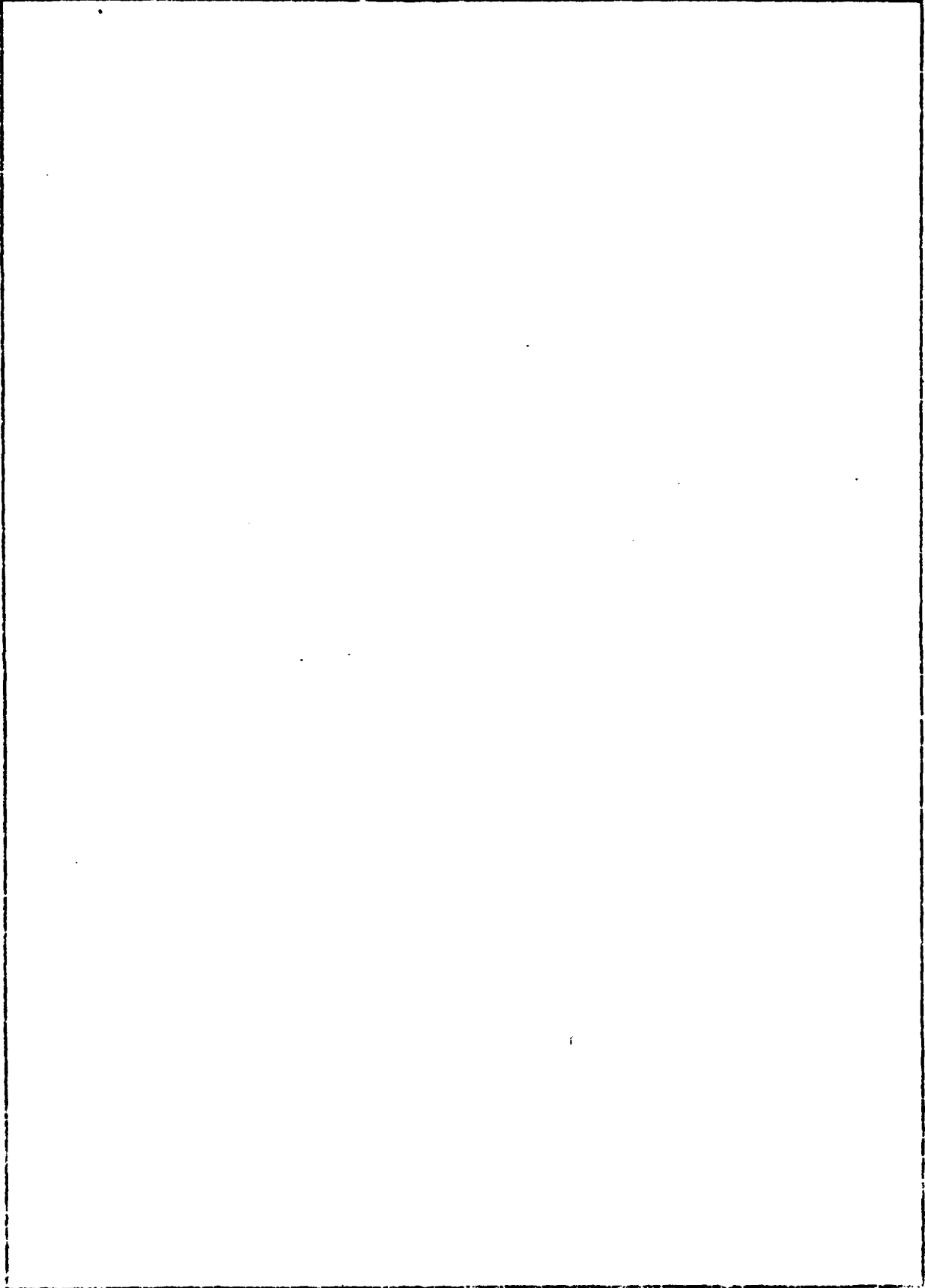
UNCLASSIFIED

SECURITY CLASSIFICATION OF THIS PAGE (When Data Entered)

4115-15

J. B

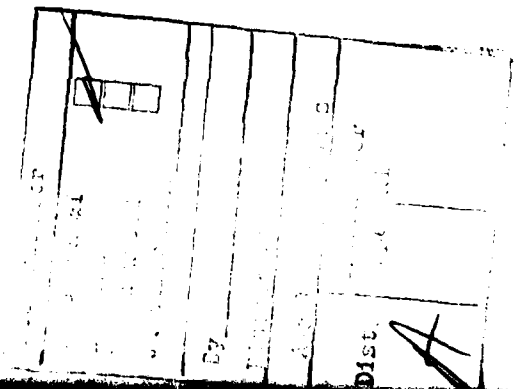
SECURITY CLASSIFICATION OF THIS PAGE(When Data Entered)



SECURITY CLASSIFICATION OF THIS PAGE(When Data Entered)

CONTENTS

	<u>Page</u>
1.0 <u>INTRODUCTION</u>	1-1
2.0 <u>TECHNICAL SUMMARY.</u>	2-1
3.0 <u>CABLE DEVELOPMENT.</u>	3-1
3.1 CABLE DESIGN	3-1
3.2 PREFORM DESIGN	3-2
3.3 DRAW PROCESS	3-2
3.4 FIBER COATING MATERIALS AND TECHNIQUES	3-4
3.5 CABLE EVALUATION.	3-7
3.6 STATIC FATIGUE CONSIDERATIONS	3-21
4.0 <u>DISPENSER DESIGN</u>	4.1-1
4.1 APPROACH	4.1-1
4.2 DISPENSER DESIGN	4.2-1
4.3 MECHANICAL AND PAYOUT TESTING	4.3-1
4.4 OPTICAL EVALUATION.	4.4-1
5.0 CABLE REQUIREMENTS	5-1
5.1 MECHANICAL RELATED REQUIREMENTS	5-1
5.2 SIGNAL TRANSMISSION RELATED REQUIREMENTS.	5-3
5.3 CONNECTOR RELATED REQUIREMENTS.	5-8
6.0 <u>ROCKET SLED TEST INSTRUMENTATION</u>	6-1
6.1 INSTRUMENTATION DESIGN.	6-1
6.2 PACKAGING	6-4
7.0 CONCLUSIONS.	7-1



LIST OF ILLUSTRATIONS

<u>Figure</u>		<u>Page</u>
3-1	Cable Design "A"	3-2
3-2	Cable Design "B"	3-3
3-3	Cable Design, Standard ITT Fiber	3-3
3-4	Schematic of Fiber Drawing Equipment	3-5
3-5	Strength Proof Test Setup Drawing.	3-12
3-6	Dynamic Strength Results. WCC-2 Coated Fiber at Start of Pull (SOP)	3-14
3-7	Dynamic Strength Test Results. WCC-2 Coated Fiber at end of Pull (EOP).	3-15
3-6	Static Fatigue Comparison of Various Coating Materials . . .	3-17
4.2-1	Design No. 1	4.2-7
4.2-2	Design No. 2	4.2-8
4.2-3	Design No. 3	4.2-9
4.2-4	Design No. 4	4.2-10
4.2-5	Design No. 5	4.2-11
4.2-6	Design No. 6	4.2-12
4.2-7	Forces Between Layers.	4.2-25
4.2-8	Radial Interlayer Pressure Indicated for Designs	4.2-26
4.3-1	Test Bobbin 1, Spool Geometry.	4.3-2
4.3-2	Bobbin 1, Cable Force-Displacement Characteristics	4.3-3
4.3-A	Modified Bobbin Winding Machine	4.3-5
4.3-3	Bobbin 1, Spool Strain vs Number of Layers	4.3-9
4.3-4	Pressure Vessel Geometry	4.3-11
4.3-5	Photograph of Pressure Vessel.	4.3-12
4.3-6	Spool Strain vs Applied Pressure	4.3-13
4.3-B	Cable Dispensing Parameters.	4.3-14
4.3-7	Cable Tension Measurement Technique.	4.3-14
4.3-8	Bobbin 2, Spool Strain vs Number of Layers	4.3-17
4.3-9	Bobbin 2, Spool Strain vs Time	4.3-17

LIST OF ILLUSTRATIONS (Continued)

<u>Figure</u>		<u>Page</u>
4.3-10	Bobbin 3, Cable Force-Displacement Characteristics	4.3-19
4.3-11	Bobbin 3, Spool Strain vs Number of Layers	4.3-20
4.3-12	Bobbin 3, Strain vs Applied Pressure and Time.	4.3-20
4.3-13	Buffer Damage Due to Adhesive Action, Bobbin 3	4.3-21
4.3-14	Inclusion in Glass Fiber, Bobbin 3.	4.3-22
4.3-15	Bobbin 4, Cable Force-Displacement Characteristics.	4.3-23
4.3-16	Bobbin 4, Spool Strain vs Number of Layers.	4.3-24
4.3-17	Bobbin 4, Spool Strain vs Applied Pressure and Temperature.	4.3-24
4.3-18	Bobbin 5, Spool Geometry	4.3-25
4.3-19	Bobbin 5, Spool Strain vs Number of Layers.	4.3-26
4.3-20	SEM Photograph of Failed End from Bobbin 5 Payout Test.	4.3-27
4.3-21	Bobbin 6, Spool Geometry.	4.3-29
4.3-22	Bobbin 7, Cable Force-Displacement Characteristics.	4.3-30
4.3-23	Bobbin 7, Spool Strain vs Number of Layers.	4.3-31
4.3-24	Bobbin 7, Failed Ends	4.3-32
4.3-25	Photograph of Bobbin 8.	4.3-33
4.3-26	Bobbin 9, Cable Force-Displacement Characteristics.	4.3-35
4.3-27	Bobbin 9, Spool Strain vs Number of Layers.	4.3-36
4.3-28	Photograph of Bobbin 9.	4.3-37
4.3-29	Test Bobbin 10, Spool Geometry	4.3-38
4.3-30	Bobbin 10 Pressure Vessel Geometry.	4.3-39
4.3-31	Bobbin 10 Spool Strain vs Number of Layers.	4.3-40
4.3-32	Photograph of Bobbin 10	4.3-41
4.3-33	Bobbin 11, Cable Force-Displacement Characteristics	4.3-42
4.3-34	Bobbin 11, Spool Strain vs Number of Layers	4.3-43
4.3-35	Bobbin 12, Cable Force-Displacement Characteristics	4.3-44
4.3-36	Bobbin 12, Spool Strain vs Number of Layers	4.3-45
4.3-37	Photograph of Bobbin 12	4.3-46
4.3-38	Bobbin 13, Cable Force-Displacement Characteristics	4.3-48
4.3-39	Bobbin 13, Spool Strain vs Number of Layers	4.3-49
4.3-40	Bobbin 14, Cable Force-Displacement Characteristics	4.3-50
4.3-41	Bobbin 15, Spool Strain vs Number of Layers.	4.3-51

LIST OF ILLUSTRATIONS

<u>Figure</u>		<u>Page</u>
4.4-A	OTDR Schematic Diagram	4.4-6
4.4-1	Bobbin 1, OTDR Test Results	4.4-8
4.4-2	Cable Attenuation vs Interlayer Pressure.	4.4-10
4.4-3	Layer Length vs Layer Number, Bobbin 1.	4.4-11
4.4-4	Interlayer Pressure vs Layer Number, Bobbin 1	4.4-12
4.4-5	Bobbin 6, OTDR Test Results	4.4-13
4.4-6	Bobbin 7, OTDR Test Results	4.4-14
4.4-7	Bobbin 8, OTDR Test Results	4.4-15
4.4-8	Bobbin 9, OTDR Test Results	4.4-16
4.4-9	Bobbin 10, OTDR Test Results.	4.4-17
4.4-10	Bobbin 11, OTDR Test Results.	4.4-18
4.4-11	Bobbin 12, OTDR Test Results.	4.4-19
4.4-12	Bobbin 13, OTDR Test Results.	4.4-20
4.4-13	Bobbin 14, OTDR Test Results.	4.4-21
4.4-14	Bobbin 15, OTDR Test Results.	4.4-22
4.4-15	Effect of Interlayer Pressure on Cable Loss	4.4-24
4.4-16	Effect of Spool Geometry on Spooling Loss	4.4-26
4.4-17	Effect of Wavelength on Spooling Loss , Bobbin 15	4.4-28
4.4-18	Effect of Temperture on Attenuation	4.4-29
5-1	Cable Attenuation Acceptance Criterion, Bobbin Design No. 1	5-6
6-1	Downlink Transmitter Block Diagram.	6-2
6-2	Ground Station Receiver Block Diagram	6-3

LIST OF TABLES

<u>Table</u>	<u>Page</u>
3-I Details of Coating Materials.	3-8
3-II Optical Data.	3-10
3-III Optical Data WCC-2 UV-Cured Primary Jacket, Hytrel Secondary Jacket.	3-11
3-IV WCC-2 Coated Fiber Strength Summary	3-13
3-V (a) Effect of Temperature on Attenuation Constant DB/KM	3-18
3-V (b) Effect of Temperature on Pulse Dispersion NS/KM	3-18
3-VI Post-Humidity Tension Test Results	3-20
4.2-I Summary of Bobbin Design Parameters	4.2-6
4.2-II Design No. 1	4.2-13
4.2-III Design No. 2	4.2-16
4.2-IV Design No. 3	4.2-18
4.2-V Design No. 5	4.2-20
4.2-VI Design No. 6	4.2-23
4.3-I Bobbin 1 Design Tabulation - Nominal Tension.	4.3-7
4.3-II Bobbin 1 Design Tabulation - Modified Tension	4.3-8
4.3-III Summary of Experiments.	4.3-16
4.4-I Summary of Bobbin Characteristics	4.4-4
5-I Cable Requirements - Winding, Storage, Payout	5-2
5-II Cable Attenuation Parameters.	5-7
5-III Cable Parameters Influencing Connector Loss	5-12
6-I Link Budget	6-4

1.0 INTRODUCTION

Hughes Aircraft Company, under contract with USA CORADCOM, Ft. Monmouth New Jersey, is pursuing the exploratory development of a fiber optic cable payout dispenser capable of high speed payout of long lengths, up to 10 km, of fiber optic cable. The Electro Optical Products Division (EOPD) of ITT (International Telephone and Telegraph) is serving as a major subcontractor to Hughes Aircraft Company in this development and is responsible for the development of the fiber optic cable and for special instrumentation equipment to be used during future rocket sled payout tests. This report, coming at approximately midpoint of the contract, summarizes the progress accomplished and the current status of the program.

Program results continue to be very encouraging in terms of meeting the technical objectives. Fiber optic cables, which appear to satisfy the optical requirements when wound on a spool for payout, have been fabricated and tested. Successful payout tests of short lengths to 1 km have been conducted with peak payout speeds at approximately 90 percent of the objective. To date nothing has been encountered that would raise question regarding the feasibility of high speed payout of long lengths of fiber optic cable.

2.0 TECHNICAL SUMMARY

The program for the development of a high strength rapid payout fiber optic cable assembly which is being conducted by Hughes Aircraft Company under contract to CORADCOM is approximately at its midpoint. This report provides a summary of effort to date and an assessment of the overall feasibility of accomplishing the objectives of the program.

At the outset of the program, two major areas of technical risk were recognized. These are (1) the development of a fiber optic cable with sufficiently low intrinsic signal loss and with sufficiently small sensitivity to microbending loss due to the spooling stresses so as to satisfy a requirement of 60 dB for overall signal attenuation for a 10 km spooled length, and (2) obtaining adequate strength in the fiber optic cable to withstand the mechanical stresses associated with winding, storage, and payout. Both of these areas of technical risk are stated in terms of requirements on the cable. It should be recognized, however, that there is a very strong interaction between the cable requirements and the design of the wound dispenser. Achieving success in either of these areas of technical risk can be accomplished only by careful and coordinated effort in terms of improved cable design and fabrication coupled with the definition of bobbin design parameters which minimize the demands on the cable in terms of signal attenuation loss and strength.

This development program is structured into three phases. The completed first phase consisted of a rather broad investigation of cable and dispenser design alternatives with the goal of selecting two designs to be carried forward into the subsequent phase. The investigation of a minimum of five designs was called out; a total of 14 design configurations have been evaluated. A design consists of the combination of a particular cable configuration with a particular bobbin geometry; changing either cable or bobbin design parameters comprises a new design. During the initial phase, rather short lengths of cable were involved (from 0.5 to about 1.0 km). The second phase of the program, which is now in process,

3.0 CABLE DEVELOPMENT

Cable design and development efforts have been performed at the Electro Optical Products Division of International Telephone and Telegraph on a subcontract basis.[†] The results obtained to date have involved almost exclusively cable produced by ITT. A decision has been made to proceed with ITT-supplied cables for the remainder of the program; this report will describe the results of the ITT efforts.

3.1 CABLE DESIGN

The design of the fiber optic cable consisted of optimizing the transmission, mechanical and environmental properties of optical fibers specifically for payout purposes. The important data transmission properties of a missile control link fiber are low loss (less than 6 dB/km), small core to reduce bending losses (25 μm diameter), large numerical aperture (0.27 to 0.30), and minimum dispersion (2 ns per km at 0.9 μm). The important cable mechanical properties are high tensile strength (1380 N/mm²) at long lengths (up to 10 km), coating concentricity ($t_{\text{min}}/t_{\text{max}} \geq 0.67$), coating roundness ($d_{\text{max}} - d_{\text{min}} \leq 0.0001$), and an average diameter of 0.012 ± 0.001 inches (305 ± 25 μm) where d_{max} = maximum cable diameter, d_{min} = fiber glass diameter t_{max} = maximum coating thickness and t_{min} = minimum coating thickness. The important cable environmental properties are minimum high and low temperature effects on strength and attenuation, minimum effects of humidity on tensile strength and maximum fungus-growth resistance.

Cable development efforts have been directed toward the design of a small diameter cable with specific parameters tailored for the payout application. The initial design goal for cable diameter was 254 μm (0.010 in.). Because of early difficulties in obtaining suitable attenuation properties, the objective for cable diameter was increased to

[†] Hughes Research Laboratories, on an unfunded basis, has contributed samples from an ongoing effort to develop high strength metallic coated optical fibers.

305 μm (0.012 in.). In addition a special cable with a diameter of 380 μm (0.015 in.) was designed and tested. The result of this effort was two basic Preliminary Design Model (PDM) cable configurations with two variations of one of these configurations. Figure 3-1 illustrates the cross section, nominal dimensions, and structure of the 380 μm (0.015 in.) diameter cable. This cable was similar in structure to a standard production cable, but with reduced diameter of both the core and fiber diameters. The dimensions of the Sylgard RTV and Hytrel coatings were scaled to provide the overall diameter of 380 μm (0.015 in.). The second design, illustrated in figure 3-2, involves a cable diameter of 305 μm (0.012 in.). This cable utilizes a 100 μm (0.004 in.) fiber with small diameter (25 - 30 μm) core and a single coating as a buffer. Several coating materials were investigated and two, Polyene-polythiol-ester (WCC-2) and an epoxy acrylate (DeSoto 8), were found to have suitable properties. The basic cable geometry is similar to either of these coatings.

In addition to the two special cable configurations, a standard production cable, 500 μm (0.020 in.) in diameter with a fiber diameter of 125 μm (0.005 in.) and a core diameter of about 55 μm was evaluated. This standard production cable is illustrated in figure 3-3.

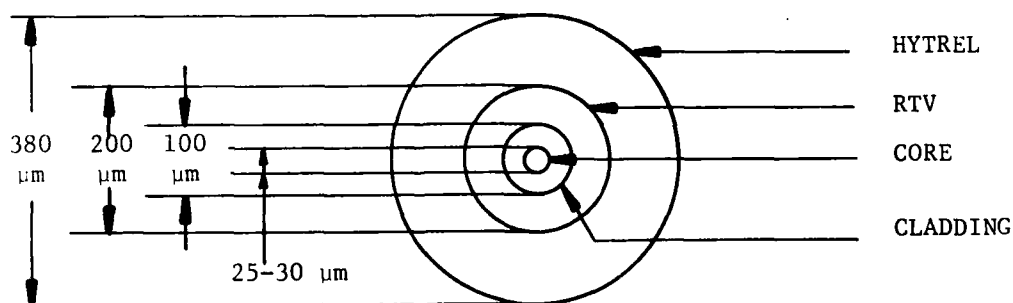
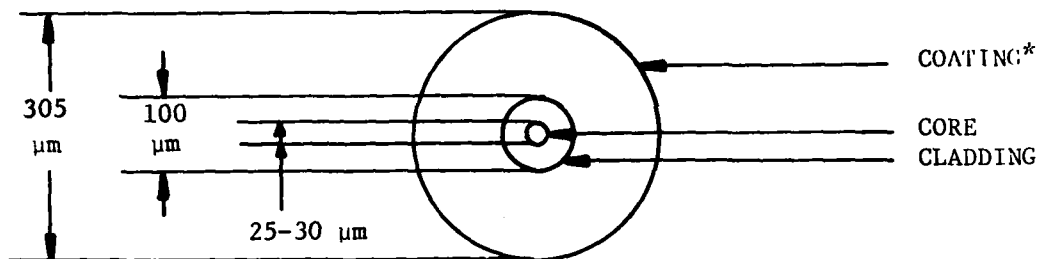


Figure 3-1 Cable Design "A"



*Alternate coatings:

WCC-2 - Design B1

DeSoto 8 - Design B2

Figure 3-2. Cable Design "B"

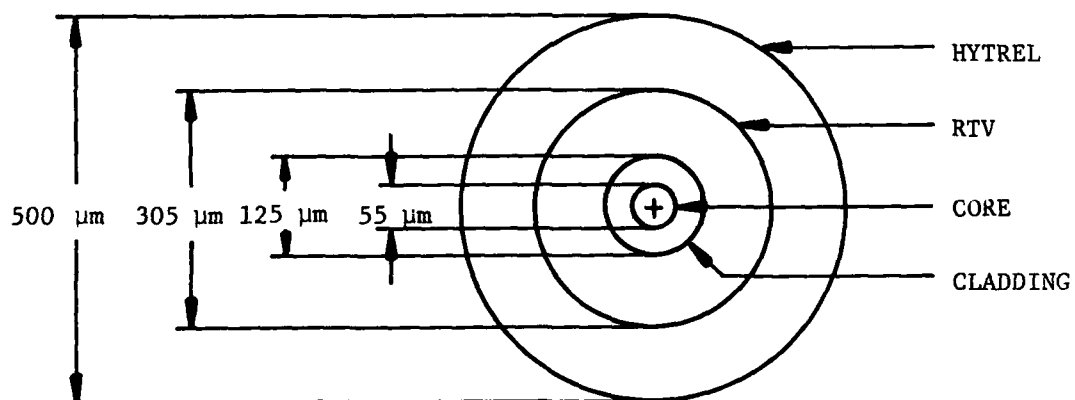


Figure 3-3. Cable Design, Standard ITT Fiber

3.2 PREFORM DESIGN

Preform development was concentrated on achieving a core diameter of 25 μm core in a 100 μm diameter fiber, a numerical aperture (NA) of 0.3, a loss of ≤ 6 dB/km, and a dispersion of ≤ 2 ns/km. The approach has been to modify, as needed, the techniques currently in use at ITT EOPD for fabrication of low loss 55 μm core graded index fibers. This was done by adjusting the fabrication conditions and the core and cladding glass compositions. Experimental preforms were produced with NA values ranging from 0.2 to 0.35 and with core diameters ranging from 20 to 40 μm . After the conditions were established to achieve an NA = 0.3 and a core diameter = 25 μm , the refractive index profile was optimized to achieve the desired loss and dispersion values.

3.3 DRAW PROCESS

After the preform has been fabricated, it is mounted on the preform feed mechanism of the fiber draw tower. A schematic of the fiber drawing equipment is shown in figure 3-4. Oxy-hydrogen torches are used as a heat source to raise the temperature of the preform tip to the point where it can be drawn into fiber. As part of fiber strength preservation techniques, both the hydrogen and the oxygen supplied to the torches are filtered through a 0.1 μm particle filter prior to entering the torches.

A Milmaster SSE-5R diameter monitor along with an SEC-1 closed loop feedback process controller were used to monitor and control the fiber OD just below the melt zone. Diameter control on fibers drawn from preforms developed for this program was maintained to within ± 3 percent with this system.

Just below the diameter monitor, the jacket material is applied by dipcoating. Concentricity of this coating is maintained by two means: (1) alignment of the dipcoater orifice with the fiber which centers the fiber in the dipcoater before the coating material is added; and (2) monitoring the viscosity of the coating material. The viscosity of

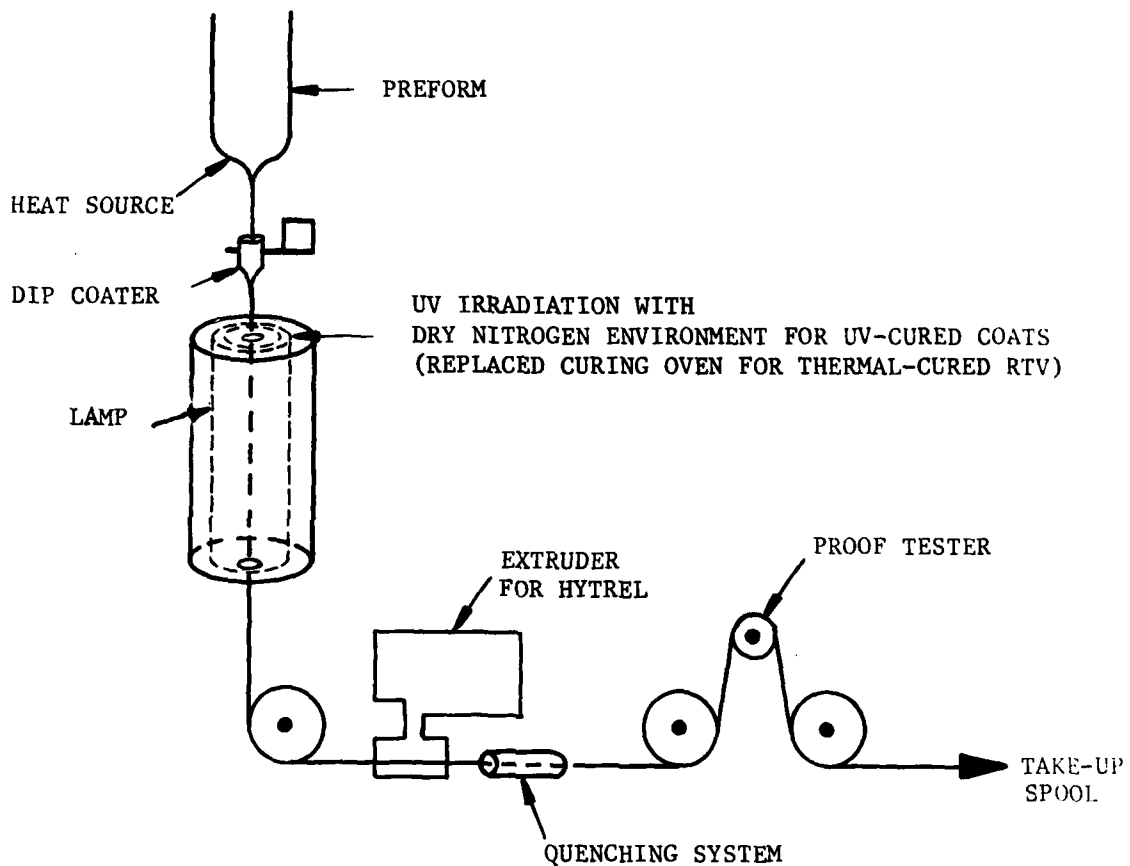


Figure 3-4. Schematic of Fiber Drawing Equipment

UV-curable resins is temperature dependent. If the resin viscosity is properly maintained, and the dipcoater is well centered around the fiber, the fluid pressure of the viscous resins helps to center the fiber within the coating.

After the coating has been applied, it is immediately cured by exposure to UV radiation. A filtered nitrogen atmosphere is provided around the fiber as it passes through the UV irradiator to promote a higher cure rate. After the coating is cured, the fiber is proof tested at the specified level (see section 3.5) and taken up on a plastic spool. The fiber is respooled on a metal spool supplied by Hughes before it is sent for optical evaluation.

The draw procedure, as shown in figure 3-4, for fibers coated with silicone RTV and Hytrel is the same as that for UV-cured fibers except for the following:

- a. Since the silicone RTV is thermally cured, a curing oven is used in place of the UV irradiator. The RTV is cured in ambient atmosphere.
- b. The Hytrel secondary coating is applied by tube extrusion after the fiber exits the silicone curing oven and before the fiber is proof tested. It is quenched by the use of a water bath, and immediately dried using a high pressure air wipe.

3.4 FIBER COATING MATERIALS AND TECHNIQUES

The following coating materials and coating approaches were chosen for evaluation as protective coatings for the proposed fiber optic cable design: Silicone-Kynar, UV-curable resins, Isonel 200D, direct extrusion of polymers, and dip-coating. In selecting suitable protective coatings, there are some properties which are quite important and others which are unimportant. So far as cable strength is concerned, it is important that the coating elongation at failure is greater than that of the glass fiber. This insures that the glass will fail before the coating. The modulus of the coating tends to have little effect on cable strength since the glass carries the bulk of the load. Typically, the modulus of elasticity for organic or silicon plastics is on the order of a few hundred pounds per

square inch, while that of fused silica is about 10^7 psi. For the coating to share one half of the load, the cross-sectional area of the coating would have to be 25 to 50 times the area of the glass. Since, in the configurations of interest the ratio of coating area to glass area is about 8, it is clear that the coating modulus will have little effect. It is important, however, that the integrity of the coating be maintained. Any failure of the coating in payout will almost certainly result in a failure of the cable.

A summary of the results of the investigations of the various coating materials is as follows:

Silicone-Kynar. This approach was to provide a soft inner cushion (a silicone layer, applied by a dipcoating technique and cured thermally) and a hard, well-finished, tack-free outer coating. However, this approach was not investigated in detail because of associated problems in obtaining a smooth, uniform coating of Kynar dispersions.

UV-Curable Resins. UV-curable resins have been employed as a protective coating for optical fibers. A range of UV-curable resins, namely urethane acrylates, epoxy-acrylates, polyene/polythiol esters, urethane/epoxy acrylates have been attempted. The object was to obtain a single coating which would provide the required mechanical and environmental protection. The coating should also provide a well-finished, smooth, tack-free surface required for high-speed payout tests. Two UV-curable resins were chosen from several that were investigated as the candidate coating materials for the fibers. This selection was based on the desirable mechanical and optical performance of the coated fiber. The details of these two coating materials are listed in table 3-1.

Isonel-200 D. Isonel-200 D, a thermally curable, polyurethane was also investigated. This is a typical enamel coating used for coating copper wires and contains glycol ether as a solvent with some aromatic hydrocarbon dilutents. This composition has about 15 percent solvents. On-line coating of optical fibers with this material did not give promising results. The maximum thickness of coating that can be cured

in one pass is about 1/6 of a mil. A large number of passes is required to build a minimum coating thickness to provide the required mechanical and environmental protection. In the process of coating, in such a multiple pass coating system, the fiber strength will be greatly reduced which is not desirable. Hence, further evaluation was discontinued.

TABLE 3-I. DETAILS OF COATING MATERIALS

Material	Chemical Nature	Viscosity CP (at 28° C)	Tensile Strength (PSI)	Elongation at Break (1%)	Modulus at 1% Elongation (PSI)	Refractive Index
WCC-2 (W. R. Grace & Co.)	Polyene/ Polythiol Ester	≈4000	1500	30	100,000	≈1.5
DeSoto 8 (DeSoto Inc.)	Urethane/ Epoxy Acrylates	6000	4500	15	63,000	1.535

Direct Extrusion of Polymer. This procedure of forming a protective coating was not investigated in depth because preliminary evaluation has shown that the fiber loses its initial high strength during the extrusion process. A tube extrusion method was employed. During extrusion, the bare fiber has to be aligned in the cross-head. On-line centering of a drawing fiber in the extruder is a difficult task to perform. Any excursions of the uncoated fiber from the extruder center-line causes glass abrasion and thus results in greatly reduced fiber strength.

Dip-Coating Technique Employed. A dip-coating technique, using a flexible nozzle, was employed for on-line coating of the fibers with both Silicone RTV and UV-curable resins. A concentric coating was obtained by adjusting the position of the dip-coater nozzle. The concentricity is retained throughout the draw by the dynamics of the dip-coater nozzle design and the maintenance of a constant viscosity of the coating material. The concentricity was checked during the draw, using a microscope to observe the coated fiber in two perpendicular directions at 90° and normal to the axis of the fiber. The thickness of the coating was controlled by the diameter of the flexible nozzle orifice.

A Fusion System UV lamp with a variable power supply was used to cure the UV-cure resin coatings. The lamp delivers a power of 300 watts/inch of the lamp at full power setting. A nitrogen purge was used to increase the cure rate. The fiber runs parallel to the lamp system and is exposed to a maximum total UV energy of 3000 watts at any given time. Figure 3-4 shows a schematic of the drawing-curing process.

3.5 CABLE EVALUATION

The manufactured cable was evaluated for conformance to specific optical, mechanical and environmental performance requirements that were considered important and necessary for cable success.

Optical Cable Evaluation. Prior to delivery of each of the PDM cables, several optical parameters were measured; included were optical signal attenuation, pulse dispersion, numerical aperture, and the diameters of the fiber and core. The evaluation provided not only a quality assurance check to insure the quality of the cable, but also provided baseline data to determine the effects of winding upon the optical parameters of the cable. The test procedures used were consistent with DOD-STD-1678, dated 30 November 1977. The numerical aperture data was obtained by measuring the included angle of a cone containing essentially 100 percent of the output energy from a 1 meter test length.

The data obtained for the three types of cables investigated is shown in tables 3-II and 3-III. The test methods and procedures are described in a Test Plan submitted to Hughes under separate cover.

TABLE 3-II. OPTICAL DATA

Material	Fiber OD (mils)	Loss (dB/km)	Dispersion (ns/km)	NA	Core Size (μ m)	Remarks**
Borden	5.0	9.95	0.99	.33	55 x 57	Poor Quality Preform Spooled
DeSoto 8	5.0	7.87	0.59	.20	53	Spooled
WCC-2	4.0	4.46	0.69	.24	41	Spooled
Hughson	4.0	4.96	1.07	.30	43	Spooled
WCC-2*	5.0	5.27	1.76	.28	54 x 56	Spooled
WCC-2*	5.0	4.26	1.25	.28	54 x 56	Strung

*Indicates same fiber.

** Spooled - These fibers were measured on their shipping spools. Multiple cross-overs and sufficient winding tension is used to prevent fiber movement during shipment

Strung - These fibers were measured while strung between two 12-inch diameter drums with a centerline distance of seven meters. This evaluation procedure eliminates spooling loss and is a true measure of the attenuation without bending losses.

TABLE 3-III. OPTICAL DATA

WCC-2 UV-CURED PRIMARY JACKET, HYTREL SECONDARY JACKET

With WCC-2 Jacket Only:

*Spooled	5.27 dB/km, 1.76 ns/km
**Strung	4.26 dB/km, 1.25 ns/km

With Hytrel Secondary Jacket:

Spooled	5.57 dB/km, 1.34 ns/km
Strung	5.01 dB/km, 1.08 ns/km

NOTE: A 300 meter piece was proof tested to 200 kpsi without breaks.

*Spooled - These fibers were measured on their shipping spools. Multiple cross-overs and sufficient winding tension is used to prevent fiber movement during shipment.

**Strung - These fibers were measured while strung between two 12-inch diameter drums with a centerline distance of seven meters. This evaluation procedure eliminates spooling losses and is a true measure of the attenuation without bending losses.

Mechanical Evaluation. All fibers were subjected to a proof test on-line as the fiber was being drawn. This means that the entire length of the fiber was subjected to a tensile load which produces a known tensile stress. This procedure eliminates weak sections of fiber if they exist. Any portion of fiber which does not have a tensile strength greater than the proof test stress will break at the proof tester. The proof test level that was employed for the fabrication of the missile payout fibers was 200 kpsi (1380 N/mm²). Some of the proof testing was done on-line with the fiber drawing equipment, and other testing was done off-line. The test setup is illustrated in figure 3-5. The load buildup occurs in about 0.5 seconds, the interval during which the proof load is applied is about 1 to 2 seconds, and unloading in about 0.5 seconds.

When the desired cable design was established, a plastic clad silica (PCS) fiber was drawn for strength evaluation. This fiber was drawn from a solid Suprasil 2 rod (synthetic high purity SiO₂) with a fiber OD of 4 mils and a jacket OD of 12.5 mils of UV-cured WCC-2. This was done to simulate draw conditions as they would be with a CVD preform required to achieve the established design. The PCS fiber was on-line proof tested at 200 kpsi, and one continuous piece 4854 meters in length was produced.

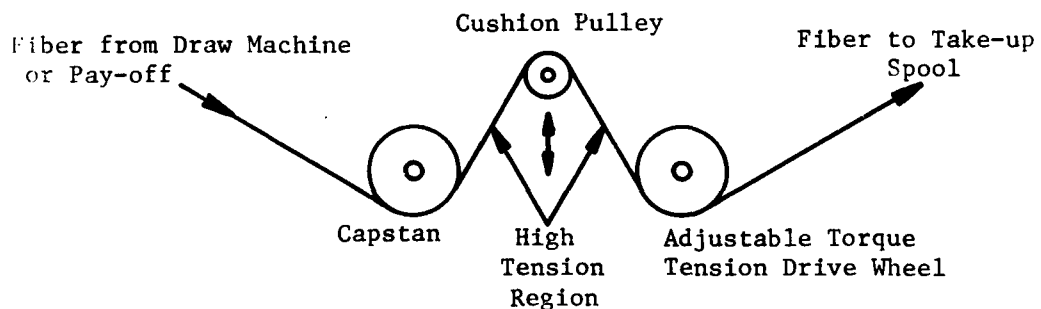


Figure 3-5. Strength Proof Test Setup Drawing

This draw established the fact that a fairly long length of fiber can be produced which can pass the 200 kpsi proof test. After the draw, short gauge length (2 meters) dynamic strength tests were performed on two sections of the fiber, one set at the start of pull (SOP) and the other at the end of pull (EOP). Table 3-IV summarizes the numerical results. In these tests, the load was applied by introducing a constant strain rate of 20 percent of the initial length per minute. At this strain rate, approximately 6 seconds are required to reach a load of 200 kpsi.

TABLE 3-IV. WCC-2 COATED FIBER STRENGTH SUMMARY

Fiber Portion	SOP	EOP
Load Rate (% elongation per minute)	20	20
Maximum Strength (kpsi)	929	947
Minimum Strength (kpsi)	785	748
Mean Strength (kpsi)	838	852
M Value (Weibull parameter)	69	59

Figure 3-6 and 3-7 are Weibull plots of the data for these two sets of dynamic strength tests. Both ends of this fiber were very strong and these results should be typical of fibers drawn and jacketed in this manner as long as high preform quality is maintained. However, occasional rare flaws (weak spots) will still be encountered as the length of the fiber increases.

Static Fatigue tests were performed on early fibers coated with DeSoto-8 and WCC-2. Testing was done by the mandrel method, in which the fiber is carefully wound onto a precision mandrel causing a known bending stress on the fiber. The elapsed time until the fiber breaks is recorded.

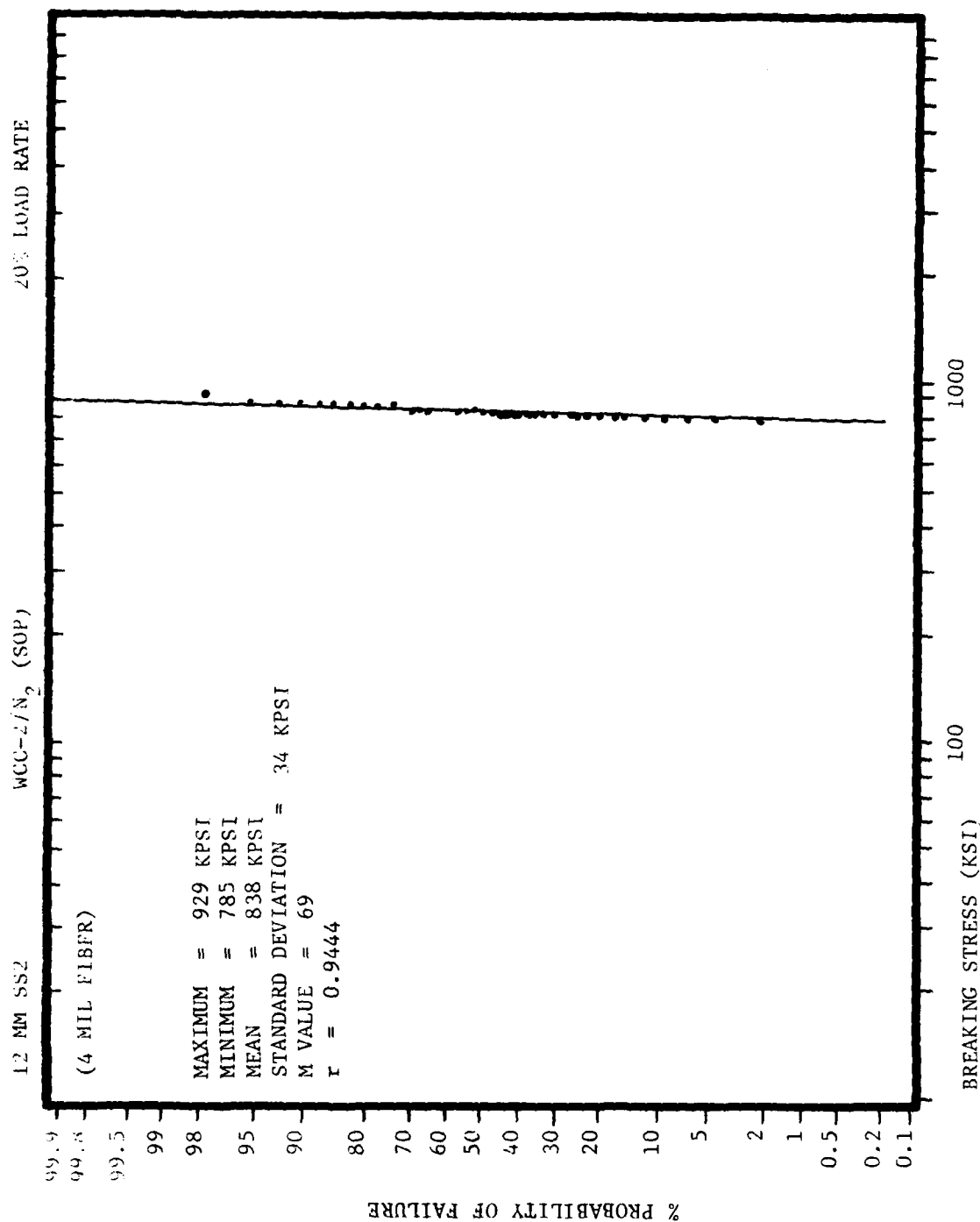


Figure 3-6. Dynamic Strength Test Results. WCC-2 Coated Fiber at Start of Pull (SOP).

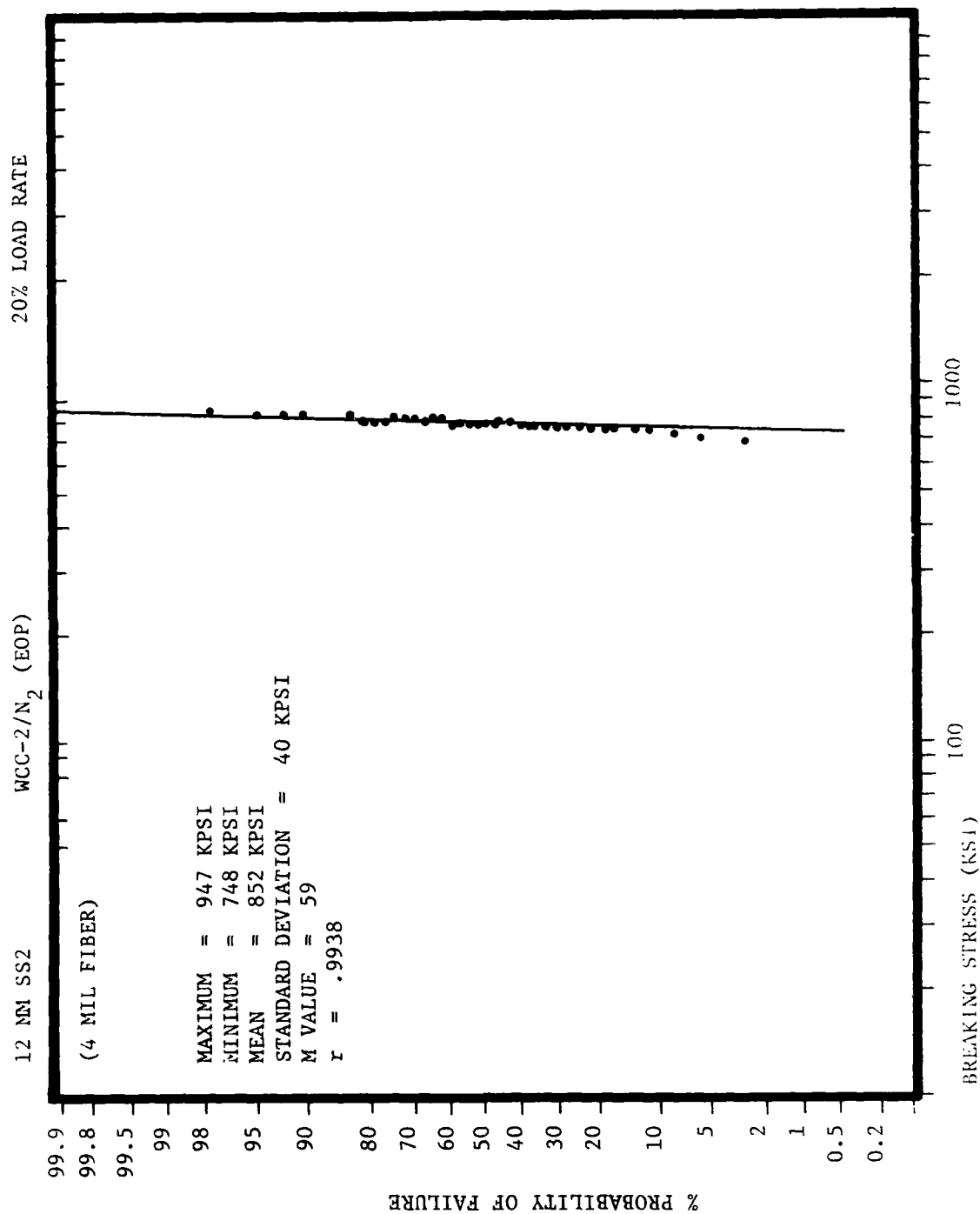


Figure 4-7. Dynamic Strength Test Results. WCC-2 Coated Fiber at End of Pull (EOP).

The stress applied to the fiber can be calculated from the equation:

$$S = \frac{Er}{R + r + t}$$

where E = Young's modulus for SiO₂ glass
R = mandrel radius
r = fiber radius
t = jacket thickness

A plot of log stress versus log time to failure tends to give a straight line, the slope of which is the fatigue value, N. A high N value is desirable for better fatigue resistance. N values for the three jacket materials evaluated in Phase I are as follows:

Silicone RTV + Hytrel	N = 20-22
DeSoto 8	N = 19-20
WCC-2	N = 30-35

Figure 3-8 shows a comparison plot of fatigue data for these materials. It may be noted that the data points do not all fall on the lines. Considering the statistical spread in the data and the small number of samples at each stress level, the departures from the straight lines are not believed to be significant.

Environmental Testing and Results. The key qualifying environmental tests performed on the preliminary design model (PDM) cables were high and low temperature versus attenuation and dispersion, tensile strength following humidity, and fungus growth in accordance with MIL-STD-810C.

High and Low Temperature Versus Attenuation. Sufficient lengths of coated fiber optical cables were subjected to the high and low temperature tests in accordance with MIL-STD-810C, Method 501.1, procedure II and Method 502.1, procedure I. One sample of each different coating material was evaluated. The cables were loosely coiled into a 12-inch diameter loop. Table 3-V shows the results of that testing. In a similar experiment performed by Hughes on ITT fibers wound on a metal bobbin, the attenuation did not change either at low or high temperatures. These results are discussed in section 4-4.

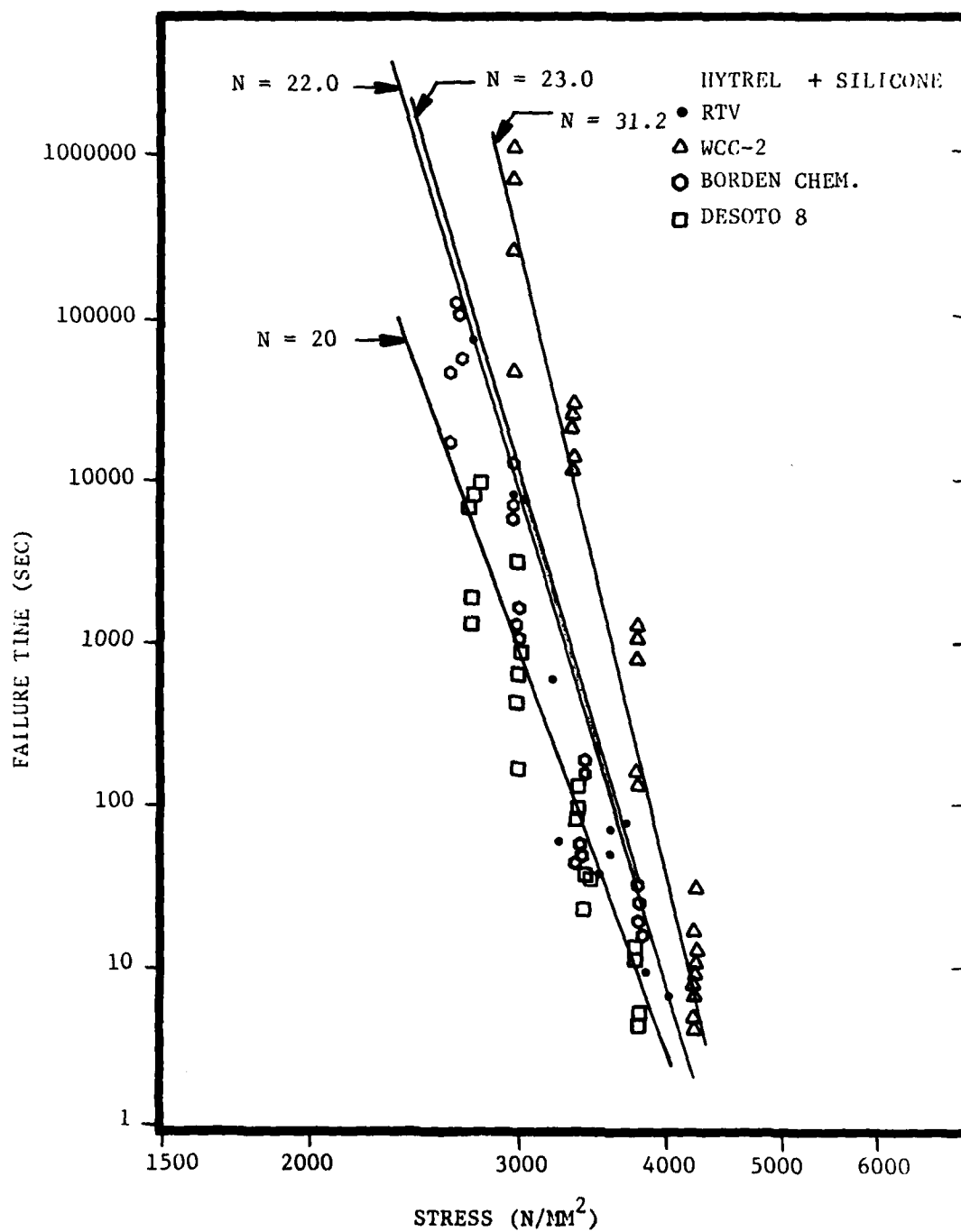


Figure 3-8. Static Fatigue Comparison of Various Coating Materials

TABLE 3-V(a). EFFECT OF TEMPERATURE ON ATTENUATION CONSTANT DB/KM

Cable Sample		Elapsed Time (Hrs)						
		0	7.0	11.5	13.25	26.5	27.5	37.5
Serial Number	Coating	Temperature (°C)						
		25	49	71	25	25	-57	25
EG20537	WCC-2	7.48	7.06	7.92	7.84	7.79	8.35	7.2
EG20592D	Sylgard & Hytrel	3.57	3.45	4.19	3.91	4.02	8.73	4.03
EG20542	DeSoto 8	3.98	4.6	4.54	4.70	4.59	6.59	4.29

TABLE 3-V(b). EFFECT OF TEMPERATURE ON PULSE DISPERSION NS/KM

Cable Sample		Elapsed Time (Hrs)						
		0	7.0	11.5	13.25	26.5	27.5	37.5
Serial Number	Coating	Temperature (°C)						
		25	49	71	25	25	-57	25
EG20537	WCC-2	2.53	-	-	2.35	-	1.85	2.21
EG20592D	Sylgard & Hytrel	0.79	-	-	0.71	-	Note 1	0.55
EG20542	DeSoto 8	1.01	-	-	1.19	-	0.85	0.69

Note 1. This value dropped below the minimum acceptable range as defined in DOD-STD-1678, method 6050-2, 4.6, step 6; hence considered too small to measure accurately with technique employed.

Post Humidity, Tensile Strength. This test was performed in accordance with method 507.1, procedure II of MIL-STD-810C. Three samples, one of each different type of coating, were placed in a test chamber and subjected to the following temperature cycle:

Steps

- a. Increased chamber temperature from $+86^{\circ}$ F to 149° F in four hours
- b. Maintained $+140^{\circ}$ F for eight hours
- c. Decreased from 149° F to $+86^{\circ}$ F in four hours
- d. Maintained $+86^{\circ}$ F for 21 hours
- e. Decreased from 86° F to $+68^{\circ}$ F in one hour
- f. Maintained $+68^{\circ}$ F for four hours
- g. Increased from $+68^{\circ}$ F to $+86^{\circ}$ F in one hour
- h. Maintained $+86^{\circ}$ F for five hours.

The samples were subjected to five continuous 48-hour cycles as described above. The relative humidity was maintained at 95 ± 4 percent during this test, except not less than 85 percent during the descending temperature periods. Following the temperature/humidity cycling, preconditioned 80-inch samples of optical fiber cables were subjected to tension tests. The tensile test was repeated on three samples from each cable type. Only one non-related break occurred outside the tensioning apparatus. The results are presented in table 3-VI.

Fungus Growth Resistance. The fungus test was performed on each cable type for MIL-STD-810, Method 508.1, procedure I. Prior to the start of the fungus test, the optic fiber samples were cleaned with isopropyl alcohol. The samples were then placed in the fungus chamber and sprayed with previously prepared and tested fungus culture. The test chamber was maintained at $+86^{\circ}$ F at 95 percent relative humidity for 28 days. Only the DeSoto 8 coated material showed light to heavy, spotty growth. The other two samples showed light and very light scattered growth for the WCC-2 and RTV-Hytrel coated samples, respectively. Cable optical and mechanical performance was not degraded as a result of fungus testing.

TABLE 3-VI. POST HUMIDITY TENSION TEST RESULTS

Cable	Tension (lbs)	Stress (ksi)	Test Duration (min)	Remarks
EG20542 (1)	3.77	200	3	No breaks*
EG20542 (2)	3.77	200	3	No breaks
EG20542 (3)	3.77	200	3	No breaks
EG20537 (1)	2.30	200	3	No breaks
EG20537 (2)	2.30	200	3	No breaks
EG20537 (3)	2.30	200	3	No breaks
EG20592D (1)	2.65	200	3	No breaks
EG20592D (2)	2.65	200	3	No breaks
EG20592D (3)	2.65	200	3	No breaks
*NOTE: Fiber broke outside test section while being removed from tensioning apparatus.				

3.6 STATIC FATIGUE CONSIDERATIONS

The tests which have been conducted to date have not specifically examined the question of static fatigue of the cable when wound on a bobbin. There has been one test result which, by accident, has provided some knowledge for application to this study. The region of the winding which is believed to be most susceptible to static fatigue is the crossover zone where one turn of the winding obliquely crosses over a turn on the layer below. In this region, in the plane of the turn, the cable is constrained by the pressure from the layers above to tend to lie along a long helix with an inside diameter equal to the cable diameter. As the crossover angle is increased, the pitch of the helix is reduced, increasing the bending stresses at the crossover. In the plane normal to the plane of the turn, the cable makes a slight "S" shaped bend as it approaches and then leaves the crossover region. This results in bending stresses in a plane normal to the plane containing the bending due to the helical path. As the pressure on a layer is increased due to the layer being located deep within the cable pack, the bending stresses in the plane of the turn appear to be the greater of the two stresses.

An approximation to the radius of the curvature, R , of the cable as it follows a helix about the turn beneath is

$$R \approx \frac{r_c}{\sin^2 \theta}$$

where r_c is the radius of the cable and θ is the angle which the helix makes relative to the axis of the lower turn. The outer fiber tensile stress, S_o , resulting from this bending, is

$$S_o = \frac{E r_f}{R} \approx \frac{r_f}{r_c} E \sin^2 \theta$$

where r_f is the fiber diameter and E is Young's modulus of the fiber. As θ is increased, the cable bending radius is reduced quite rapidly and the bending stresses are correspondingly increased.

During the testing of the wound bobbin which is described in 4.4, pressure is applied to the exterior of the test bobbin, simulating the pressure on those layers due to additional layers above. Since during the test the elevated pressure is applied for a relatively short time period, the maximum bending stress for static fatigue purposes is not applied for a sufficient time to obtain any meaningful static fatigue results. However in one test, some turns were accidentally dislodged and put back in place as carefully as was possible, but five or six turns were positioned with abnormal crossover geometry with substantially greater crossover angles. Although there were no careful measurements made on the resulting geometry, it is estimated that the resulting bending stresses as pressure was applied to these anomolous crossovers was perhaps a factor of four or five greater than that of a normal crossover. Approximately two or three minutes after application of the maximum pressure, simulating conditions deep in the cable pack, the cable failed in static fatigue at one of these anomolous crossovers. Prior to the application of the maximum pressure (simulating conditions deep in the cable pack) the cable failed in static fatigue at one of these anomolous crossovers. Prior to the application of the maximum pressure, lower pressure had been applied contributing to static fatigue at a lower rate.

The significance of this static fatigue failure is difficult to define accurately, but some broad conclusions can be made. There are several empirical models which have been described in the literature describing the relationship between the level of applied stress and the static fatigue life of a fiber. Using the straight line approximations to the failure time data in figure 3-6, a relationship of the form

$$\left(\frac{S_1}{S_2}\right)^N = \frac{t_2}{t_1}$$

is readily obtained where S_1 and S_2 are levels of applied stress, and t_1 and t_2 are the corresponding static fatigue lifetimes, and N is the slope of the straight line. Using a value of $N = 20$ corresponding to the

shallowest of the lines of figure 3-6, and a value of 4 for the approximate ratio of the anomolous bending stress in the test to the normal stress at the crossovers, the ratio between the expected lifetime at normal stress and the observed lifetime at the increased stress is

$$\frac{t_2}{t_1} = (4)^{20} = 1.1 \times 10^{12}$$

For an observed life under the increased load of approximately 2 minutes, the predicted lifetime under normal loads is about 4×10^6 years, a value which should be suitable for even the most critical of requirements.

Based on a predicted static fatigue life of over four million years, one is tempted to conclude that there is no static fatigue problem with the existing cables. There are certain considerations which tend to discourage such a conclusion without additional data. These considerations include the following:

1. There are significant uncertainties in the values used to compute the predicted static fatigue life which can significantly alter the final result. For example, if the ratio of the excess load to working load was only a factor of 2 rather than a factor of 4, and if the observed failure time was only 1 minute rather than 2 minutes, the predicted static fatigue life becomes only 2 years. This illustrates how sensitive to errors this prediction is.
2. In practice in measuring static fatigue life, where several cable samples are subjected to a given load and the time to failure for each sample is measured, there is usually a wide statistical distribution in failure times observed. For this reason, with only a single test sample, one cannot assign much statistical confidence to the result.
3. The computation involves the prediction of the storage time required for the cable to fail while wound on the bobbin. In reality, the lifetime that is of interest is that storage time which results in sufficient weakening of the cable from crack propagation due to static

fatigue that a cable just fails during the payout loads. This latter prediction is much more complex and the allowable storage life will be significantly less than that which would result from the use of the foregoing equations.

In summary, although the available data suggests that the cable configurations which have been tested will likely yield adequate static fatigue life, the available data is too incomplete to reach that conclusion with any confidence. The answer to this question must await the availability of substantially more data than is now available.

4.0 DISPENSER DESIGN

4.1 APPROACH

The dispenser development activities have proceeded along three parallel and highly interrelated lines which are:

1. Full length dispenser design,
2. Design and mechanical evaluation of test dispensers employing short length of cable (≈ 0.5 to 1.0 km), and
3. Optical evaluation of short length test dispensers.

The combined results of these efforts are the basis for an iterative sequence involving cable and dispenser design changes in order to obtain several cable and dispenser design combinations which appear capable of satisfying the full 10 km length objectives.

The sequence that follows was used for the design and evaluation of candidate dispensers to achieve final designs capable of full length payout.

Step 1. Initial cable design and characterization

Step 2. Based on:

- . Nominal outside diameter of the cable
- . Required outside diameter of a wound 10 km dispenser
- . Determined transverse compressibility modulus
Compute through model, parameters for 10 km dispenser including
- . Dimensions of the winding spool
- . Total number of layers (stepback)
- . Interlayer pressure at each layer of the cable pack for specific winding tension

Step 3. Design test spools having shorter length dimension to increase the number of layers for short cable test lengths

- Step 4. Fabricate instrumented test spool for short lengths
- Step 5. Measure spool strain prior to winding and during winding of test lengths of cable.
- Step 6. Correlate with computer results used in the design.
- Step 7. Determine optical attenuation resulting from the spooling process. Use applied pressure to simulate the effect of winding additional layers to a total of 10 km length.
- Step 8. Payout test dispenser on high speed test facility.
- Step 9. Evaluate results and apply to improved cable design.
- Step 10. Repeat the sequence.

The design sequence was used in an iterative manner with the results of one test being used to modify the cable and dispenser design parameters for subsequent items. Through this process, cable and dispenser designs capable of satisfying the geometric and attenuation requirements for full 10 km lengths have resulted.

4.2 DISPENSER DESIGN

The length of cable that can be wound on a cylindrical spool is given by

$$L = 2\pi \sum_{n=1}^N \left[b + \frac{d}{2} + (n-1) \frac{d}{2} \sqrt{4 - \frac{d_s^2}{d^2}} \right] \left[\frac{\ell}{d_s} - (n-1)i \right] \quad (4.2-1)$$

where

d = cable diameter

b = spool outer radius

d_s = winding pitch $\geq d$

N = number of layers

ℓ = spool length

i = the number of stepback turns per layer

The radius to the outside of the cable pack is

$$R_n = b + d \left(1 + \frac{N-1}{2} \sqrt{4 - \frac{d_s^2}{d^2}} \right) \quad (4.2-2)$$

These equations neglect any compression of the cable pack and spool which occurs during winding and also the effect of spool taper. In order to calculate the spool and cable pack stress, an existing computer program based on the work done on TOW was used. A definition of some of the terms used in the program follows:

Input: ES - Young's modulus for the spool material
 VS - Poisson's ratio for the spool material
 T - Spool thickness
 B - Spool outer radius
 A - Spool inner radius
 DS - Winding pitch
 EC - Young's modulus for the glass
 D - Glass diameter
 DW - Overall cable diameter
 K - Transverse stiffness of cable
 N - Number of layers
 T - Winding tension

Output 1: ESO - Spool hoop strain at inner radius
 ESX - Spool axial strain
 SSX - Spool axial stress
 US - Spool radial displacement at outer radius
 SSO - Spool hoop stress at inner radius
 SSR - Spool radial stress at outer radius
 F1 - Radial contact force between first layer and spool

Output 2: J - Layer number
 TWJ - Tensile force in layer J after N layers are wound
 FJ - Force between layer J and J-1
 VWJ - Radial displacement of layer J
 CJ - Radius to layer J

The spool hoop strain and spool hoop stress are caused by external pressure being applied to the outer radius as a result of winding on cable under tension. Since the spool hoop strain at the inner radius is measured by means of a strain gage during the performance of the experiments, a correlation can be obtained with the theoretical values. The spool axial strain and stress result from the Poisson effect and from the axial tension put into the spool by the first layer of cable. The spool radial stress is again the result of winding on cable under tension and is zero at the inner

radius and maximum at the outer radius where contact with the cable occurs. The spool radial displacement also results from the loading of the spool and is maximum at the outer radius.

The derivation of the equations in the program are based on the following assumptions:

- a. The basic equations describing the stresses and deformations resulting from winding cable on a spool are applicable only in the axially uniform regions of the wound spool and are not applicable in the tapered layer-to-layer transition regions.
- b. The effects of differential thermal expansion of the cable and spool materials are not included in the basic equations.
- c. The effect of crossovers which occur twice per turn when a layer is wound in the opposite direction over an existing layer are neglected.
- d. The force displacement relation between cables in contact is assumed to be linear; i.e., the cable lateral stiffness is constant.
- e. The effect of the coating on cable longitudinal stiffness is neglected and consists of the stiffness of the glass only.
- f. The effect of twist in the cable is neglected.
- g. The effect of spool taper is neglected.
- h. Any creep or relaxation of the cable pack material cannot be accounted for by this analysis.

The criteria which constrain the dispenser design are as follows:

- a. In order to introduce as little microbending as possible into the cable as it exists in the cable pack, the radial interlayer pressure must be kept low. This requires low winding tension and fewer layers.
- b. The spool length and number of layers are constrained by

$$l > d_g (N-1) i \quad (4.2-3)$$

c. The minimum spool radius is determined so that the first layer of cable wound on it does not yield because of winding tension and bending.

d. The maximum diameter of the dispenser is determined by the missile size.

e. The spool stress must remain below the yield or buckling stress. This places constraints on the spool material and thickness.

f. The tension in all layers in the cable pack should remain positive to avoid the possibility of local buckling of the cable.

g. Cable setback in the layer-to-layer transition regions is required for cable pack stability. In the present designs this was set at nine turns per layer ($4\frac{1}{2}$ at each end).

The parameters for six different designs are summarized in table 4.2-I. As described above, test bobbins were fabricated to expedite the evaluation of the various designs; the corresponding design parameters for the test bobbins are shown in parenthesis, if different from those of the basic design. Cross sections are shown in figures 4.2-1 through 4.2-6. Three of these designs, numbers 1, 2, and 5, represent variations of standard bobbin geometry with the spool length substantially greater than the diameter. Design No. 3 involves a large diameter dispenser with the length less than the diameter. Design No. 6 falls in between these extremes. Design number 4 involves a configuration where dispensing is accomplished from the inside of the cable pack. The computer output for all the designs with the exception of number 4 is shown in tables 4.2-II through 4.2-VI. Number 4 has low internal stresses since it relaxes when the spool is removed. The computer printout for each design consists of the input parameters and two sets of output. The input parameters define the spool material constants, the spool thickness and radius, the winding pitch, the glass material constant, the overall diameter of the cable and the diameter of the glass inside it, the transverse cable stiffness (which is measured as described in the next section), the number of layers, and

the winding tension. The first set of output gives the tension of each layer as it is wound on, the strains stresses and radial displacement of the spool as each layer is applied, and the radial force per unit length between the first layer and the spool as each layer is applied. The second set of output gives the cable tension, force between layers, layer radial displacement, radius to a given layer, etc., as a function of layer number after the winding is completed.

Radial interlayer pressure can be derived from the second set of computer output by considering figure 4.2-7.

$$p_j = \frac{2 F_j \cos \alpha}{d_s} \quad (4.2-4)$$

where $\alpha = \sin^{-1} \frac{d_s}{2d_w}$ (4.2-5)

The radial interlayer pressure is shown in figure 4.2-8 for all designs except number 4, where it is small.

Radial interlayer pressure tends to increase as the total number of layers, cable lateral stiffness, winding tension and spool stiffness (or thickness) increase, and tends to decrease as cable diameter, spool diameter and cable spacing increase. The least pressure occurs in design number 3, which has the largest diameter spool and relatively few layers. Design number 5 has the next higher pressure, even though it has the most layers, due to larger cable diameter and the lowest cable lateral stiffness. Design number 6 ranks next because of the highest cable lateral stiffness and smaller diameter cable. Design number 1 is next, even though it has the largest diameter cable because of the higher winding tension, smallest diameter spool, and large number of layers. Design number 2 exhibits the highest interlayer pressure, even though it has relatively few layers, because of the small diameter cable of high lateral stiffness wound on the smallest diameter spool.

The yield strength of 6061-T6 aluminum alloy is 35,000 psi. Examination of the maximum SS0 in the computer output yields 10,150 in table 4.2-IV and 10,430 pis in table 4.2-IV.

TABLE 4.2-1. SUMMARY OF BOBBIN DESIGN PARAMETERS

Parameter	Design No. 1	Design No. 2	Design No. 3	(Inside Payout) Design No. 4	Design No. 5	Design No. 6
Cable Length - km	10 (1.2)	10 (.6)	10 (1)	10 (.6)	10 (1)	10 (1)
Cable O.D. - in	.020	.0107	.010 (.008)	.01	.015	.0125 (.013)
Glass O.D. - in	.005	.00415	.005 (.004)	.005	.005 (.004)	.004 (.0042)
Average Spool O.D. - in	3.5	3.5 (3.552)	7.73 (7.8)	5 (3.53)	4 (3.53)	5 (3.53)
Wound Spool Length - in	14.4 (6)	12 (3)	6 (2)	10 (4.5)	10.5 (4.5)	10.5 (4.5)
Spool Thickness - in	.1	.1	.050	.1	.1	.050 (.1)
Spool Taper - deg	1	1	1	1	1	1
Number of Layers	68 (17)	33 (8)	35 (10)	27 (6.5)	70 (18)	35 (12)
Setback per Layer - turns	9	9	9	9	9	9
Average Overall Wound O.D. - in	5.9 (4.1)	4 (3.6)	8.34 (8)	5.47 (3.62)	5.82 (4.0)	5.76 (3.8)
Cable Lateral Stiffness - psi	6000	12,800	12,800 (62,000)	27,500	4,500	26,600
Winding Tension - lb	.5 (.93)	.28 (.39)	.25 (.42)	.25 (.4)	.25 (.47)	.25 (.36)
Spool Material	6061-T6	6061-T6	6061-T6	--	6061-T6	6061-T6

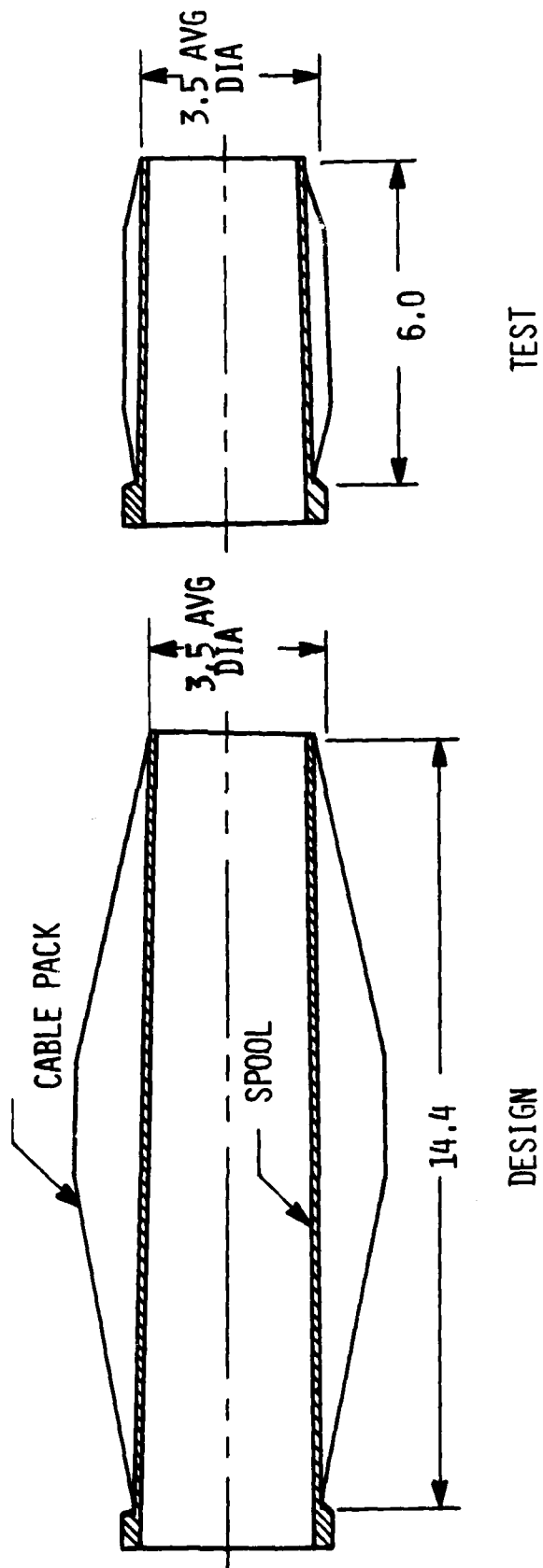


Figure 4.2-1. Design No. 1

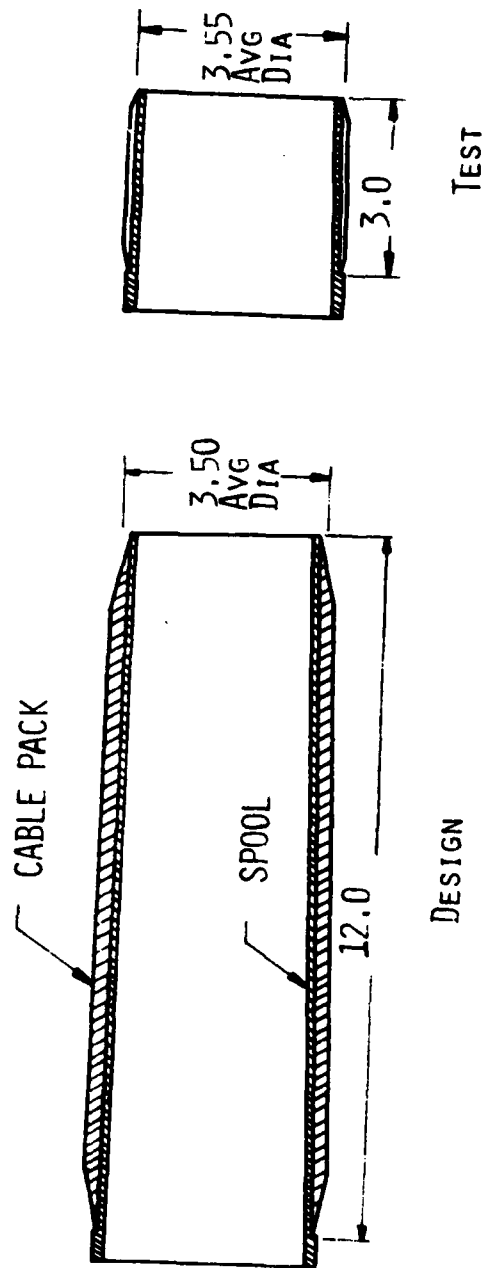


Figure 4.2-2. Design No. 2

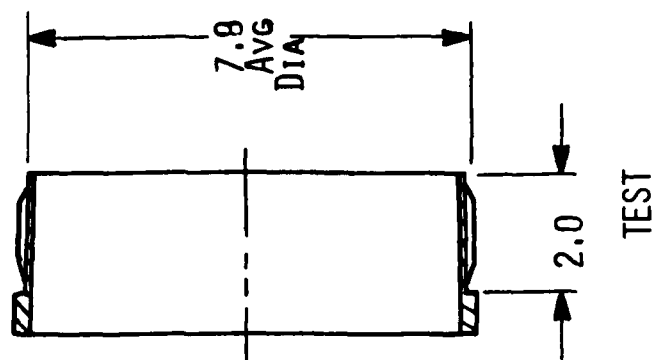
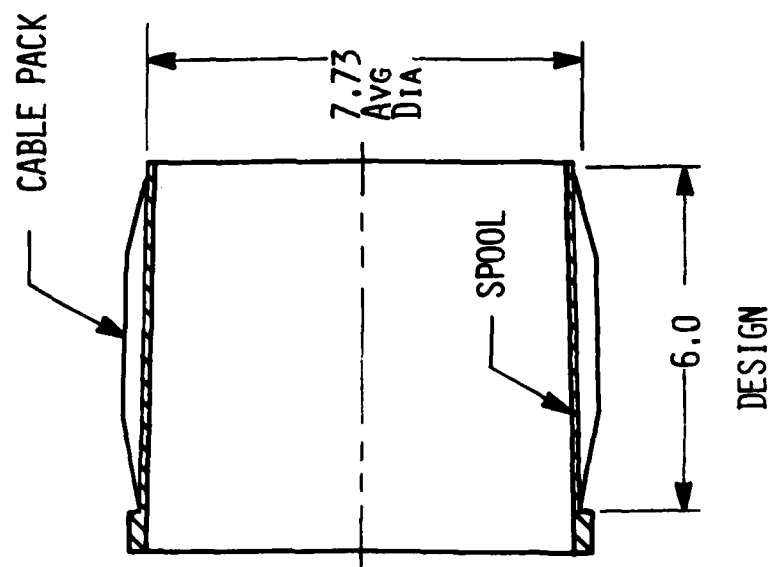


Figure 4.2-3. Design No. 3

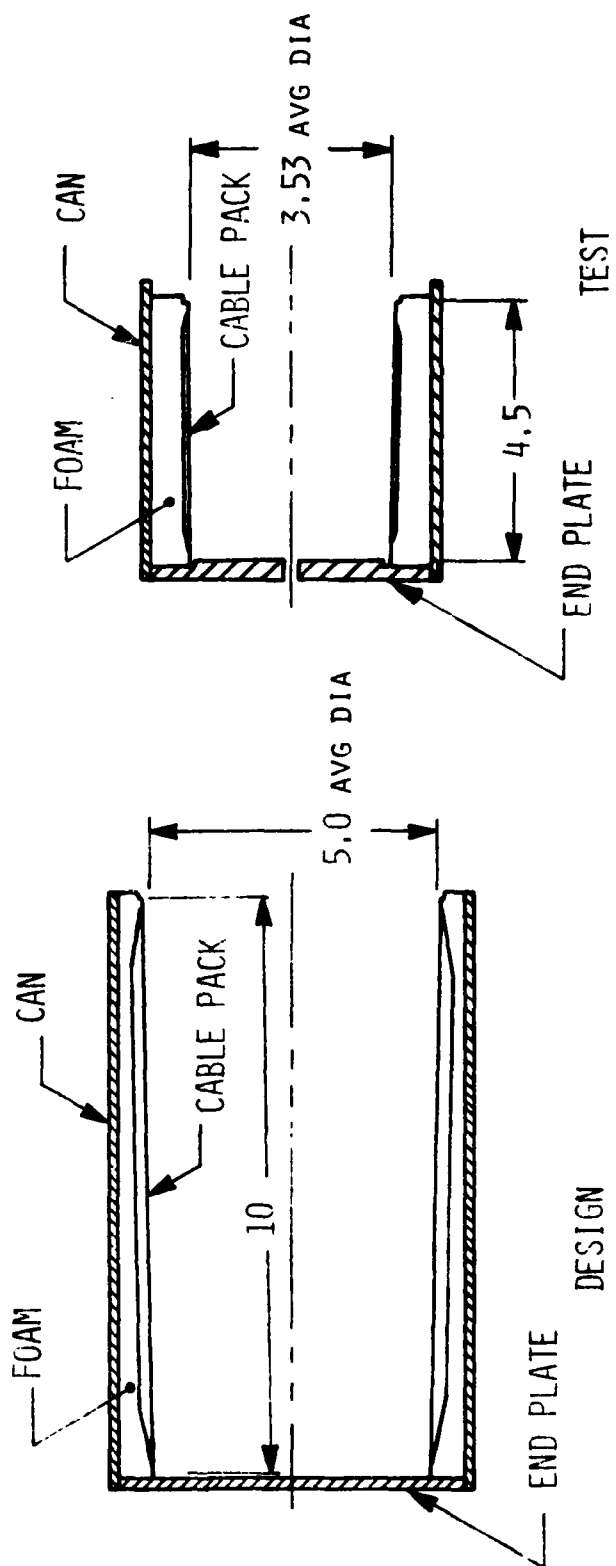


Figure 4.2-4. Design No. 4

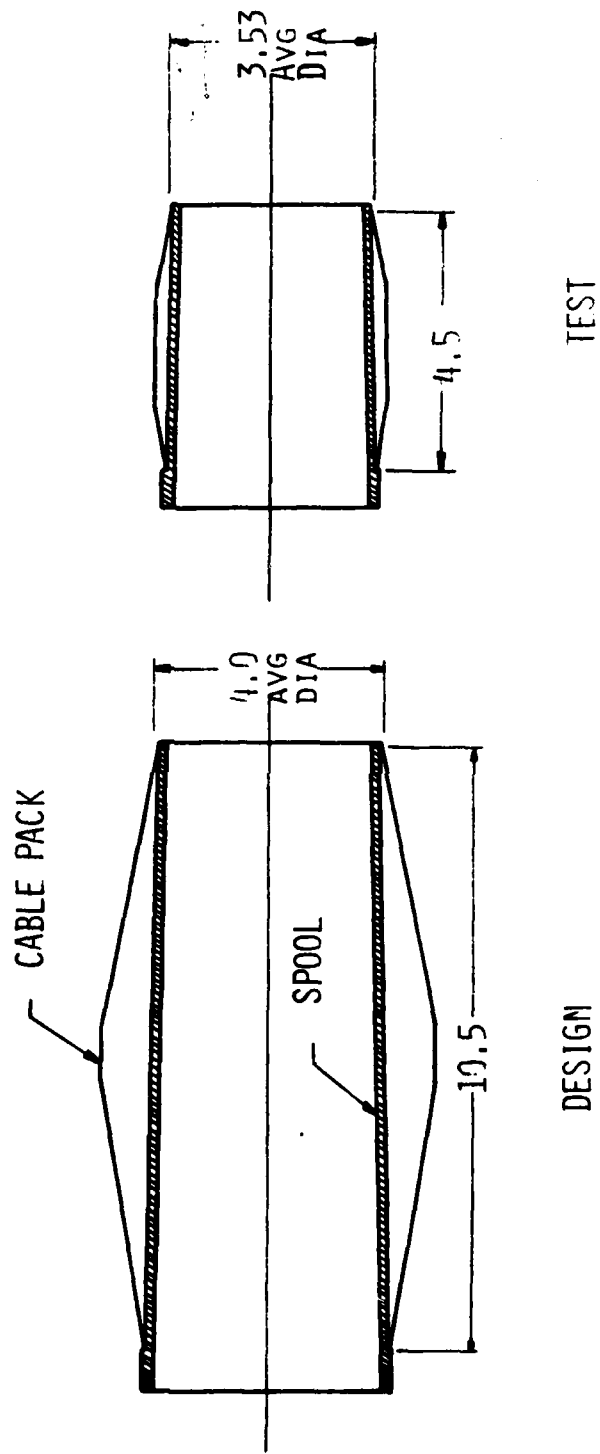


Figure 4.2-5. Design No. 5

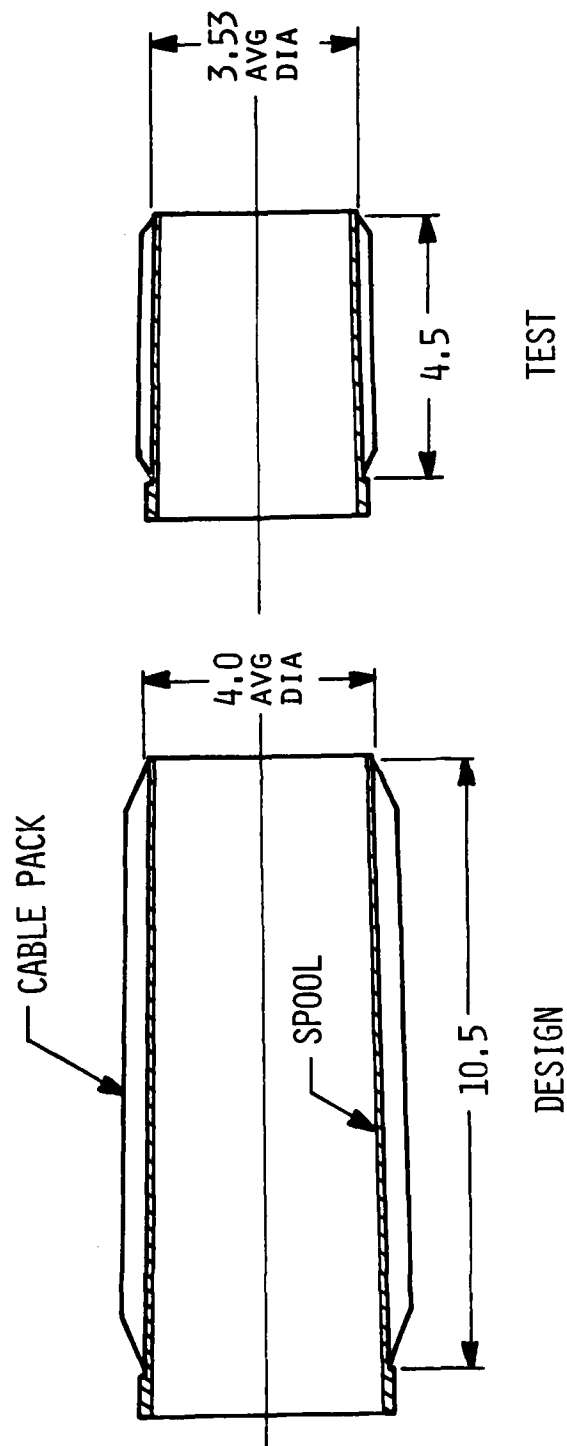


Figure 4.2-6. Design No. 6

TABLE 4.2-II. DESIGN NO. 1

SPOOL			WIRE-PACK			BOBBIN			DATE 02/11/78	
ES=	0.1010E+08	B= 0.1750E+01	EC=	0.1050E+08	DDW= 0.	S=	0.9928E-01			
VS=	0.3300E+00	A= 0.1650E+01	D=	0.4920E-02	K= 0.6000E+04	DELIC=	0.1704E-01			
T=	0.1000E+00	DS= 0.1968E-01	DD=	0.	E= 0.5952E+06	N=	68			
DT=	0.	DDS= 0.	DW=	0.1968E-01	ALFA= 0.8738E+01					
N	T	DELT	ESO	ESX	SSX	US	SSO	SSR	F1	
1	0.5000E+00	0.	-0.2589E-04	0.8545E-05	-0.5211E-06	-0.4197E-04	-0.2615E+03	-0.1452E+02	0.2857E+00	
2	0.5000E+00	0.	-0.5145E-04	0.1706E-04	0.9076E+00	-0.8339E-04	-0.5193E+03	-0.2883E+02	0.5674E+00	
3	0.5000E+00	0.	-0.7652E-04	0.2548E-04	0.2637E+01	-0.1240E-03	-0.7720E+03	-0.4285E+02	0.8434E+00	
4	0.5000E+00	0.	-0.1010E-03	0.3377E-04	0.5159E+01	-0.1637E-03	-0.1010E+04	-0.5651E+02	0.1112E+01	
5	0.5000E+00	0.	-0.1247E-03	0.4188E-04	0.8436E+01	-0.2021E-03	-0.1256E+04	-0.6974E+02	0.1372E+01	
6	0.5000E+00	0.	-0.1475E-03	0.4978E-04	0.1243E+02	-0.2391E-03	-0.1486E+04	-0.8248E+02	0.1623E+01	
7	0.5000E+00	0.	-0.1695E-03	0.5743E-04	0.1708E+02	-0.2747E-03	-0.1706E+04	-0.9469E+02	0.1864E+01	
8	0.5000E+00	0.	-0.1904E-03	0.6481E-04	0.2236E+02	-0.3087E-03	-0.1916E+04	-0.1064E+03	0.2093E+01	
9	0.5000E+00	0.	-0.2104E-03	0.7192E-04	0.2821E+02	-0.3412E-03	-0.2116E+04	-0.1175E+03	0.2311E+01	
10	0.5000E+00	0.	-0.2294E-03	0.7875E-04	0.3458E+02	-0.3719E-03	-0.2305E+04	-0.1280E+03	0.2519E+01	
11	0.5000E+00	0.	-0.2474E-03	0.8529E-04	0.4144E+02	-0.4011E-03	-0.2485E+04	-0.1379E+03	0.2714E+01	
12	0.5000E+00	0.	-0.2644E-03	0.9154E-04	0.4873E+02	-0.4287E-03	-0.2654E+04	-0.1473E+03	0.2899E+01	
13	0.5000E+00	0.	-0.2804E-03	0.9751E-04	0.5642E+02	-0.4547E-03	-0.2813E+04	-0.1562E+03	0.3073E+01	
14	0.5000E+00	0.	-0.2955E-03	0.1032E-03	0.6448E+02	-0.4792E-03	-0.2963E+04	-0.1645E+03	0.3237E+01	
15	0.5000E+00	0.	-0.3097E-03	0.1086E-03	0.7287E+02	-0.5023E-03	-0.3104E+04	-0.1723E+03	0.3391E+01	
16	0.5000E+00	0.	-0.3231E-03	0.1138E-03	0.8157E+02	-0.5240E-03	-0.3236E+04	-0.1796E+03	0.3535E+01	
17	0.5000E+00	0.	-0.3356E-03	0.1187E-03	0.9054E+02	-0.5443E-03	-0.3360E+04	-0.1865E+03	0.3670E+01	
18	0.5000E+00	0.	-0.3474E-03	0.1234E-03	0.9977E+02	-0.5634E-03	-0.3476E+04	-0.1929E+03	0.3797E+01	
19	0.5000E+00	0.	-0.3584E-03	0.1279E-03	0.1092E+03	-0.5814E-03	-0.3584E+04	-0.1990E+03	0.3915E+01	
20	0.5000E+00	0.	-0.3688E-03	0.1322E-03	0.1189E+03	-0.5982E-03	-0.3686E+04	-0.2046E+03	0.4026E+01	
21	0.5000E+00	0.	-0.3785E-03	0.1363E-03	0.1288E+03	-0.6140E-03	-0.3780E+04	-0.2099E+03	0.4130E+01	
22	0.5000E+00	0.	-0.3876E-03	0.1402E-03	0.1388E+03	-0.6289E-03	-0.3869E+04	-0.2148E+03	0.4227E+01	
23	0.5000E+00	0.	-0.3962E-03	0.1439E-03	0.1491E+03	-0.6428E-03	-0.3952E+04	-0.2194E+03	0.4318E+01	
24	0.5000E+00	0.	-0.4042E-03	0.1475E-03	0.1595E+03	-0.6558E-03	-0.4030E+04	-0.2237E+03	0.4403E+01	
25	0.5000E+00	0.	-0.4118E-03	0.1509E-03	0.1700E+03	-0.6681E-03	-0.4103E+04	-0.2277E+03	0.4482E+01	
26	0.5000E+00	0.	-0.4188E-03	0.1542E-03	0.1807E+03	-0.6796E-03	-0.4171E+04	-0.2315E+03	0.4556E+01	
27	0.5000E+00	0.	-0.4255E-03	0.1573E-03	0.1915E+03	-0.6905E-03	-0.4234E+04	-0.2350E+03	0.4626E+01	
28	0.5000E+00	0.	-0.4317E-03	0.1603E-03	0.2025E+03	-0.7006E-03	-0.4294E+04	-0.2384E+03	0.4691E+01	
29	0.5000E+00	0.	-0.4376E-03	0.1633E-03	0.2136E+03	-0.7102E-03	-0.4350E+04	-0.2414E+03	0.4752E+01	
30	0.5000E+00	0.	-0.4432E-03	0.1661E-03	0.2248E+03	-0.7192E-03	-0.4402E+04	-0.2443E+03	0.4809E+01	
31	0.5000E+00	0.	-0.4484E-03	0.1688E-03	0.2361E+03	-0.7277E-03	-0.4451E+04	-0.2471E+03	0.4862E+01	
32	0.5000E+00	0.	-0.4533E-03	0.1714E-03	0.2476E+03	-0.7357E-03	-0.4496E+04	-0.2496E+03	0.4912E+01	
33	0.5000E+00	0.	-0.4579E-03	0.1740E-03	0.2591E+03	-0.7433E-03	-0.4539E+04	-0.2520E+03	0.4959E+01	
34	0.5000E+00	0.	-0.4623E-03	0.1764E-03	0.2708E+03	-0.7504E-03	-0.4580E+04	-0.2542E+03	0.5003E+01	
35	0.5000E+00	0.	-0.4664E-03	0.1788E-03	0.2825E+03	-0.7571E-03	-0.4617E+04	-0.2563E+03	0.5044E+01	
36	0.5000E+00	0.	-0.4703E-03	0.1812E-03	0.2944E+03	-0.7635E-03	-0.4653E+04	-0.2583E+03	0.5083E+01	
37	0.5000E+00	0.	-0.4740E-03	0.1834E-03	0.3064E+03	-0.7695E-03	-0.4686E+04	-0.2601E+03	0.5119E+01	

TABLE 4.2-II. DESIGN NO. 1 (Continued)

38	0.5000E+00	0.	-0.4774E-03	0.1856E-03	0.3184E+03	-0.7752E-03	-0.4717E+04	-0.2618E+03	0.5153E+01
39	0.5000E+00	0.	-0.4807E-03	0.1878E-03	0.3306E+03	-0.7806E-03	-0.4746E+04	-0.2635E+03	0.5185E+01
40	0.5000E+00	0.	-0.4838E-03	0.1899E-03	0.3428E+03	-0.7857E-03	-0.4774E+04	-0.2650E+03	0.5215E+01
41	0.5000E+00	0.	-0.4868E-03	0.1920E-03	0.3552E+03	-0.7905E-03	-0.4799E+04	-0.2664E+03	0.5243E+01
42	0.5000E+00	0.	-0.4896E-03	0.1940E-03	0.3676E+03	-0.7951E-03	-0.4824E+04	-0.2678E+03	0.5270E+01
43	0.5000E+00	0.	-0.4923E-03	0.1960E-03	0.3802E+03	-0.7995E-03	-0.4847E+04	-0.2690E+03	0.5295E+01
44	0.5000E+00	0.	-0.4948E-03	0.1979E-03	0.3928E+03	-0.8037E-03	-0.4868E+04	-0.2702E+03	0.5318E+01
45	0.5000E+00	0.	-0.4972E-03	0.1999E-03	0.4055E+03	-0.8076E-03	-0.4888E+04	-0.2713E+03	0.5340E+01
46	0.5000E+00	0.	-0.4995E-03	0.2018E-03	0.4183E+03	-0.8114E-03	-0.4907E+04	-0.2724E+03	0.5361E+01
47	0.5000E+00	0.	-0.5017E-03	0.2036E-03	0.4313E+03	-0.8150E-03	-0.4925E+04	-0.2734E+03	0.5380E+01
48	0.5000E+00	0.	-0.5038E-03	0.2055E-03	0.4443E+03	-0.8184E-03	-0.4942E+04	-0.2743E+03	0.5399E+01
49	0.5000E+00	0.	-0.5058E-03	0.2073E-03	0.4573E+03	-0.8217E-03	-0.4958E+04	-0.2752E+03	0.5416E+01
50	0.5000E+00	0.	-0.5077E-03	0.2091E-03	0.4705E+03	-0.8249E-03	-0.4973E+04	-0.2760E+03	0.5432E+01
51	0.5000E+00	0.	-0.5095E-03	0.2108E-03	0.4838E+03	-0.8279E-03	-0.4987E+04	-0.2768E+03	0.5448E+01
52	0.5000E+00	0.	-0.5113E-03	0.2126E-03	0.4971E+03	-0.8308E-03	-0.5000E+04	-0.2775E+03	0.5462E+01
53	0.5000E+00	0.	-0.5130E-03	0.2143E-03	0.5106E+03	-0.8335E-03	-0.5012E+04	-0.2782E+03	0.5476E+01
54	0.5000E+00	0.	-0.5146E-03	0.2160E-03	0.5241E+03	-0.8362E-03	-0.5024E+04	-0.2789E+03	0.5489E+01
55	0.5000E+00	0.	-0.5161E-03	0.2178E-03	0.5377E+03	-0.8388E-03	-0.5035E+04	-0.2795E+03	0.5501E+01
56	0.5000E+00	0.	-0.5176E-03	0.2195E-03	0.5514E+03	-0.8412E-03	-0.5046E+04	-0.2801E+03	0.5512E+01
57	0.5000E+00	0.	-0.5190E-03	0.2211E-03	0.5652E+03	-0.8436E-03	-0.5055E+04	-0.2806E+03	0.5523E+01
58	0.5000E+00	0.	-0.5204E-03	0.2228E-03	0.5791E+03	-0.8459E-03	-0.5065E+04	-0.2811E+03	0.5533E+01
59	0.5000E+00	0.	-0.5217E-03	0.2245E-03	0.5931E+03	-0.8481E-03	-0.5074E+04	-0.2816E+03	0.5543E+01
60	0.5000E+00	0.	-0.5230E-03	0.2262E-03	0.6072E+03	-0.8502E-03	-0.5082E+04	-0.2821E+03	0.5552E+01
61	0.5000E+00	0.	-0.5242E-03	0.2278E-03	0.6213E+03	-0.8523E-03	-0.5090E+04	-0.2825E+03	0.5560E+01
62	0.5000E+00	0.	-0.5254E-03	0.2295E-03	0.6356E+03	-0.8543E-03	-0.5097E+04	-0.2829E+03	0.5568E+01
63	0.5000E+00	0.	-0.5266E-03	0.2311E-03	0.6499E+03	-0.8562E-03	-0.5104E+04	-0.2833E+03	0.5576E+01
64	0.5000E+00	0.	-0.5277E-03	0.2327E-03	0.6643E+03	-0.8581E-03	-0.5111E+04	-0.2837E+03	0.5583E+01
65	0.5000E+00	0.	-0.5288E-03	0.2344E-03	0.6788E+03	-0.8599E-03	-0.5117E+04	-0.2840E+03	0.5590E+01
66	0.5000E+00	0.	-0.5298E-03	0.2360E-03	0.6934E+03	-0.8617E-03	-0.5123E+04	-0.2844E+03	0.5596E+01
67	0.5000E+00	0.	-0.5309E-03	0.2377E-03	0.7080E+03	-0.8634E-03	-0.5128E+04	-0.2847E+03	0.5602E+01
68	0.5000E+00	0.	-0.5319E-03	0.2393E-03	0.7228E+03	-0.8651E-03	-0.5133E+04	-0.2850E+03	0.5608E+01
N	T	DELT	ESO	ESX	SSX	US	SSO	SSR	F1

J	TWJ	FJ	UWJ	QJ	STWJ	CJ	PJ
68	0.5000E+00	0.9978E-01	-0.3731E-03	0.5000E+00	0.5000E+00	0.2893E+01	8.6
67	0.4748E+00	0.1957E+00	-0.7275E-03	0.9748E+00	0.9748E+00	0.2876E+01	
66	0.4507E+00	0.2879E+00	-0.1064E-02	0.1425E+01	0.1425E+01	0.2859E+01	
65	0.4274E+00	0.3764E+00	-0.1383E-02	0.1853E+01	0.1853E+01	0.2842E+01	32.6
64	0.4051E+00	0.4615E+00	-0.1685E-02	0.2258E+01	0.2258E+01	0.2825E+01	
63	0.3837E+00	0.5432E+00	-0.1971E-02	0.2642E+01	0.2642E+01	0.2808E+01	
62	0.3631E+00	0.6216E+00	-0.2242E-02	0.3005E+01	0.3005E+01	0.2791E+01	
61	0.3434E+00	0.6969E+00	-0.2498E-02	0.3348E+01	0.3348E+01	0.2774E+01	
60	0.3245E+00	0.7691E+00	-0.2740E-02	0.3673E+01	0.3673E+01	0.2757E+01	66.6
59	0.3063E+00	0.8385E+00	-0.2968E-02	0.3979E+01	0.3979E+01	0.2740E+01	
58	0.2889E+00	0.9050E+00	-0.3184E-02	0.4268E+01	0.4268E+01	0.2723E+01	
57	0.2722E+00	0.9687E+00	-0.3387E-02	0.4540E+01	0.4540E+01	0.2706E+01	
56	0.2562E+00	0.1030E+01	-0.3577E-02	0.4796E+01	0.4796E+01	0.2689E+01	
55	0.2408E+00	0.1088E+01	-0.3757E-02	0.5037E+01	0.5037E+01	0.2672E+01	94.2
54	0.2262E+00	0.1145E+01	-0.3925E-02	0.5263E+01	0.5263E+01	0.2655E+01	
53	0.2121E+00	0.1198E+01	-0.4083E-02	0.5475E+01	0.5475E+01	0.2638E+01	
52	0.1986E+00	0.1250E+01	-0.4230E-02	0.5674E+01	0.5674E+01	0.2621E+01	
51	0.1858E+00	0.1299E+01	-0.4368E-02	0.5859E+01	0.5860E+01	0.2603E+01	
50	0.1735E+00	0.1347E+01	-0.4497E-02	0.6033E+01	0.6033E+01	0.2586E+01	116.6

TABLE 4.2-II. DESIGN NO. 1 (Continued)

49	0.1617E+00	0.1392E+01	-0.4617E-02	0.6195E+01	0.6195E+01	0.2569E+01	
48	0.1505E+00	0.1435E+01	-0.4728E-02	0.6345E+01	0.6345E+01	0.2552E+01	
47	0.1397E+00	0.1477E+01	-0.4831E-02	0.6485E+01	0.6485E+01	0.2535E+01	
46	0.1295E+00	0.1516E+01	-0.4926E-02	0.6614E+01	0.6615E+01	0.2518E+01	
45	0.1197E+00	0.1554E+01	-0.5013E-02	0.6734E+01	0.6734E+01	0.2501E+01	134.6
44	0.1104E+00	0.1591E+01	-0.5094E-02	0.6844E+01	0.6845E+01	0.2484E+01	
43	0.1015E+00	0.1625E+01	-0.5167E-02	0.6946E+01	0.6946E+01	0.2467E+01	
42	0.9302E-01	0.1659E+01	-0.5234E-02	0.7038E+01	0.7039E+01	0.2450E+01	
41	0.8498E-01	0.1690E+01	-0.5294E-02	0.7123E+01	0.7124E+01	0.2433E+01	
40	0.7734E-01	0.1721E+01	-0.5348E-02	0.7201E+01	0.7201E+01	0.2416E+01	149.0
39	0.7009E-01	0.1750E+01	-0.5397E-02	0.7271E+01	0.7271E+01	0.2399E+01	
38	0.6322E-01	0.1778E+01	-0.5439E-02	0.7334E+01	0.7335E+01	0.2382E+01	
37	0.5672E-01	0.1804E+01	-0.5476E-02	0.7391E+01	0.7391E+01	0.2365E+01	
36	0.5059E-01	0.1830E+01	-0.5508E-02	0.7441E+01	0.7442E+01	0.2348E+01	
35	0.4482E-01	0.1854E+01	-0.5534E-02	0.7486E+01	0.7487E+01	0.2331E+01	160.6
34	0.3940E-01	0.1878E+01	-0.5556E-02	0.7525E+01	0.7526E+01	0.2314E+01	
33	0.3433E-01	0.1900E+01	-0.5572E-02	0.7560E+01	0.7561E+01	0.2297E+01	
32	0.2961E-01	0.1922E+01	-0.5584E-02	0.7589E+01	0.7590E+01	0.2280E+01	
31	0.2524E-01	0.1943E+01	-0.5591E-02	0.7614E+01	0.7615E+01	0.2263E+01	
30	0.2122E-01	0.1963E+01	-0.5593E-02	0.7635E+01	0.7637E+01	0.2246E+01	170.0
29	0.1756E-01	0.1983E+01	-0.5590E-02	0.7653E+01	0.7654E+01	0.2229E+01	
28	0.1427E-01	0.2002E+01	-0.5582E-02	0.7667E+01	0.7668E+01	0.2211E+01	
27	0.1137E-01	0.2020E+01	-0.5570E-02	0.7678E+01	0.7680E+01	0.2194E+01	
26	0.0864E-02	0.2038E+01	-0.5552E-02	0.7687E+01	0.7689E+01	0.2177E+01	
25	0.6780E-02	0.2056E+01	-0.5530E-02	0.7694E+01	0.7695E+01	0.2160E+01	178.1
24	0.5145E-02	0.2074E+01	-0.5501E-02	0.7699E+01	0.7701E+01	0.2143E+01	
23	0.3992E-02	0.2092E+01	-0.5467E-02	0.7703E+01	0.7705E+01	0.2126E+01	
22	0.3364E-02	0.2109E+01	-0.5427E-02	0.7706E+01	0.7708E+01	0.2109E+01	
21	0.3311E-02	0.2127E+01	-0.5380E-02	0.7709E+01	0.7711E+01	0.2092E+01	
20	0.3892E-02	0.2146E+01	-0.5327E-02	0.7713E+01	0.7715E+01	0.2075E+01	185.8
19	0.5179E-02	0.2165E+01	-0.5265E-02	0.7718E+01	0.7720E+01	0.2058E+01	
18	0.7257E-02	0.2185E+01	-0.5194E-02	0.7726E+01	0.7728E+01	0.2041E+01	
17	0.1023E-01	0.2207E+01	-0.5115E-02	0.7736E+01	0.7738E+01	0.2024E+01	
16	0.1421E-01	0.2229E+01	-0.5024E-02	0.7750E+01	0.7752E+01	0.2007E+01	
15	0.1934E-01	0.2254E+01	-0.4921E-02	0.7769E+01	0.7771E+01	0.1990E+01	195.2
14	0.2578E-01	0.2281E+01	-0.4805E-02	0.7795E+01	0.7797E+01	0.1973E+01	
13	0.3373E-01	0.2311E+01	-0.4674E-02	0.7829E+01	0.7831E+01	0.1956E+01	
12	0.4340E-01	0.2344E+01	-0.4526E-02	0.7872E+01	0.7874E+01	0.1939E+01	
11	0.5505E-01	0.2381E+01	-0.4358E-02	0.7927E+01	0.7929E+01	0.1922E+01	
10	0.6896E-01	0.2424E+01	-0.4169E-02	0.7996E+01	0.7998E+01	0.1905E+01	209.9
9	0.8548E-01	0.2472E+01	-0.3954E-02	0.8081E+01	0.8084E+01	0.1888E+01	
8	0.1050E+00	0.2527E+01	-0.3712E-02	0.8186E+01	0.8189E+01	0.1871E+01	
7	0.1279E+00	0.2590E+01	-0.3439E-02	0.8314E+01	0.8317E+01	0.1854E+01	
6	0.1547E+00	0.2662E+01	-0.3131E-02	0.8469E+01	0.8471E+01	0.1837E+01	
5	0.1859E+00	0.2746E+01	-0.2783E-02	0.8655E+01	0.8657E+01	0.1819E+01	237.8
4	0.2222E+00	0.2843E+01	-0.2393E-02	0.8877E+01	0.8880E+01	0.1802E+01	
3	0.2641E+00	0.2956E+01	-0.1954E-02	0.9141E+01	0.9144E+01	0.1785E+01	
2	0.3124E+00	0.3086E+01	-0.1463E-02	0.9453E+01	0.9456E+01	0.1768E+01	
1	0.3678E+00	0.3238E+01	-0.8651E-03	0.9814E+01	0.9824E+01	0.1750E+01	280.4
J	TWJ	FJ	UWJ	QJ	STWJ	CJ	

TABLE 4.2-III. DESIGN NO. 2

SPOOL			WIRE-PACK			BOBBIN			DATE 16 JAN 79	
ES=	0.1010E+08	B= 0.1750E+01	EC=	0.1050E+08	DDW=	0.	S=	0.2250E+00		
VS=	0.3300E+00	A= 0.1650E+01	D=	0.4150E-02	K=	0.1280E+05	DEL=	0.9266E-02		
T=	0.1000E+00	DS= 0.1070E-01	DD=	0.	E=	0.1432E+07	N=	33		
DT=	0.	DDS= 0.	DW=	0.1070E-01	ALFA=	0.9282E+01				
N	T	DELT	ESO	ESX	SSX	US	SSO	SSR	F1	
1	0.2800E+00	0.	-0.2667E-04	0.8801E-05	-0.3779E-06	-0.4323E-04	-0.2694E+03	-0.1495E+02	0.1600E+00	
2	0.2800E+00	0.	-0.5297E-04	0.1752E-04	0.5084E+00	-0.8585E-04	-0.5348E+03	-0.2969E+02	0.3177E+00	
3	0.2800E+00	0.	-0.7887E-04	0.2616E-04	0.1400E+01	-0.1278E-03	-0.7961E+03	-0.4419E+02	0.4728E+00	
4	0.2800E+00	0.	-0.1043E-03	0.3468E-04	0.2906E+01	-0.1691E-03	-0.1053E+04	-0.5843E+02	0.6252E+00	
5	0.2800E+00	0.	-0.1293E-03	0.4309E-04	0.4775E+01	-0.2096E-03	-0.1304E+04	-0.7240E+02	0.7747E+00	
6	0.2800E+00	0.	-0.1537E-03	0.5136E-04	0.7074E+01	-0.2492E-03	-0.1550E+04	-0.8606E+02	0.9289E+00	
7	0.2800E+00	0.	-0.1776E-03	0.5948E-04	0.9790E+01	-0.2880E-03	-0.1791E+04	-0.9941E+02	0.1064E+01	
8	0.2800E+00	0.	-0.2010E-03	0.6746E-04	0.1291E+02	-0.3258E-03	-0.2026E+04	-0.1124E+03	0.1203E+01	
9	0.2800E+00	0.	-0.2237E-03	0.7527E-04	0.1642E+02	-0.3627E-03	-0.2254E+04	-0.1251E+03	0.1339E+01	
10	0.2800E+00	0.	-0.2458E-03	0.8292E-04	0.2030E+02	-0.3985E-03	-0.2476E+04	-0.1375E+03	0.1471E+01	
11	0.2800E+00	0.	-0.2673E-03	0.9039E-04	0.2453E+02	-0.4334E-03	-0.2692E+04	-0.1494E+03	0.1599E+01	
12	0.2800E+00	0.	-0.2882E-03	0.9769E-04	0.2911E+02	-0.4673E-03	-0.2902E+04	-0.1611E+03	0.1723E+01	
13	0.2800E+00	0.	-0.3085E-03	0.1048E-03	0.3402E+02	-0.5002E-03	-0.3105E+04	-0.1723E+03	0.1844E+01	
14	0.2800E+00	0.	-0.3281E-03	0.1117E-03	0.3924E+02	-0.5320E-03	-0.3301E+04	-0.1832E+03	0.1961E+01	
15	0.2800E+00	0.	-0.3471E-03	0.1185E-03	0.4476E+02	-0.5628E-03	-0.3491E+04	-0.1938E+03	0.2074E+01	
16	0.2800E+00	0.	-0.3655E-03	0.1251E-03	0.5056E+02	-0.5926E-03	-0.3675E+04	-0.2040E+03	0.2183E+01	
17	0.2800E+00	0.	-0.3833E-03	0.1315E-03	0.5663E+02	-0.6215E-03	-0.3853E+04	-0.2139E+03	0.2288E+01	
18	0.2800E+00	0.	-0.4005E-03	0.1377E-03	0.6295E+02	-0.6493E-03	-0.4024E+04	-0.2234E+03	0.2390E+01	
19	0.2800E+00	0.	-0.4170E-03	0.1438E-03	0.6952E+02	-0.6762E-03	-0.4189E+04	-0.2325E+03	0.2488E+01	
20	0.2800E+00	0.	-0.4330E-03	0.1496E-03	0.7632E+02	-0.7022E-03	-0.4348E+04	-0.2414E+03	0.2583E+01	
21	0.2800E+00	0.	-0.4485E-03	0.1553E-03	0.8335E+02	-0.7272E-03	-0.4502E+04	-0.2499E+03	0.2674E+01	
22	0.2800E+00	0.	-0.4633E-03	0.1609E-03	0.9058E+02	-0.7513E-03	-0.4650E+04	-0.2581E+03	0.2762E+01	
23	0.2800E+00	0.	-0.4777E-03	0.1663E-03	0.9800E+02	-0.7746E-03	-0.4792E+04	-0.2660E+03	0.2846E+01	
24	0.2800E+00	0.	-0.4915E-03	0.1715E-03	0.1056E+03	-0.7970E-03	-0.4929E+04	-0.2736E+03	0.2928E+01	
25	0.2800E+00	0.	-0.5040E-03	0.1766E-03	0.1134E+03	-0.8186E-03	-0.5061E+04	-0.2809E+03	0.3006E+01	
26	0.2800E+00	0.	-0.5176E-03	0.1815E-03	0.1214E+03	-0.8394E-03	-0.5188E+04	-0.2880E+03	0.3081E+01	
27	0.2800E+00	0.	-0.5299E-03	0.1863E-03	0.1295E+03	-0.8595E-03	-0.5310E+04	-0.2947E+03	0.3154E+01	
28	0.2800E+00	0.	-0.5418E-03	0.1910E-03	0.1378E+03	-0.8788E-03	-0.5427E+04	-0.3013E+03	0.3223E+01	
29	0.2800E+00	0.	-0.5533E-03	0.1955E-03	0.1462E+03	-0.8973E-03	-0.5540E+04	-0.3075E+03	0.3290E+01	
30	0.2800E+00	0.	-0.5643E-03	0.1999E-03	0.1548E+03	-0.9152E-03	-0.5648E+04	-0.3135E+03	0.3355E+01	
31	0.2800E+00	0.	-0.5749E-03	0.2041E-03	0.1635E+03	-0.9324E-03	-0.5752E+04	-0.3193E+03	0.3417E+01	
32	0.2800E+00	0.	-0.5851E-03	0.2083E-03	0.1723E+03	-0.9490E-03	-0.5852E+04	-0.3249E+03	0.3476E+01	
33	0.2800E+00	0.	-0.5949E-03	0.2123E-03	0.1813E+03	-0.9649E-03	-0.5948E+04	-0.3302E+03	0.3533E+01	
N	T	DELT	ESO	ESX	SSX	US	SSO	SSR	F1	

TABLE 4.2-III. DESIGN NO. 2 (Continued)

J	TWJ	FJ	UWJ	QJ	STWJ	CJ	PJ
33	0.2800E+00	0.7896E-01	-0.1594E-03	0.2800E+00	0.2800E+00	0.2047E+01	12.8
32	0.2692E+00	0.1556E+00	-0.3108E-03	0.5492E+00	0.5492E+00	0.2038E+01	
31	0.2688E+00	0.2299E+00	-0.4545E-03	0.8079E+00	0.8079E+00	0.2029E+01	
30	0.2488E+00	0.3021E+00	-0.5906E-03	0.1057E+01	0.1057E+01	0.2019E+01	48.9
29	0.2393E+00	0.3723E+00	-0.7191E-03	0.1296E+01	0.1296E+01	0.2010E+01	
28	0.2303E+00	0.4404E+00	-0.8400E-03	0.1526E+01	0.1526E+01	0.2001E+01	
27	0.2216E+00	0.5067E+00	-0.9536E-03	0.1748E+01	0.1748E+01	0.1992E+01	
26	0.2135E+00	0.5712E+00	-0.1060E-02	0.1961E+01	0.1961E+01	0.1982E+01	
25	0.2057E+00	0.6341E+00	-0.1159E-02	0.2167E+01	0.2167E+01	0.1973E+01	102.6
24	0.1985E+00	0.6955E+00	-0.1250E-02	0.2366E+01	0.2366E+01	0.1964E+01	
23	0.1916E+00	0.7554E+00	-0.1334E-02	0.2557E+01	0.2557E+01	0.1955E+01	
22	0.1853E+00	0.8139E+00	-0.1411E-02	0.2742E+01	0.2743E+01	0.1945E+01	
21	0.1794E+00	0.8713E+00	-0.1481E-02	0.2922E+01	0.2922E+01	0.1936E+01	
20	0.1740E+00	0.9277E+00	-0.1542E-02	0.3096E+01	0.3096E+01	0.1927E+01	150.2
19	0.1691E+00	0.9831E+00	-0.1597E-02	0.3265E+01	0.3265E+01	0.1918E+01	
18	0.1647E+00	0.1038E+01	-0.1643E-02	0.3430E+01	0.3430E+01	0.1908E+01	
17	0.1609E+00	0.1092E+01	-0.1681E-02	0.3591E+01	0.3591E+01	0.1899E+01	
16	0.1576E+00	0.1145E+01	-0.1712E-02	0.3748E+01	0.3748E+01	0.1890E+01	193.9
15	0.1549E+00	0.1198E+01	-0.1734E-02	0.3903E+01	0.3903E+01	0.1880E+01	
14	0.1520E+00	0.1251E+01	-0.1747E-02	0.4056E+01	0.4056E+01	0.1871E+01	
13	0.1513E+00	0.1305E+01	-0.1752E-02	0.4207E+01	0.4207E+01	0.1862E+01	
12	0.1505E+00	0.1358E+01	-0.1748E-02	0.4358E+01	0.4358E+01	0.1853E+01	
11	0.1504E+00	0.1412E+01	-0.1734E-02	0.4508E+01	0.4508E+01	0.1843E+01	
10	0.1510E+00	0.1467E+01	-0.1710E-02	0.4659E+01	0.4659E+01	0.1834E+01	237.5
9	0.1524E+00	0.1522E+01	-0.1676E-02	0.4811E+01	0.4811E+01	0.1825E+01	
8	0.1546E+00	0.1579E+01	-0.1631E-02	0.4966E+01	0.4966E+01	0.1816E+01	
7	0.1576E+00	0.1638E+01	-0.1576E-02	0.5124E+01	0.5124E+01	0.1806E+01	
6	0.1616E+00	0.1698E+01	-0.1508E-02	0.5235E+01	0.5235E+01	0.1797E+01	
5	0.1666E+00	0.1761E+01	-0.1429E-02	0.5452E+01	0.5452E+01	0.1788E+01	285.1
4	0.1725E+00	0.1826E+01	-0.1337E-02	0.5624E+01	0.5624E+01	0.1779E+01	295.6
3	0.1796E+00	0.1894E+01	-0.1231E-02	0.5804E+01	0.5804E+01	0.1769E+01	
2	0.1878E+00	0.1966E+01	-0.1112E-02	0.5992E+01	0.5992E+01	0.1760E+01	
1	0.1972E+00	0.2040E+01	-0.9649E-03	0.6183E+01	0.6189E+01	0.1750E+01	330.2
J	TWJ	FJ	UWJ	QJ	STWJ	CJ	

TABLE 4.2-IV. DESIGN NO. 3

SPOOL				WIRE-PACK				BOBBIN				DATE 02/02/79			
ES=	0.1010E+08	B=	0.3900E+01	EC=	0.1050E+08	DDW=	0.	S=	0.1352E+01						
VS=	0.3300E+00	A=	0.3850E+01	D=	0.5000E-02	K=	0.1280E+05	DELIC=	0.8660E-02						
T=	0.5000E-01	DS=	0.1000E-01	DD=	0.	E=	0.2381E+07	N=	35						
DT=	0.	DDS=	0.	DW=	0.1000E-01	ALFA=	0.1197E+02								
N	T	DELT	ESO	ESX	SSX	US	SSO	SSR	F1						
1	0.2500E+00	0.	-0.4982E-04	0.1644E-04	0.9441E-07	-0.1910E-03	-0.5032E+03	-0.6410E+01	0.6410E-01						
2	0.2500E+00	0.	-0.9757E-04	0.3223E-04	0.3928E+00	-0.3741E-03	-0.9853E+03	-0.1255E+02	0.1255E+00						
3	0.2500E+00	0.	-0.1435E-03	0.4745E-04	0.1136E+01	-0.5502E-03	-0.1449E+04	-0.1846E+02	0.1846E+00						
4	0.2500E+00	0.	-0.1877E-03	0.6214E-04	0.2217E+01	-0.7197E-03	-0.1895E+04	-0.2414E+02	0.2414E+00						
5	0.2500E+00	0.	-0.2303E-03	0.7633E-04	0.3624E+01	-0.8831E-03	-0.2325E+04	-0.2962E+02	0.2962E+00						
6	0.2500E+00	0.	-0.2714E-03	0.9005E-04	0.5346E+01	-0.1041E-02	-0.2740E+04	-0.3490E+02	0.3490E+00						
7	0.2500E+00	0.	-0.3111E-03	0.1033E-03	0.7374E+01	-0.1193E-02	-0.3140E+04	-0.3999E+02	0.3999E+00						
8	0.2500E+00	0.	-0.3494E-03	0.1162E-03	0.9697E+01	-0.1340E-02	-0.3526E+04	-0.4491E+02	0.4491E+00						
9	0.2500E+00	0.	-0.3864E-03	0.1286E-03	0.1231E+02	-0.1481E-02	-0.3899E+04	-0.4966E+02	0.4966E+00						
10	0.2500E+00	0.	-0.4222E-03	0.1407E-03	0.1520E+02	-0.1619E-02	-0.4259E+04	-0.5425E+02	0.5425E+00						
11	0.2500E+00	0.	-0.4568E-03	0.1524E-03	0.1836E+02	-0.1751E-02	-0.4607E+04	-0.5869E+02	0.5869E+00						
12	0.2500E+00	0.	-0.4903E-03	0.1637E-03	0.2178E+02	-0.1880E-02	-0.4944E+04	-0.6298E+02	0.6298E+00						
13	0.2500E+00	0.	-0.5227E-03	0.1747E-03	0.2546E+02	-0.2004E-02	-0.5271E+04	-0.6714E+02	0.6714E+00						
14	0.2500E+00	0.	-0.5541E-03	0.1854E-03	0.2939E+02	-0.2124E-02	-0.5586E+04	-0.7116E+02	0.7116E+00						
15	0.2500E+00	0.	-0.5845E-03	0.1958E-03	0.3356E+02	-0.2241E-02	-0.5892E+04	-0.7506E+02	0.7506E+00						
16	0.2500E+00	0.	-0.6140E-03	0.2060E-03	0.3797E+02	-0.2354E-02	-0.6189E+04	-0.7884E+02	0.7884E+00						
17	0.2500E+00	0.	-0.6426E-03	0.2158E-03	0.4262E+02	-0.2464E-02	-0.6476E+04	-0.8250E+02	0.8250E+00						
18	0.2500E+00	0.	-0.6703E-03	0.2254E-03	0.4749E+02	-0.2570E-02	-0.6755E+04	-0.8604E+02	0.8604E+00						
19	0.2500E+00	0.	-0.6973E-03	0.2347E-03	0.5258E+02	-0.2673E-02	-0.7025E+04	-0.8949E+02	0.8949E+00						
20	0.2500E+00	0.	-0.7234E-03	0.2438E-03	0.5788E+02	-0.2774E-02	-0.7287E+04	-0.9283E+02	0.9283E+00						
21	0.2500E+00	0.	-0.7488E-03	0.2527E-03	0.6340E+02	-0.2871E-02	-0.7542E+04	-0.9607E+02	0.9607E+00						
22	0.2500E+00	0.	-0.7734E-03	0.2613E-03	0.6912E+02	-0.2965E-02	-0.7789E+04	-0.9922E+02	0.9922E+00						
23	0.2500E+00	0.	-0.7974E-03	0.2698E-03	0.7505E+02	-0.3057E-02	-0.8029E+04	-0.1023E+03	0.1023E+01						
24	0.2500E+00	0.	-0.8206E-03	0.2780E-03	0.8118E+02	-0.3146E-02	-0.8262E+04	-0.1052E+03	0.1052E+01						
25	0.2500E+00	0.	-0.8433E-03	0.2860E-03	0.8749E+02	-0.3233E-02	-0.8488E+04	-0.1081E+03	0.1081E+01						
26	0.2500E+00	0.	-0.8652E-03	0.2938E-03	0.9400E+02	-0.3318E-02	-0.8708E+04	-0.1109E+03	0.1109E+01						
27	0.2500E+00	0.	-0.8866E-03	0.3015E-03	0.1007E+03	-0.3400E-02	-0.8922E+04	-0.1136E+03	0.1136E+01						
28	0.2500E+00	0.	-0.9074E-03	0.3089E-03	0.1076E+03	-0.3479E-02	-0.9130E+04	-0.1163E+03	0.1163E+01						
29	0.2500E+00	0.	-0.9277E-03	0.3162E-03	0.1146E+03	-0.3557E-02	-0.9332E+04	-0.1189E+03	0.1189E+01						
30	0.2500E+00	0.	-0.9474E-03	0.3234E-03	0.1219E+03	-0.3632E-02	-0.9528E+04	-0.1214E+03	0.1214E+01						
31	0.2500E+00	0.	-0.9665E-03	0.3304E-03	0.1292E+03	-0.3706E-02	-0.9719E+04	-0.1238E+03	0.1238E+01						
32	0.2500E+00	0.	-0.9852E-03	0.3372E-03	0.1368E+03	-0.3777E-02	-0.9905E+04	-0.1262E+03	0.1262E+01						
33	0.2500E+00	0.	-0.1003E-02	0.3439E-03	0.1445E+03	-0.3847E-02	-0.1009E+05	-0.1285E+03	0.1285E+01						
34	0.2500E+00	0.	-0.1021E-02	0.3504E-03	0.1524E+03	-0.3915E-02	-0.1026E+05	-0.1307E+03	0.1307E+01						
35	0.2500E+00	0.	-0.1038E-02	0.3568E-03	0.1605E+03	-0.3981E-02	-0.1043E+05	-0.1329E+03	0.1329E+01						
N	T	DELT	ESO	ESX	SSX	US	SSO	SSR	F1						

TABLE 4.2-IV. DESIGN NO. 3 (Continued)

J	TWJ	FJ	UWJ	QJ	STWJ	CJ	PJ
35	0.2500E+00	0.3441E-01	-0.1358E-03	0.2500E+00	0.2500E+00	0.4195E+01	6.0
34	0.2434E+00	0.6804E-01	-0.2690E-03	0.4934E+00	0.4934E+00	0.4186E+01	
33	0.2369E+00	0.1009E+00	-0.3997E-03	0.7303E+00	0.7303E+00	0.4178E+01	
32	0.2305E+00	0.1330E+00	-0.5281E-03	0.9608E+00	0.9608E+00	0.4169E+01	
31	0.2242E+00	0.1644E+00	-0.6541E-03	0.1185E+01	0.1185E+01	0.4160E+01	
30	0.2179E+00	0.1951E+00	-0.7779E-03	0.1403E+01	0.1403E+01	0.4152E+01	33.8
29	0.2118E+00	0.2250E+00	-0.8997E-03	0.1615E+01	0.1615E+01	0.4143E+01	
28	0.2057E+00	0.2542E+00	-0.1019E-02	0.1820E+01	0.1820E+01	0.4134E+01	
27	0.1997E+00	0.2827E+00	-0.1137E-02	0.2020E+01	0.2020E+01	0.4126E+01	
26	0.1937E+00	0.3104E+00	-0.1253E-02	0.2214E+01	0.2214E+01	0.4117E+01	
25	0.1879E+00	0.3375E+00	-0.1368E-02	0.2402E+01	0.2402E+01	0.4109E+01	58.5
24	0.1821E+00	0.3638E+00	-0.1481E-02	0.2584E+01	0.2584E+01	0.4100E+01	
23	0.1763E+00	0.3895E+00	-0.1592E-02	0.2760E+01	0.2760E+01	0.4091E+01	
22	0.1706E+00	0.4144E+00	-0.1702E-02	0.2930E+01	0.2931E+01	0.4083E+01	
21	0.1649E+00	0.4387E+00	-0.1811E-02	0.3095E+01	0.3095E+01	0.4074E+01	
20	0.1592E+00	0.4622E+00	-0.1919E-02	0.3255E+01	0.3255E+01	0.4065E+01	80.1
19	0.1536E+00	0.4851E+00	-0.2026E-02	0.3408E+01	0.3408E+01	0.4057E+01	
18	0.1480E+00	0.5072E+00	-0.2132E-02	0.3556E+01	0.3556E+01	0.4048E+01	
17	0.1425E+00	0.5287E+00	-0.2237E-02	0.3699E+01	0.3699E+01	0.4039E+01	
16	0.1369E+00	0.5494E+00	-0.2342E-02	0.3836E+01	0.3836E+01	0.4031E+01	
15	0.1313E+00	0.5695E+00	-0.2447E-02	0.3967E+01	0.3967E+01	0.4022E+01	98.6
14	0.1258E+00	0.5888E+00	-0.2551E-02	0.4093E+01	0.4093E+01	0.4013E+01	
13	0.1202E+00	0.6074E+00	-0.2656E-02	0.4213E+01	0.4213E+01	0.4005E+01	
12	0.1146E+00	0.6253E+00	-0.2760E-02	0.4327E+01	0.4327E+01	0.3996E+01	
11	0.1089E+00	0.6424E+00	-0.2865E-02	0.4436E+01	0.4436E+01	0.3987E+01	
10	0.1032E+00	0.6588E+00	-0.2970E-02	0.4540E+01	0.4540E+01	0.3979E+01	114.1
9	0.9746E-01	0.6744E+00	-0.3077E-02	0.4637E+01	0.4637E+01	0.3970E+01	
8	0.9164E-01	0.6892E+00	-0.3184E-02	0.4729E+01	0.4729E+01	0.3961E+01	
7	0.8574E-01	0.7032E+00	-0.3292E-02	0.4814E+01	0.4814E+01	0.3953E+01	
6	0.7975E-01	0.7164E+00	-0.3402E-02	0.4894E+01	0.4894E+01	0.3944E+01	
5	0.7366E-01	0.7288E+00	-0.3514E-02	0.4968E+01	0.4968E+01	0.3935E+01	126.2
4	0.6743E-01	0.7403E+00	-0.3628E-02	0.5035E+01	0.5035E+01	0.3927E+01	
3	0.6107E-01	0.7510E+00	-0.3744E-02	0.5096E+01	0.5096E+01	0.3918E+01	
2	0.5455E-01	0.7607E+00	-0.3863E-02	0.5151E+01	0.5151E+01	0.3909E+01	132.9
1	0.4785E-01	0.7673E+00	-0.3981E-02	0.5183E+01	0.5199E+01	0.3900E+01	
J	TWJ	FJ	UWJ	QJ	STWJ	CJ	

TABLE 4.2-V. DESIGN NO. 5

SPOOL			WIRE-PACK			BOBBIN			DATE 03/07/79	
ES=	0.1010E+00	B= 0.2000E+01	EC=	0.1050E+00	DDW= 0.	S=	0.1320E+00			
VS=	0.3300E+00	A= 0.1900E+01	D=	0.5000E-02	K= 0.4500E+04	DEL=	0.1299E-01			
T=	0.1000E+00	DS= 0.1500E-01	DD=	0.	E= 0.1050E+07	N=	70			
DT=	0.	DDS= 0.	DW=	0.1500E-01	ALFA= 0.1345E+02					
N	T	DELT	ESO	ESX	SSX	US	SSO	SSR	F1	
1	0.2500E+00	0.	-0.1692E-04	0.5585E-05	-0.1810E-06	-0.3165E-04	-0.1709E+03	-0.8333E+01	0.1250E+00	
2	0.2500E+00	0.	-0.3356E-04	0.1111E-04	0.3948E+00	-0.6276E-04	-0.3388E+03	-0.1652E+02	0.2477E+00	
3	0.2500E+00	0.	-0.4980E-04	0.1654E-04	0.1146E+01	-0.9315E-04	-0.5026E+03	-0.2450E+02	0.3675E+00	
4	0.2500E+00	0.	-0.6556E-04	0.2183E-04	0.2238E+01	-0.1226E-03	-0.6615E+03	-0.3225E+02	0.4837E+00	
5	0.2500E+00	0.	-0.8077E-04	0.2698E-04	0.3654E+01	-0.1511E-03	-0.8146E+03	-0.3971E+02	0.5957E+00	
6	0.2500E+00	0.	-0.9536E-04	0.3194E-04	0.5374E+01	-0.1784E-03	-0.9614E+03	-0.4687E+02	0.7030E+00	
7	0.2500E+00	0.	-0.1093E-03	0.3672E-04	0.7376E+01	-0.2044E-03	-0.1101E+04	-0.5369E+02	0.8054E+00	
8	0.2500E+00	0.	-0.1225E-03	0.4129E-04	0.9638E+01	-0.2292E-03	-0.1234E+04	-0.6018E+02	0.9027E+00	
9	0.2500E+00	0.	-0.1351E-03	0.4565E-04	0.1214E+02	-0.2527E-03	-0.1360E+04	-0.6631E+02	0.9947E+00	
10	0.2500E+00	0.	-0.1469E-03	0.4979E-04	0.1486E+02	-0.2748E-03	-0.1479E+04	-0.7210E+02	0.1081E+01	
11	0.2500E+00	0.	-0.1581E-03	0.5373E-04	0.1777E+02	-0.2957E-03	-0.1591E+04	-0.7754E+02	0.1163E+01	
12	0.2500E+00	0.	-0.1685E-03	0.5746E-04	0.2086E+02	-0.3153E-03	-0.1695E+04	-0.8264E+02	0.1240E+01	
13	0.2500E+00	0.	-0.1783E-03	0.6098E-04	0.2412E+02	-0.3337E-03	-0.1793E+04	-0.8742E+02	0.1311E+01	
14	0.2500E+00	0.	-0.1875E-03	0.6431E-04	0.2752E+02	-0.3508E-03	-0.1885E+04	-0.9189E+02	0.1378E+01	
15	0.2500E+00	0.	-0.1961E-03	0.6745E-04	0.3105E+02	-0.3669E-03	-0.1970E+04	-0.9605E+02	0.1441E+01	
16	0.2500E+00	0.	-0.2041E-03	0.7041E-04	0.3469E+02	-0.3819E-03	-0.2050E+04	-0.9993E+02	0.1499E+01	
17	0.2500E+00	0.	-0.2116E-03	0.7321E-04	0.3845E+02	-0.3959E-03	-0.2124E+04	-0.1036E+03	0.1553E+01	
18	0.2500E+00	0.	-0.2185E-03	0.7584E-04	0.4230E+02	-0.4089E-03	-0.2193E+04	-0.1069E+03	0.1604E+01	
19	0.2500E+00	0.	-0.2250E-03	0.7833E-04	0.4623E+02	-0.4210E-03	-0.2257E+04	-0.1100E+03	0.1651E+01	
20	0.2500E+00	0.	-0.2310E-03	0.8068E-04	0.5025E+02	-0.4323E-03	-0.2317E+04	-0.1130E+03	0.1694E+01	
21	0.2500E+00	0.	-0.2367E-03	0.8289E-04	0.5434E+02	-0.4429E-03	-0.2372E+04	-0.1157E+03	0.1735E+01	
22	0.2500E+00	0.	-0.2419E-03	0.8499E-04	0.5850E+02	-0.4527E-03	-0.2424E+04	-0.1182E+03	0.1772E+01	
23	0.2500E+00	0.	-0.2468E-03	0.8697E-04	0.6272E+02	-0.4618E-03	-0.2472E+04	-0.1205E+03	0.1807E+01	
24	0.2500E+00	0.	-0.2513E-03	0.8884E-04	0.6700E+02	-0.4703E-03	-0.2516E+04	-0.1227E+03	0.1840E+01	
25	0.2500E+00	0.	-0.2555E-03	0.9062E-04	0.7133E+02	-0.4782E-03	-0.2557E+04	-0.1247E+03	0.1870E+01	
26	0.2500E+00	0.	-0.2595E-03	0.9231E-04	0.7572E+02	-0.4856E-03	-0.2596E+04	-0.1265E+03	0.1898E+01	
27	0.2500E+00	0.	-0.2631E-03	0.9391E-04	0.8014E+02	-0.4925E-03	-0.2631E+04	-0.1283E+03	0.1924E+01	
28	0.2500E+00	0.	-0.2666E-03	0.9543E-04	0.8462E+02	-0.4989E-03	-0.2664E+04	-0.1299E+03	0.1948E+01	
29	0.2500E+00	0.	-0.2698E-03	0.9688E-04	0.8913E+02	-0.5049E-03	-0.2695E+04	-0.1314E+03	0.1971E+01	
30	0.2500E+00	0.	-0.2727E-03	0.9827E-04	0.9369E+02	-0.5105E-03	-0.2724E+04	-0.1328E+03	0.1992E+01	
31	0.2500E+00	0.	-0.2755E-03	0.9959E-04	0.9828E+02	-0.5157E-03	-0.2750E+04	-0.1341E+03	0.2011E+01	
32	0.2500E+00	0.	-0.2781E-03	0.1009E-03	0.1029E+03	-0.5206E-03	-0.2775E+04	-0.1353E+03	0.2029E+01	
33	0.2500E+00	0.	-0.2805E-03	0.1021E-03	0.1076E+03	-0.5251E-03	-0.2798E+04	-0.1364E+03	0.2046E+01	
34	0.2500E+00	0.	-0.2828E-03	0.1032E-03	0.1123E+03	-0.5294E-03	-0.2819E+04	-0.1374E+03	0.2062E+01	
35	0.2500E+00	0.	-0.2849E-03	0.1043E-03	0.1170E+03	-0.5334E-03	-0.2839E+04	-0.1384E+03	0.2076E+01	
36	0.2500E+00	0.	-0.2869E-03	0.1054E-03	0.1218E+03	-0.5371E-03	-0.2858E+04	-0.1393E+03	0.2090E+01	
37	0.2500E+00	0.	-0.2888E-03	0.1065E-03	0.1266E+03	-0.5406E-03	-0.2875E+04	-0.1401E+03	0.2102E+01	
38	0.2500E+00	0.	-0.2905E-03	0.1075E-03	0.1314E+03	-0.5439E-03	-0.2891E+04	-0.1409E+03	0.2114E+01	
39	0.2500E+00	0.	-0.2922E-03	0.1084E-03	0.1363E+03	-0.5470E-03	-0.2906E+04	-0.1417E+03	0.2125E+01	
40	0.2500E+00	0.	-0.2937E-03	0.1094E-03	0.1412E+03	-0.5499E-03	-0.2920E+04	-0.1423E+03	0.2135E+01	
41	0.2500E+00	0.	-0.2951E-03	0.1103E-03	0.1461E+03	-0.5526E-03	-0.2933E+04	-0.1430E+03	0.2145E+01	
42	0.2500E+00	0.	-0.2965E-03	0.1112E-03	0.1510E+03	-0.5552E-03	-0.2945E+04	-0.1436E+03	0.2153E+01	
43	0.2500E+00	0.	-0.2978E-03	0.1120E-03	0.1560E+03	-0.5576E-03	-0.2956E+04	-0.1441E+03	0.2162E+01	
44	0.2500E+00	0.	-0.2990E-03	0.1129E-03	0.1610E+03	-0.5599E-03	-0.2966E+04	-0.1446E+03	0.2169E+01	

TABLE 4.2-V. DESIGN NO. 5 (Continued)

45	0.2500E+00	0.	-0.3001E-03	0.1137E-03	0.1661E+03	-0.5620E-03	-0.2976E+04	-0.1451E+03	0.2176E+01
46	0.2500E+00	0.	-0.3012E-03	0.1145E-03	0.1711E+03	-0.5640E-03	-0.2985E+04	-0.1455E+03	0.2183E+01
47	0.2500E+00	0.	-0.3022E-03	0.1153E-03	0.1762E+03	-0.5659E-03	-0.2994E+04	-0.1460E+03	0.2189E+01
48	0.2500E+00	0.	-0.3031E-03	0.1160E-03	0.1813E+03	-0.5677E-03	-0.3002E+04	-0.1463E+03	0.2195E+01
49	0.2500E+00	0.	-0.3040E-03	0.1168E-03	0.1865E+03	-0.5694E-03	-0.3009E+04	-0.1467E+03	0.2201E+01
50	0.2500E+00	0.	-0.3049E-03	0.1175E-03	0.1916E+03	-0.5711E-03	-0.3016E+04	-0.1470E+03	0.2206E+01
51	0.2500E+00	0.	-0.3057E-03	0.1183E-03	0.1968E+03	-0.5726E-03	-0.3023E+04	-0.1474E+03	0.2210E+01
52	0.2500E+00	0.	-0.3065E-03	0.1190E-03	0.2021E+03	-0.5741E-03	-0.3029E+04	-0.1477E+03	0.2215E+01
53	0.2500E+00	0.	-0.3072E-03	0.1197E-03	0.2073E+03	-0.5755E-03	-0.3034E+04	-0.1479E+03	0.2219E+01
54	0.2500E+00	0.	-0.3079E-03	0.1204E-03	0.2126E+03	-0.5768E-03	-0.3040E+04	-0.1482E+03	0.2223E+01
55	0.2500E+00	0.	-0.3086E-03	0.1211E-03	0.2179E+03	-0.5780E-03	-0.3045E+04	-0.1484E+03	0.2226E+01
56	0.2500E+00	0.	-0.3092E-03	0.1217E-03	0.2232E+03	-0.5792E-03	-0.3049E+04	-0.1486E+03	0.2230E+01
57	0.2500E+00	0.	-0.3098E-03	0.1224E-03	0.2286E+03	-0.5804E-03	-0.3053E+04	-0.1489E+03	0.2233E+01
58	0.2500E+00	0.	-0.3104E-03	0.1231E-03	0.2340E+03	-0.5815E-03	-0.3057E+04	-0.1490E+03	0.2236E+01
59	0.2500E+00	0.	-0.3109E-03	0.1237E-03	0.2394E+03	-0.5825E-03	-0.3061E+04	-0.1492E+03	0.2238E+01
60	0.2500E+00	0.	-0.3114E-03	0.1244E-03	0.2448E+03	-0.5835E-03	-0.3065E+04	-0.1494E+03	0.2241E+01
61	0.2500E+00	0.	-0.3119E-03	0.1250E-03	0.2503E+03	-0.5845E-03	-0.3068E+04	-0.1496E+03	0.2243E+01
62	0.2500E+00	0.	-0.3124E-03	0.1257E-03	0.2558E+03	-0.5854E-03	-0.3071E+04	-0.1497E+03	0.2246E+01
63	0.2500E+00	0.	-0.3129E-03	0.1263E-03	0.2613E+03	-0.5863E-03	-0.3074E+04	-0.1498E+03	0.2248E+01
64	0.2500E+00	0.	-0.3133E-03	0.1269E-03	0.2668E+03	-0.5871E-03	-0.3076E+04	-0.1500E+03	0.2250E+01
65	0.2500E+00	0.	-0.3137E-03	0.1276E-03	0.2724E+03	-0.5880E-03	-0.3079E+04	-0.1501E+03	0.2251E+01
66	0.2500E+00	0.	-0.3142E-03	0.1282E-03	0.2780E+03	-0.5888E-03	-0.3081E+04	-0.1502E+03	0.2253E+01
67	0.2500E+00	0.	-0.3146E-03	0.1288E-03	0.2836E+03	-0.5895E-03	-0.3083E+04	-0.1503E+03	0.2255E+01
68	0.2500E+00	0.	-0.3149E-03	0.1295E-03	0.2893E+03	-0.5903E-03	-0.3085E+04	-0.1504E+03	0.2256E+01
69	0.2500E+00	0.	-0.3153E-03	0.1301E-03	0.2949E+03	-0.5910E-03	-0.3087E+04	-0.1505E+03	0.2258E+01
70	0.2500E+00	0.	-0.3157E-03	0.1307E-03	0.3006E+03	-0.5917E-03	-0.3089E+04	-0.1506E+03	0.2259E+01
N	T	DELT	ES0	ESX	SSX	US	SS0	SSR	F1

J	TWJ	FJ	UWJ	QJ	STWJ	CJ	PJ
70	0.2500E+00	0.4982E-01	-0.2120E-03	0.2500E+00	0.2500E+00	0.2897E+01	5.8
69	0.2353E+00	0.9715E-01	-0.4115E-03	0.4853E+00	0.4853E+00	0.2884E+01	
68	0.2214E+00	0.1421E+00	-0.5992E-03	0.7067E+00	0.7067E+00	0.2871E+01	
67	0.2082E+00	0.1848E+00	-0.7757E-03	0.9149E+00	0.9149E+00	0.2858E+01	
66	0.1956E+00	0.2253E+00	-0.9415E-03	0.1111E+01	0.1111E+01	0.2845E+01	
65	0.1837E+00	0.2638E+00	-0.1097E-02	0.1294E+01	0.1294E+01	0.2832E+01	30.5
64	0.1724E+00	0.3003E+00	-0.1243E-02	0.1467E+01	0.1467E+01	0.2819E+01	
63	0.1617E+00	0.3350E+00	-0.1380E-02	0.1628E+01	0.1628E+01	0.2806E+01	
62	0.1515E+00	0.3678E+00	-0.1509E-02	0.1780E+01	0.1780E+01	0.2793E+01	
61	0.1418E+00	0.3990E+00	-0.1629E-02	0.1921E+01	0.1922E+01	0.2780E+01	
60	0.1327E+00	0.4285E+00	-0.1741E-02	0.2054E+01	0.2054E+01	0.2767E+01	49.5
59	0.1240E+00	0.4566E+00	-0.1846E-02	0.2178E+01	0.2178E+01	0.2754E+01	
58	0.1158E+00	0.4831E+00	-0.1945E-02	0.2294E+01	0.2294E+01	0.2741E+01	
57	0.1080E+00	0.5083E+00	-0.2036E-02	0.2402E+01	0.2402E+01	0.2728E+01	
56	0.1007E+00	0.5321E+00	-0.2121E-02	0.2503E+01	0.2503E+01	0.2715E+01	
55	0.9368E-01	0.5546E+00	-0.2201E-02	0.2596E+01	0.2596E+01	0.2702E+01	64.0
54	0.8708E-01	0.5760E+00	-0.2274E-02	0.2683E+01	0.2683E+01	0.2689E+01	
53	0.8083E-01	0.5962E+00	-0.2343E-02	0.2764E+01	0.2764E+01	0.2677E+01	
52	0.7493E-01	0.6154E+00	-0.2406E-02	0.2839E+01	0.2839E+01	0.2664E+01	
51	0.6935E-01	0.6335E+00	-0.2465E-02	0.2908E+01	0.2909E+01	0.2651E+01	
50	0.6407E-01	0.6506E+00	-0.2519E-02	0.2972E+01	0.2973E+01	0.2638E+01	75.1
49	0.5909E-01	0.6669E+00	-0.2568E-02	0.3031E+01	0.3032E+01	0.2625E+01	

TABLE 4.2-V. DESIGN NO. 5 (Continued)

48	0.5438E-01	0.6822E+00	-0.2614E-02	0.3086E+01	0.3086E+01	0.2612E+01	
47	0.4994E-01	0.6967E+00	-0.2656E-02	0.3136E+01	0.3136E+01	0.2599E+01	
46	0.4575E-01	0.7104E+00	-0.2694E-02	0.3181E+01	0.3182E+01	0.2586E+01	
45	0.4179E-01	0.7234E+00	-0.2729E-02	0.3223E+01	0.3224E+01	0.2573E+01	83.5
44	0.3807E-01	0.7356E+00	-0.2761E-02	0.3261E+01	0.3262E+01	0.2560E+01	
43	0.3456E-01	0.7472E+00	-0.2789E-02	0.3296E+01	0.3296E+01	0.2547E+01	
42	0.3127E-01	0.7581E+00	-0.2815E-02	0.3327E+01	0.3328E+01	0.2534E+01	
41	0.2816E-01	0.7685E+00	-0.2838E-02	0.3355E+01	0.3356E+01	0.2521E+01	
40	0.2525E-01	0.7783E+00	-0.2858E-02	0.3380E+01	0.3381E+01	0.2508E+01	89.9
39	0.2252E-01	0.7875E+00	-0.2876E-02	0.3403E+01	0.3403E+01	0.2495E+01	
38	0.1996E-01	0.7963E+00	-0.2891E-02	0.3423E+01	0.3423E+01	0.2482E+01	
37	0.1758E-01	0.8046E+00	-0.2904E-02	0.3440E+01	0.3441E+01	0.2469E+01	
36	0.1535E-01	0.8124E+00	-0.2915E-02	0.3456E+01	0.3456E+01	0.2456E+01	
35	0.1328E-01	0.8199E+00	-0.2923E-02	0.3469E+01	0.3470E+01	0.2443E+01	94.7
34	0.1136E-01	0.8270E+00	-0.2930E-02	0.3480E+01	0.3481E+01	0.2430E+01	
33	0.9589E-02	0.8337E+00	-0.2935E-02	0.3490E+01	0.3491E+01	0.2417E+01	
32	0.7967E-02	0.8401E+00	-0.2937E-02	0.3498E+01	0.3499E+01	0.2404E+01	
31	0.6491E-02	0.8462E+00	-0.2938E-02	0.3504E+01	0.3505E+01	0.2391E+01	
30	0.5160E-02	0.8521E+00	-0.2937E-02	0.3509E+01	0.3510E+01	0.2378E+01	98.4
29	0.3977E-02	0.8577E+00	-0.2934E-02	0.3513E+01	0.3514E+01	0.2365E+01	
28	0.2945E-02	0.8632E+00	-0.2929E-02	0.3516E+01	0.3517E+01	0.2352E+01	
27	0.2068E-02	0.8685E+00	-0.2922E-02	0.3518E+01	0.3519E+01	0.2339E+01	
26	0.1353E-02	0.8736E+00	-0.2914E-02	0.3519E+01	0.3521E+01	0.2326E+01	
25	0.8100E-03	0.8787E+00	-0.2903E-02	0.3520E+01	0.3521E+01	0.2313E+01	101.5
24	0.4500E-03	0.8838E+00	-0.2889E-02	0.3520E+01	0.3522E+01	0.2300E+01	
23	0.2883E-03	0.8889E+00	-0.2874E-02	0.3521E+01	0.3522E+01	0.2287E+01	
22	0.3435E-03	0.8940E+00	-0.2855E-02	0.3521E+01	0.3522E+01	0.2274E+01	
21	0.6384E-03	0.8993E+00	-0.2834E-02	0.3522E+01	0.3523E+01	0.2261E+01	
20	0.1201E-02	0.9048E+00	-0.2810E-02	0.3523E+01	0.3524E+01	0.2248E+01	104.5
19	0.2063E-02	0.9106E+00	-0.2782E-02	0.3525E+01	0.3526E+01	0.2235E+01	
18	0.3267E-02	0.9168E+00	-0.2750E-02	0.3528E+01	0.3530E+01	0.2222E+01	
17	0.4858E-02	0.9234E+00	-0.2714E-02	0.3533E+01	0.3534E+01	0.2209E+01	
16	0.6893E-02	0.9307E+00	-0.2672E-02	0.3540E+01	0.3541E+01	0.2196E+01	
15	0.9439E-02	0.9387E+00	-0.2625E-02	0.3549E+01	0.3551E+01	0.2183E+01	108.4
14	0.1257E-01	0.9476E+00	-0.2571E-02	0.3562E+01	0.3563E+01	0.2170E+01	
13	0.1639E-01	0.9577E+00	-0.2510E-02	0.3578E+01	0.3580E+01	0.2157E+01	
12	0.2099E-01	0.9692E+00	-0.2440E-02	0.3599E+01	0.3601E+01	0.2144E+01	
11	0.2650E-01	0.9822E+00	-0.2360E-02	0.3625E+01	0.3627E+01	0.2131E+01	
10	0.3305E-01	0.9973E+00	-0.2269E-02	0.3658E+01	0.3660E+01	0.2118E+01	115.2
9	0.4082E-01	0.1015E+01	-0.2164E-02	0.3699E+01	0.3701E+01	0.2105E+01	
8	0.4999E-01	0.1035E+01	-0.2046E-02	0.3749E+01	0.3751E+01	0.2092E+01	
7	0.6076E-01	0.1058E+01	-0.1910E-02	0.3810E+01	0.3812E+01	0.2079E+01	
6	0.7336E-01	0.1085E+01	-0.1756E-02	0.3883E+01	0.3885E+01	0.2066E+01	
5	0.8805E-01	0.1117E+01	-0.1581E-02	0.3971E+01	0.3973E+01	0.2053E+01	129.0
4	0.1051E+00	0.1154E+01	-0.1382E-02	0.4076E+01	0.4078E+01	0.2040E+01	
3	0.1248E+00	0.1197E+01	-0.1157E-02	0.4201E+01	0.4203E+01	0.2027E+01	
2	0.1476E+00	0.1247E+01	-0.9030E-03	0.4349E+01	0.4351E+01	0.2014E+01	
1	0.1737E+00	0.1304E+01	-0.5917E-03	0.4518E+01	0.4524E+01	0.2000E+01	150.6
J	TWJ	FJ	UNJ	QJ	STWJ	CJ	

TABLE 4.2-VI. DESIGN NO. 6

SPOOL			WIRE-PACK			BOBBIN			DATE 04/25/79	
ES=	0.1010E+08	B=	0.2500E+01	EC=	0.1050E+08	DDW=	0.	S=	0.7938E+00	
VS=	0.3300E+00	A=	0.2450E+01	D=	0.4000E-02	K=	0.2660E+05	DELC=	0.1083E-01	
T=	0.5000E-01	DS=	0.1250E-01	DD=	0.	E=	0.9751E+06	N=	35	
IT=	0.	DDS=	0.	DW=	0.1250E-01	ALFA=	0.5312E+01			
N	T	DELT	ESO	ESX	SSX	US	SSO	SSR	F1	
1	0.2500E+00	0.	-0.4000E-04	0.1320E-04	-0.1372E-05	-0.9738E-04	-0.4040E+03	-0.8000E+01	0.1000E+00	
2	0.2500E+00	0.	-0.7915E-04	0.2617E-04	0.6214E+00	-0.1927E-03	-0.7992E+03	-0.1582E+02	0.1978E+00	
3	0.2500E+00	0.	-0.1175E-03	0.3894E-04	0.1807E+01	-0.2861E-03	-0.1186E+04	-0.2349E+02	0.2936E+00	
4	0.2500E+00	0.	-0.1551E-03	0.5150E-04	0.3546E+01	-0.3776E-03	-0.1566E+04	-0.3100E+02	0.3875E+00	
5	0.2500E+00	0.	-0.1920E-03	0.6386E-04	0.5827E+01	-0.4673E-03	-0.1937E+04	-0.3835E+02	0.4794E+00	
6	0.2500E+00	0.	-0.2281E-03	0.7603E-04	0.8638E+01	-0.5552E-03	-0.2301E+04	-0.4556E+02	0.5694E+00	
7	0.2500E+00	0.	-0.2635E-03	0.8800E-04	0.1197E+02	-0.6414E-03	-0.2657E+04	-0.5261E+02	0.6576E+00	
8	0.2500E+00	0.	-0.2982E-03	0.9979E-04	0.1581E+02	-0.7258E-03	-0.3006E+04	-0.5952E+02	0.7440E+00	
9	0.2500E+00	0.	-0.3321E-03	0.1114E-03	0.2015E+02	-0.8085E-03	-0.3348E+04	-0.6629E+02	0.8286E+00	
10	0.2500E+00	0.	-0.3655E-03	0.1228E-03	0.2497E+02	-0.8896E-03	-0.3683E+04	-0.7292E+02	0.9115E+00	
11	0.2500E+00	0.	-0.3981E-03	0.1340E-03	0.3028E+02	-0.9691E-03	-0.4011E+04	-0.7941E+02	0.9927E+00	
12	0.2500E+00	0.	-0.4301E-03	0.1451E-03	0.3605E+02	-0.1047E-02	-0.4332E+04	-0.8577E+02	0.1072E+01	
13	0.2500E+00	0.	-0.4614E-03	0.1560E-03	0.4228E+02	-0.1123E-02	-0.4647E+04	-0.9200E+02	0.1150E+01	
14	0.2500E+00	0.	-0.4922E-03	0.1667E-03	0.4896E+02	-0.1198E-02	-0.4955E+04	-0.9810E+02	0.1226E+01	
15	0.2500E+00	0.	-0.5223E-03	0.1773E-03	0.5608E+02	-0.1271E-02	-0.5257E+04	-0.1041E+03	0.1301E+01	
16	0.2500E+00	0.	-0.5518E-03	0.1877E-03	0.6364E+02	-0.1343E-02	-0.5552E+04	-0.1099E+03	0.1374E+01	
17	0.2500E+00	0.	-0.5807E-03	0.1980E-03	0.7161E+02	-0.1414E-02	-0.5842E+04	-0.1157E+03	0.1446E+01	
18	0.2500E+00	0.	-0.6091E-03	0.2081E-03	0.8000E+02	-0.1483E-02	-0.6125E+04	-0.1213E+03	0.1516E+01	
19	0.2500E+00	0.	-0.6369E-03	0.2180E-03	0.8880E+02	-0.1550E-02	-0.6403E+04	-0.1268E+03	0.1585E+01	
20	0.2500E+00	0.	-0.6641E-03	0.2278E-03	0.9800E+02	-0.1617E-02	-0.6675E+04	-0.1322E+03	0.1652E+01	
21	0.2500E+00	0.	-0.6908E-03	0.2375E-03	0.1076E+03	-0.1682E-02	-0.6942E+04	-0.1375E+03	0.1718E+01	
22	0.2500E+00	0.	-0.7170E-03	0.2470E-03	0.1176E+03	-0.1746E-02	-0.7203E+04	-0.1426E+03	0.1783E+01	
23	0.2500E+00	0.	-0.7427E-03	0.2564E-03	0.1279E+03	-0.1808E-02	-0.7459E+04	-0.1477E+03	0.1846E+01	
24	0.2500E+00	0.	-0.7678E-03	0.2656E-03	0.1386E+03	-0.1869E-02	-0.7710E+04	-0.1526E+03	0.1908E+01	
25	0.2500E+00	0.	-0.7925E-03	0.2747E-03	0.1497E+03	-0.1929E-02	-0.7955E+04	-0.1575E+03	0.1969E+01	
26	0.2500E+00	0.	-0.8167E-03	0.2837E-03	0.1611E+03	-0.1988E-02	-0.8196E+04	-0.1623E+03	0.2028E+01	
27	0.2500E+00	0.	-0.8404E-03	0.2926E-03	0.1729E+03	-0.2046E-02	-0.8431E+04	-0.1669E+03	0.2087E+01	
28	0.2500E+00	0.	-0.8637E-03	0.3013E-03	0.1850E+03	-0.2103E-02	-0.8662E+04	-0.1715E+03	0.2144E+01	
29	0.2500E+00	0.	-0.8865E-03	0.3100E-03	0.1975E+03	-0.2158E-02	-0.8888E+04	-0.1760E+03	0.2200E+01	
30	0.2500E+00	0.	-0.9089E-03	0.3185E-03	0.2102E+03	-0.2213E-02	-0.9110E+04	-0.1804E+03	0.2255E+01	
31	0.2500E+00	0.	-0.9308E-03	0.3269E-03	0.2233E+03	-0.2266E-02	-0.9327E+04	-0.1847E+03	0.2309E+01	
32	0.2500E+00	0.	-0.9523E-03	0.3352E-03	0.2368E+03	-0.2319E-02	-0.9540E+04	-0.1889E+03	0.2361E+01	
33	0.2500E+00	0.	-0.9734E-03	0.3433E-03	0.2505E+03	-0.2370E-02	-0.9749E+04	-0.1930E+03	0.2413E+01	
34	0.2500E+00	0.	-0.9941E-03	0.3514E-03	0.2645E+03	-0.2420E-02	-0.9953E+04	-0.1971E+03	0.2463E+01	
35	0.2500E+00	0.	-0.1014E-02	0.3594E-03	0.2789E+03	-0.2470E-02	-0.1015E+05	-0.2010E+03	0.2513E+01	
N	T	DELT	ESO	ESX	SSX	US	SSO	SSR	F1	

TABLE 4.2-VI. DESIGN NO. 6 (Continued)

J	TWJ	FJ	UWJ	QJ	STWJ	CJ	PJ
35	0.2500E+00	0.5031E-01	-0.1075E-03	0.2500E+00	0.2500E+00	0.2069E+01	7.0
34	0.2451E+00	0.1000E+00	-0.2126E-03	0.4951E+00	0.4951E+00	0.2858E+01	
33	0.2403E+00	0.1491E+00	-0.3154E-03	0.7354E+00	0.7354E+00	0.2847E+01	
32	0.2355E+00	0.1976E+00	-0.4160E-03	0.9709E+00	0.9709E+00	0.2836E+01	
31	0.2308E+00	0.2455E+00	-0.5143E-03	0.1202E+01	0.1202E+01	0.2826E+01	
30	0.2262E+00	0.2929E+00	-0.6104E-03	0.1428E+01	0.1428E+01	0.2815E+01	40.6
29	0.2216E+00	0.3396E+00	-0.7043E-03	0.1650E+01	0.1650E+01	0.2804E+01	
28	0.2171E+00	0.3858E+00	-0.7959E-03	0.1867E+01	0.1867E+01	0.2793E+01	
27	0.2127E+00	0.4315E+00	-0.8854E-03	0.2079E+01	0.2079E+01	0.2782E+01	
26	0.2084E+00	0.4766E+00	-0.9727E-03	0.2288E+01	0.2288E+01	0.2771E+01	
25	0.2041E+00	0.5211E+00	-0.1058E-02	0.2492E+01	0.2492E+01	0.2761E+01	72.2
24	0.1999E+00	0.5652E+00	-0.1141E-02	0.2692E+01	0.2692E+01	0.2750E+01	
23	0.1958E+00	0.6087E+00	-0.1222E-02	0.2888E+01	0.2888E+01	0.2739E+01	
22	0.1917E+00	0.6516E+00	-0.1300E-02	0.3079E+01	0.3079E+01	0.2728E+01	
21	0.1877E+00	0.6941E+00	-0.1377E-02	0.3267E+01	0.3267E+01	0.2717E+01	
20	0.1837E+00	0.7361E+00	-0.1452E-02	0.3451E+01	0.3451E+01	0.2707E+01	102.0
19	0.1799E+00	0.7776E+00	-0.1524E-02	0.3630E+01	0.3630E+01	0.2696E+01	
18	0.1761E+00	0.8186E+00	-0.1594E-02	0.3807E+01	0.3807E+01	0.2685E+01	
17	0.1724E+00	0.8591E+00	-0.1663E-02	0.3979E+01	0.3979E+01	0.2674E+01	
16	0.1687E+00	0.8992E+00	-0.1729E-02	0.4148E+01	0.4148E+01	0.2663E+01	
15	0.1652E+00	0.9388E+00	-0.1793E-02	0.4313E+01	0.4313E+01	0.2652E+01	130.1
14	0.1617E+00	0.9780E+00	-0.1855E-02	0.4474E+01	0.4474E+01	0.2642E+01	
13	0.1582E+00	0.1017E+01	-0.1915E-02	0.4633E+01	0.4633E+01	0.2631E+01	
12	0.1549E+00	0.1055E+01	-0.1973E-02	0.4788E+01	0.4788E+01	0.2620E+01	
11	0.1516E+00	0.1093E+01	-0.2029E-02	0.4939E+01	0.4939E+01	0.2609E+01	
10	0.1484E+00	0.1130E+01	-0.2083E-02	0.5088E+01	0.5088E+01	0.2598E+01	156.6
9	0.1453E+00	0.1168E+01	-0.2135E-02	0.5233E+01	0.5233E+01	0.2587E+01	
8	0.1422E+00	0.1204E+01	-0.2185E-02	0.5375E+01	0.5375E+01	0.2577E+01	
7	0.1393E+00	0.1241E+01	-0.2232E-02	0.5514E+01	0.5514E+01	0.2566E+01	
6	0.1364E+00	0.1277E+01	-0.2278E-02	0.5651E+01	0.5651E+01	0.2555E+01	
5	0.1336E+00	0.1313E+01	-0.2321E-02	0.5784E+01	0.5784E+01	0.2544E+01	181.9
4	0.1308E+00	0.1349E+01	-0.2363E-02	0.5915E+01	0.5915E+01	0.2533E+01	
3	0.1282E+00	0.1383E+01	-0.2402E-02	0.6043E+01	0.6043E+01	0.2522E+01	
2	0.1257E+00	0.1418E+01	-0.2440E-02	0.6169E+01	0.6169E+01	0.2512E+01	
1	0.1232E+00	0.1451E+01	-0.2470E-02	0.6292E+01	0.6292E+01	0.2500E+01	201.1
J	TWJ	FJ	UWJ	QJ	STWJ	CJ	

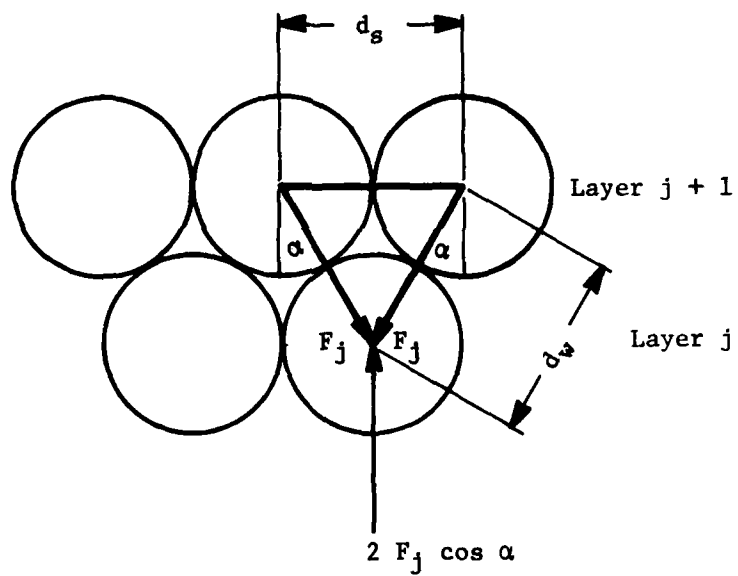


Figure 4.2-7. Forces Between Layers

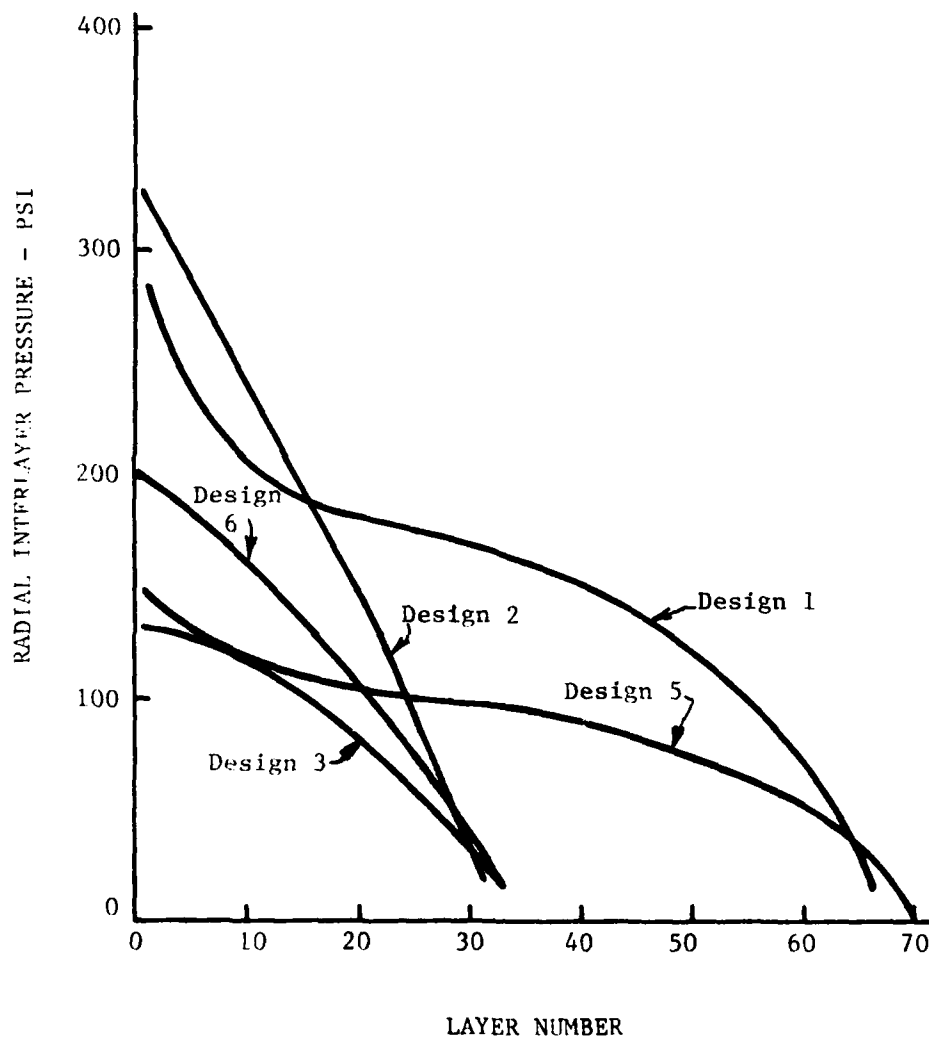


Figure 4.2-8. Radial Interlayer Pressure Indicated for Designs

4.3 MECHANICAL AND PAYOUT TESTING

The dispenser design effort described above has been performed in parallel with supporting experimental activity. This concurrent effort has served to provide certain data available only by direct measurement and to verify the results of the design analysis. For each of the full length bobbin designs there has been a design of an experimental bobbin adapted to the available length of cable. These experimental bobbins have been very useful in understanding the internal mechanics of the cable pack.

The experimental results from the various bobbins tested to date are described below. The testing performed has been quite varied and has included: (1) the measurement of the transverse compressive modulus of the cable (performed by squeezing a short length of cable between two plates and determining the force-displacement relationship), (2) the determination of the compressive force on the spool resulting from the squeezing action of the various layers and providing an indication of the magnitude of the residual tension in the various layers, and (3) high speed payout of the wound bobbins. The results of this testing for the various bobbins is described below. The discussion is somewhat more detailed for Bobbin 1 than for the others, since the experimental techniques are described there in some detail.

Bobbin 1. The first experiment was representative of design number 1 in table 4.2-I. One and two tenths km (3900 ft) of 0.02 inch diameter cable was available for the experiment. Choosing a spool diameter of 3.5 inch, $i = 9$, $l = 6$ inches, and $N = 17$ layers, equation 4.2-1 results in $L = 3820$ feet which was satisfactory. The spool is shown in figure 4.3-1. In order to calculate the cable pack stresses using the computer programs, the transverse stiffness of the cable is required. This was obtained by squeezing the cable between two precision steel blocks, 6 inches long and plotting the force/unit length against the compression. The result is shown in figure 4.3-2. An indication of the creep characteristics can be seen also.

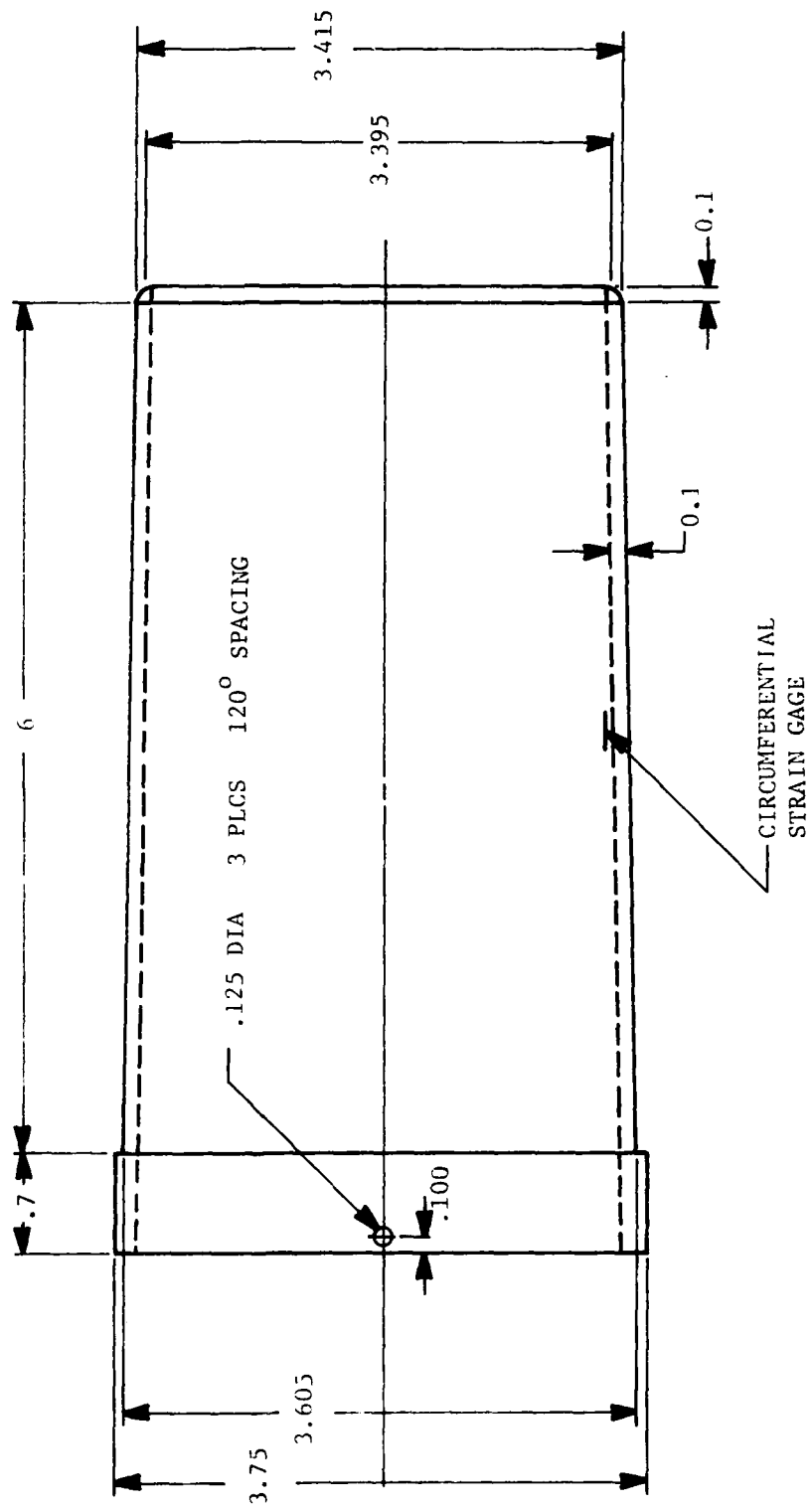


Figure 4.3-1. Test Robbin 1, Spec Geometry

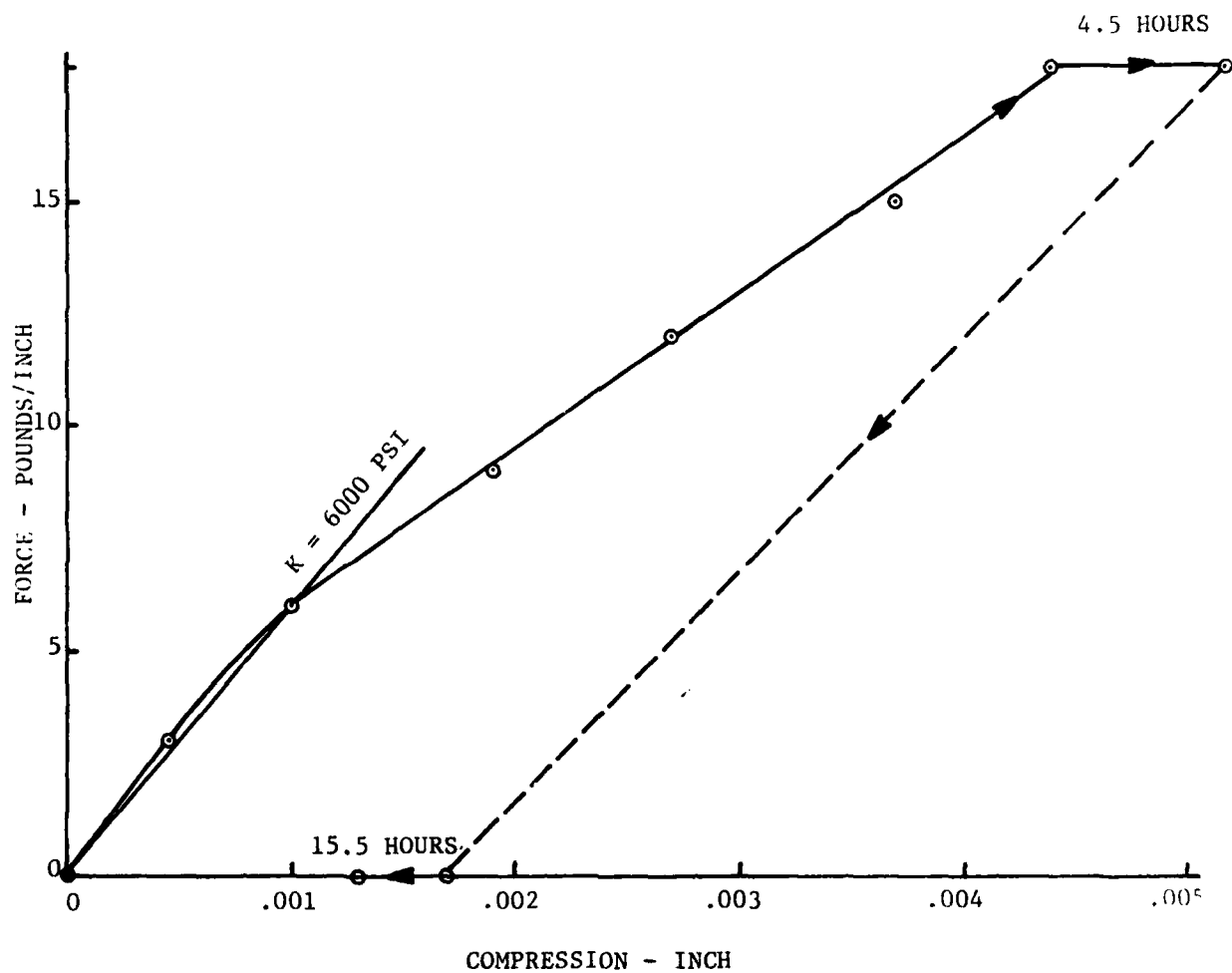


Figure 4.3-2. Bobbin 1, Cable Force-Displacement Characteristics

Since the program handles only linear transverse force deflection characteristics, a linear approximation was made as shown. (Table 4.2-II shows maximum $F_1 = 5.6$ lb/in.) The computer output is shown in table 4.3-I for this test bobbin which is essentially the same calculation as shown in table 4.2-II with $N = 15$ here.

The bobbin winding has been accomplished using a modified TOW base layer winding machine. This machine is much simpler than the machine used to wind the TOW bobbins, and for the TOW program, is used to wind a single layer of wire, always in the same direction. The modified machine is illustrated in figure 4.3-A. The modifications which were incorporated included the following:

1. The machine was modified to permit winding in both directions, allowing the winding of multiple layers. This modification also permits the adjustment of the lag angle which is the angle between the cable at the laydown point and the plane of the turn being wound.
2. The tension control mechanism was modified to permit operation at substantially lower tensions than were available with the original design. The resulting tension control mechanism is only marginally satisfactory. At the low tension levels involved, any pulley friction or other disturbances downstream from the tension control can significantly alter the winding tension. The current design, although adequate for its current purpose, does require a large amount of operator attention. The machine which has resulted is quite flexible and has demonstrated the ability to wind cables of various dimensions on bobbins of substantially different sizes.

The machine currently has no provision for applying adhesive to the cable as it is being wound, as is the case with the TOW production winders. In this series of experiments no adhesive was employed except acrylic lacquer, which was applied manually to stabilize the transition regions at the end of each layer.

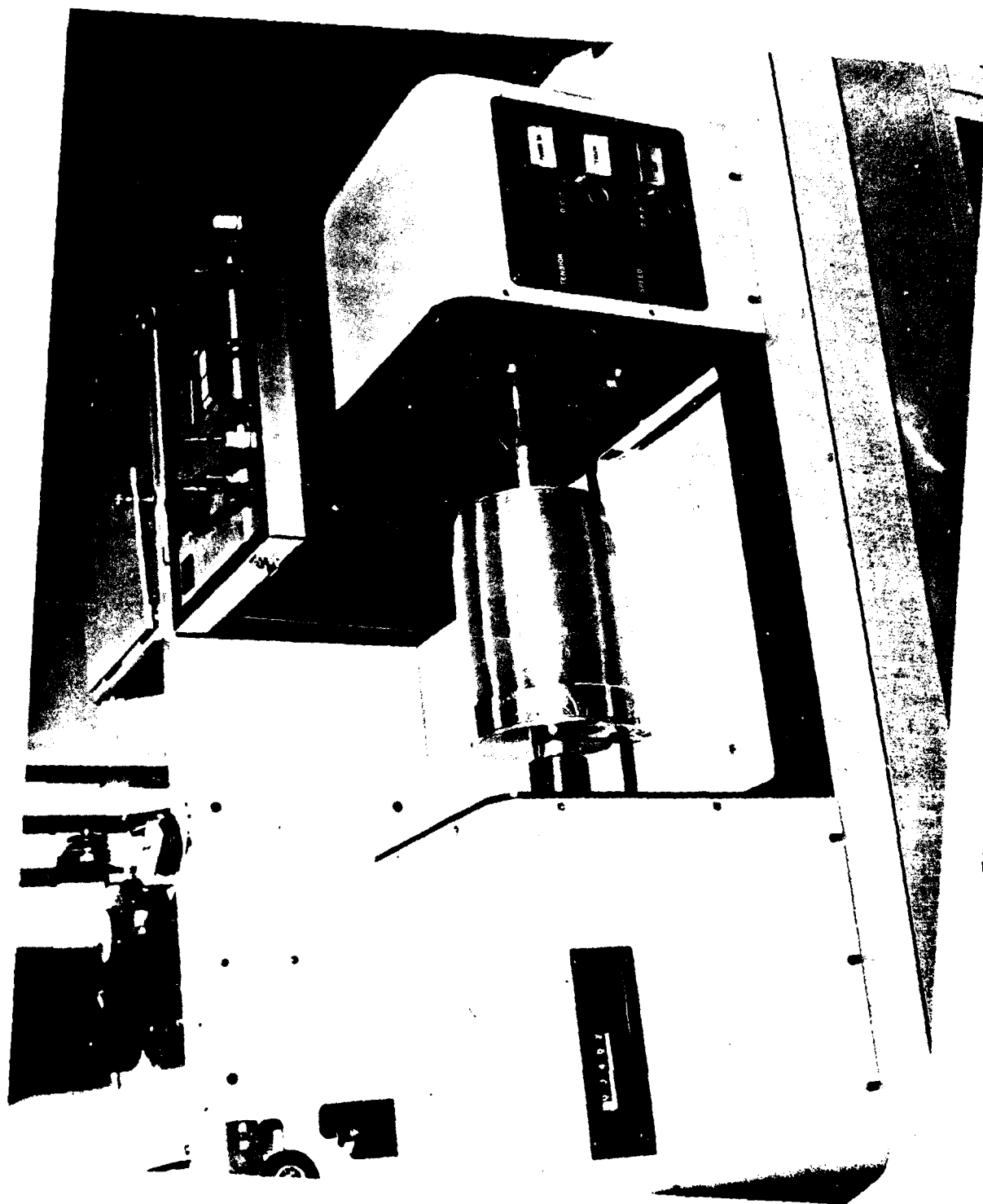


Figure 4.3-A. Modified Bobbin Winding Machine

The cable winding procedure was outlined as follows:

1. Set winding tension = 0.5 lbs.
2. Mount spool on winder with ends of strain gage leads protruding through hole in small end plate.
3. Read strain gage.
4. Begin winding on large end of spool, leaving 6 feet of cable unwound but taped down to the flange avoiding sharp bends.
5. Wind down to the small end, step back 4-1/2 turns and wind to the large end locking in the cable end.
6. Read strain gage.
7. Wind two more layers, stepping back 4-1/2 turns at each end.
8. Read strain gage.
9. Repeat steps 7 and 8 until cable is used up.

NOTE: Strain gage leads should not be free to move around inside the spool during winding.

A plot of the strain during winding versus layer number is shown in figure 4.3-3. Also shown is the theoretical strain ESO from table 4.3-I for T = 0.5 pound. The difference is due to an error in setting the cable tension during winding. The circumferential strain on the inner surface of the spool with external pressure p is

$$\epsilon_t = \frac{2}{E} \frac{pb^2}{b^2 - a^2} \quad (4.3-1)$$

TABLE 4.3-I. BOBBIN 1 DESIGN TABULATION - NOMINAL TENSION

SPOOL				WIRE-PACK				BOBBIN		DATE 02/11/74
ES=	0.1010E+00	B=	0.1750E+01	EC=	0.1050E+00	DDW=	0.	S=	0.9920E-01	
VS=	0.3300E+00	A=	0.1650E+01	D=	0.4920E-02	K=	0.6000E+04	DELC=	0.1704E-01	
T=	0.1000E+00	DS=	0.1968E-01	DD=	0.	E=	0.5952E+06	N=	15	
DT=	0.	DDS=	0.	DM=	0.1968E-01	ALFA=	0.8730E+01			
N	T	DELT	ESO	ESI	SSI	US	SSO	SSR	FI	
1	0.5000E+00	0.	-0.2589E-04	0.8545E-05	-0.5211E-06	-0.4197E-04	-0.2615E+03	-0.1452E+02	0.2857E+00	
2	0.5000E+00	0.	-0.5145E-04	0.1706E-04	0.9076E+00	-0.8339E-04	-0.5193E+03	-0.2883E+02	0.5674E+00	
3	0.5000E+00	0.	-0.7652E-04	0.2548E-04	0.2637E+01	-0.1240E-03	-0.7720E+03	-0.4285E+02	0.8494E+00	
4	0.5000E+00	0.	-0.1010E-03	0.3377E-04	0.5159E+01	-0.1637E-03	-0.1018E+04	-0.5651E+02	0.1111E-01	
5	0.5000E+00	0.	-0.1247E-03	0.4188E-04	0.8436E+01	-0.2021E-03	-0.1256E+04	-0.6974E+02	0.1372E+01	
6	0.5000E+00	0.	-0.1475E-03	0.4978E-04	0.1243E+02	-0.2391E-03	-0.1486E+04	-0.8248E+02	0.1623E+01	
7	0.5000E+00	0.	-0.1695E-03	0.5743E-04	0.1708E+02	-0.2747E-03	-0.1706E+04	-0.9469E+02	0.1864E+01	
8	0.5000E+00	0.	-0.1904E-03	0.6481E-04	0.2236E+02	-0.3087E-03	-0.1916E+04	-0.1064E+03	0.2093E+01	
9	0.5000E+00	0.	-0.2104E-03	0.7192E-04	0.2821E+02	-0.3412E-03	-0.2116E+04	-0.1175E+03	0.2311E+01	
10	0.5000E+00	0.	-0.2294E-03	0.7875E-04	0.3458E+02	-0.3719E-03	-0.2305E+04	-0.1280E+03	0.2519E+01	
11	0.5000E+00	0.	-0.2474E-03	0.8529E-04	0.4144E+02	-0.4011E-03	-0.2485E+04	-0.1379E+03	0.2714E+01	
12	0.5000E+00	0.	-0.2644E-03	0.9154E-04	0.4873E+02	-0.4287E-03	-0.2654E+04	-0.1473E+03	0.2899E+01	
13	0.5000E+00	0.	-0.2804E-03	0.9751E-04	0.5642E+02	-0.4547E-03	-0.2813E+04	-0.1562E+03	0.3073E+01	
14	0.5000E+00	0.	-0.2955E-03	0.1032E-03	0.6448E+02	-0.4792E-03	-0.2963E+04	-0.1645E+03	0.3237E+01	
15	0.5000E+00	0.	-0.3097E-03	0.1086E-03	0.7287E+02	-0.5023E-03	-0.3104E+04	-0.1723E+03	0.3391E+01	

J	TMJ	FJ	UMJ	QJ	STMJ	CJ
15	0.5000E+00	0.1451E+00	-0.3155E-03	0.5000E+00	0.5000E+00	0.1990E+01
14	0.4696E+00	0.2837E+00	-0.5952E-03	0.9696E+00	0.9696E+00	0.1973E+01
13	0.4423E+00	0.4168E+00	-0.8391E-03	0.1412E+01	0.1412E+01	0.1956E+01
12	0.4181E+00	0.5449E+00	-0.1047E-02	0.1830E+01	0.1830E+01	0.1939E+01
11	0.3971E+00	0.6691E+00	-0.1210E-02	0.2227E+01	0.2227E+01	0.1922E+01
10	0.3796E+00	0.7901E+00	-0.1351E-02	0.2607E+01	0.2607E+01	0.1905E+01
9	0.3657E+00	0.9091E+00	-0.1445E-02	0.2972E+01	0.2972E+01	0.1888E+01
8	0.3550E+00	0.1027E+01	-0.1498E-02	0.3328E+01	0.3328E+01	0.1871E+01
7	0.3499E+00	0.1146E+01	-0.1508E-02	0.3678E+01	0.3678E+01	0.1854E+01
6	0.3487E+00	0.1266E+01	-0.1474E-02	0.4027E+01	0.4027E+01	0.1837E+01
5	0.3523E+00	0.1389E+01	-0.1392E-02	0.4379E+01	0.4379E+01	0.1819E+01
4	0.3612E+00	0.1518E+01	-0.1260E-02	0.4740E+01	0.4740E+01	0.1802E+01
3	0.3760E+00	0.1654E+01	-0.1075E-02	0.5116E+01	0.5116E+01	0.1785E+01
2	0.3971E+00	0.1800E+01	-0.8331E-03	0.5513E+01	0.5513E+01	0.1768E+01
1	0.4251E+00	0.1958E+01	-0.5023E-03	0.5934E+01	0.5938E+01	0.1750E+01

TABLE 4.3-II. BOBBIN 1 DESIGN TABULATION - MODIFIED TENSION

SPOOL				WIRE-PACK				BOBBIN		DATE 12/19/78	
ES=	0.1010E+08	B=	0.1750E+01	EC=	0.1050E+08	DDW=	0.	S=	0.9928E-01		
VS=	0.3300E+00	A=	0.1650E+01	D=	0.4920E-02	K=	0.6000E+04	DELC=	0.1704E-01		
T=	0.1000E+00	DS=	0.1968E-01	DD=	0.	E=	0.5952E+06	N=	15		
DT=	0.	DDS=	0.	DW=	0.1968E-01	ALFA=	0.8738E+01				
N	T	DELT	ESO	ESX	SSX	US	SSO	SSR	F1		
1	0.9270E+00	0.	-0.4801E-04	0.1584E-04	-0.1186E-05	-0.7781E-04	-0.4849E+03	-0.2692E+02	0.5297E+00		
2	0.9270E+00	0.	-0.9539E-04	0.3163E-04	0.1683E+01	-0.1546E-03	-0.9629E+03	-0.5345E+02	0.1052E+01		
3	0.9270E+00	0.	-0.1419E-03	0.4725E-04	0.4889E+01	-0.2300E-03	-0.1431E+04	-0.7945E+02	0.1564E+01		
4	0.9270E+00	0.	-0.1872E-03	0.6262E-04	0.9564E+01	-0.3034E-03	-0.1887E+04	-0.1048E+03	0.2062E+01		
5	0.9270E+00	0.	-0.2311E-03	0.7765E-04	0.1564E+02	-0.3747E-03	-0.2329E+04	-0.1293E+03	0.2544E+01		
6	0.9270E+00	0.	-0.2735E-03	0.9228E-04	0.2304E+02	-0.4434E-03	-0.2755E+04	-0.1529E+03	0.3009E+01		
7	0.9270E+00	0.	-0.3142E-03	0.1065E-03	0.3167E+02	-0.5093E-03	-0.3163E+04	-0.1756E+03	0.3455E+01		
8	0.9270E+00	0.	-0.3531E-03	0.1202E-03	0.4145E+02	-0.5724E-03	-0.3552E+04	-0.1972E+03	0.3881E+01		
9	0.9270E+00	0.	-0.3901E-03	0.1333E-03	0.5230E+02	-0.6325E-03	-0.3923E+04	-0.2178E+03	0.4285E+01		
10	0.9270E+00	0.	-0.4253E-03	0.1460E-03	0.6411E+02	-0.6896E-03	-0.4274E+04	-0.2373E+03	0.4669E+01		
11	0.9270E+00	0.	-0.4586E-03	0.1581E-03	0.7682E+02	-0.7437E-03	-0.4607E+04	-0.2557E+03	0.5033E+01		
12	0.9270E+00	0.	-0.4901E-03	0.1697E-03	0.9035E+02	-0.7948E-03	-0.4921E+04	-0.2731E+03	0.5375E+01		
13	0.9270E+00	0.	-0.5199E-03	0.1808E-03	0.1046E+03	-0.8430E-03	-0.5216E+04	-0.2895E+03	0.5698E+01		
14	0.9270E+00	0.	-0.5479E-03	0.1913E-03	0.1196E+03	-0.8885E-03	-0.5494E+04	-0.3050E+03	0.6002E+01		
15	0.9270E+00	0.	-0.5742E-03	0.2014E-03	0.1351E+03	-0.9312E-03	-0.5755E+04	-0.3194E+03	0.6287E+01		

	TWJ	FJ	UWJ	QJ	STWJ	CJ	LB/IN	PJ
1	0.9270E+00	0.2690E+00	-0.5849E-03	0.9270E+00	0.9270E+00	0.1990E+01	.466	23.7
14	0.8796E+00	0.5261E+00	-0.1103E-02	0.1798E+01	0.1798E+01	0.1973E+01	.911	46.3
13	0.8199E+00	0.7727E+00	-0.1556E-02	0.2618E+01	0.2618E+01	0.1956E+01	1.338	68.0
12	0.7751E+00	0.1010E+01	-0.1941E-02	0.3393E+01	0.3393E+01	0.1939E+01	1.749	88.9
11	0.7362E+00	0.1240E+01	-0.2257E-02	0.4129E+01	0.4129E+01	0.1922E+01	2.148	109.1
10	0.7038E+00	0.1465E+01	-0.2504E-02	0.4833E+01	0.4833E+01	0.1905E+01	2.537	128.9
9	0.6701E+00	0.1685E+01	-0.2678E-02	0.5511E+01	0.5511E+01	0.1888E+01	2.919	148.3
8	0.6596E+00	0.1904E+01	-0.2777E-02	0.6170E+01	0.6170E+01	0.1871E+01	3.298	167.6
7	0.6488E+00	0.2124E+01	-0.2796E-02	0.6819E+01	0.6819E+01	0.1854E+01	3.679	186.9
6	0.6464E+00	0.2347E+01	-0.2733E-02	0.7465E+01	0.7466E+01	0.1837E+01	4.065	206.6
5	0.6521E+00	0.2576E+01	-0.2581E-02	0.8118E+01	0.8119E+01	0.1819E+01	4.462	226.7
4	0.6777E+00	0.2815E+01	-0.2336E-02	0.8788E+01	0.8788E+01	0.1802E+01	4.876	247.8
3	0.6971E+00	0.3067E+01	-0.1993E-02	0.9485E+01	0.9485E+01	0.1785E+01	5.312	269.9
2	0.7362E+00	0.3337E+01	-0.1545E-02	0.1022E+02	0.1022E+02	0.1768E+01	5.780	293.7
1	0.7892E+00	0.3630E+01	-0.9312E-03	0.1100E+02	0.1101E+02	0.1750E+01	6.287	319.5

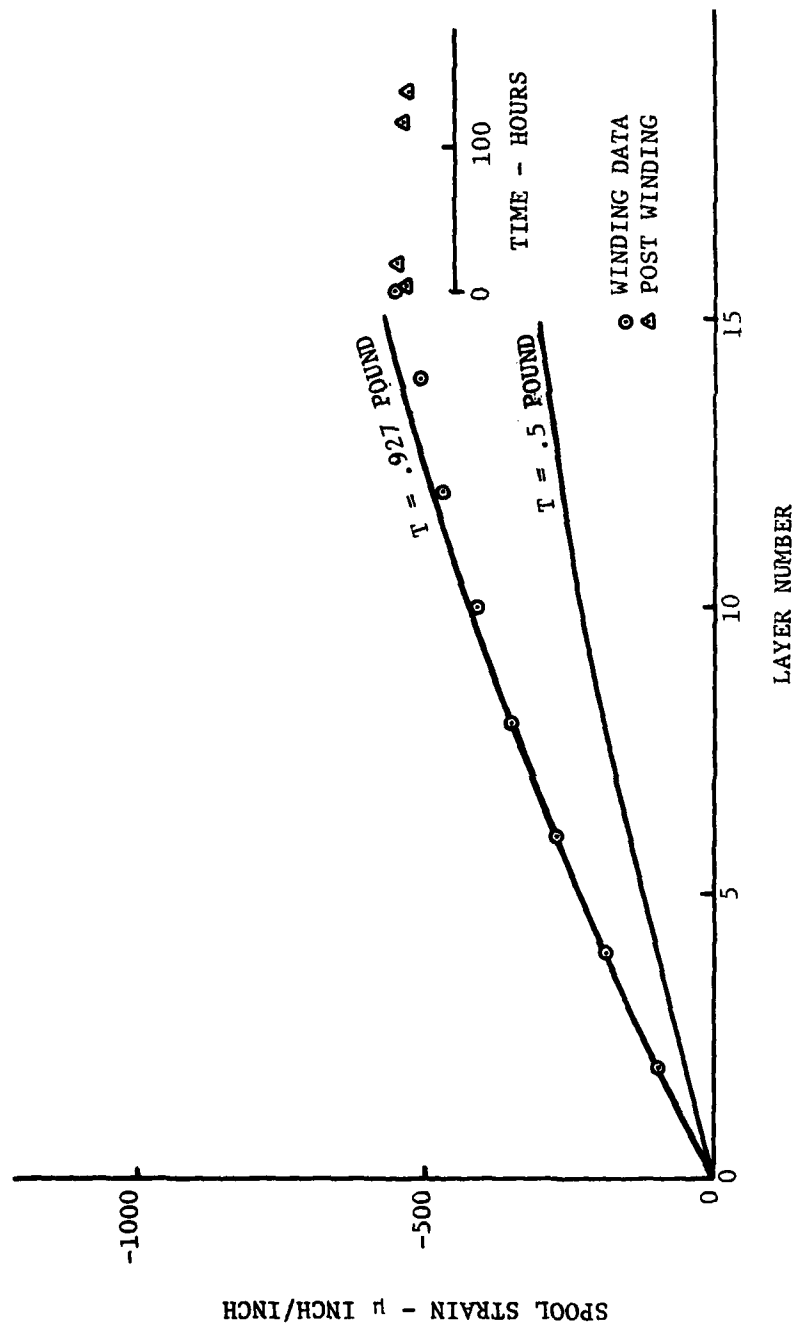


Figure 4.3-3. Bobbin 1, Spool Strain Versus Number of Layers

The pressure due to winding one layer of cable is

$$P = \frac{T}{b d_s} \quad (4.3-2)$$

Eliminating P from 4.3-1 and 4.3-2 leads to

$$T = E d_s \frac{b^2 - a^2}{2b} \epsilon_t \quad (4.3-3)$$

For the present case, 4.3-3 becomes

$$T = .0193 \epsilon_t \quad (4.3-4)$$

The actual strain after winding one layer of cable was $\epsilon_t = 48 \mu$ in/in. Introducing this into (4.3-4) results in $T = 0.93$ pound which was the actual winding tension. The computer run for this tension is shown in table 4.3-II, and the spool strain is also plotted in figure 4.3-3. The disagreement at higher layer numbers could be due to creep in the cable coating. Some relaxation is evident with time as shown in figure 4.3-3. To simulate the effect on the cable of 68 layers being wound on a spool, a pressure vessel was designed to apply pressure to the top layer of cable. A cross section of the vessel is shown in figure 4.3-4. The bobbin was inserted into the vessel with a special rubber bladder between the top layer of cable and the vessel inside diameter as shown in figure 4.3-5. The valve stem protruded through the hole in the side. Referring back to figure 4.2-8, the interlayer pressure for 15 layers is 195 psi for design number 1. Strain as a function of pressure is shown in figure 4.3-6 and appears to be quite linear. The assembly was then placed in an oven at 160° F overnight and the strain is shown as a function of time, increasing as the spool warms up. The next morning the pressure was down to zero at 160° F because the valve stem had failed during the night. This point is shown in figure 4.3-6. After cooling to room temperature, the relaxation of the cable pack due to the pressure/temperature cycle can be seen.

This bobbin was dispensed on the TOW high speed payout test facility. The bobbin was held in a fixture which measures axial bobbin force; i.e., the force acting on the bobbin in the direction of payout. The cable is wound on a drum driven by a speed-controlled air turbine.

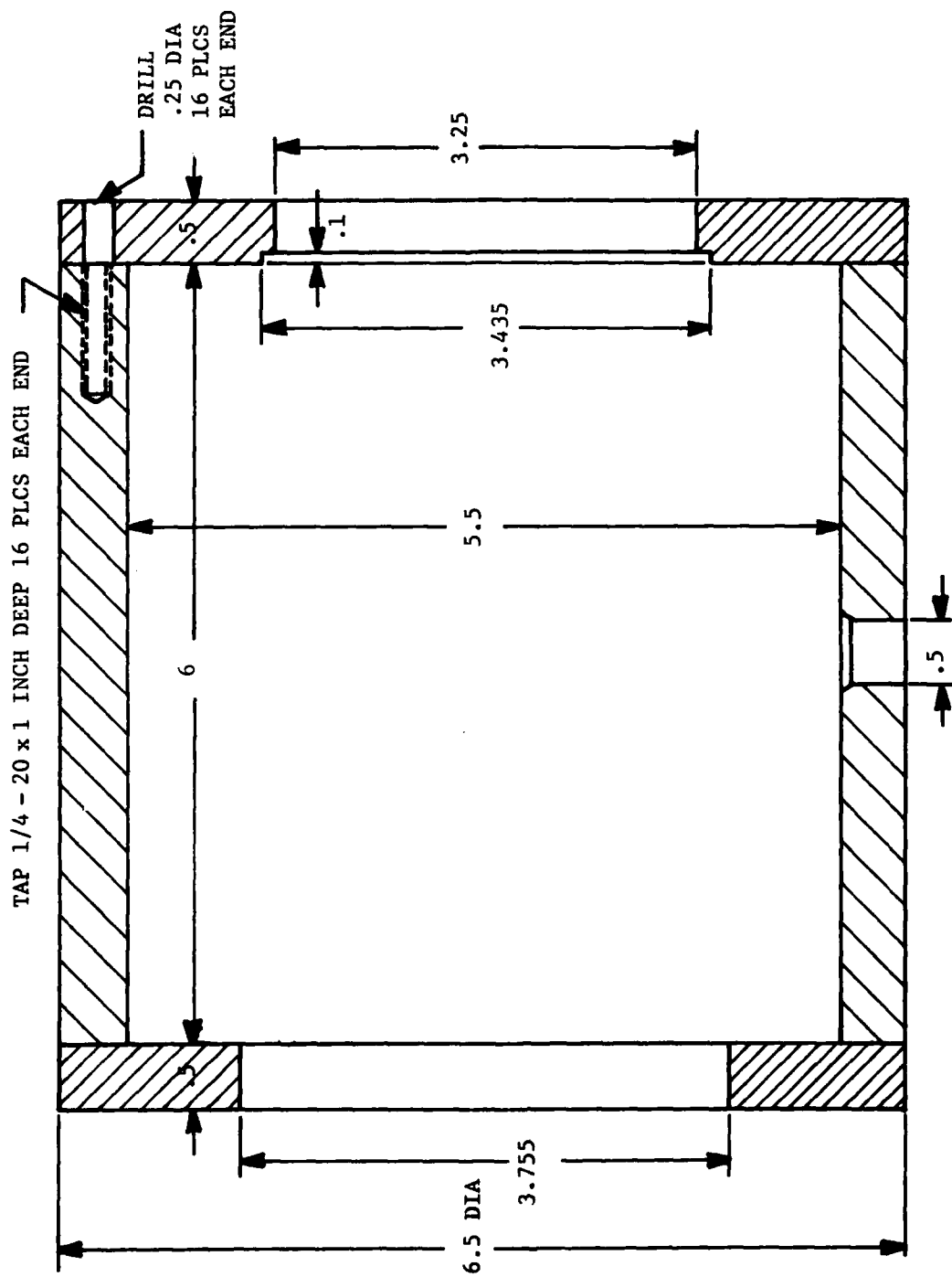


Figure 4.3-4. Pressure Vessel Geometry

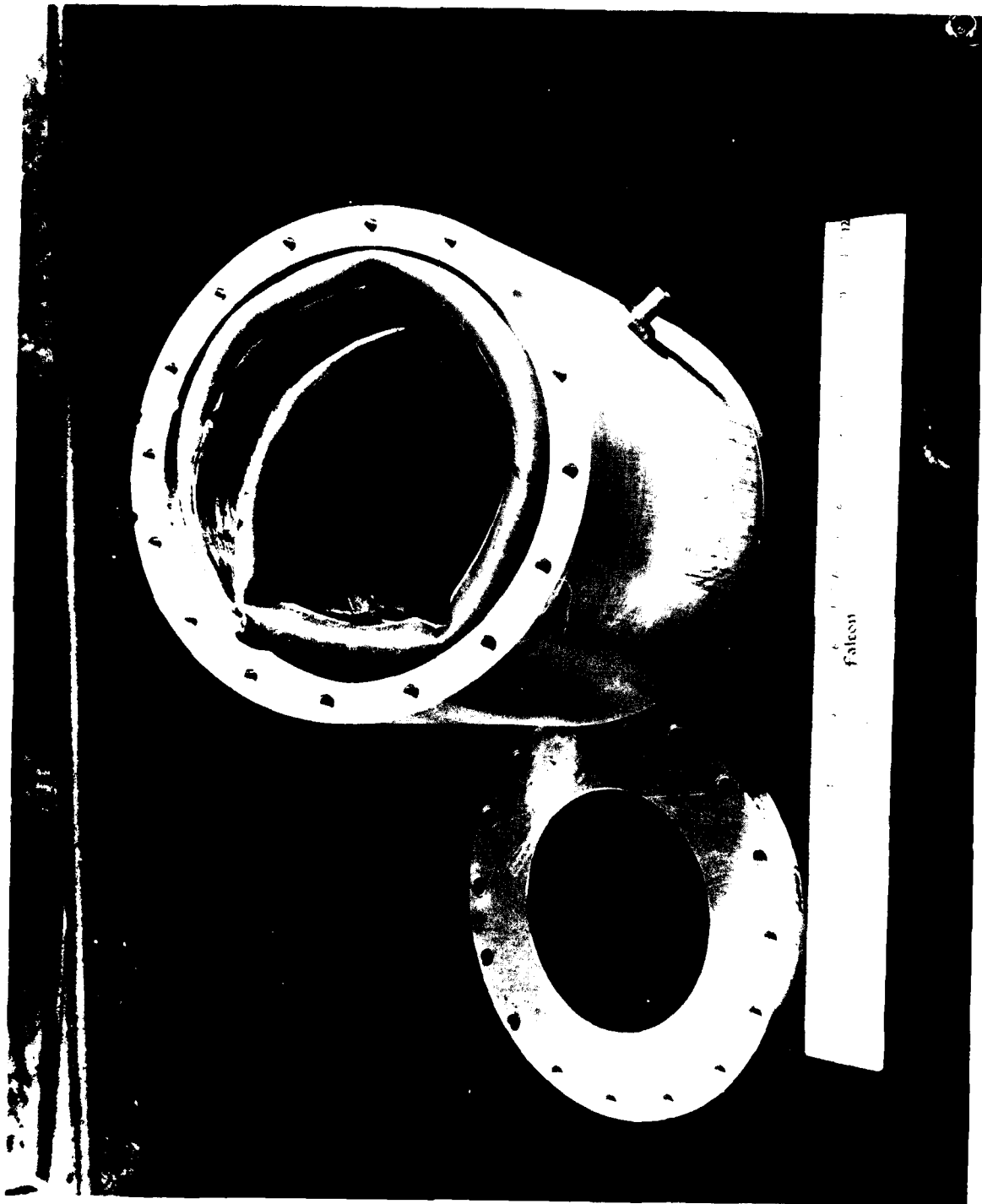


Figure 4.3-5. Photograph of Pressure Vessel

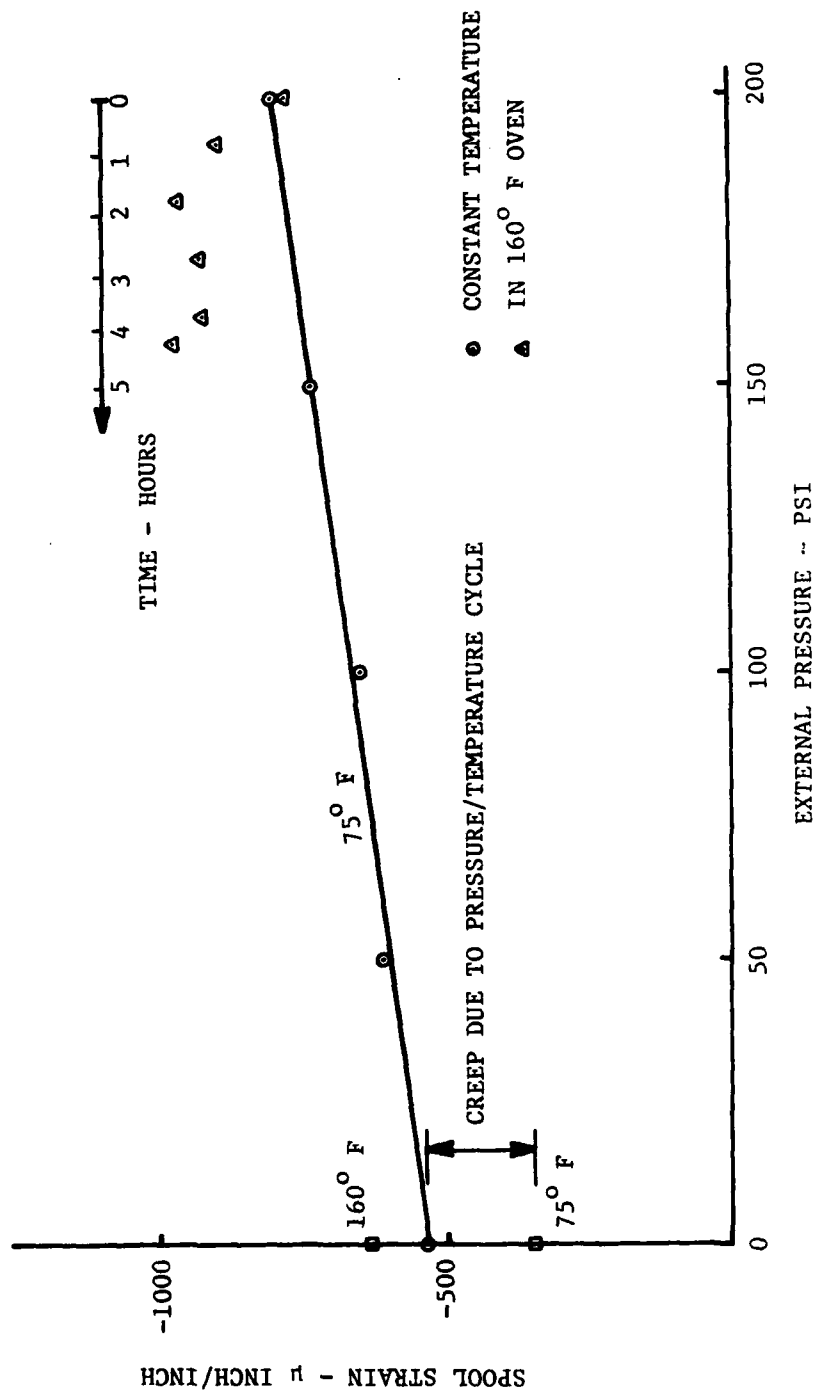


Figure 4.3-6. Spool Strain Versus Applied Pressure

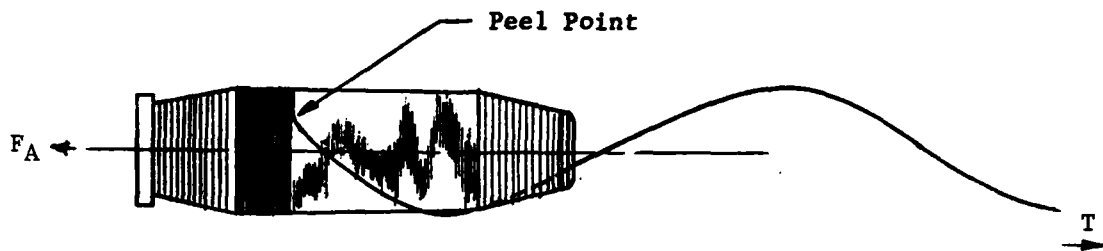


Figure 4.3-B. Cable Dispensing Parameters

The tension T required to dispense cable at a large distance from the bobbin at velocity V is given by

$$T = (1.5 + \alpha)\rho'V^2 + F_A \quad (4.3-4a)$$

where ρ' is the cable lineal density, F_A is the axial bobbin force, and α is an aerodynamic drag factor. The axial bobbin force is generated by friction at the peel point (see figure 4.3-B) and wherever else the cable being dispensed may be touching the bobbin, and depends on the character of the cable coating. The axial bobbin force, spool strain and turbine speed were recorded during the test. The bobbin was successfully dispensed at the first attempt. Cable tension at the turbine was also recorded by a method involving running the cable through three eyes which are offset and then measuring the lateral force on the center eye (see figure 4.3-7). This force can then be related to the tension.

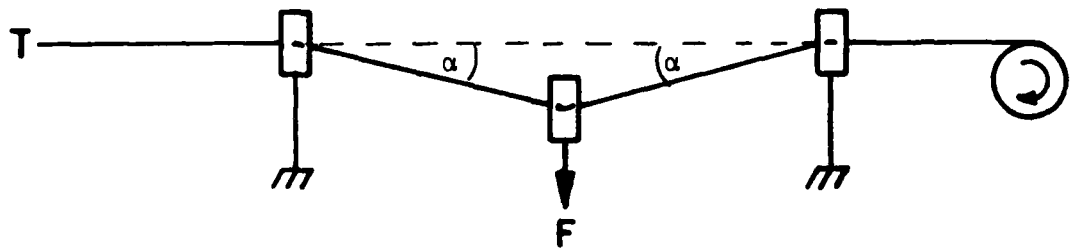


Figure 4.3-7. Cable Tension Measurement Technique

$$T = \rho' v^2 + \frac{F}{2 \sin \alpha} \quad (4.3-5)$$

The axial bobbin force was roughly an order of magnitude higher than was typical for TOW wire, indicating high surface friction on the coating. All pertinent parameters and results are summarized in table 4.3-III.

Bobbin 2. The second experiment consisted of a nonwaveguide cable wound on a spool similar to experiment 1 (see table 4.3-III). The spool strain as a function of layer number is shown in figure 4.3-8. Some relaxation is also evident after winding. The bobbin was placed in a 160° F oven overnight and strain as a function of time is shown in figure 4.3-9. Considerable relaxation had occurred as a result of the temperature cycle. The bobbin was successfully dispensed on the first attempt. The axial bobbin force was more than double that of Bobbin 1.

TABLE 4.3-III. SUMMARY OF EXPERIMENTS

BOBBIN NO	CABLE PARAMETERS						SPOOL PARAMETERS						DISPENSER PARAMETERS				CONDITIONING			PAYOUT TESTING RESULTS					COMMENTS
	Fiber Dia In	Cable Dia In	Coating	* 1 Kfc P lb	Transverse Stiffness K-lb	Length In	Ave Dia In	Length In	Thickness In	Taper Deg	Material	Winding Tension-lb	No of Layers	Max Cable Load lb/in	External Pressure-psi	Temp of Peak Speed-rps	Speed at Failure-rps	Peak Axial Bobbin Force -gm	Peak Tension Force -gm						
1 .029	.005	Hytrel/Svigard		6	1.0	3.5	6	.1	1	6061-T6	.93	15.5	6.3	200	160	400	-	200	600	Successful					
2 .011	.005	WCC-2	Not Waveguide		.83	3.5	6	.1	1	6061-T6	.54	8		0	160	400	-	500	400	Successful					
3 .013	.005	WCC-2		27.5	1.22	3.5	6	.1	1	6061-T6	.2	9.5				320	320	190	370	Multiple breaks					
4 .0104	.004	DeSoto 8		12.8	.53	3.5	6	.1	1	6061-T6	.3	3.5				540	480	170	600	Partially successful					
5 .0107	.005	DeSoto 8			.48	3.55	3	.1	1	6061-T6	.39	10				550	450	80	550	Partially successful					
6 .010	.005	WCC-2		27.5	.63	3.5	4.5	Inside payout	1	-		6.5				300	300	20	250	Multiple breaks					
7 .008	.004	WCC-2		62	.99	3.5	4.5	.1	1	6061-T6	.28	8								Could not be dispensed					
8 .008	.004	WCC-2		62	.79	3.5	4.5	Inside payout	1	-		7								Could not be dispensed					
9 .012	.0042	WCC-2	14.5	14	.50	3.5	3	.1	1	6061-T6	.34	10				330	330	60	-	1 bobbin break & additional during restraining					
10 .008	.004	WCC-2		62	.98	7.8	2	.05	1	6061-T6	.42	10								Could not be dispensed					
11 .012	.0042	DeSoto 8	15.7	15.6	1.16	3.5	4.5	.1	1	6061-T6	.39	14				400	-	120	-	Successful					
12 .016	.004	Hytrel/Svigard		4.5	.98	3.5	4.5	.1	1	6061-T6	.54	18													
13 0.13	.00415	WCC-2		26.6	1.01	3.5	4.5	.1	1	6061-T6	.36	12								To be dispensed in the future					
14 .013	.009	A1		13	.1	3.5	4.5	.1	1	6061-T6		3													
15 .012	.004	DeSoto 8			.86	3.5	6	.1	1	6061-T6	.4	7.5													

*P = cable lineal density

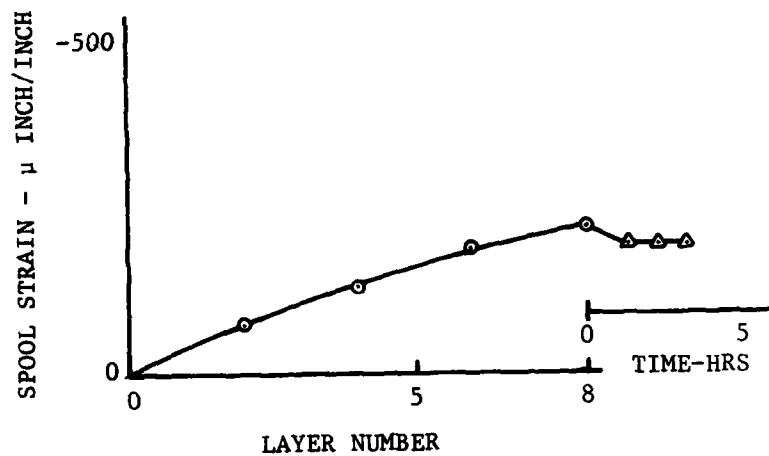


Figure 4.3-8. Bobbin 2, Spool Strain Versus Number of Layers

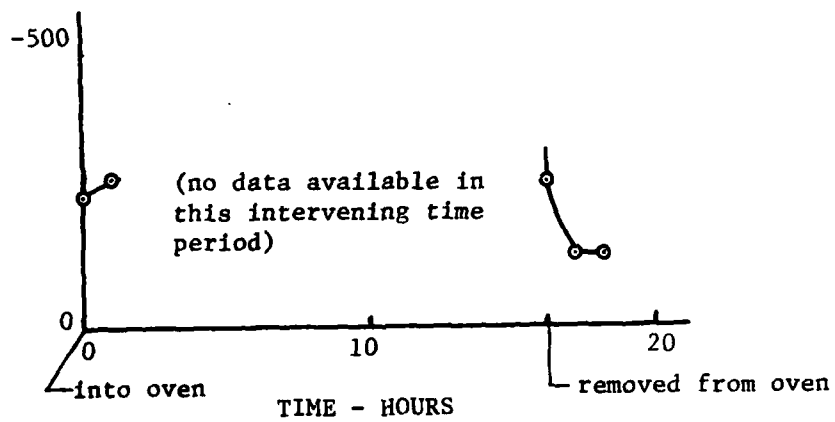


Figure 4.3-9. Bobbin 2, Spool Strain Versus Time

Bobbin 3. This bobbin was wound as shown in table 4.3-III. The results of the squeeze test are shown in figure 4.3-10. The stiffness of the WCC-2 coating is higher than that previously measured on Bobbin 1. The spool strain due to winding is shown in figure 4.3-11 as a function of layer number. The effect on spool strain due to pressure and subsequent temperature is shown in figure 4.3-12. Four attempts at payout of Bobbin 3 resulted in breakage at the takeup reel, making the means of attachment to the reel suspect. The attachment mode was changed, and on the fifth attempt failure occurred at the bobbin. This made the cable itself suspect. The remainder of the cable was returned to ITT for proof testing. It was discovered that the adhesive was damaging the coating and ITT submitted photographs shown in figure 4.3-13. Examination of break ends with the scanning electron microscope (SEM) revealed an inclusion in the glass fiber in one of the ends; a SEM photograph is shown in figure 4.3-14.

Bobbin 4. This bobbin was wound with a cable having a different coating. The results of the squeeze test are shown in figure 4.3-15. The spool strain during winding is shown in figure 4.3-16 as a function of layer number. The effect due to pressure and subsequent temperature is shown in figure 4.3-17. The creep due to the pressure/temperature cycle is slight because of the small number of layers. Bobbin 4 dispensed successfully down to the bottom layer and failed after dispensing 1/3 of this layer. Examination of the end showed a large eccentricity between the fiber and the buffer coating. The payout failure is believed to be the result of this large eccentricity.

Bobbin 5. When short lengths of smaller diameter cable are wound, only a few layers result on the 6-inch long spool; therefore a 3-inch long spool was designed as shown in figure 4.3-18. This bobbin was representative of design number 2. The spool strain resulting from winding cable is shown in figure 4.3-19. Since the spool is short, the last layers have relatively few turns because of the step back for each layer. Thus the effect of the spool ends is to reduce the strain as shown in figure 4.3-19. Bobbin 5 dispensed successfully down to the bottom layer and failed after dispensing 1/2 of this layer. The end also showed a large eccentricity between the fiber and the buffer coating. A SEM photograph is shown in figure 4.3-20. An examination of figure 4.3-20 indicates that the first point of initiation of the fracture of the glass was adjacent to the thinnest

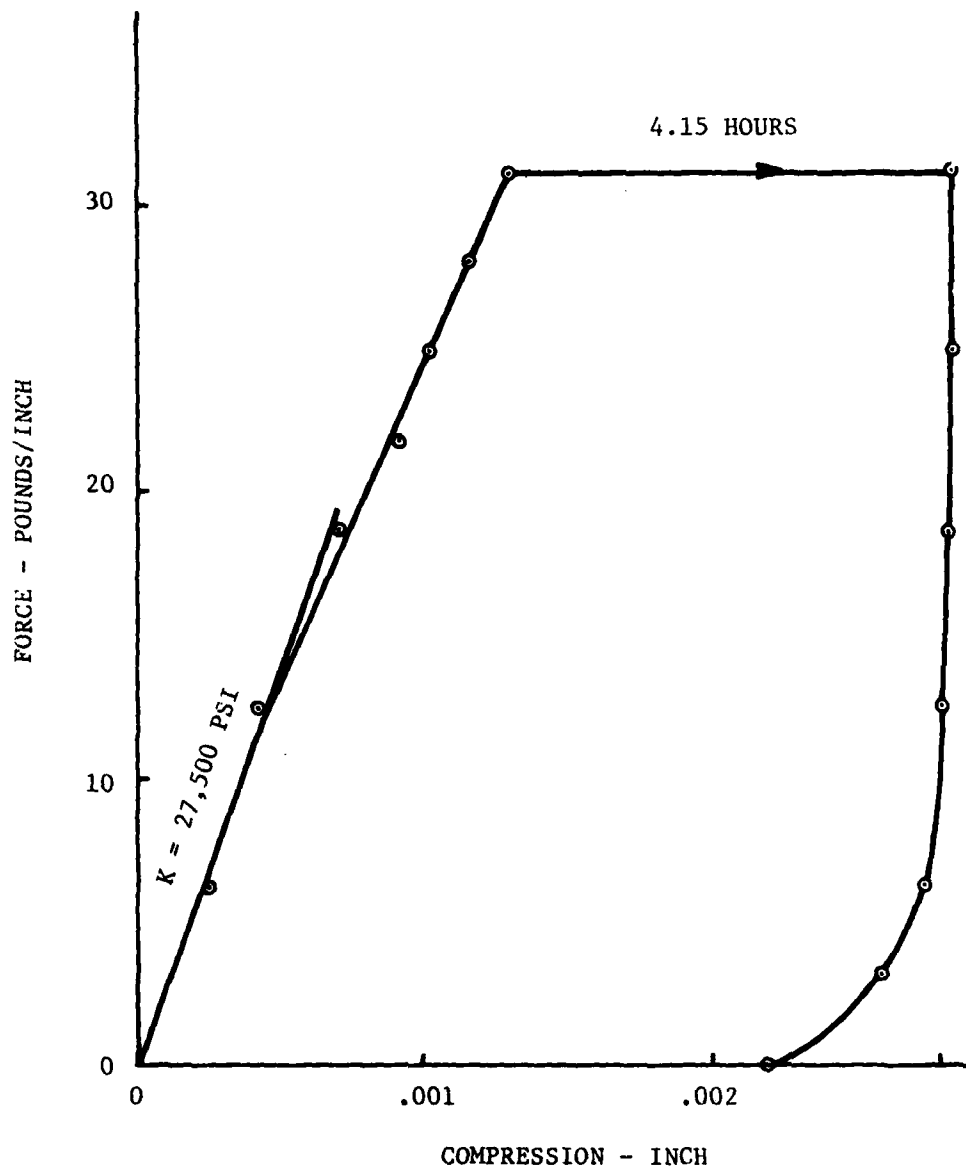


Figure 4.3-10. Bobbin 3, Cable Force-Displacement Characteristics

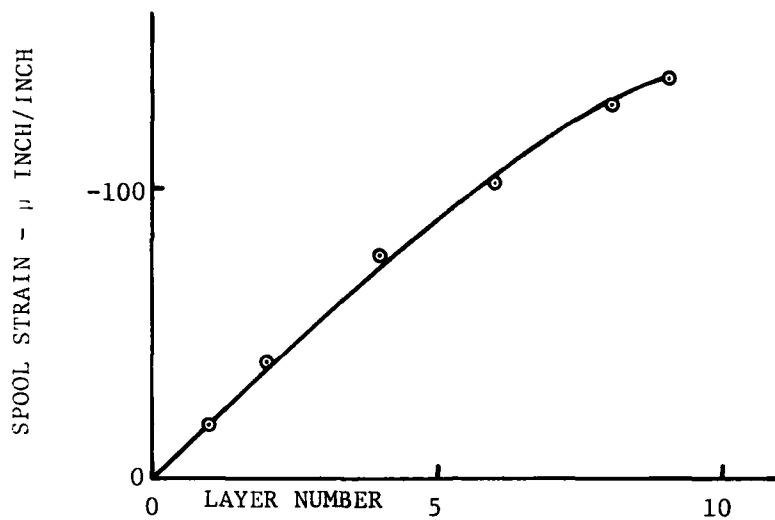


Figure 4.3-11. Bobbin 3, Spool Strain Versus Number of Layers

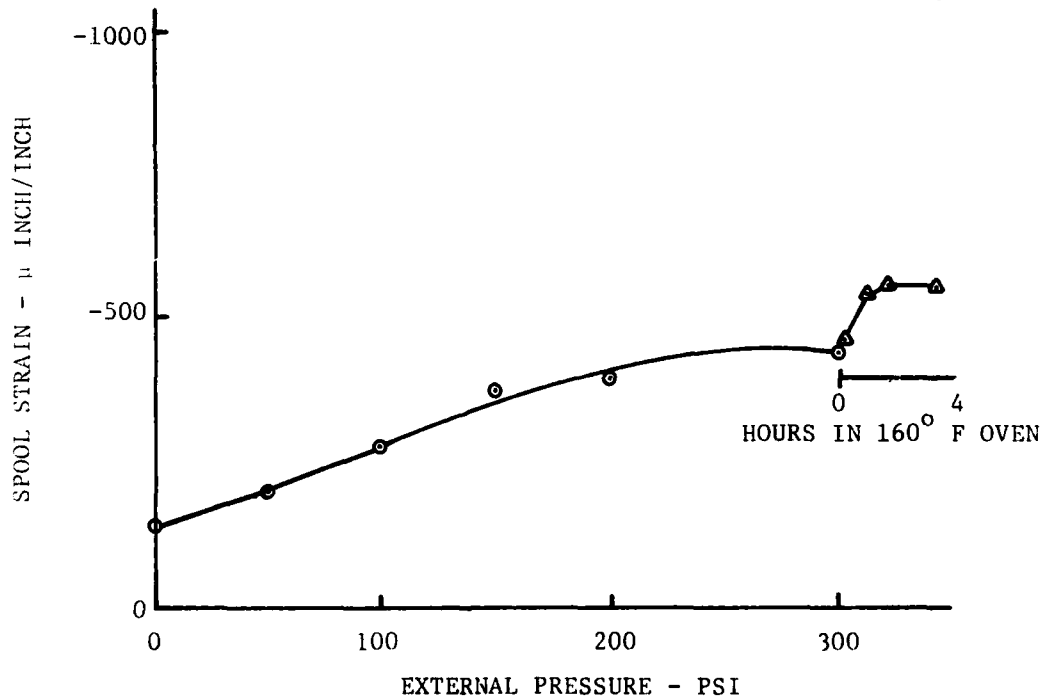
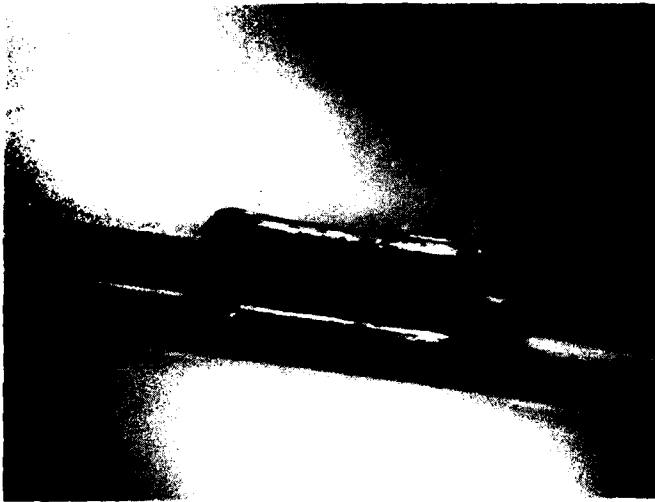


Figure 4.3-12. Bobbin 3, Spool Strain Versus Applied Pressure and Time



Photograph No. 1

.020" of fiber coating attached to adjacent wrap. Note inside diameter of fiber coating. Approximately same diameter as glass.



Photograph No. 2

Similar to photograph No. 1, except at another location.



Photograph No. 3

Glass core of fiber (cable) intact. Cable jacket stripped away.



Figure 4.3-14. Inclusion in Glass Fiber - Bobbin 3

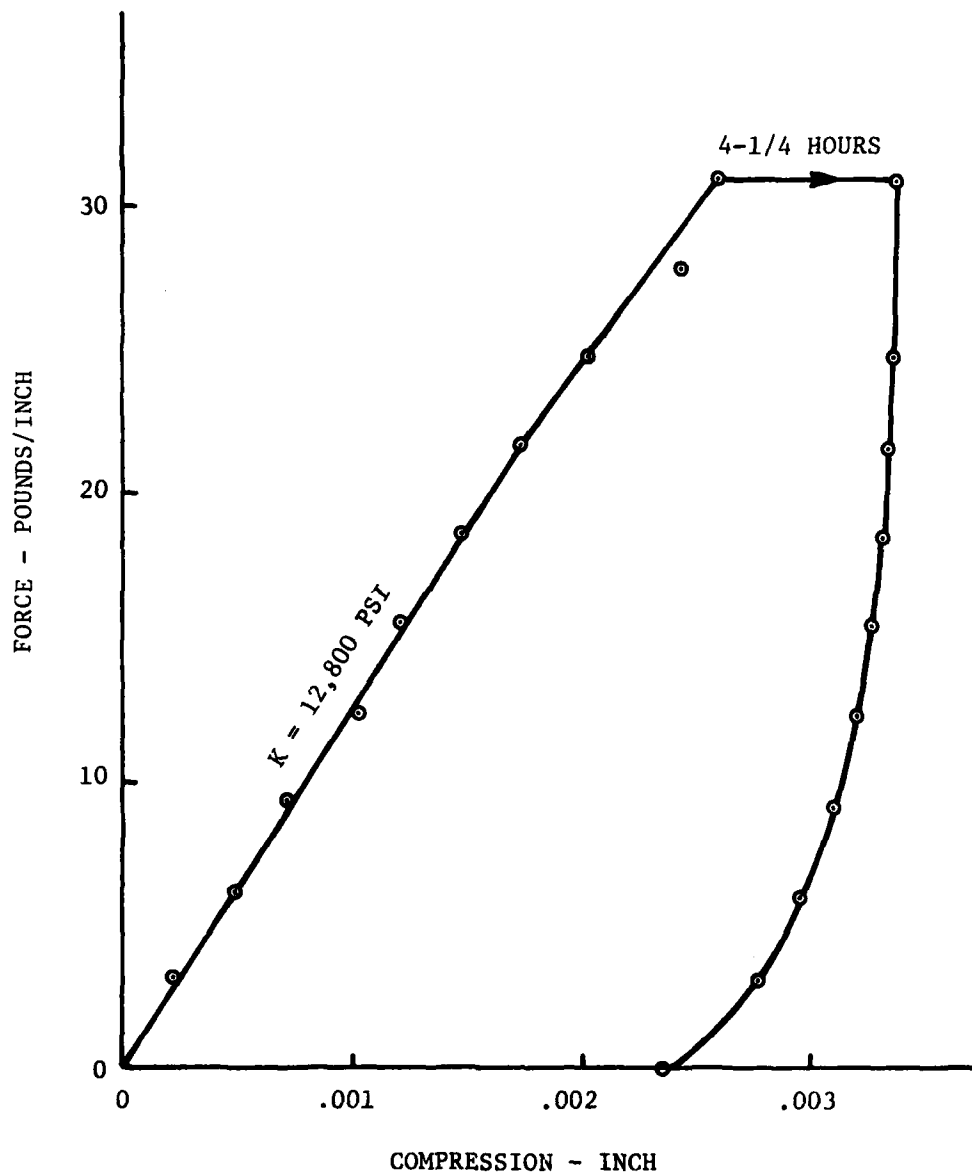


Figure 4.3-15. Bobbin 4, Cable Force-Displacement Characteristics

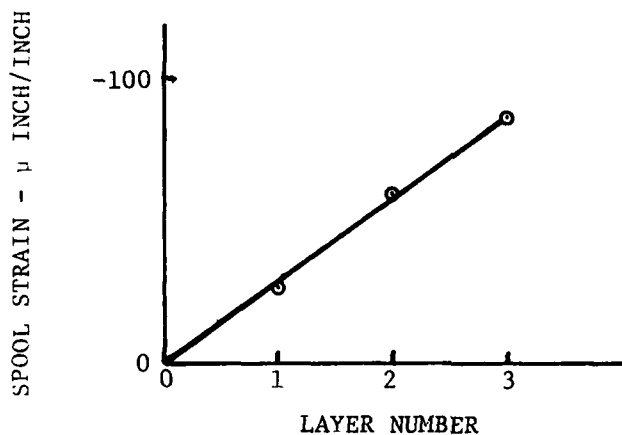


Figure 4.3-16. Bobbin 4, Spool Strain Versus Number of Layers

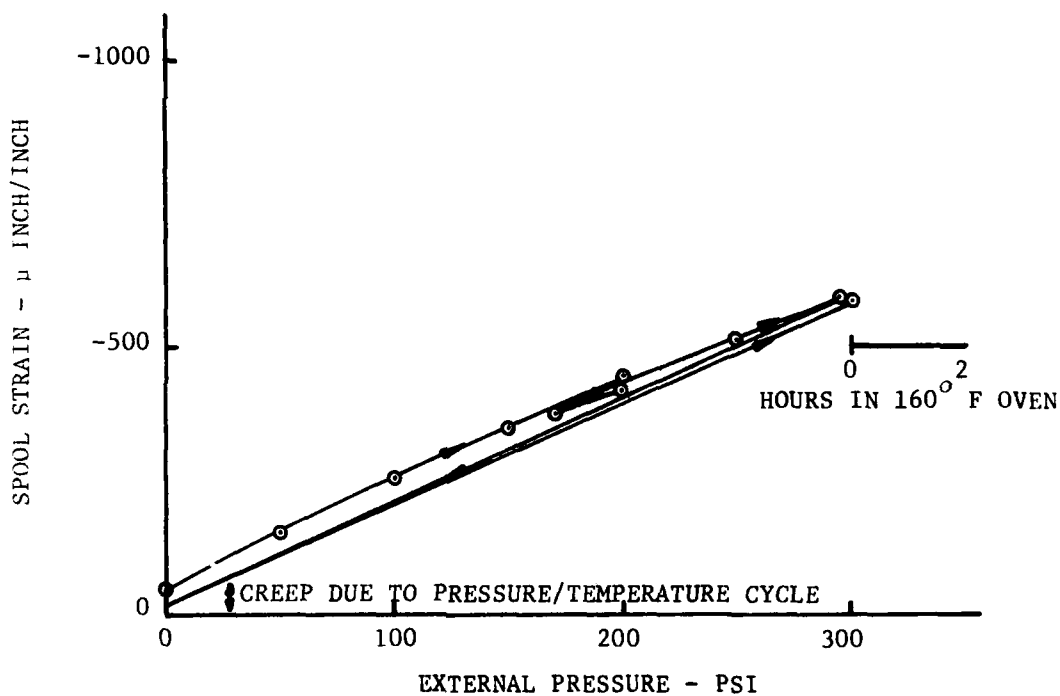


Figure 4.3-17. Bobbin 4, Spool Strain Versus Applied Pressure and Temperature

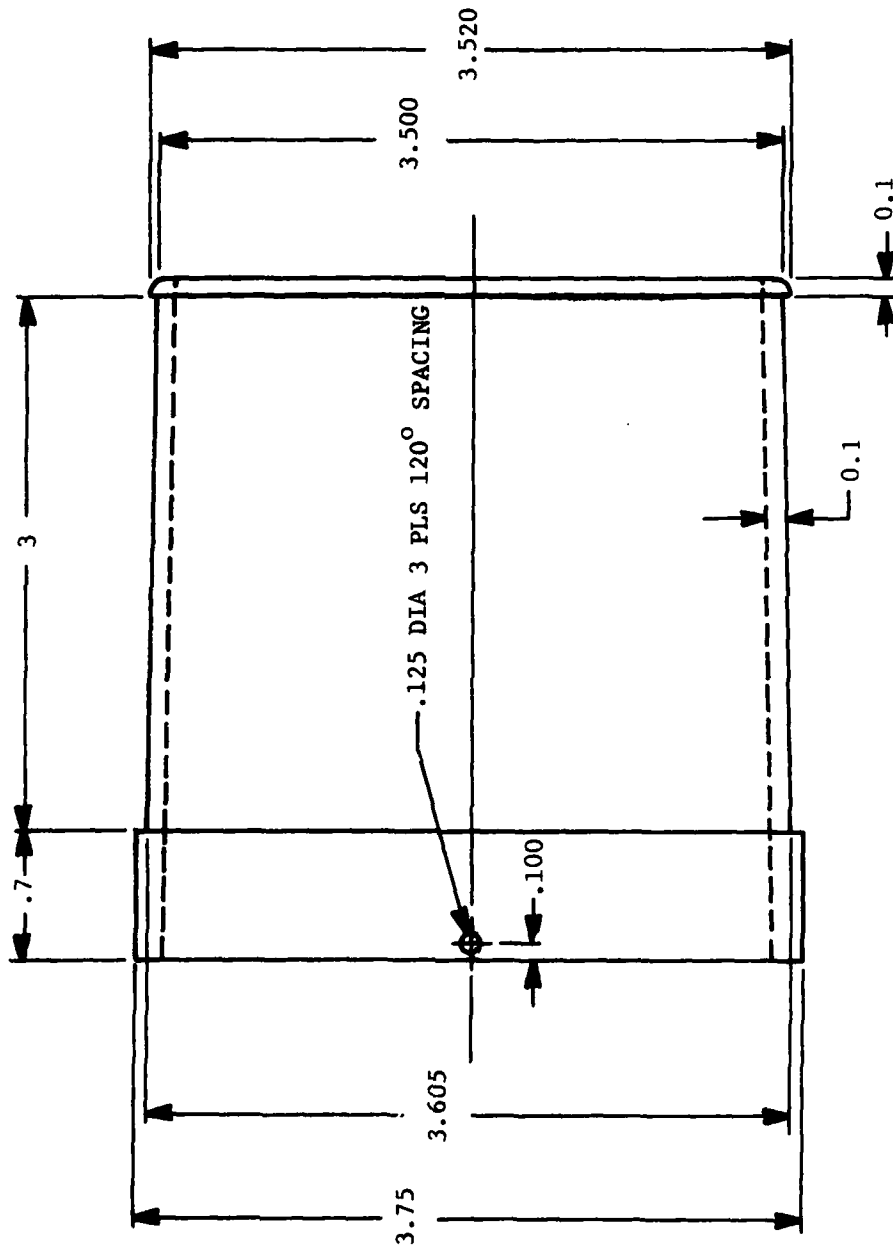


Figure 4.3-18. Bobbin 5, Spool Gear Try

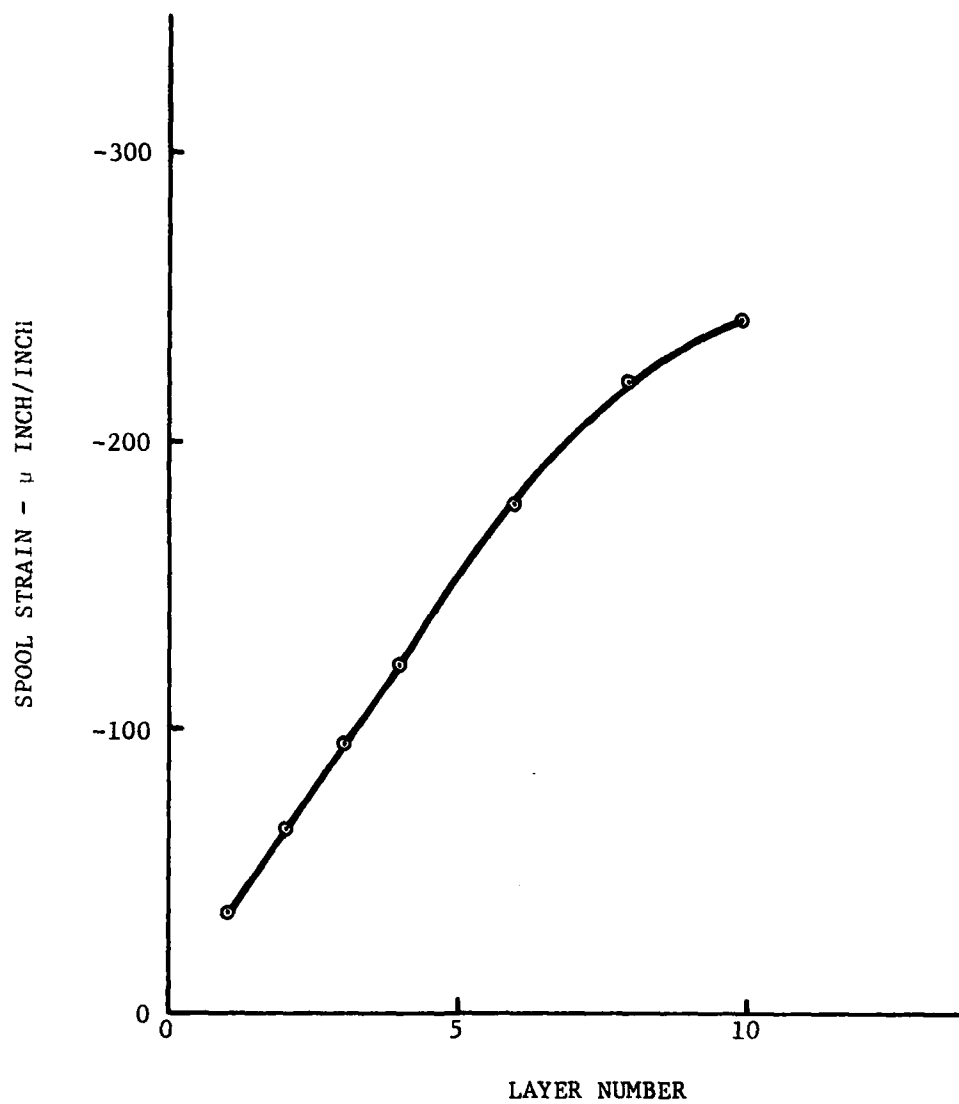


Figure 4.3-19. Bobbin 5, Spool Strain Versus Number of Layers



Figure 4.3-20. SEM Photograph of Failed End
From Bobbin 5 Payout Test

section of the buffer coating which was less than 0.001 inch (25 μ m) in thickness at that point. The large eccentricity between fiber and buffer coating is the result of a difficulty in manufacturing.

Bobbin 6. Bobbin 6 was an attempt to wind a bobbin which would dispense from the inside out and was representative of design number 4. A spool measuring 4-1/2 inches in length was designed as shown in figure 4.3-21. Two layers of number 30 enamelled wire with an OD of 0.0114 inch were wound on the spool for a base. Both wound in the same direction in two pieces. On top of these the fiber optic cable was wound and each layer was sprayed with an acrylic adhesive. Upon completion of winding, a "can" was placed over the bobbin and the space between was filled with foam. After the foam had set, the base layers were pulled out so that the spool could be withdrawn exposing the inner layer of cable which could now be dispensed from the inside. Such a cable pack has very little interlayer pressure but must be held together with adhesive. Three attempts were made to dispense Bobbin 6. In each case failure occurred at the peel point before maximum speed was reached. Failure has been attributed to the buffer-adhesive incompatibility as described with Bobbin 3.

Bobbin 7. Bobbin 7 was wound on a 4-1/2 inch long spool with small diameter cable (0.008 inch). The results of the squeeze test are plotted in figure 4.3-22 and reveal a high stiffness. The spool strain as a result of winding is shown in figure 4.3-23. The data suggests a drop in winding tensions subsequent to the second layer. Bobbin 7 could not be dispensed on the payout test facility because the adhesive damaged the coating such that the glass was exposed. Figure 4.3-24 shows the damage.

Bobbin 8. This was another inside payout bobbin, similar to Bobbin 6. Two layers of 0.009 inch enamel-coated wire were wound on the spool to facilitate removal of the spool after encapsulation of the cable pack. A photograph is shown in figure 4.3-25. This bobbin could not be dispensed for the same reason as number 6 and 7.

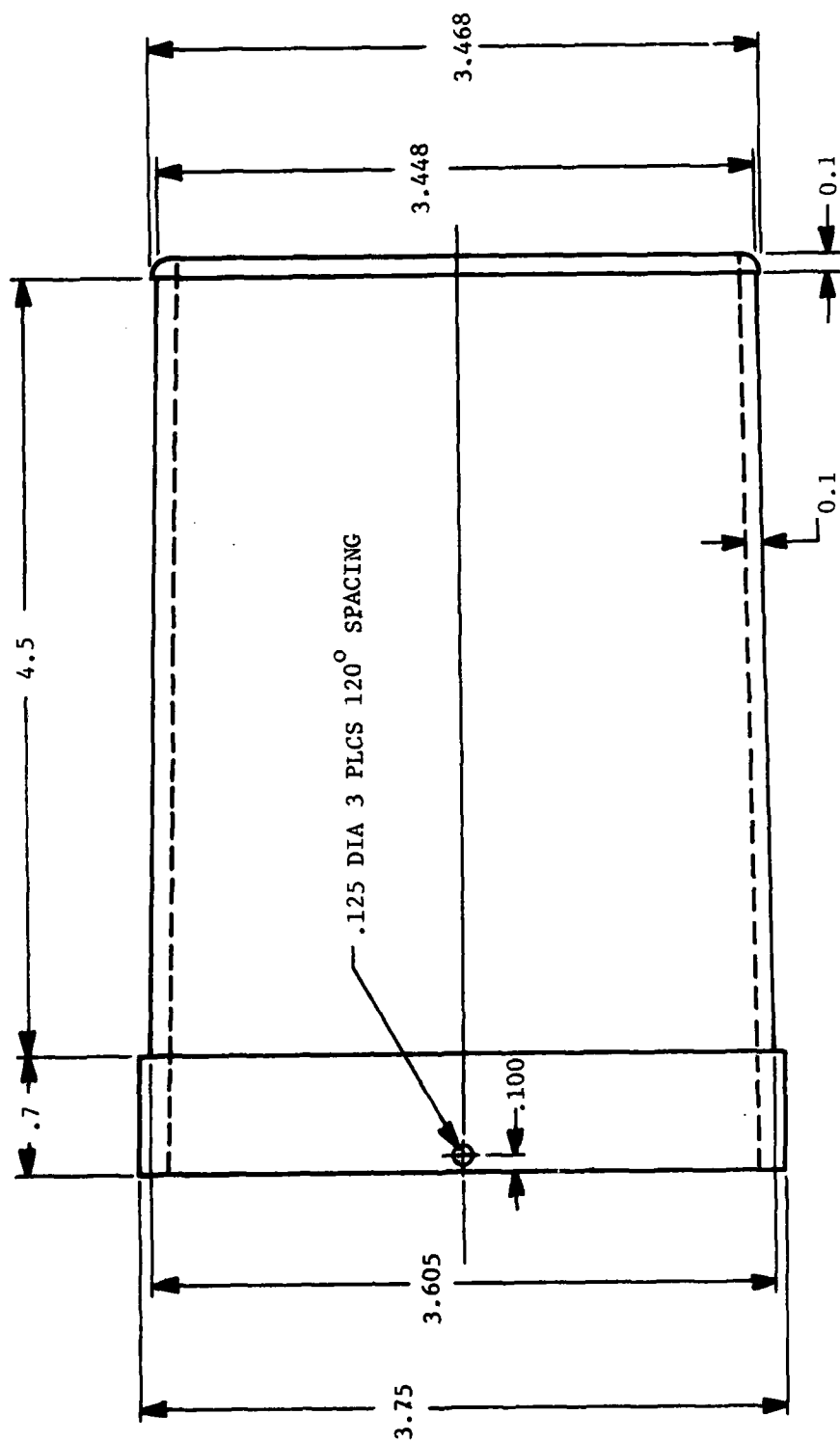


Figure 4.3-21. Bobbin 6, Spool Geometry

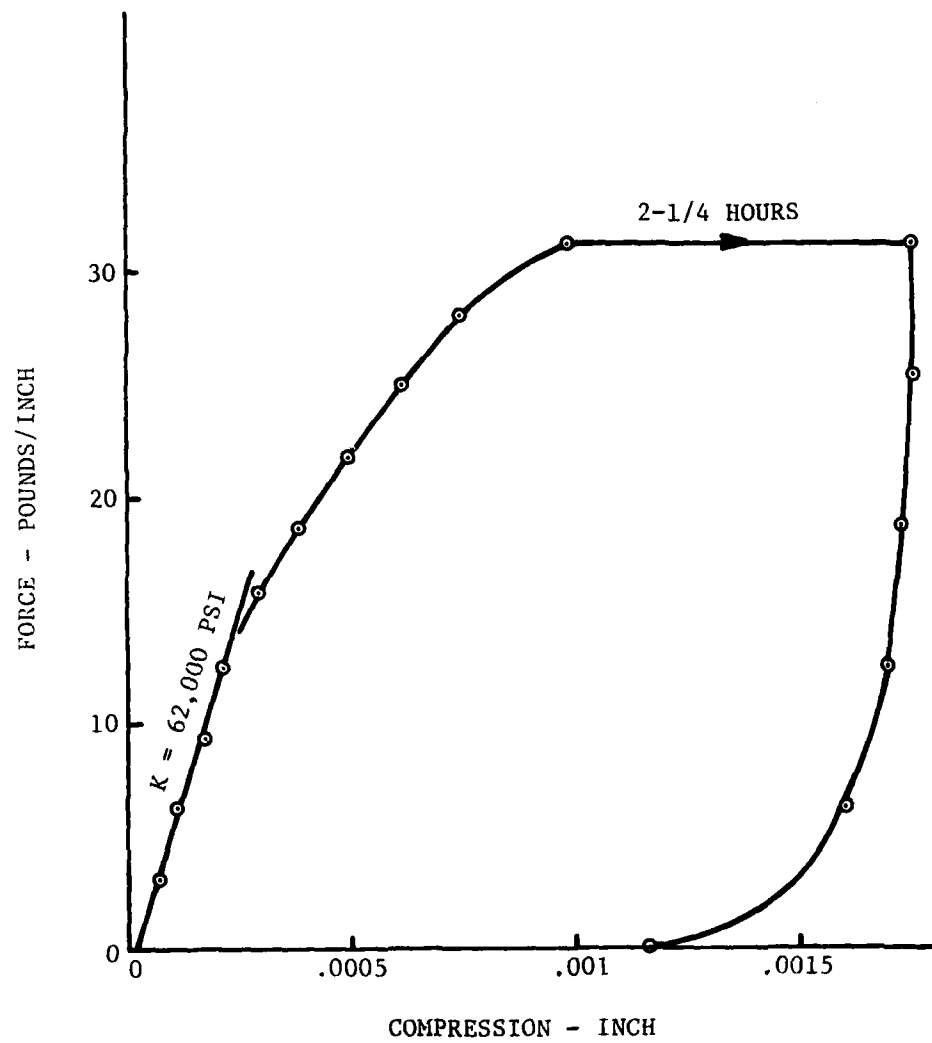


Figure 4.3-22. Bobbin 7, Cable Force-Displacement Characteristics

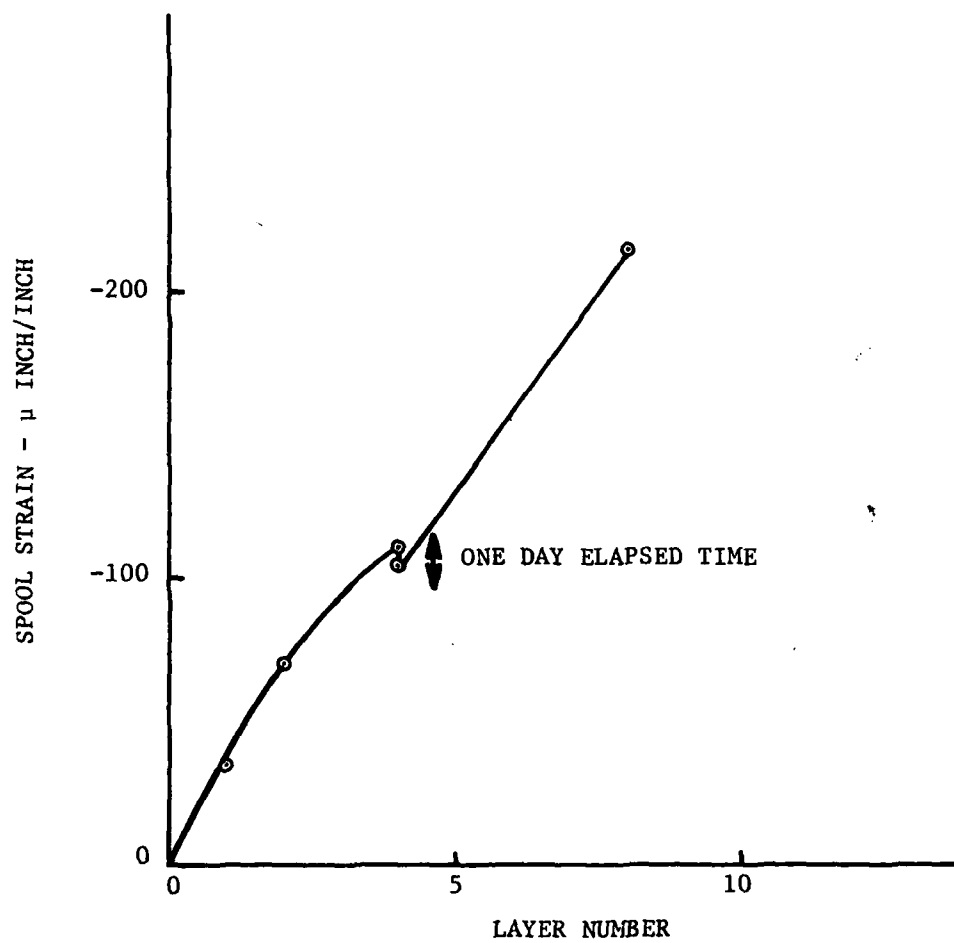


Figure 4.3-23. Bobbin 7, Spool Strain Versus Number of Layers

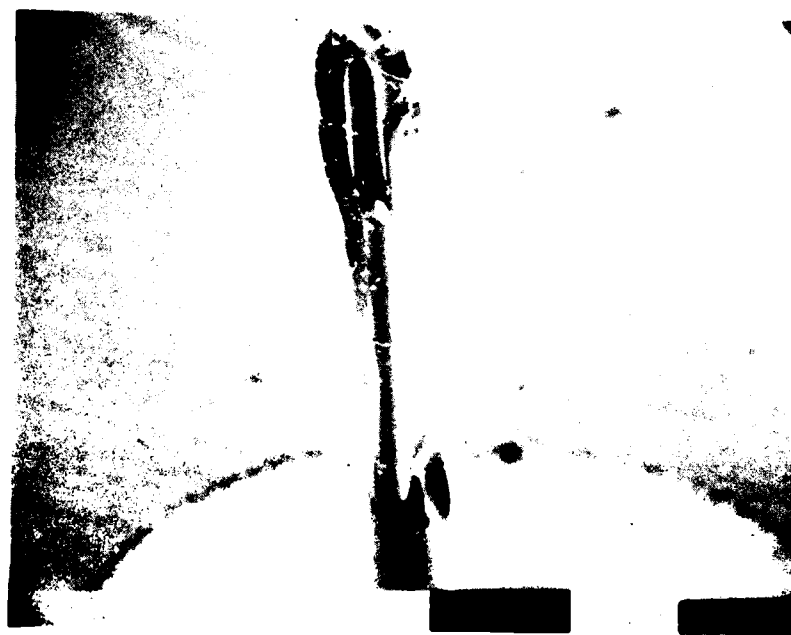


Figure 4.3-24. Bobbin 7 - Failed Ends

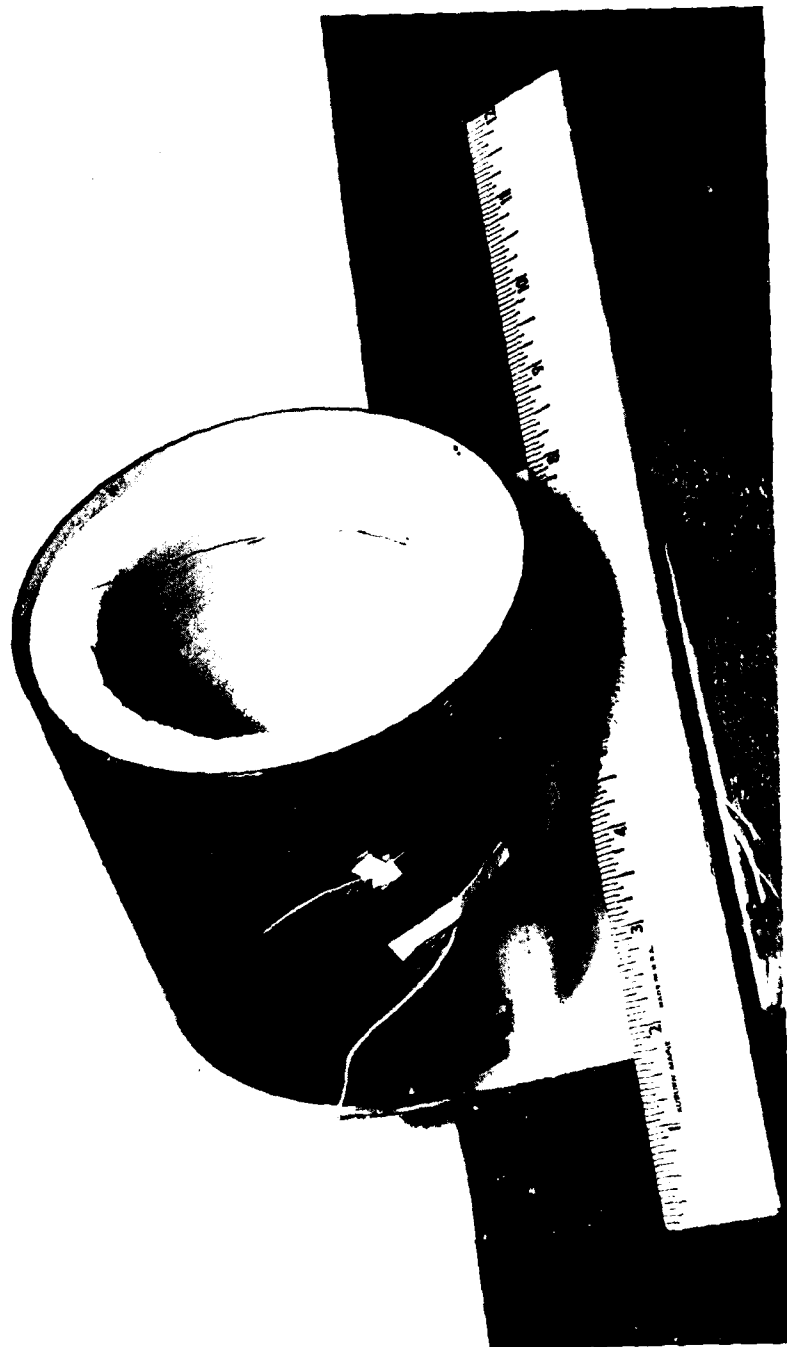


Figure 4.3-25. Photograph of Bobbin 8

AD-A079 633

HUGHES AIRCRAFT CO TUCSON AZ MISSILE DEVELOPMENT DIV
HIGH STRENGTH RAPID PAYOUT FIBER OPTIC CABLE ASSEMBLY. (U)
AUG 79 D S FOX, R A EISENTRAUT

F/G 20/6

DAAB07-78-C-2964

UNCLASSIFIED

FR7956-0003

CORADCOM-78-2964-1

NL

2 of 2
ALC 2
10/20/80



END
DATE
FILED
2 - 80

DDC

Bobbin 9. Bobbin 9 was wound on a short spool of the same diameter as Bobbin 7, but with larger diameter cable (see table 4.3-III). The squeeze test data is plotted in figure 4.3-26 and is linear in the region tested. Creep recovery is almost complete also. The spool strain resulting from winding is shown in figure 4.3-27. It reveals the end effects of the short spool and a change in winding tension subsequent to layer four. A photograph is shown in figure 4.3-28. One attempt was made to dispense this bobbin on the turbine pay out facility. The cable broke on the bobbin almost immediately, and on restringing, additional breaks occurred. Again, adhesive-buffer incompatibility was concluded to be the cause of failure.

Bobbin 10. Bobbin 10 was representative of dispenser design number 3, employing the large diameter spool. The test spool is shown in figure 4.3-29, and the pressure vessel which was designed for the 6-inch long spool is shown in figure 4.3-30. An adapter was designed such that the shorter test spool would fit into the pressure vessel. The spool strain is shown in figure 4.3-31. Again the effect of a short spool with rapidly decreasing number of turns per layer can be seen. A photograph of the bobbin is shown in figure 4.3-32. This one could not be dispensed because of coating damage from the adhesive.

Bobbin 11. Bobbin 11 was a 3-1/2 inch diameter spool wound with a cable having a thicker coating of DeSoto 8 than used in earlier bobbin experiments (see table 4.3-III). The results of the squeeze test are shown in figure 4.3-34. This one dispensed successfully on the second attempt. On the first attempt, the cable broke at the take-up reel after pulling off approximately one layer. Failures at the take-up reel are encountered quite frequently and are not normally considered as payout failures.

Bobbin 12. Bobbin 12, which was representative of design number 5, was wound with a coating similar to Bobbin 1. The cable diameter was reduced from that used in Bobbin 1, but significantly larger than all other prior experiments. The squeeze test data is shown in figure 4.3-35 and is the first to show a stiffening effect. Creep recovery was also limited. The spool strain resulting from the winding is shown in figure 4.3-36. The wound bobbin is illustrated in figure 4.3-37. The effect of creep can be seen especially in the decrease in strain overnight. An increase in winding tension is also suggested on the second day.

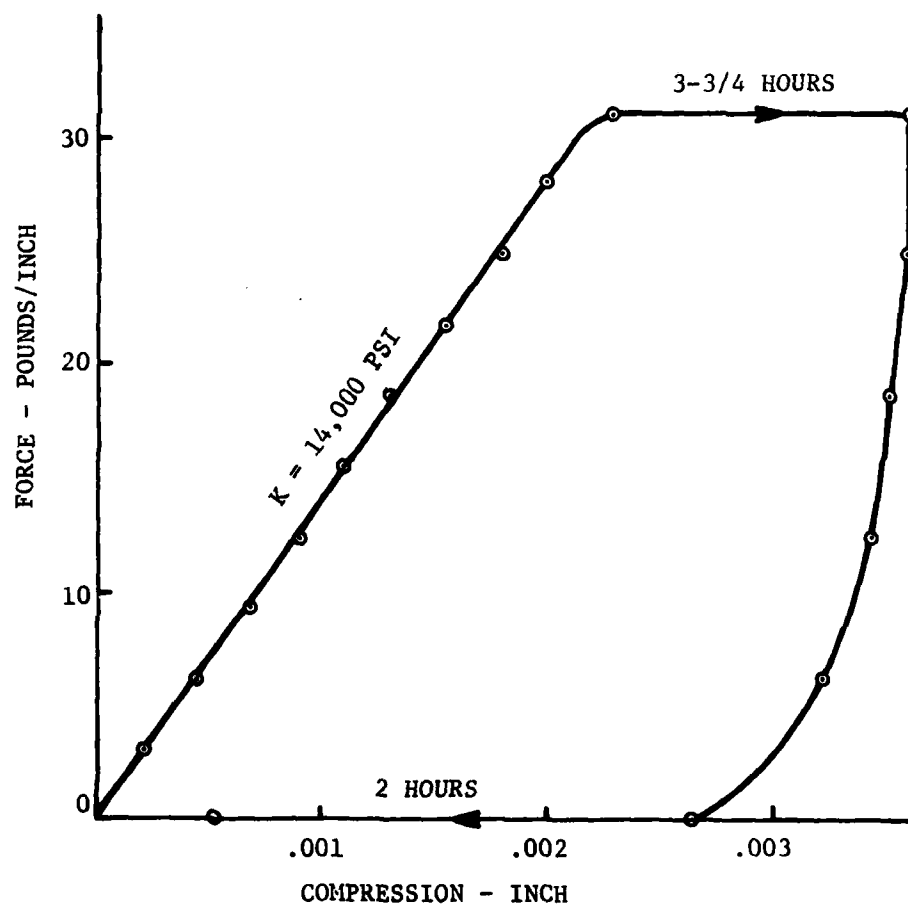


Figure 4.3-26. Bobbin 9, Cable Force-Displacement Characteristics

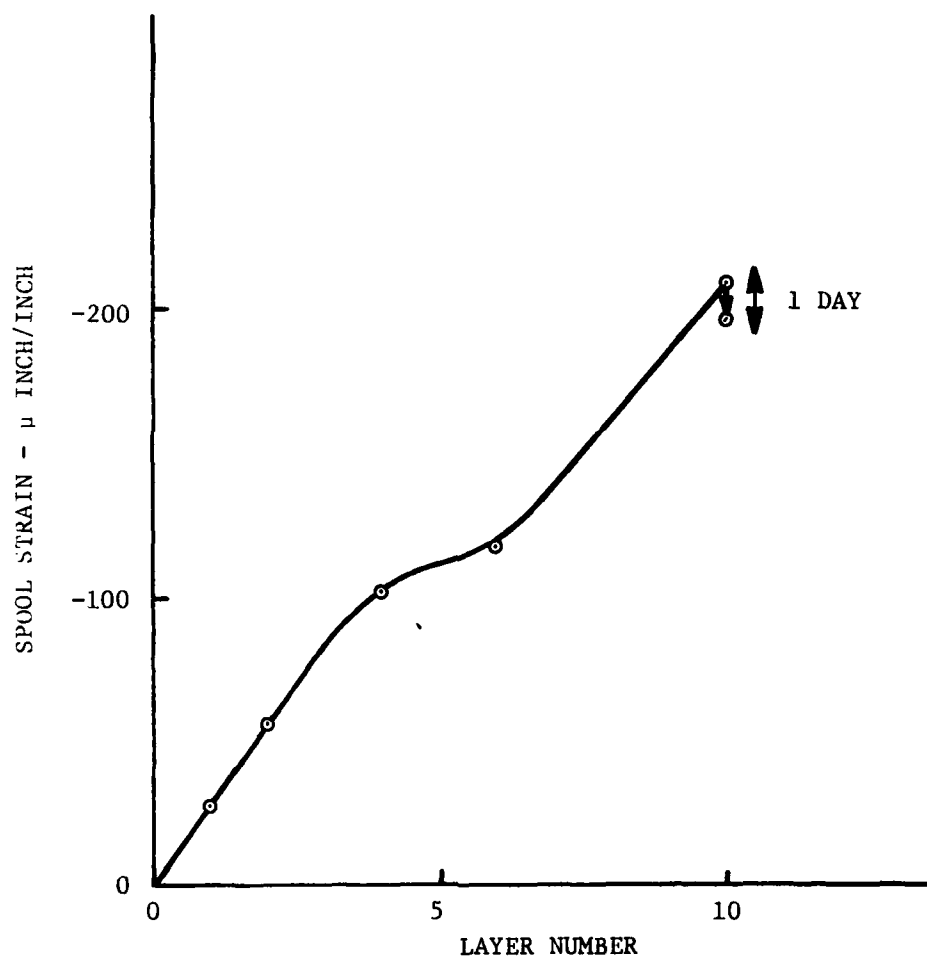


Figure 4.3-27. Bobbin 9, Spool Strain Versus Number of Layers



Figure 4.3-28. Photograph of Bobbin 9

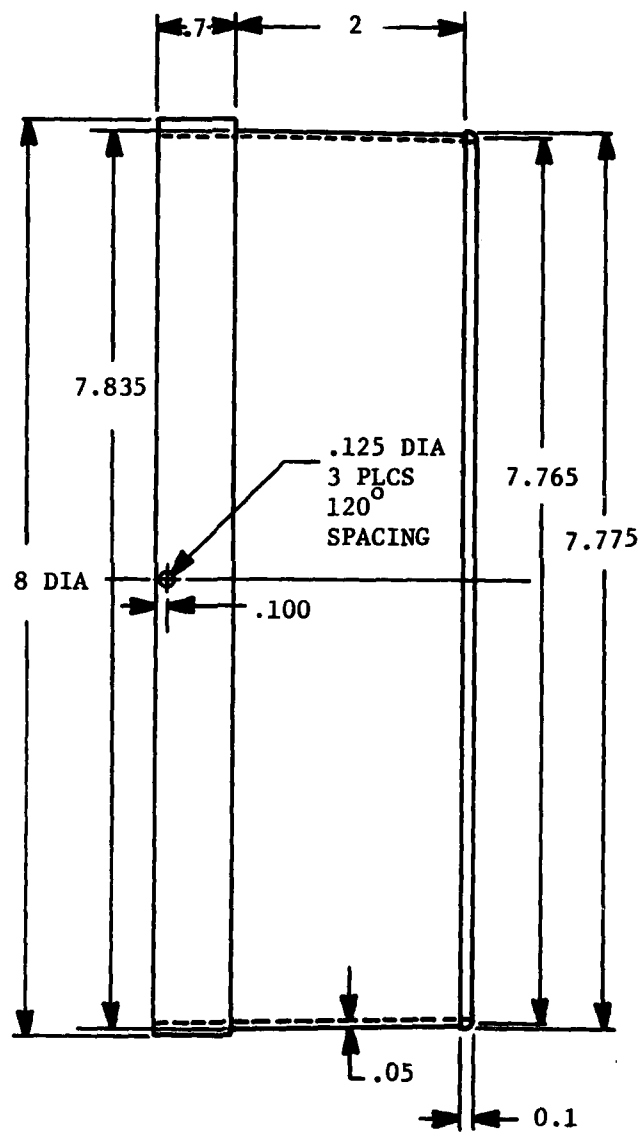


Figure 4.3-29. Test Bobbin 10, Spool Geometry

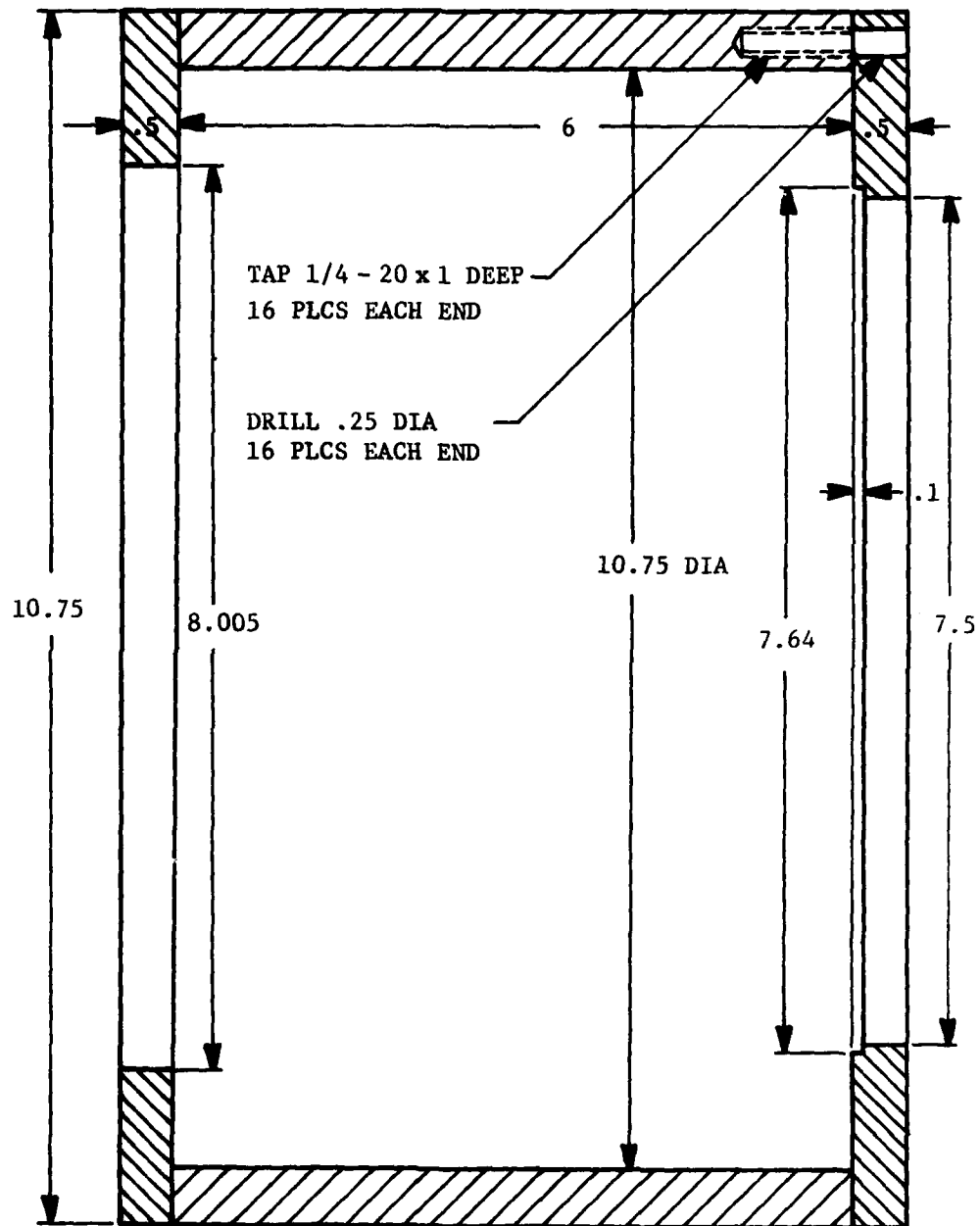


Figure 4.3-30. Bobbin 10, Pressure Vessel Geometry

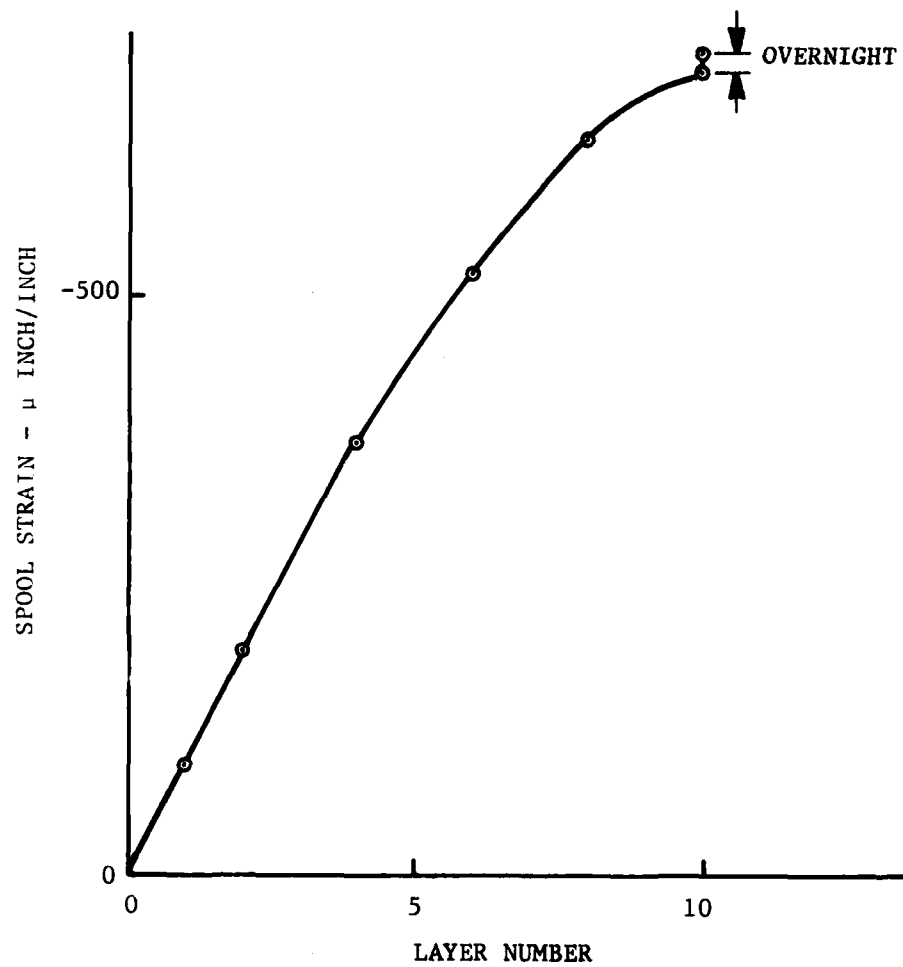


Figure 4.3-31. Bobbin 10, Spool Strain Versus Number of Layers

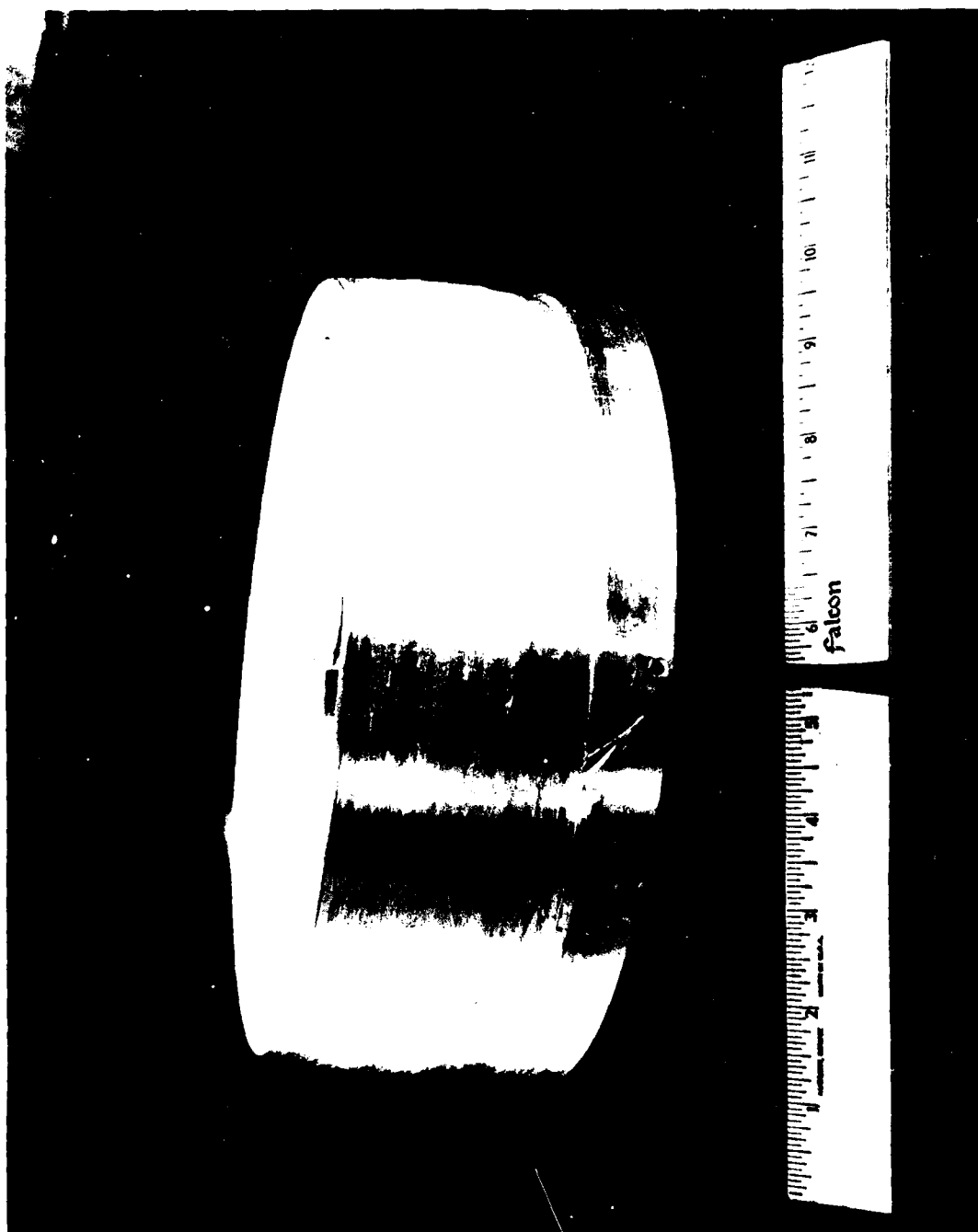


Figure 4.3-32. Photograph of Bobbin 10

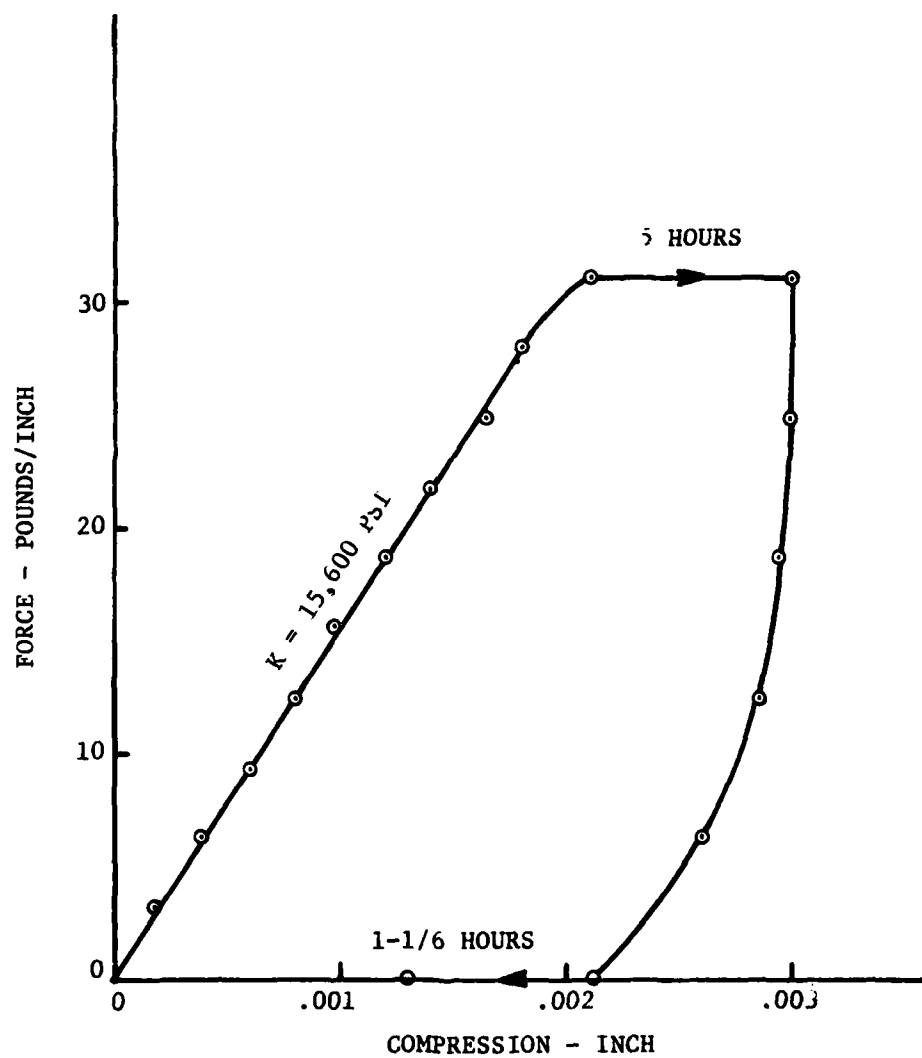


Figure 4.3-33. Bobbin 11, Cable Force-Displacement Characteristics

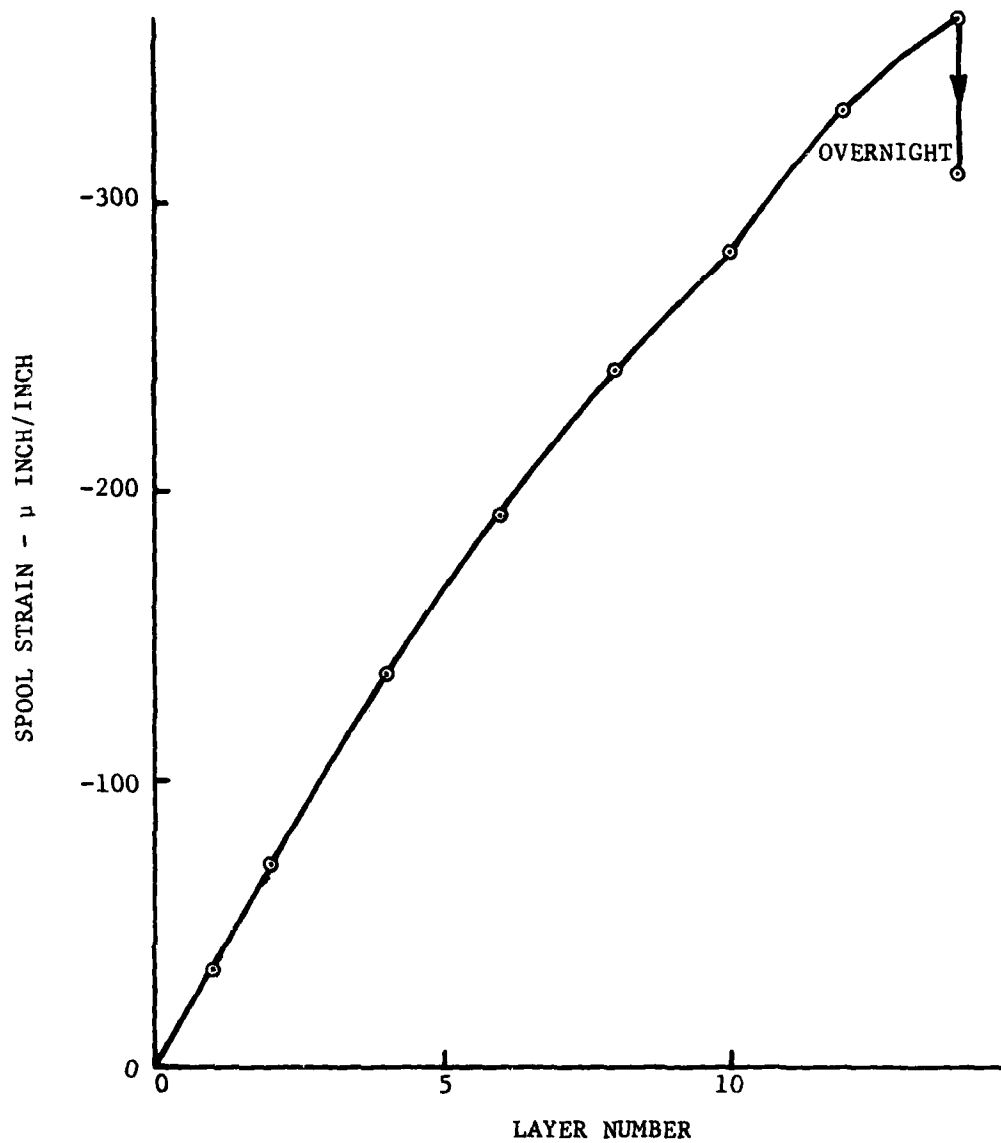


Figure 4.3-34. Bobbin 11, Spool Strain Versus Number of Layers

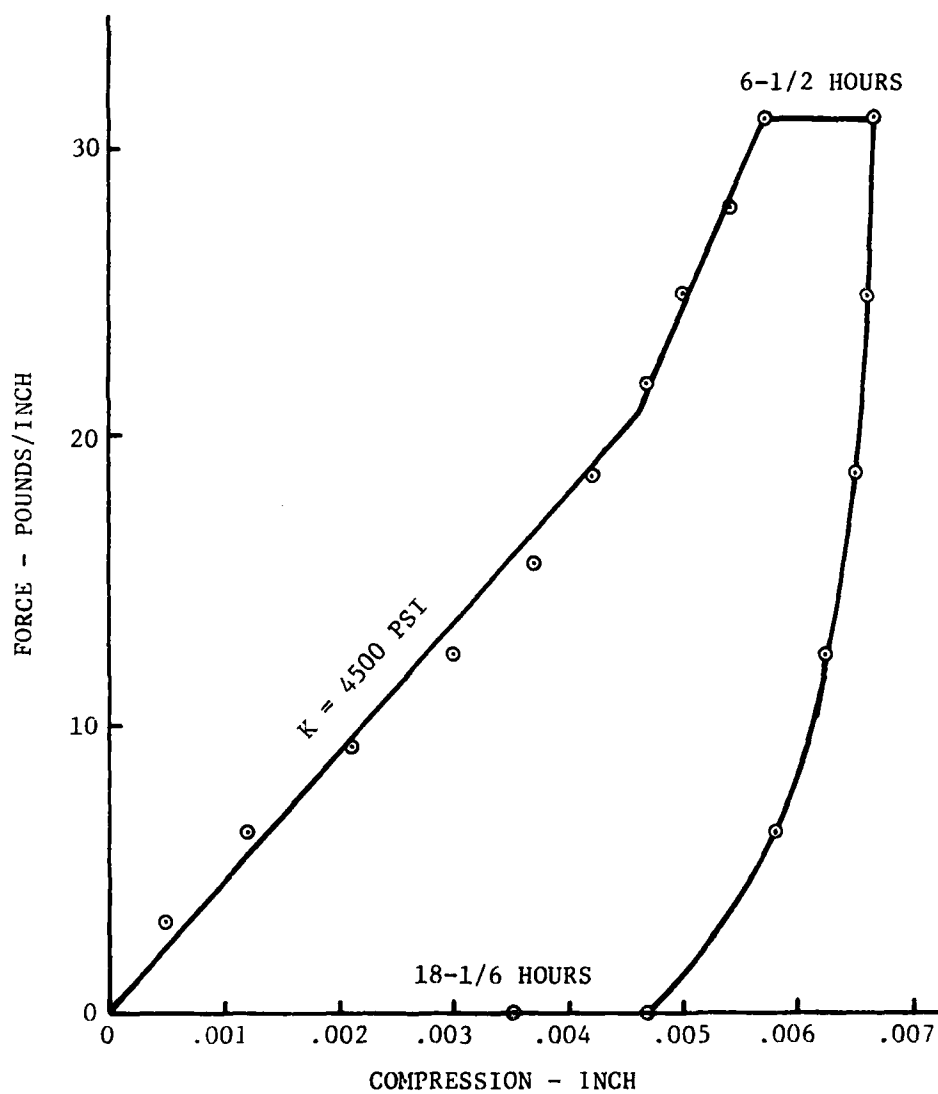


Figure 4.3-35. Bobbin 12, Cable Force-Displacement Characteristics

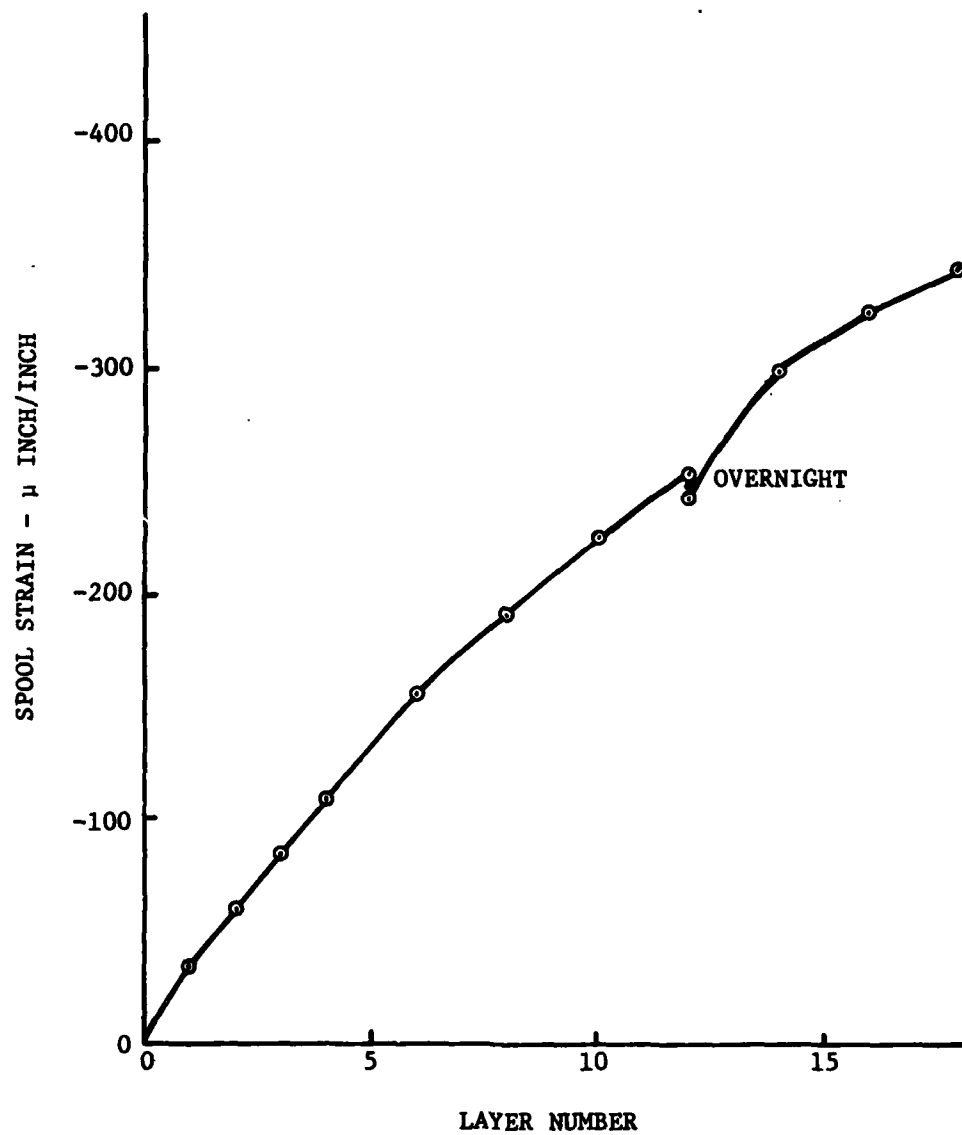


Figure 4.3-36. Bobbin 12, Spool Strain Versus Number of Layers

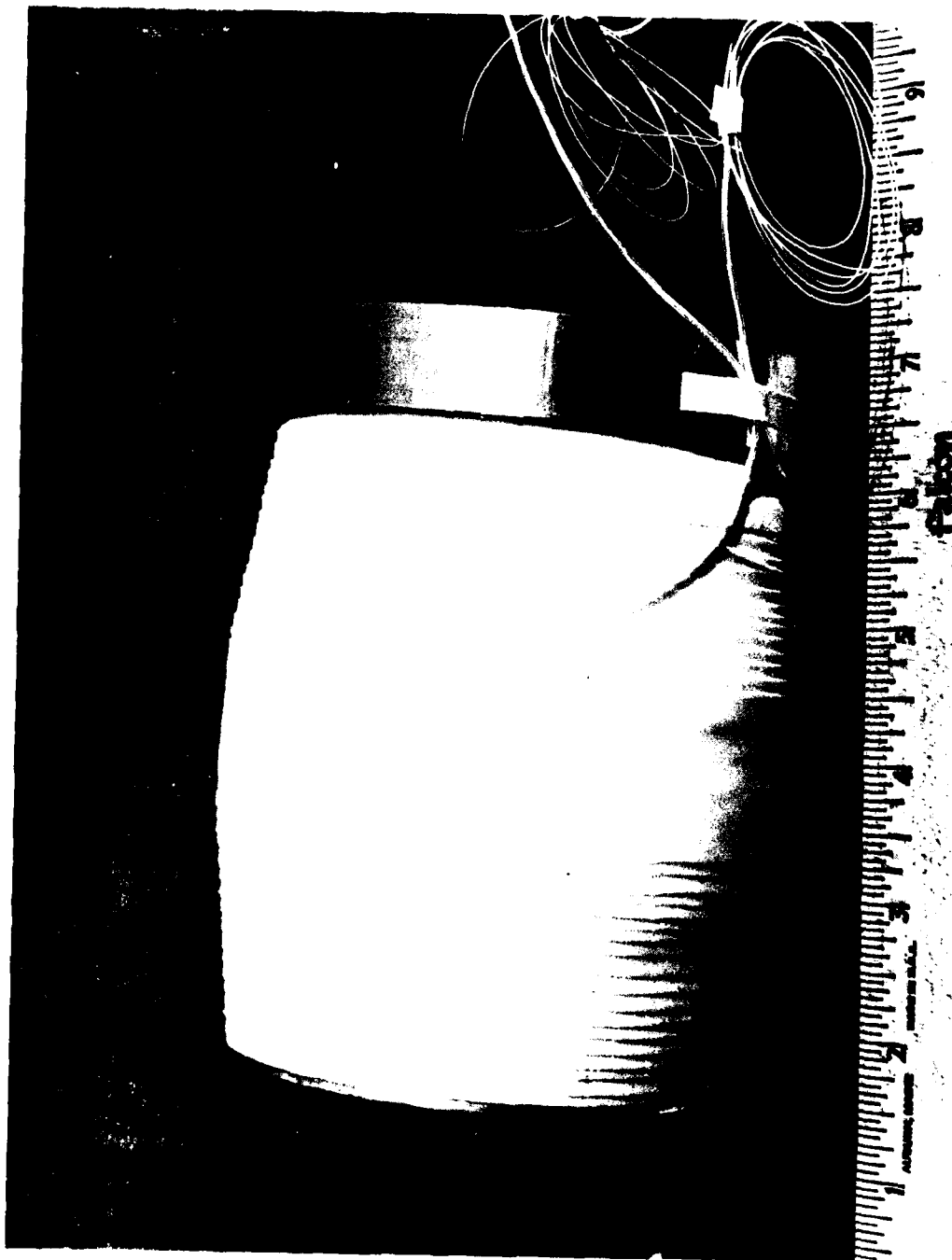


Figure 4.3-37. Photograph of Bobbin 12

Bobbin 13. Bobbin 13, which was representative of design number 6, was wound on a 3.5 inch diameter spool with a cable about 0.012 inch in diameter; the cable coating was WCC-2. The squeeze test data is shown in figure 4.3-38. The coating is quite stiff and shows considerable creep with fair recovery. The spool strain as a function of layer number is shown in figure 4.3-39. Again, the effect of the creep of the cable is evident. This bobbin has not yet been payout tested.

Bobbin 14. Bobbin 14 was wound with HRL aluminum-coated cable. The squeeze test results are shown in figure 4.3-40. Creep recovery is very slight. There is no data available for spool strain versus layer number. The initial length of cable was relatively short and, because of difficulties encountered in winding, the cable was broken during winding. The net result was that there were only two layers wound, precluding obtaining any meaningful spool strain data. This bobbin was not subjected to payout testing.

Bobbin 15. The spool strain resulting from winding is shown in figure 4.3-41. The data is remarkably linear. This bobbin has not yet received payout testing.

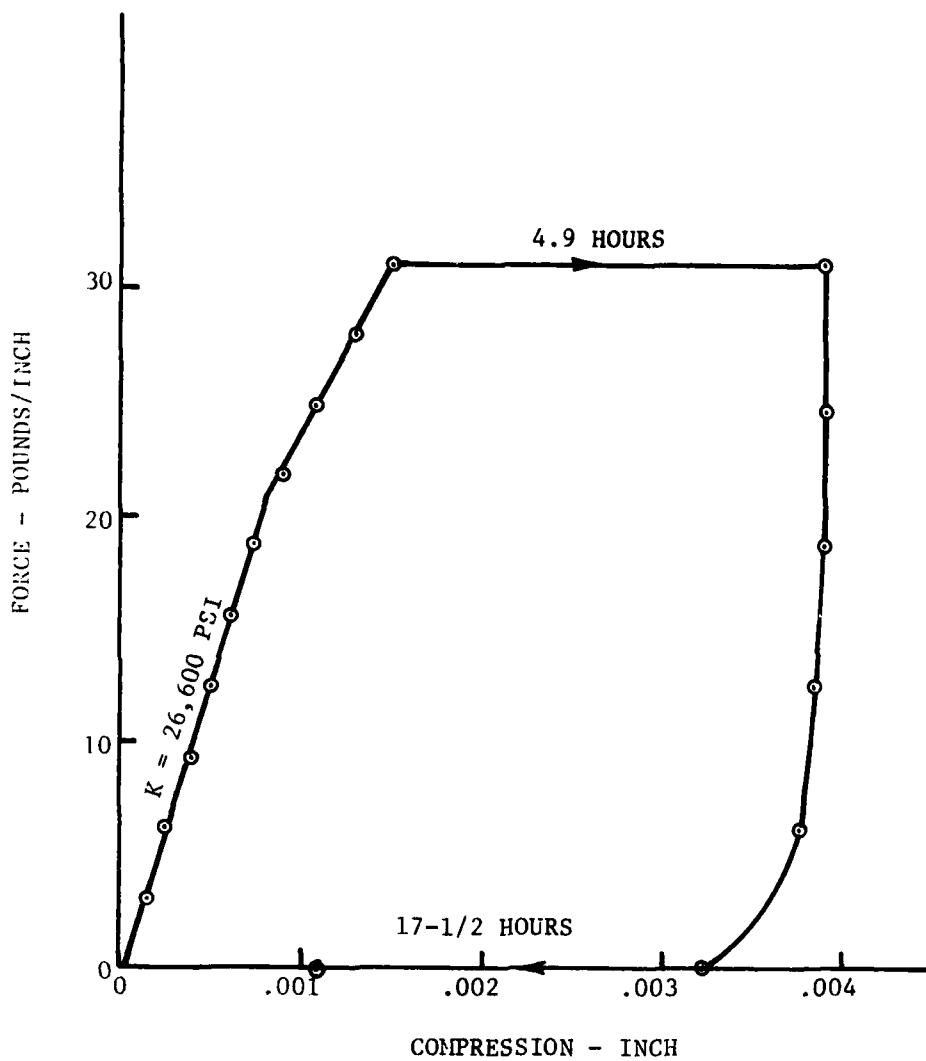


Figure 4.3-38. Bobbin 13, Cable Force-Displacement Characteristics

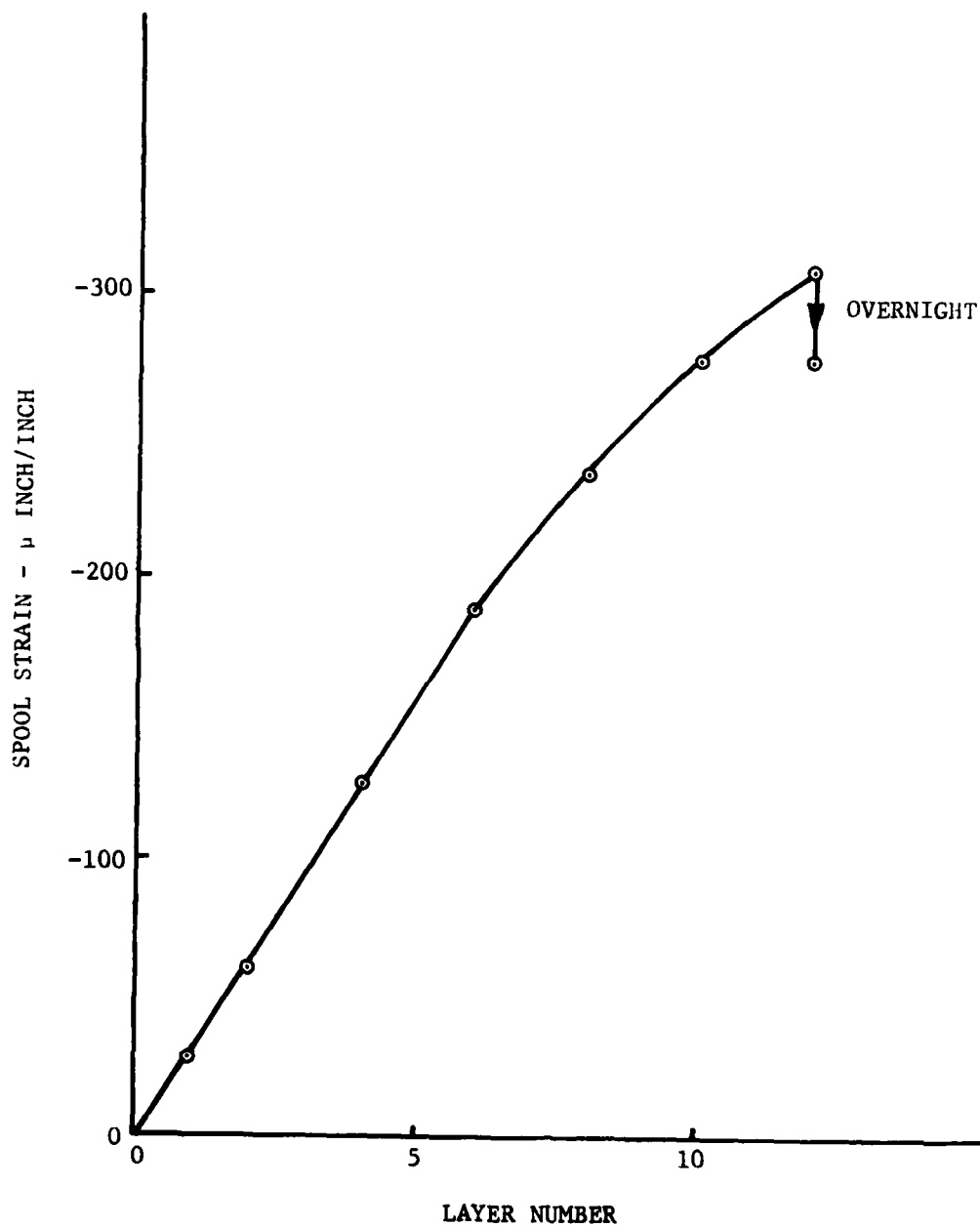


Figure 4.3-39. Bobbin 13, Spool Strain Versus Number of Layers

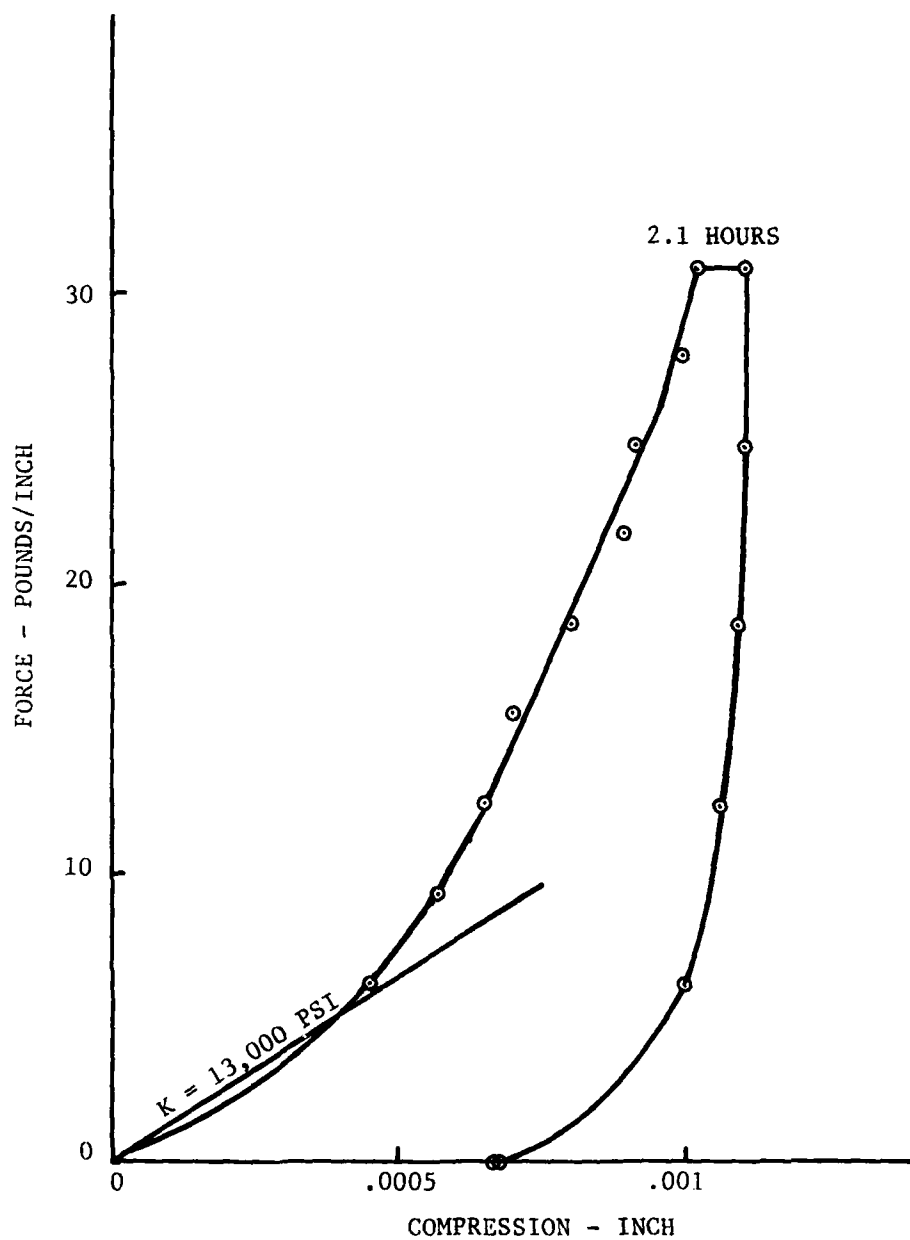


Figure 4.3-40. Bobbin 14, Cable Force-Displacement Characteristics

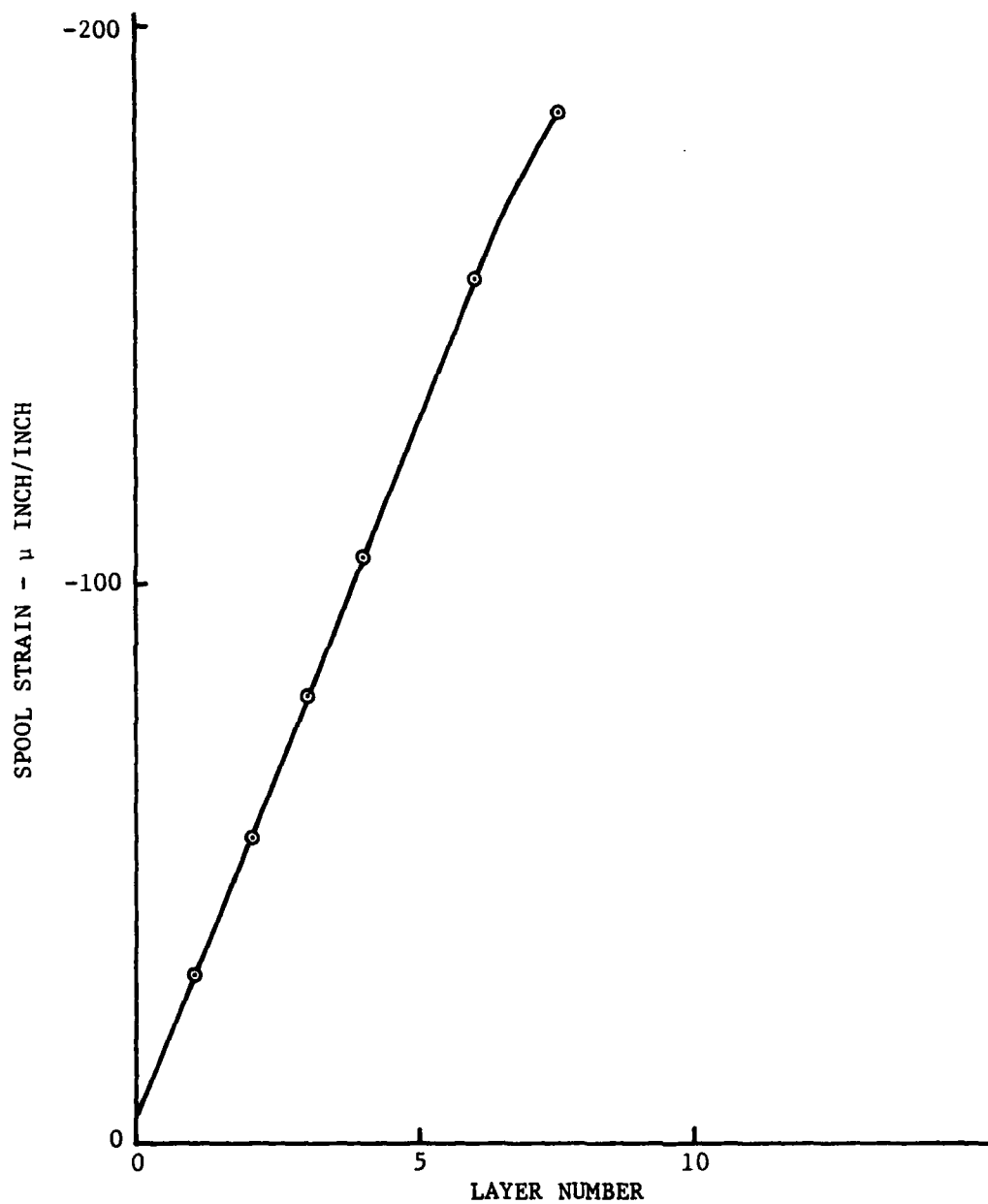


Figure 4.3-41. Bobbin 15, Spool Strain Versus Number of Layers

4.4 OPTICAL EVALUATION

The program for the development of the fiber optic cable dispenser involves the use of short lengths of cable (≈ 1 km) for all tests except those to be conducted in the final phase of the program. This provides a genuine saving in cost but results in an element of risk to the program, since some of the mechanisms important to dispenser design do not scale linearly with cable length. To minimize this risk, attention has been given to define experiments which will help in understanding these nonlinear mechanisms. With this knowledge, full length performance can be predicted based on measurement data obtained from short lengths of cable. As an example, the optical attenuation resulting from microbending within the wound spool increases in a nonlinear manner with cable length. The attenuation in a given layer increases as the interlayer pressure forcing that layer into the layer beneath is increased. It is known that the interlayer pressure increases as the number of layers is increased to accommodate a longer length of cable. Therefore, the attenuation measured with a short length of cable is less than the attenuation of the same length and layers of cable when wound as part of a full-length dispenser.

After a review of various alternatives, a procedure has been selected to provide an indication of the long-length attenuation based on measurements with short lengths. This procedure involves winding the short length of cable on an instrumented spool; this spool is then enclosed in a fixture which contains a bladder which may be pressurized to simulate the interlayer pressure from the upper layers in a fully wound bobbin. The equivalent position of the wound layers depends upon the pressure applied. By determining the attenuation as a function of pressure, the total attenuation in a fully wound bobbin can be predicted.

An example of a test fixture used in determining the optical attenuation as a function of interlayer pressure is described in section 4.3, figure 4.3-5. This fixture was used for evaluating the performance of test bobbins which were less than 5 inches (0.13 m) in diameter and 6 inches (0.15 m) in length. The bladder was fabricated from a piece of an automotive innertube, sealed on the ends with the valve stem attached to the exterior surface.

Prior to a review of the data obtained from the use of this technique, it is appropriate to review some of the potential limitations or uncertainties. There are several possible sources of error which are inherent in this approach. Among these error sources are the following:

1. The technique assumes that interlayer pressure is constant over the full length of a layer. With the type of winding being used, where each succeeding layer is shorter than the layer beneath, the center of a layer is subjected to greater pressure than the ends of the layer. Since the interlayer pressure ascribed to a layer corresponds to the pressure at the center, and since optical attenuation increases as pressure increases, this assumption will predict higher attenuation levels than will actually be encountered.
2. The computer models used to predict interlayer pressure for the full length bobbins assume linear elastic behavior of any coatings on the cable. Since the elastic parameters can be determined only approximately with short lengths of cable, and since most cable coatings tend to exhibit visco-plastic characteristics, errors in predicted interlayer pressure will result. The errors in predicted pressure due to uncertainties in the cable transverse modulus of compression can be either positive or negative. The errors due to ignoring the visco-plastic characteristics will result in the predicted pressure being somewhat greater than the actual interlayer pressure.
3. Errors in the measurements of optical signal attenuation versus pressure result from various sources. With the technique used for pressurizing the cable pack, the full length of the spool is subjected to the applied pressure. There is evidence that the attenuation at the layer-to-layer transitions may be particularly sensitive to pressure. In real life, these layer-to-layer transitions are not subjected to the interlayer pressure, but in the test they experience full pressure. The resulting attenuation at the transition causes the overall observed attenuation to be somewhat greater than the corresponding true attenuation in a full

length bobbin. In addition, some difficulty has been experienced in leading the ends of the winding out of the pressure vessel without subjecting some local spots to high bending stress which can add attenuation. Furthermore, with a test bobbin which consists of a relatively small number of layers, the inner and outer layers, which experience somewhat unique interface conditions, represent a relatively large fraction of the total cable length. Any unusual attenuation conditions which result from the unique interface conditions can influence the overall data on attenuation versus pressure. Since the inner surface of the bladder which is used to pressurize the windings is not completely smooth, and since there are other non-uniformities in the interface due to leading out the cable ends, it is expected that due to these contributions the true excess loss versus pressure is somewhat less than that indicated by the experiment.

In spite of these limitations on the technique for comparing the spooling losses of various cables, the technique is believed to represent the best approach thus far identified. Results of tests conducted to date have been extremely useful in making program decisions. It must be recognized that any predictions of full length bobbin attenuation represent a substantial extrapolation. Nevertheless, the technique is believed to represent a valuable tool for use at this phase of the program.

To date, optical attenuation measurements have been made on 14 of the 15 bobbins wound and tested, with cable lengths varying from about 0.5 to 1.2 km. The characteristics of these bobbins and the cables with which they were wound are indicated in table 4.4-I. Of the 14 bobbins, 12 were of a configuration suitable for measurement of attenuation versus pressure; the remaining two bobbins were designed for payout from the inside of the spool. An inside payout geometry involves substantially smaller and different pressure distribution throughout the cable pack than is experienced with a conventional winding geometry. The inside payout geometry is incapable of supporting high interlayer pressures, hence the attenuation versus pressure measurement is meaningless and cannot be performed.

TABLE 4.4-I. SUMMARY OF BOBBIN CHARACTERISTICS

CABLE PARAMETERS						SPOOL PARAMETERS			OPTICAL PARAMETERS	
Bobbin	Cable Dia (inch)	Fiber Dia (inch)	Core Dia (microns)	Coating	Length (km)	Dia (inch)	Length (inch)	Number of Layers	Unspooled (dB/km)	10 km Extrap
1	.020	.005	55	Hytrel/Silicon Rubber	1.0	3.5	6.0	16	3.8	61 dB
2	.011	.005	-	WCC-2	0.83	3.5	6.0	8	Not wave-guide	
3	.010	.005	44	WCC-2	1.22	3.5	6.0	9½	2.3	Very large
4	.0104	.004	45	DeSoto 8	.53	3.5	6.0	3½	13*	Very large
5	.0107	.005	51	DeSoto 8	.48	3.5	3.0	10	3.4	Very large
6	.010	.005	50	WCC-2	.63	3.5	4.5	6½	2.3	63 dB
(Inside payout)										
7	.008	.004	41	WCC-2	.99	3.5	4.5	8	≈4.5*	Very large
8	.008	.004	41	WCC-2					≈4.5	120 dB
(Inside payout)										
9	.012	.0042	44	WCC-2	.50	3.5	3.0	10	12*	Very large
10	.008	.004	41	WCC-2	.98	7.8	2.0	10	4.5	≈100 dB
11	.012	.0042	44	DeSoto 8	1.16	3.5	4.5	14	6.5*	Very large
12	.016	.004	27	Hytrel/Sylgard	.98	3.5	4.5	18	7.2*	68 dB
13	.013	.00415	25	WCC-2	1.01	3.5	4.5	12	6.4*	≈95 dB
14	.010	.009	25	AL	.3	3.5	4.5	3	13	Very large
15	.012	.004	25	DeSoto 8	.85	3.5	6.0	7½	3.5	45 dB

* ITT insertion loss data on shipping spool. This data is frequently much larger than OTDR measurement on a straight section.

* ITT insertion loss data on shipping spool. This data is frequently much larger than OTDR measurement on a straight section.

An examination of table 4.4-I indicates that of the 14 configurations examined for optical properties to date, only four show any promise of satisfying the attenuation goal of 60 dB in a 10 km length. Bobbin 1, which utilized a standard production ITT cable with a diameter of 0.020 inch, extrapolates to a full length attenuation of about 61 dB. Bobbin 6, with the inside payout geometry, demonstrated about 6.3 dB/km. The extrapolation of the short length attenuation data for an inside payout bobbin to a full length bobbin is not as well understood as is the situation with the outside payout geometry; however, with the inside payout geometry, the attenuation is expected to scale much more linearly with length than does the outside payout geometry. Assuming linear dependence with length, an attenuation of about 63 dB is expected for a full length bobbin with the parameters of bobbin 6.

Bobbins 12, 13, and 15 utilized cables which were specially fabricated for payout purposes. Of these, bobbins 12 and 15 indicate acceptable or near acceptable attenuation. The cable for bobbin 13 had a rather high intrinsic loss; hence, even though the excess loss due to spooling was acceptable, the high intrinsic loss resulted in an overall attenuation level which was excessive.

The attenuation data was obtained, for most of the bobbins, using an optical time delay reflectometer (OTDR). This highly useful instrument, illustrated in figure 4.4-A is essentially an optical pulse radar which launches a very short pulse of optical energy down a length of optical fiber and detects the Rayleigh backscattered energy as a function of time. Since the Rayleigh scattered light at any point is proportional to the intensity of the transmitted pulse at that point, the time history of the backscattered radiation provides a means of determining attenuation as a function of position along the fiber. The OTDR which has been used for most of the data gathering operates at a wavelength of 0.9 micron with a pulse length of 130 nanoseconds. It utilizes a Laser Diode Laboratories' LD60 laser as the transmitter, and an RCA 30818 Avalanche Photo diode with an integral pre-amplifier as a detector. The backscattered signal is processed through a logarithmic amplifier. As a result, the slope of the response curve is

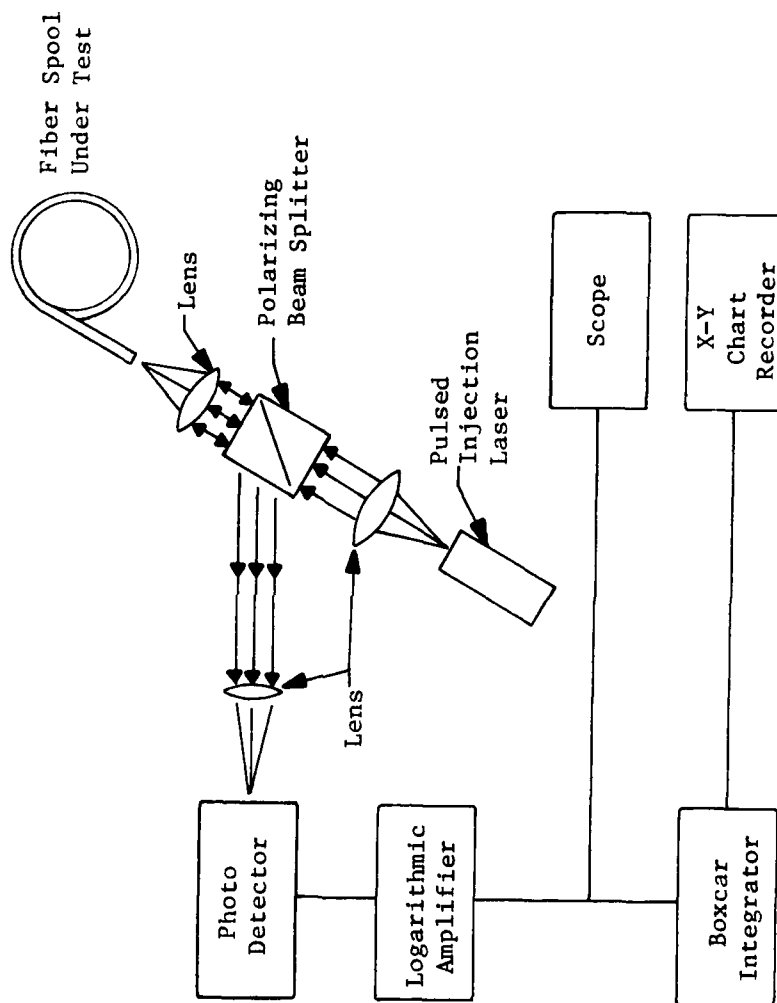


Figure 4.4-A OTDR Schematic Diagram

proportional to the attenuation in dB/km. At the end of the fiber, part of the transmitted pulse undergoes Fresnel reflection; this is readily observed as a large amplitude response at the end of the response curve. With the test bobbin installed in the pressure vessel and the bladder pressure at ambient, an end of the fiber (usually the top end was used) is connected to the OTDR, and a response curve is taken. The bladder pressure is then increased in steps and additional response curves are taken. In most cases, the pressure was increased stepwise and then reduced stepwise in order to obtain data on any hysteresis characteristics which may be present.

To understand more fully the extrapolated attenuation data presented in table 4.4-I, it is appropriate to review the test and data analysis procedures in somewhat more detail. Using bobbin 1 as an example, let us go step by step through the test and analysis sequence.

The OTDR data for bobbin 1 is presented in figure 4.4-1. Each of the traces correspond to a particular applied pressure. It may be noted that the length of the optical fiber under test is about 475 meters in length. The actual winding involved about 1 km of cable but, due to an experimental problem, the cable was broken during test very near the center. The length of the section selected for test was then slightly less than 0.5 km. At the higher pressure levels, at a position of 165 meters, there is a short region of high attenuation indicated by the steps in the curves. This region has been traced to a large defect in the winding which resulted from a large clump of foreign material which was adhering to the cable. The fact that this winding defect was observed to cause a very substantial attenuation has made it apparent that such defects cannot be allowed in the winding. In fact, all subsequent windings were free of such defects and no similar regions of high attenuation were observed. In determining the loss for the various values of applied pressure, the average slopes of the traces between about 200 and 475 meters were used. The resulting data, providing signal attenuation versus applied pressure, is plotted in figure 4.4-2.

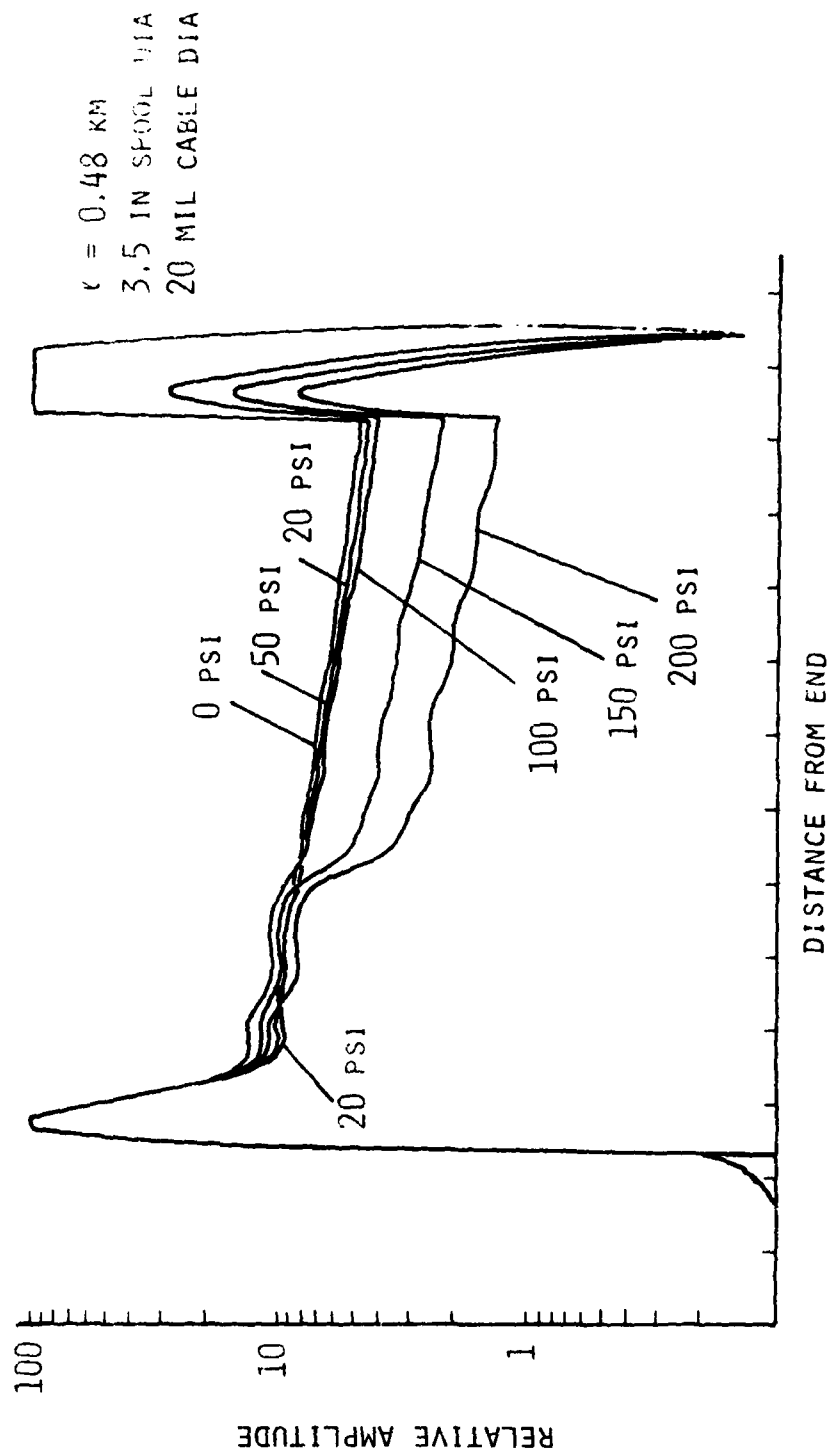


Figure 4.4-1. Bobbin 1, OTDR Test Results

Based on data obtained from the bobbin design studies for interlayer pressure at each layer and the wound length of each layer, the total predicted loss in dB may be computed from equation 4.4-1.

$$L_{\text{total}} = \sum_{i=1}^N X_i L(P_i) \quad 4.4-1$$

where X_i is the length of the i^{th} layer in km, P_i is the interlayer pressure at the i^{th} layer, and $L(P)$ is the loss in dB/km as a function of pressure as indicated in figure 4.4-2. The values of X_i and P_i are presented in figures 4.4-3 and 4.4-4. The resulting value of total attenuation computed in this manner for bobbin 1 is 61 dB.

The OTDR data for several other bobbins are presented in figures 4.4-5 through 4.4-14. The detailed analysis conducted for bobbin 1 was not performed for most of the bobbins because it was quite apparent from inspection that the design was far from satisfying attenuation requirements. It may be noted from a review of figures 4.4-5 through 4.4-14 that, for some cases, the range of applied pressure was somewhat less than for bobbin 1. In the case of bobbin 10, this resulted from the fact that the maximum value of applied pressure for a full length bobbin is only about half of that for the other configurations. In other cases, the limited range of applied pressure resulted from the fact that attenuation was increasing so rapidly that taking of data at the higher pressures was considered to be meaningless.

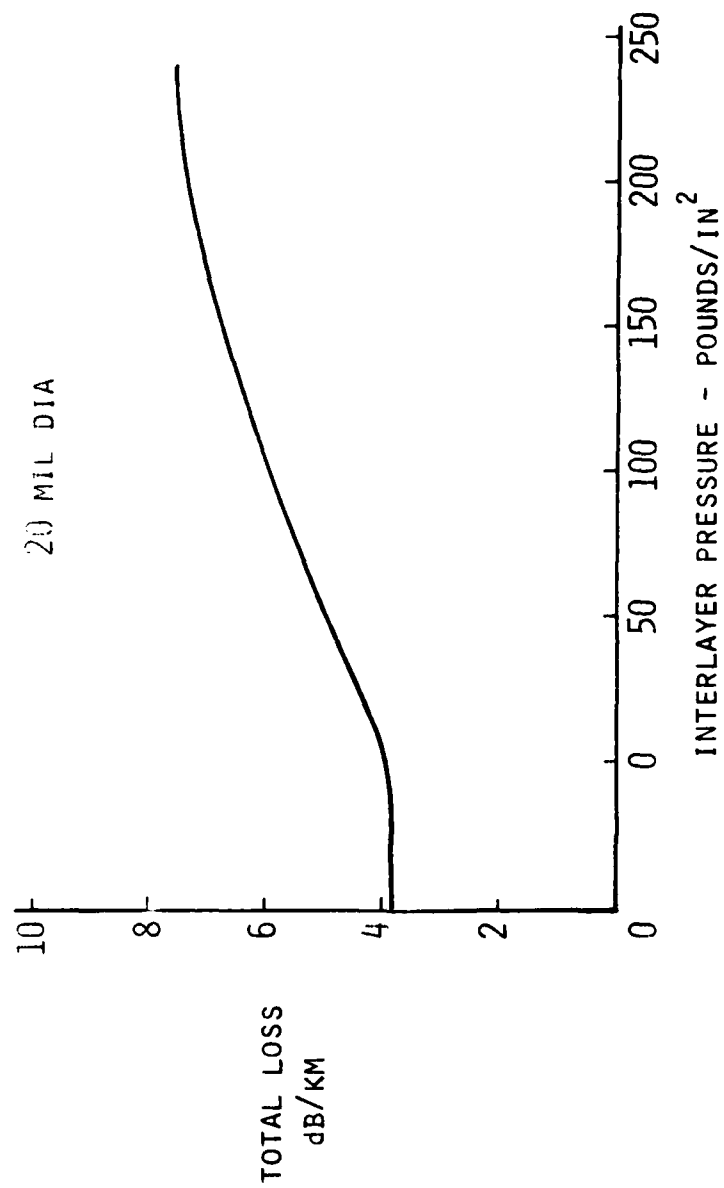


Figure 4.4-2. Cable Attenuation vs Interlayer Pressure

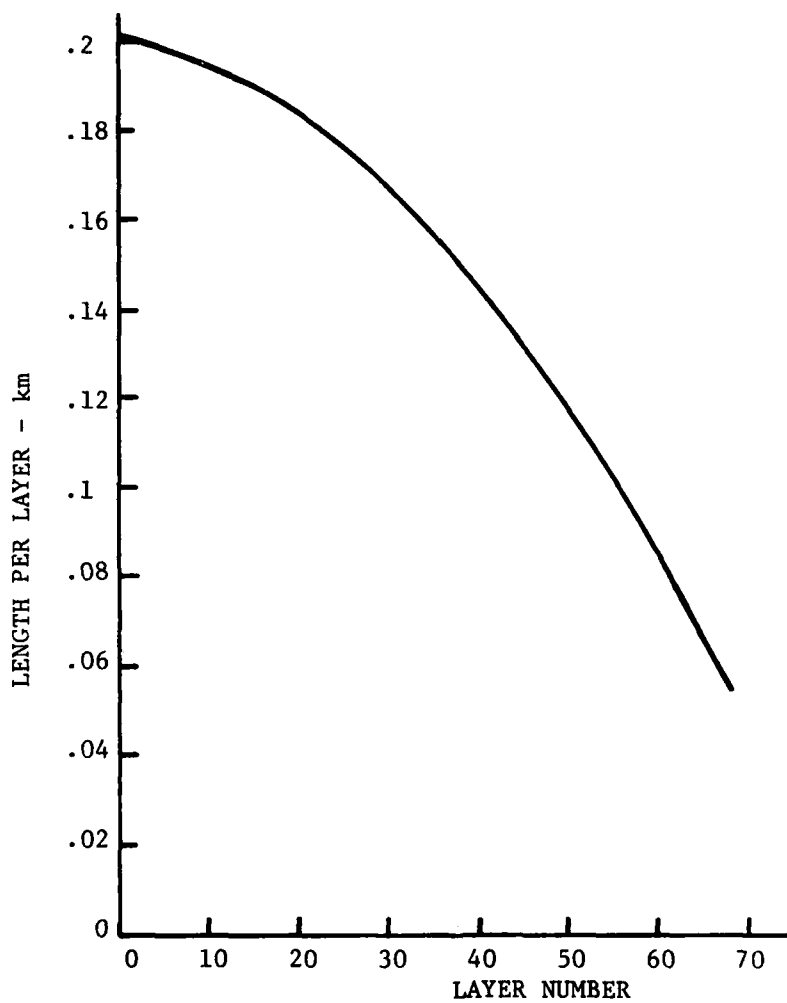


Figure 4.4-3. Layer Length vs Layer Number, Bobbin 1

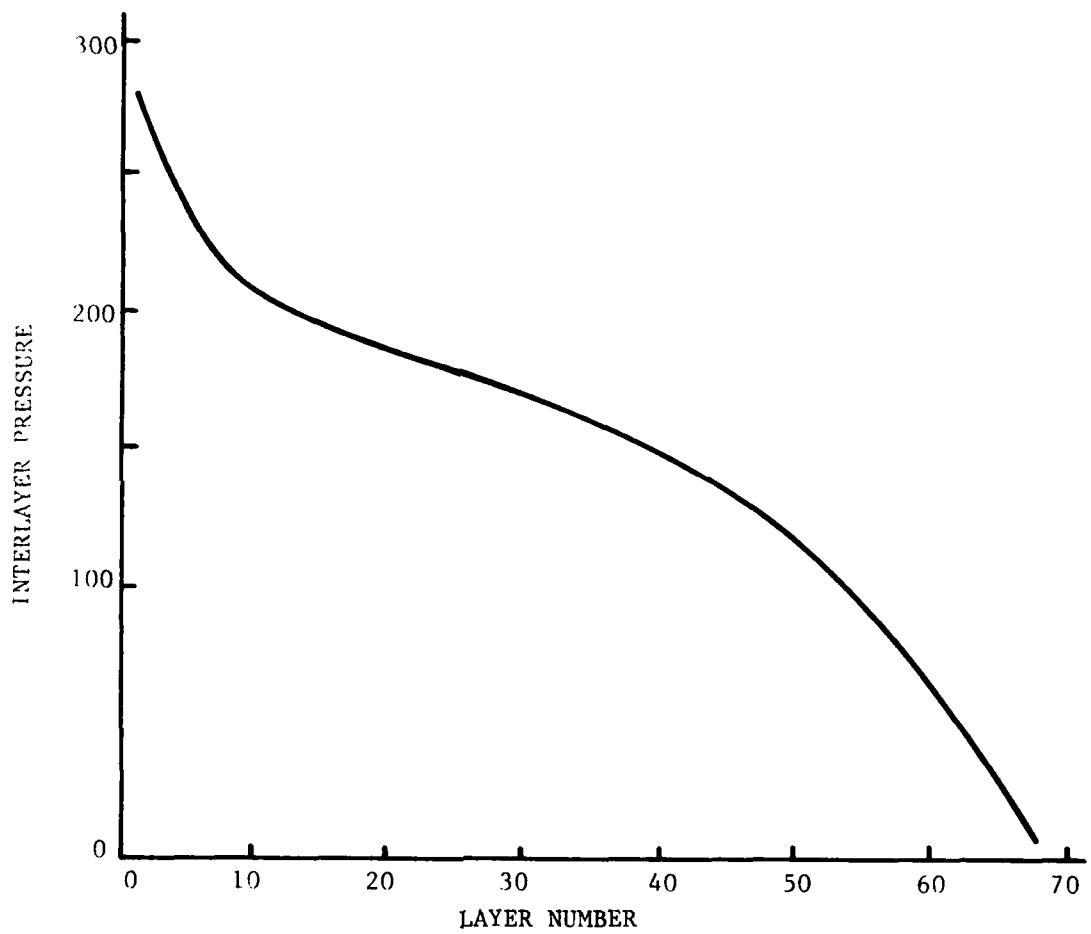


Figure 4.4-4. Interlayer Pressure vs Layer Number, Bobbin 1

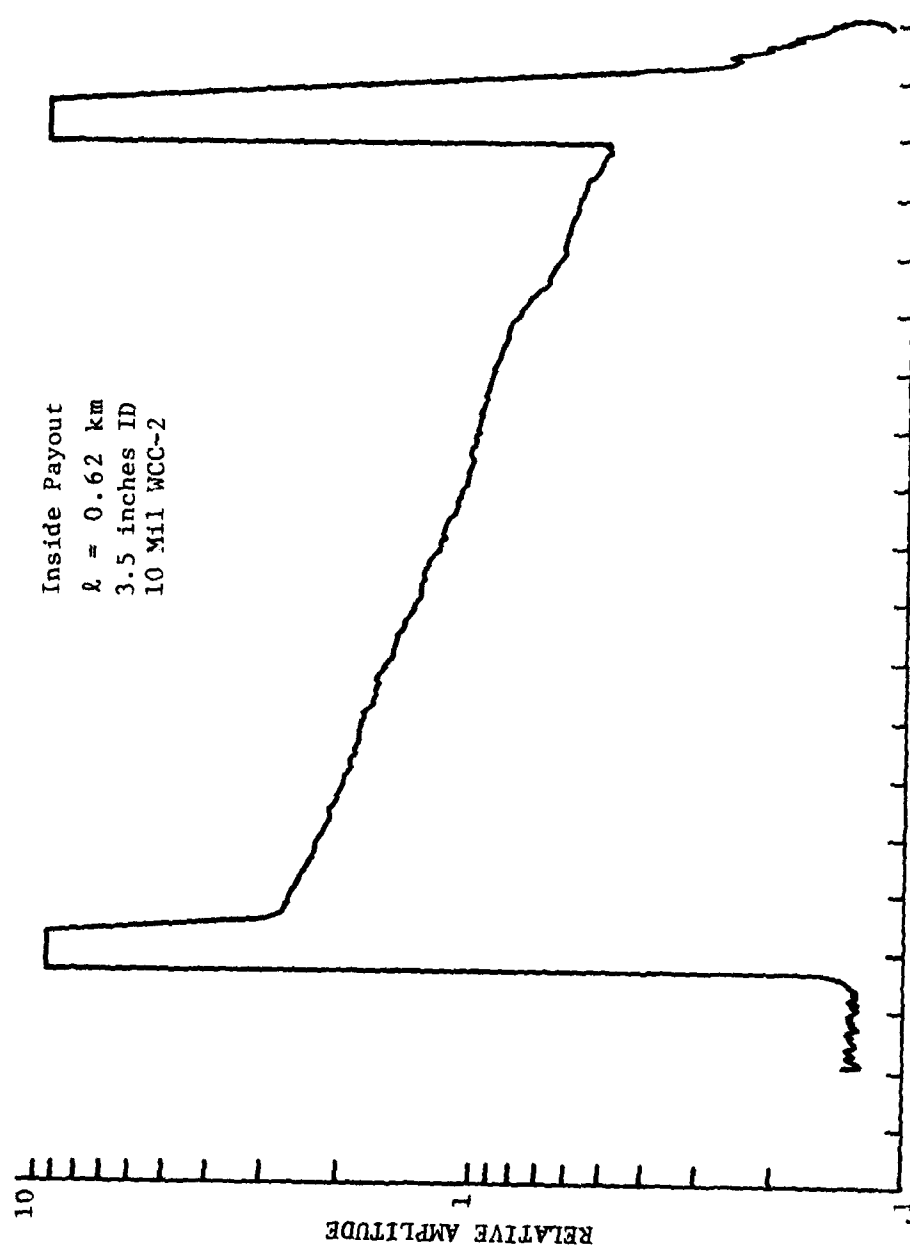


Figure 4.4-5. Bobbin 6, OTDR Test Results

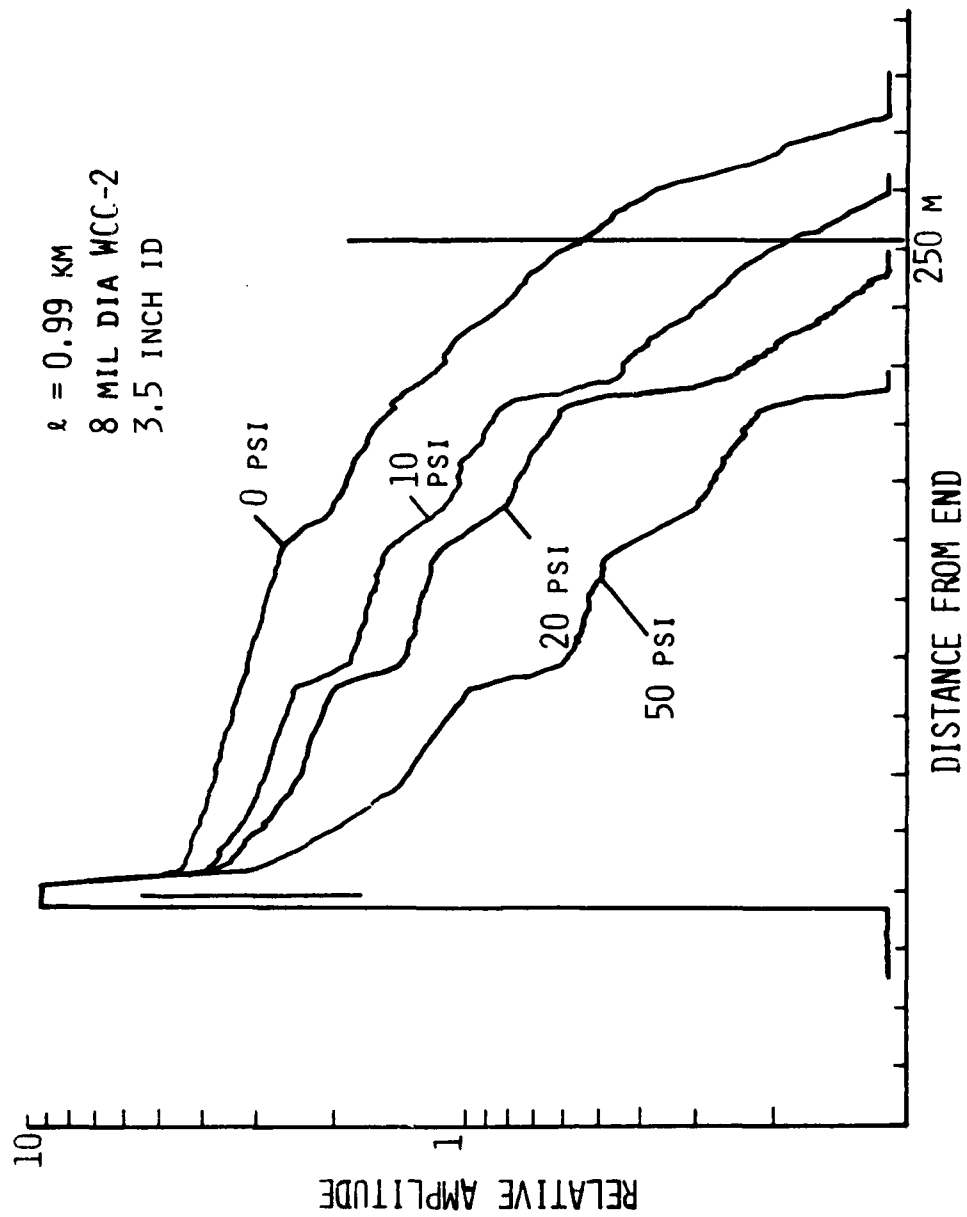


Figure 4.4-6. Bobbin 7, OTDR Test Results

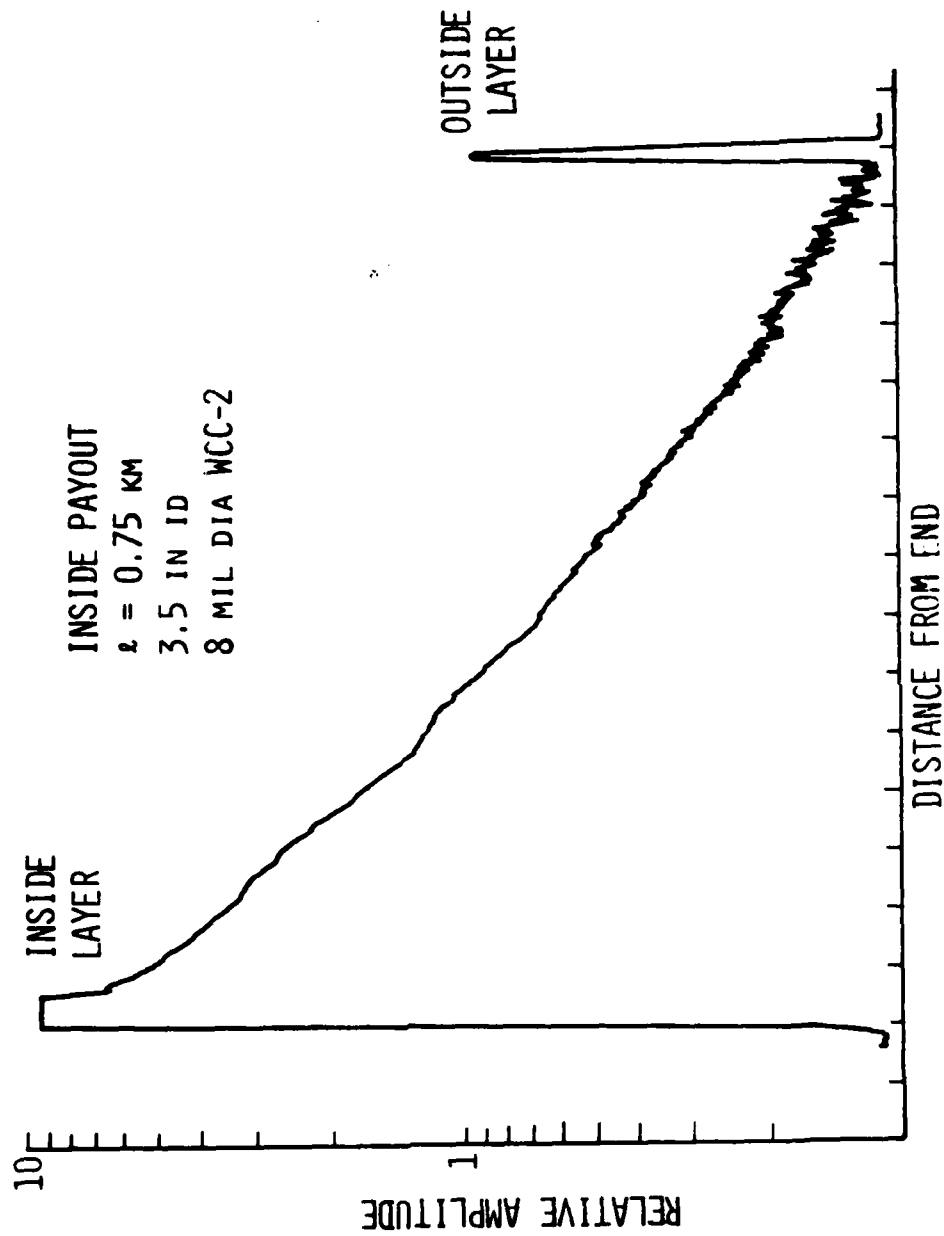


Figure 4.4-7. Bobbin 8, JTDR Test Results

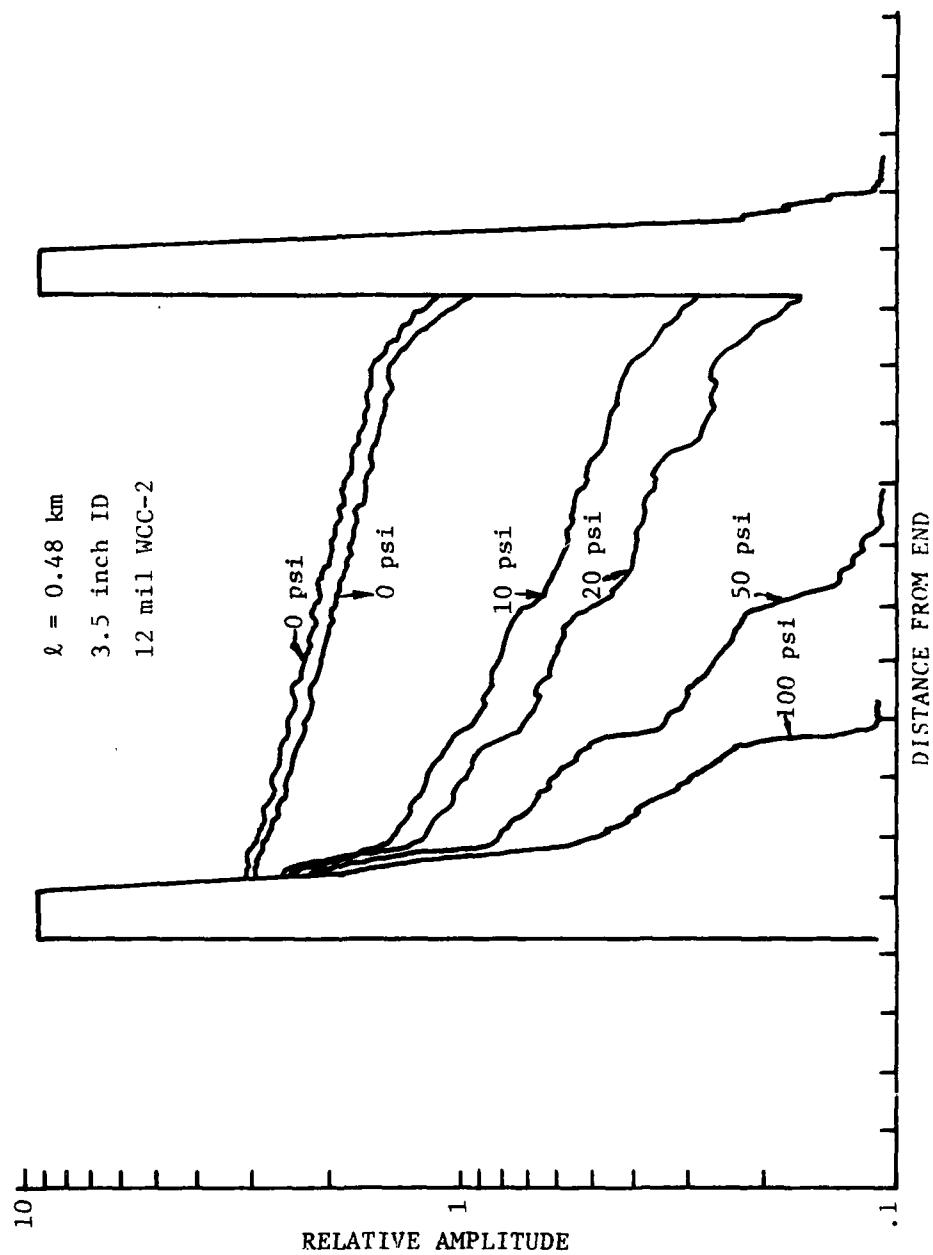


Figure 4.4-8. Bobbin 9, OTDR Test Results

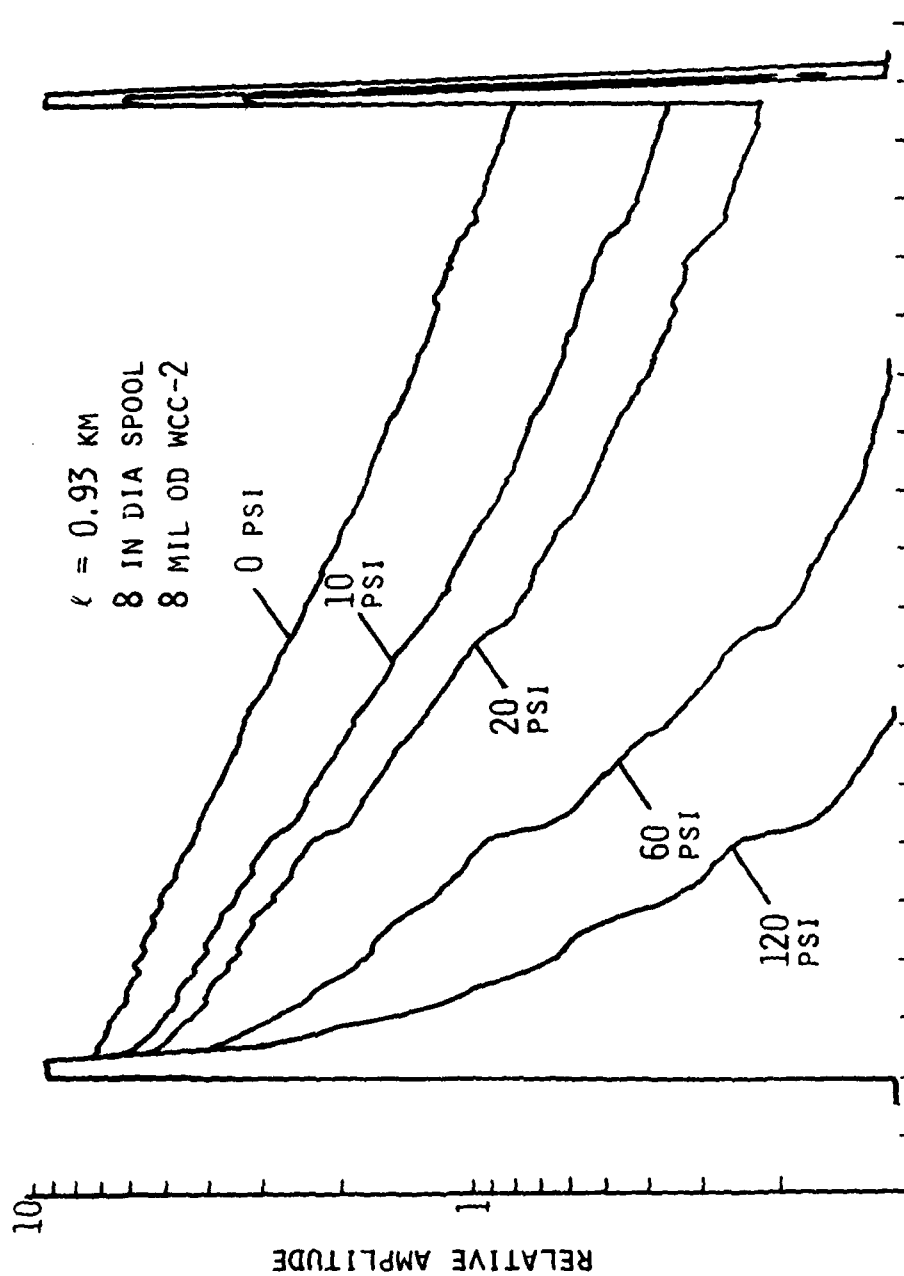


Figure 4.4-9. Bobbin 10, OTDR Test Results

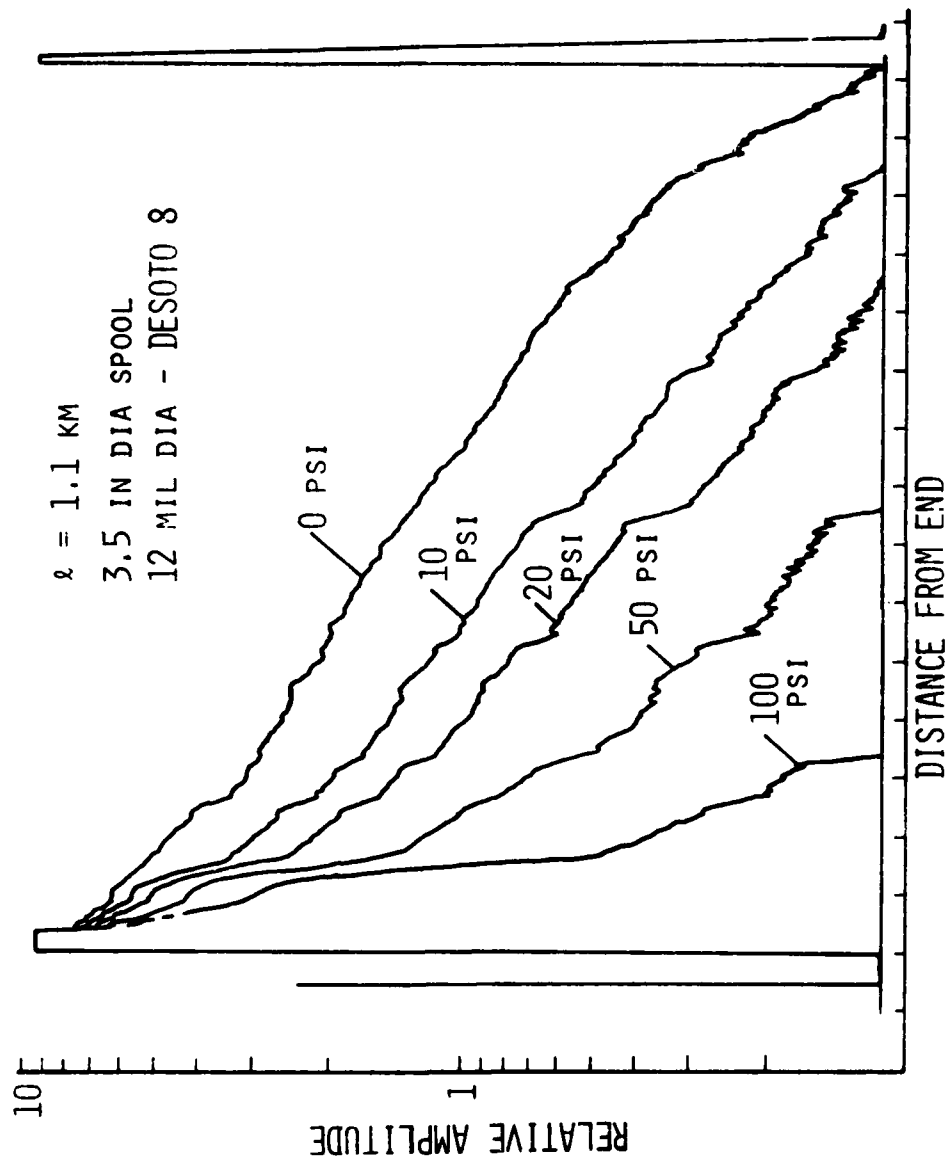


Figure 4.4-10. Bobbin 11, OTDR Test Results

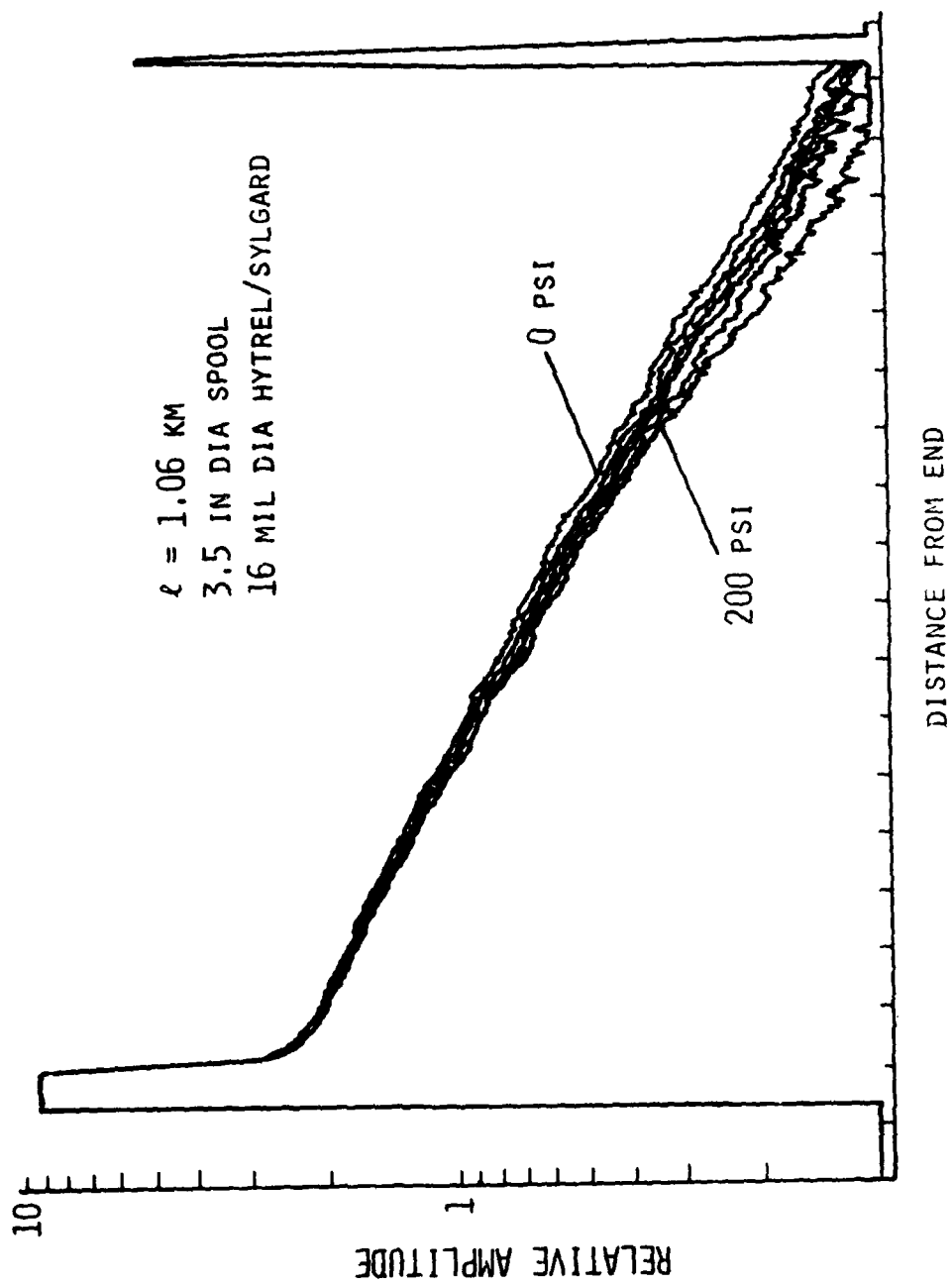


Figure 4.4-11. Bobbin 12, OTDR Test Results

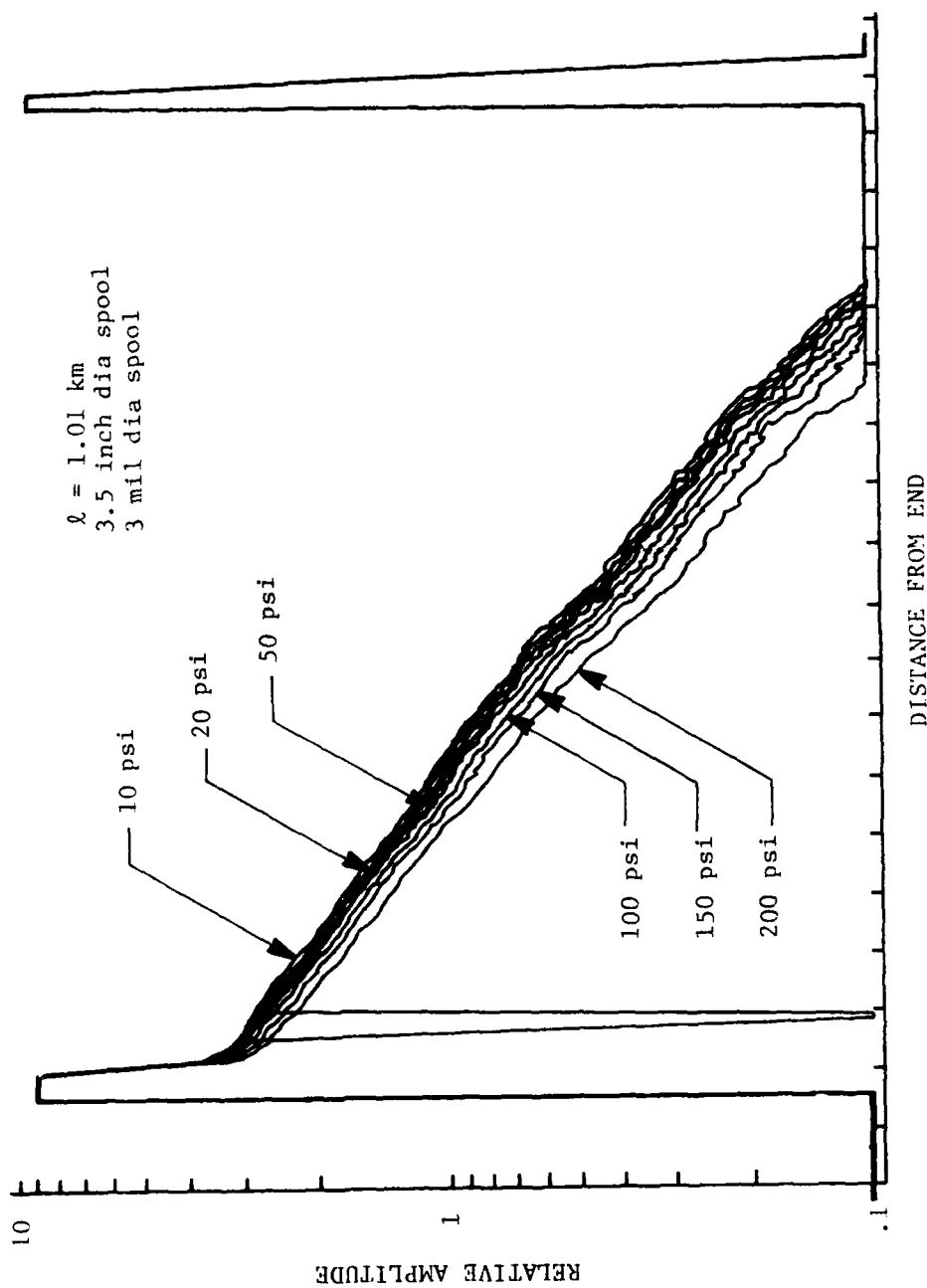


Figure 4.4-12. Bobbin 13, OTDR Test Results

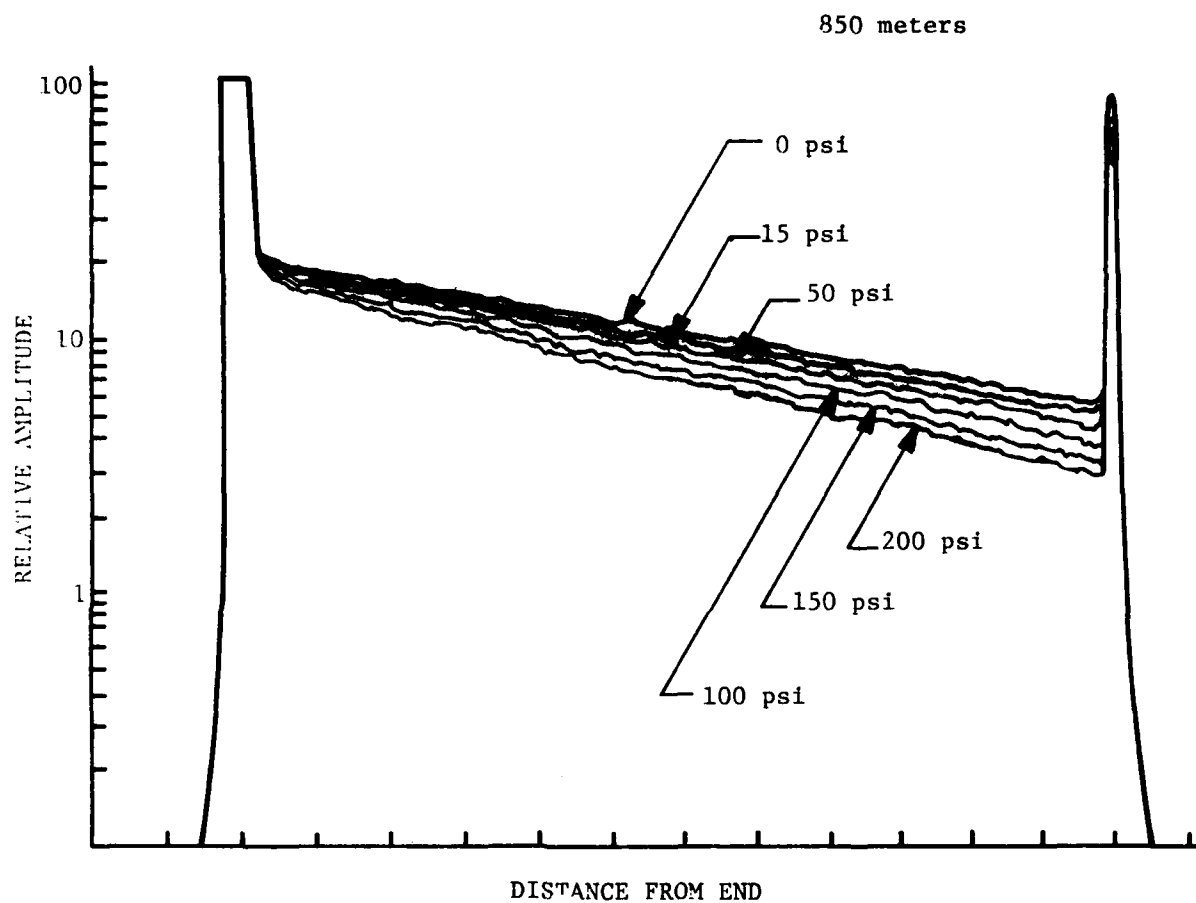


Figure 4.4-14. Bobbin 15, OTDR Test Results

Special comment should be made regarding the data for bobbins 6 and 8 which were designed to be payed out from the inside of the cable pack. With this geometry, there is no spool on the inside to support the cumulative interlayer pressure; hence interlayer pressures must be very small. This geometry is fabricated by winding on a spool and then removing the spool. This results in an adjustment of the cable pack with the substantial reduction in interlayer pressure. Since these bobbins were designed to minimize the interlayer pressure, and since the pressure distribution within this type of winding is not as well understood as with the conventional geometry, it was considered meaningless to apply external pressure to these bobbins. For this reason, only a single OTDR trace is found on figures 4.4-5 and 4.4-7.

It was noted above that only four of the 14 bobbins evaluated optically show promise for satisfying the overall attenuation requirements. The optical attenuation characteristics of these four, along with the data for three less promising candidates, are presented in figure 4.4-15. The four cables corresponding to the four bottom lines in this figure appear satisfactory from the standpoint of attenuation for use in full length bobbins. Of these, one represents the standard production ITT cable configuration. This cable demonstrated very good optical properties but is somewhat larger in diameter than desired with a diameter of 0.020 inch compared to a goal of 0.010 inch. However, it appears that full length bobbins with up to 0.020 inch cable can be wound within reasonable bobbin length and diameter constraints. The diameter of the other three acceptable cable configurations ranges from 0.012 to 0.016 inch which, although slightly larger than the initial goal, is quite acceptable for full length bobbin application.

It is significant that for all of the cables acceptable for optical attenuation, except the 0.020 inch diameter cable, the diameter of the fiber core relative to the fiber diameter has been reduced by a factor of almost two. This change was made to reduce the sensitivity of the cable to microbending loss due to winding. The reduction in the core diameter was quite successful in achieving the goal but does invoke a penalty in other areas. Because of the smaller core diameter, it is somewhat more difficult to launch light

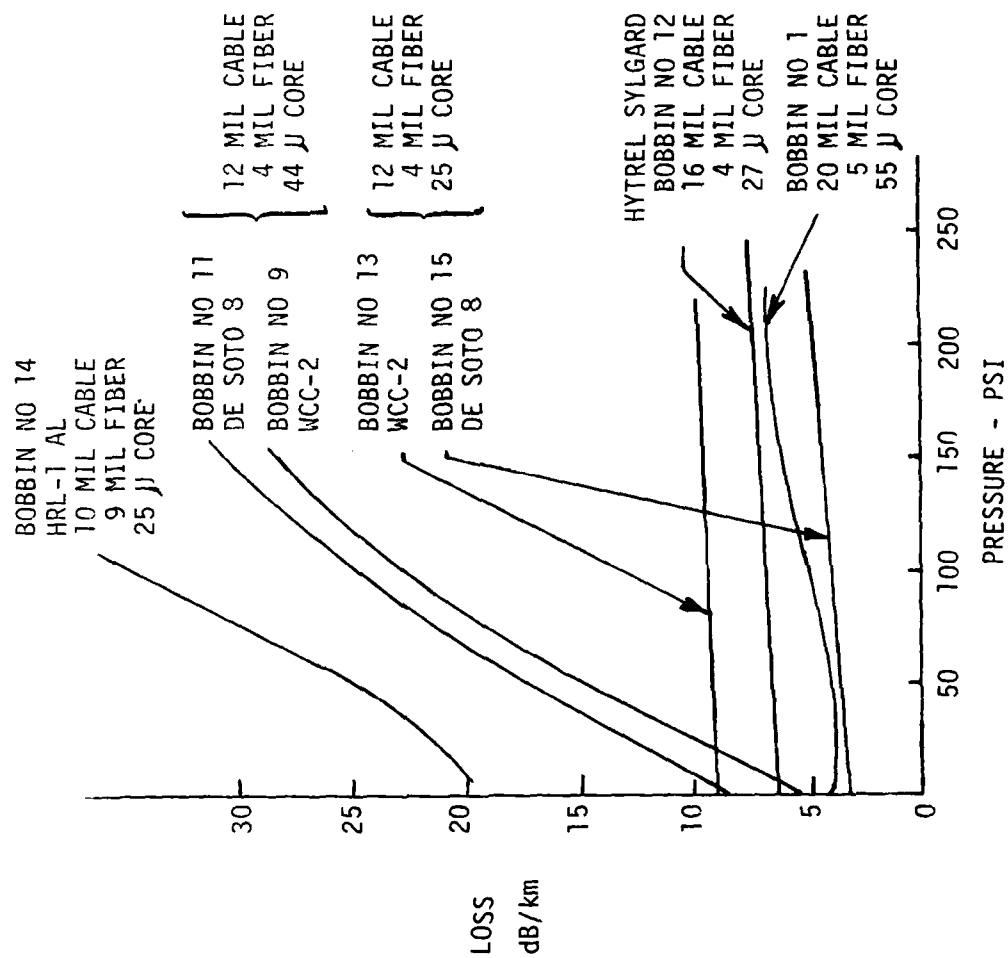


Figure 4.4-15. Effect of Interlayer Pressure on Cable Loss

into the cable which may require somewhat more complex optical coupling techniques at each end of the cable.

Recognizing that optical attenuation is a very important parameter in the design of the cable and dispenser, two special bobbin designs were pursued to determine how much relief in terms of cable microbending loss susceptibility could be achieved through novel dispenser design. A large diameter design provides two mechanisms which tend to reduce cable microbending loss. The first of these involves a reduction in interlayer pressure. As the cable is wound, the force with which a turn is pulled against the lower turns is proportional to the tension in the cable and inversely proportional to the diameter on which it is being wound. The larger spool results in reduced interlayer pressure per layer; in addition, the larger spool requires fewer layers to achieve the required length, further reducing interlayer pressure. Secondly, with the large diameter spool, the number of turns required to wind the full length is reduced. Since the number of crossovers within the cable pack, where one turn crosses diagonally over the turn beneath, is roughly equal to twice the number of turns, the larger spool results in a reduction in the number of crossovers. Crossovers are believed to be the sites of microbending where loss can occur, hence the reduced number of crossovers should result in reduced signal attenuation.

The second special design involves payout from the inside of the bobbin. As described above, this approach reduces interlayer pressure by eliminating the spool at the center of winding, thereby removing the means of supporting sizeable interlayer pressure. The effect of these designs on attenuation is illustrated in figure 4.4-16, where cable loss is plotted as a function of interlayer pressure for a conventional configuration, labeled 3.5 inch diameter spool. All of these bobbins were wound using cable from the same supply spool, hence uncertainties due to variability of cable parameters were largely eliminated from the experiment.

From an examination of figure 4.4-16, it is apparent that spool design can substantially alter the requirements on the cable in terms of sensitivity to spooling conditions. If one compares the data for the 3.5 inch diameter

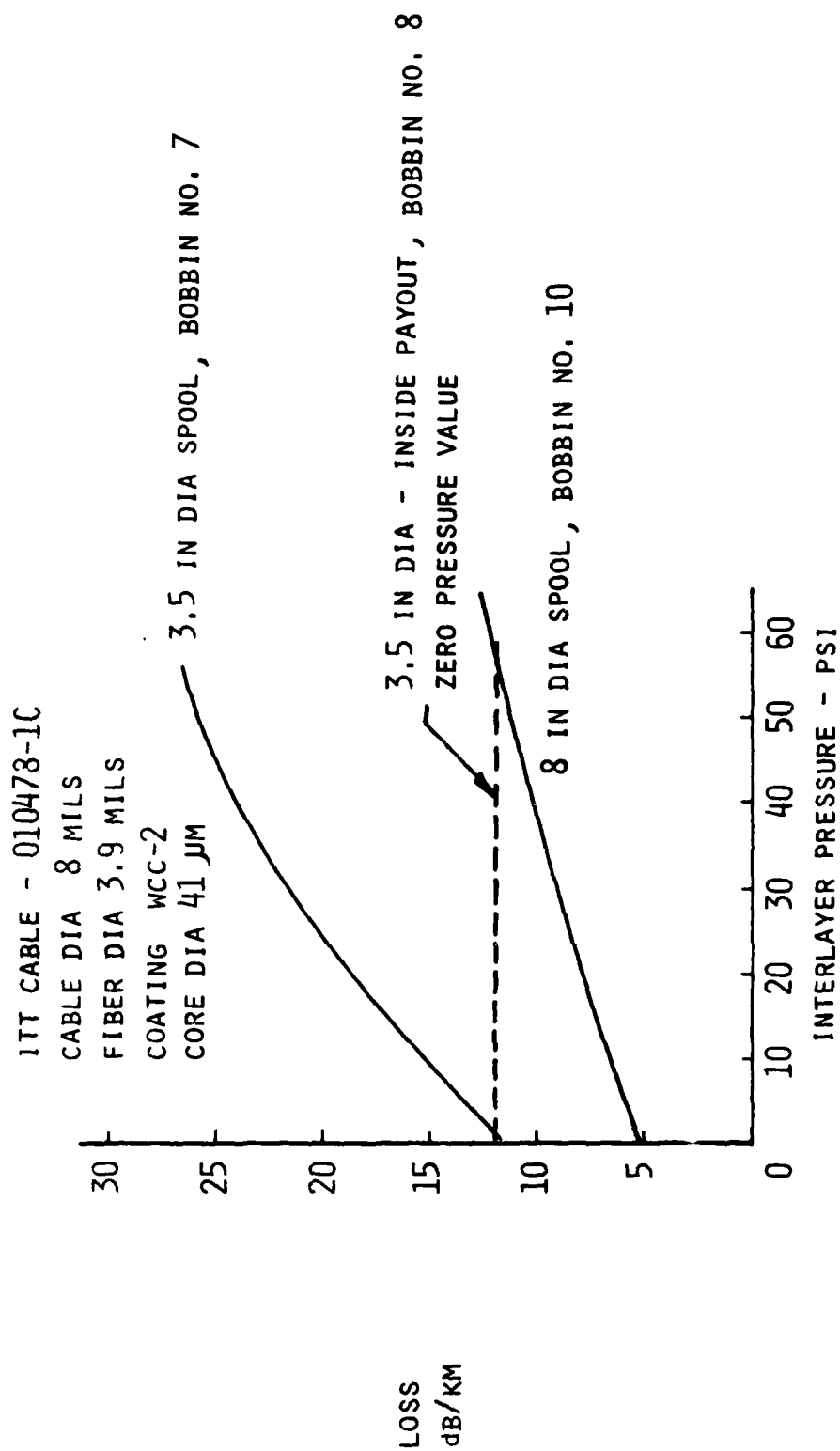


Figure 4.4-16. Effect of Spool Geometry on Spooling Loss

spool with that for the 8 inch diameter spool, a marked difference is noted. Both the attenuation value at zero applied pressure and the slope as pressure is increased are less with the larger spool configuration. If one adds to this the fact that the maximum interlayer pressure for a full length bobbin with the large diameter spool is only about one-half of that for the 3.5 inch diameter spool, the marked advantage of the increased diameter may be recognized.

Of course, the special configurations involve other disadvantages and risks. For this reason the main stream effort of the program will place emphasis on the small diameter, conventional geometry dispensers.

It was stated above that most of the OTDR data has been taken at a wavelength of 0.9 micron. Recently a second OTDR, operating at a wavelength of 0.85 micron has become available and comparative data has been obtained on one bobbin. Figure 4.4-17 illustrates this data. It may be noted that there is a substantial increase in the value of attenuation at zero applied pressure for the 0.85 micron wavelength, but the two lines are very nearly parallel. This indicates that the pressure-induced loss is probably almost independent of wavelength, but the intrinsic attenuation of the cable is definitely wavelength-sensitive. An increase in the zero pressure attenuation is expected at the shorter wavelength but an increase of 5 dB/km is somewhat larger than anticipated. The reason for this large increase is not known at this time. Additional data on the effect of wavelength on spooling losses will be obtained.

The effect of temperature on cable attenuation has also been evaluated for three cable types. ITT conducted tests of attenuation at various temperatures for these cables in a relaxed or loosely spooled condition. These cables were also wound into bobbins and subjected to temperature extremes. The results of these tests are plotted in figure 4.4-18. Note that this figure illustrates the change in attenuation rather than total attenuation. The data is relative to the initial room temperature attenuation. It is interesting to note that, for all three cable types, the variation in attenuation is less in the wound bobbin than for the unspooled cable. This trend is encouraging, but because of the small data sample, it is premature to draw definite conclusions.

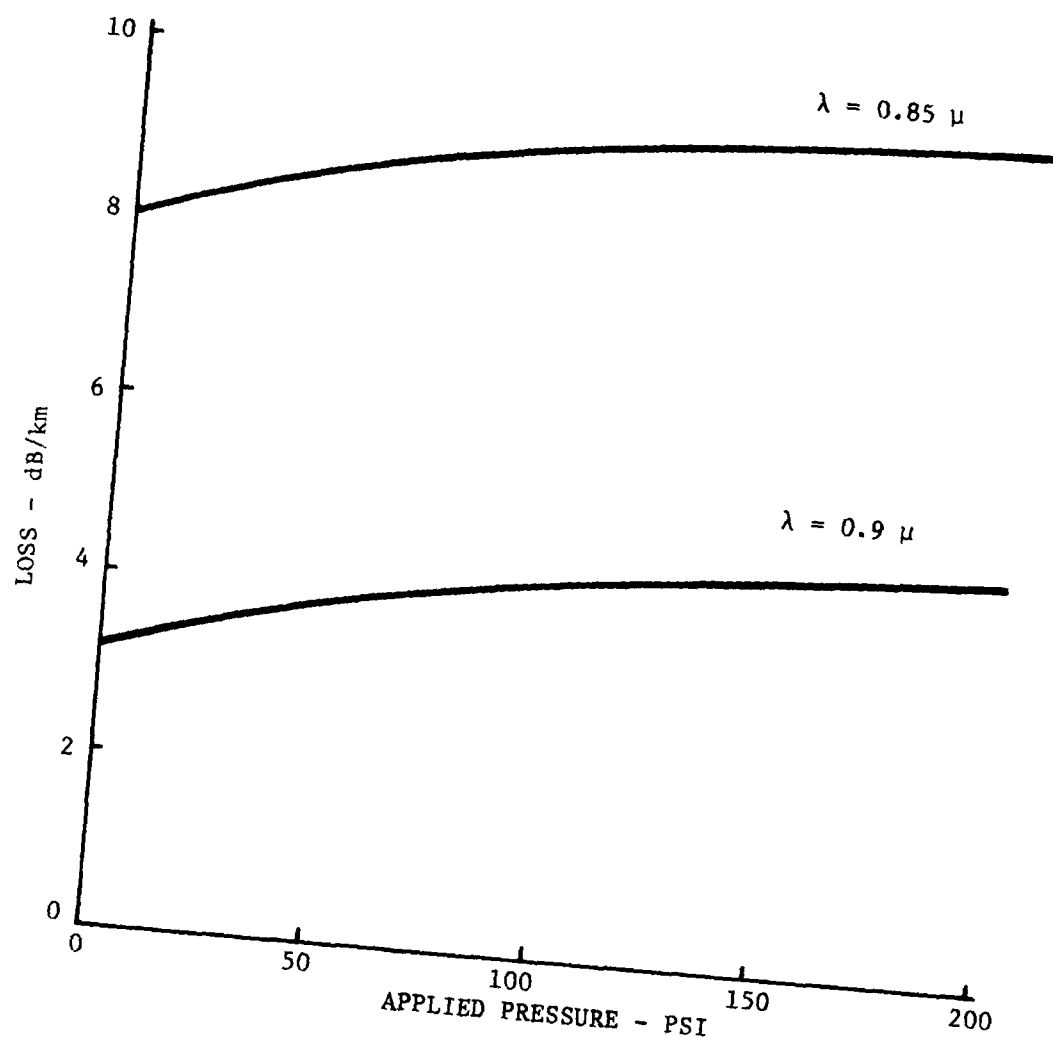


Figure 4.4-17. Effect of Wavelength on Spooling Loss, Bobbin 15

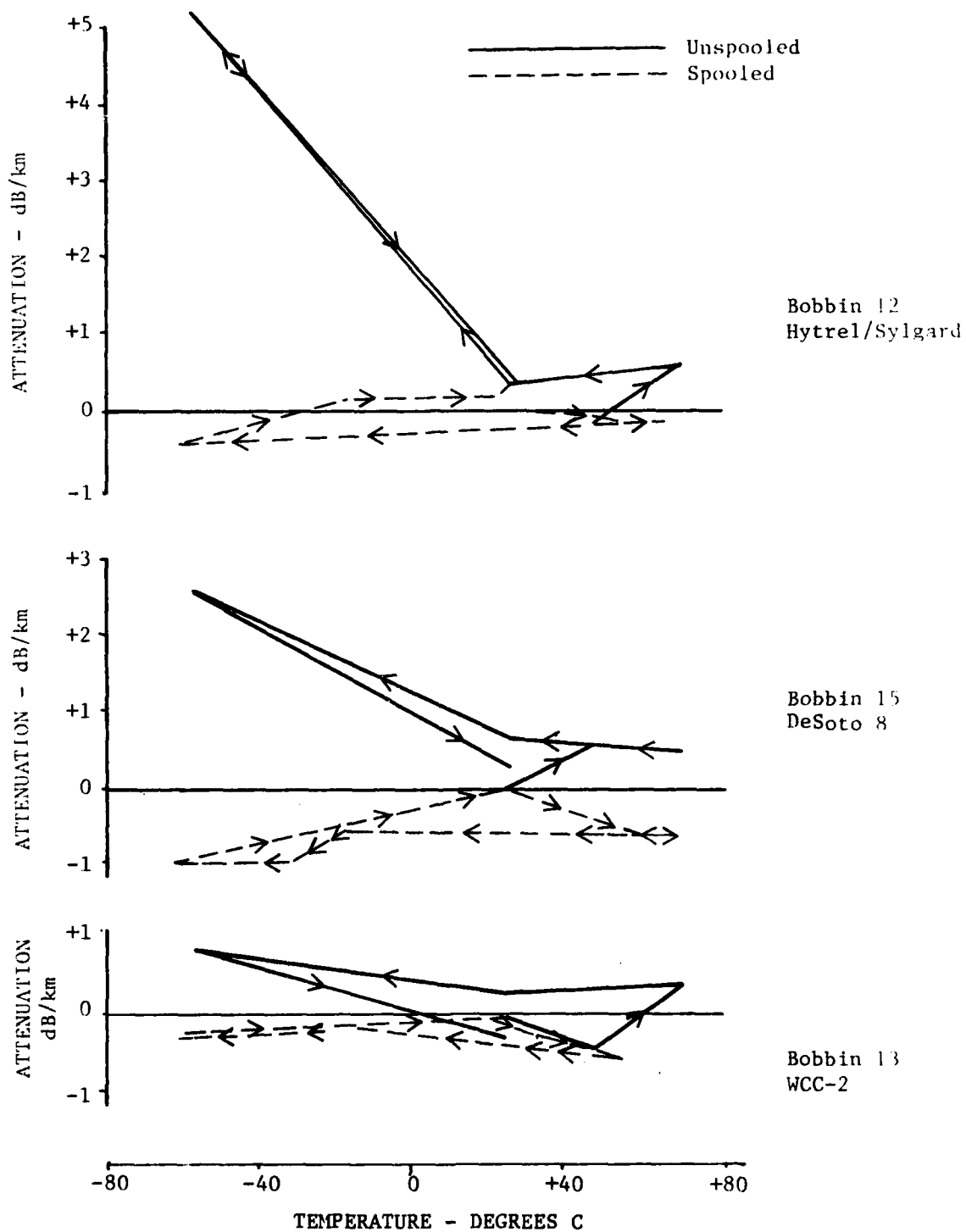


Figure 4.4-18. Effect of Temperature on Attenuation

An additional attenuation mechanism, which has potential impact on the performance of a fiber optic data link during payout, is the tendency for excess loss to increase as the cable is placed under tension. Although this phenomenon is not yet completely understood, it is believed to result from microbending due to mechanical stresses induced by the cable buffer material. For payout applications, a certain amount of strain-induced attenuation in the length of dispensed cable can be beneficial. This is due to the fact that the loss will tend to offset the increase in signal due to the elimination of spooling losses. The experiment to evaluate strain-related and other payout-related effects for this cable involves the following:

1. The basic optical properties and mechanical characteristics of the cable must be determined.
2. Strain-induced excess loss of the cable must be measured prior to any handling of the cable which could alter the mechanical properties of the buffer.
3. The cable must be wound in a typical geometry for payout, and subjected to mechanical and high-temperature stress to cause plastic deformations of the buffer corresponding to that expected in a full length (10 km) dispenser.
4. The optical parameters of the cable as wound on the spool must be measured.
5. The cable must be unwound and the strain-induced excess loss measured as rapidly as possible after unwinding. Since the buffer material is expected to exhibit viscoplastic behavior, it is important to perform the measurement rapidly in order to determine the cable properties prior to any substantial change in the shape of the deformations of the buffer.

A 1.2 km length of standard ITT production cable with a diameter of 0.02 inch (508 microns) was subjected to the full experiment consisting of all five steps. There was no observable strain-induced attenuation prior

to or after winding. Several additional samples of cable were subjected to the measurement of strain-induced loss prior to winding without any substantial effect being observed. Because of the difficulty and time required to perform the measurement after spooling, and because there was no indication of any strain-induced effects with any of the plastic coated cables, the latter part of the experiment was not performed for the additional cables. It was concluded that strain-induced attenuation is not an important phenomenon with the cable types being used.

5.0 CABLE REQUIREMENTS

In conjunction with the development of the fiber optic cable dispenser, substantial information has become available relative to the ultimate requirements which must be imposed on the cable as this program moves from a technology development phase into a full missile development and production phase. The cable requirements, as specified in the Technical Requirement in the contract, represent the starting point for the long range requirements. Data resulting from analysis, tests, and experience obtained with the TOW missile development and production have served to enlarge and, in some cases, modify the initial requirements. In some cases, particular parameters are recognized as needing a specification but data to define the format and/or numerical values for the requirements are not available. In these cases, these requirements are indicated as yet to be defined (TBD).

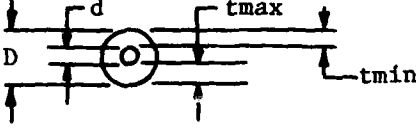
For purposes of understanding the reasons for the need for a particular requirement, the cable requirements can be grouped according to the function which imposes the requirement. In the work done to date, cable requirements arising from the following functions have been considered:

1. Mechanical - winding, storage, payout
2. Signal propagation - attenuation, pulse dispersion
3. Connector/splice considerations.

5.1 MECHANICAL RELATED REQUIREMENTS

The requirements which arise from the mechanical related functions are summarized in table 5-1. The nominal values presented are based on a particular cable design which shows substantial promise for payout purposes; these parameters would, of course, be changed if a different cable were to be selected. They are included to emphasize that control of such parameters is important. Even though suitable dispenser designs can be accomplished over a substantial range of some of these parameters, once the design has been frozen, the cable parameters must closely conform to the nominal values.

TABLE 5-I. CABLE REQUIREMENTS - WINDING, STORAGE, PAYOUT

Continuous Length	10 km
Number of Optical Fibers in Cable	1
Nominal Fiber Diameter	.004 inch
Fiber Out-of-Roundness	$\frac{d(\max) - d(\min)}{d(\min)} < .016$
Cable Cast-Helix Diameter	>8 inches
Cable Residual Twist	90°/foot max
Nominal Cable Lineal Density	6.7×10^{-5} pounds/foot
Coating Thickness	.004 inch
Coating Concentricity	$\frac{t(\min)}{t(\max)} \geq .67$
	
Cable Out-of-Roundness	$\frac{d(\max) - d(\min)}{d(\max)} < .008$
Cable Average Diameter	.012 ±.0002 inch
Maximum Deviation From Average Cable Diameter	$\frac{\Delta \text{Dia}}{\text{Ave Dia}} \pm .0083$
Cable Transverse Compressibility Modulus (nominal)	10 KSI
Fiber Tensile Strength	>200 KSI
Coating Tensile Strength	>1500 PSI
Coating Surface Friction	TBD
Coating Toughness	TBD
Cable Transverse Compressive Creep	TBD
Cable Cold Temperature Bending Stiffness	TBD
Humidity Resistance	TBD
Static Fatigue Resistance	TBD
Storage Temperature Range	-62° to 68° C -80° to 155° F
Operating Temperature Range	-32° to 60° C -25° to 140° F

Two of the parameters called out, cast and residual twist, are probably unfamiliar; these parameters are included because of experience with the TOW missile wire dispenser and relate to nonuniform residual stresses in the cable due to manufacturing processes. The term "cast" refers to the diameter of the helix which the cable attempts to form if relieved of all external forces. This is a measure of the residual bending stress in the cable. The residual twist is a measure of the residual torsion stress in the cable.

Several of the mechanical-related requirements are yet to be defined. In fact, probably most of these will not be defined during this program. This does not imply, however, that these parameters are not important. For example, static fatigue resistance is believed to be a very important characteristic of the cable. At this time, however, we cannot define specific numerical requirements, nor do we even understand the best format for specifying such requirements.

5.2 SIGNAL TRANSMISSION RELATED REQUIREMENTS

The signal transmission related requirements include pulse dispersion and attenuation. The contractual technical requirement specifies a maximum allowable pulse dispersion as 2.0 ns/km. This value is established by the maximum expected transmission frequency. Since there is no effort in this contract which involves the definition of transmission bandwidths and frequency, there is no basis to modify this requirement. It is well to emphasize, however, that the pulse dispersion requirement applies over the full operating temperature range of -32°C to $+60^{\circ}\text{C}$.

The specification of required attenuation characteristics is complex. Based on state-of-the-art optical transmitter and receiver characteristics and expected losses in other parts of the transmission path, the maximum allowable attenuation for the fiber optic cable, either spooled or laid out straight, is about 60 dB. The spooled state is the most restrictive of these conditions because of the spooling losses. The total loss of the cable may be divided into the unspooled losses (referred to as the intrinsic loss) and the spooling losses (those additional losses which are experienced upon

winding the cable into a bobbin). Since these two losses are additive, and since total attenuation is the parameter of interest, there exists a situation where one type of loss can be traded off against the other type of loss. For example, consider two cables, one which has relatively high intrinsic loss but very low sensitivity to spooling stresses, while the other has very low intrinsic loss but substantial sensitivity to spooling stresses. If both of these cables satisfy the overall requirement of 60 dB total attenuation as spooled, then both must be considered as acceptable from the standpoint of signal attenuation. This ability to interchange intrinsic loss and spooling loss significantly complicates the matter of specification.

A scheme has been defined which accounts for the interchangeability of spooling and intrinsic losses. A loss model has been formulated based on the observation that the data of loss versus interlayer pressure appears to fit a function of the form

$$\alpha(\text{dB/km}) = A + BP^C \quad (5-1)$$

where α is the total attenuation constant, P is the interlayer pressure, and A , B , and C are constants which describe a particular cable. It may be noted that the parameter A includes the intrinsic loss of the cable plus contributions from the spooling-induced losses. Based on equation 5-1, we may describe L_i , the loss of the i^{th} layer of the winding, as

$$L_i = \alpha_i \ell_i = (A + BP_i^C) \ell_i \quad (5-2)$$

where ℓ_i is the length of that layer and P_i is the corresponding interlayer pressure. The total attenuation of the wound bobbin, L_{total} , is

$$L_{\text{total}} = \sum_{i=1}^N \alpha_i \ell_i = \sum_{i=1}^N \ell_i (A + BP_i^C) = A \sum_{i=1}^N \ell_i + B \sum_{i=1}^N \ell_i P_i^C \quad (5-3)$$

where N is the total number of layers. Please note that $\sum_{i=1}^N \ell_i = \ell_t$, the total length of cable in the wound bobbin.

The condition for an acceptable cable is that L_{total} is less than L_0 where L_0 is the maximum allowable attenuation ($L_0 = 60$ dB for the case of interest).

$$L_{total} \leq L_0 \quad (5-4)$$

Combining equations 5-3 and 5-4 yields

$$L_0 - A l_t \leq B \sum_{i=1}^N l_i P_i^C \quad (5-5)$$

Since l_i and P_i are determined by the bobbin design, for a given bobbin design, the summation $\sum_{i=1}^N l_i P_i^C$ can be evaluated for various values of C . By evaluating this summation for the particular bobbin design parameters for various values of C , equation 5-5 provides a functional relationship between A , B , and C defining the conditions of acceptability. For a given cable, based on the type of pressure vessel tests described in section 4, the corresponding values of A , B , and C may be evaluated to determine if the cable conforms to the requirements.

Figure 5-1 illustrates the cable attenuation acceptance criterion based on bobbin design number 1 (see section 4.2). This design utilizes a cable 0.020 inch (508 microns) in diameter. The attenuation data obtained from the use of the corresponding test bobbin has been analyzed to determine the values of A , B , and C for that cable; these values are also plotted on figure 5-1. Since the value of A for the cable is 2.07, the location of the point must be compared with a curve for $A = 2.07$. Such a curve would fall slightly below the curve for $A = 2.0$ which is provided. It appears that the location of the point falls slightly above the curve location for $A = 2.07$; whereas to be acceptable, the point should fall on or below the curve. This observation is consistent with a predicted total loss for this cable of 61 dB compared to a requirement of 60 dB.

Table 5-II presents the attenuation parameters for the cables used in winding test bobbins 1, 12, 13, and 15 which represent the more promising cable configurations. Since the characteristics of a cable enter into the

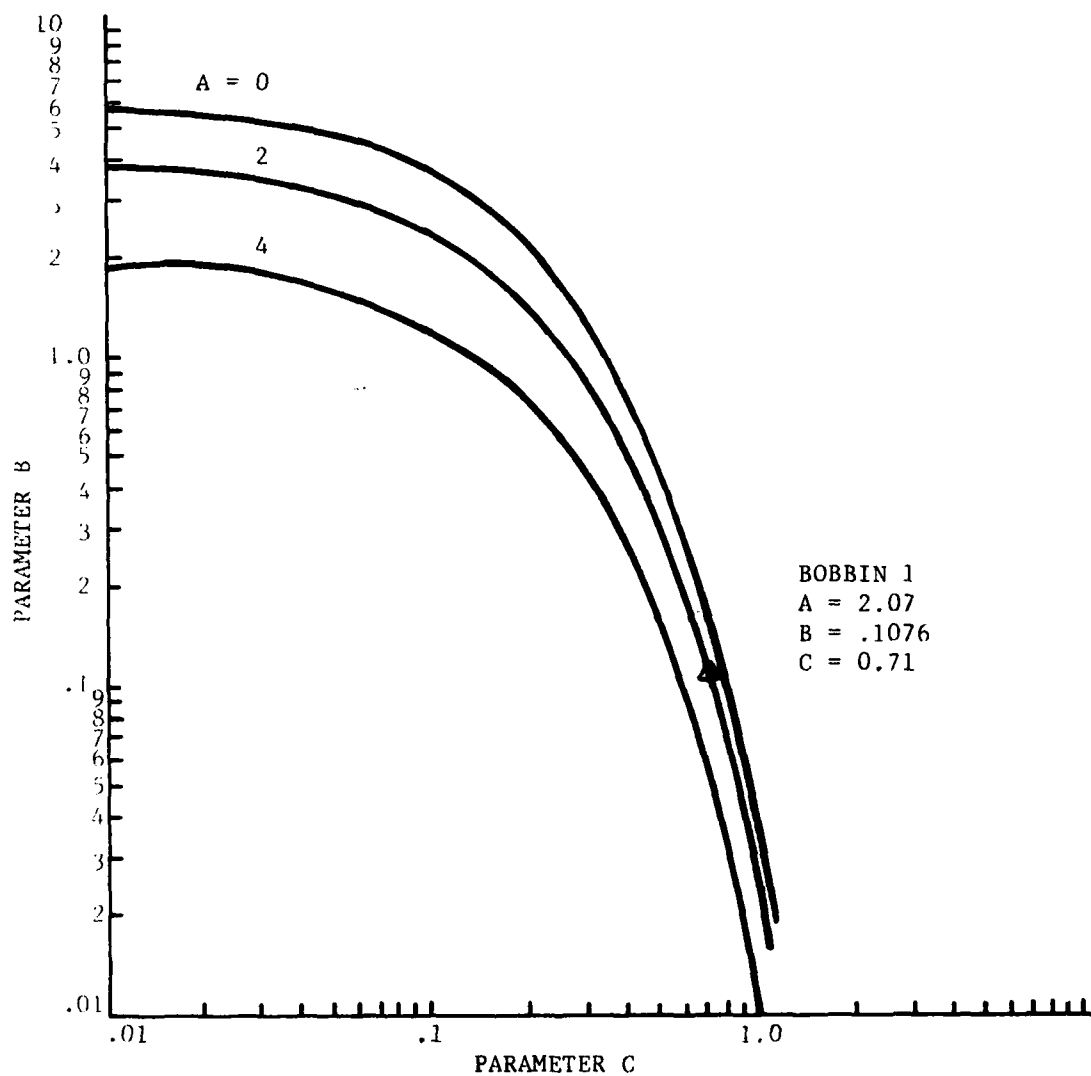


Figure 5-1. Cable Attenuation Acceptance Criterion
Bobbin Design No. 1

TABLE 5-II. CABLE ATTENUATION PARAMETERS

Cable	A	B	C
Bobbin 1 .020" Hyt/Syl 50 μ core 125 μ fiber	2.07	.1076	.71
Bobbin 12 .016" Hyt/Syl 25 μ core 100 μ fiber	6.32	.0048	1.0
Bobbin 13 .012" WCC-2 25 μ core 100 μ fiber	8.58	.0044	1.0
Bobbin 15 .012" DeSoto 8 25 μ core 100 μ fiber	3.37	.0074	.966

design of the bobbin utilizing that cable, the cable acceptance criterion must correspond to the appropriate bobbin configuration. Since the criterion presented in figure 5-1 is based on bobbin 1, the parameters for the other three cables should not be compared with that particular criterion.

5.3 CONNECTOR RELATED REQUIREMENTS

The contractual technical requirement establishes a design goal for cable connectors to be provided of 1.5 dB per connector pair. Since connector losses are influenced by various characteristics of the cable, it is apparent that the connector requirements must be reflected into requirements on those particular cable parameters.

Six specific cable parameters have been identified which directly influence connector attenuation. These are fiber diameter fluctuations, fiber ellipticity, core diameter fluctuations, core eccentricity, core ellipticity, and numerical aperture fluctuations. In considering loss mechanisms, effects of core and fiber geometry imperfections have been treated as though they are independent. In practice, however, some fiber and core imperfections are closely correlated. For example, fluctuations of the diameter of the fiber will almost always be accompanied by fluctuations in the diameter of the core. In addition, there can be separate, independent fluctuations in the diameter of the core. Since, however, the mechanisms wherein fiber and core diameter fluctuations influence connector loss are different, it is convenient to consider them separately. At this time there has been no attempt to establish numerical values for the various connector-related loss parameters. To do so requires establishing formal loss budgets, allocating overall connector loss between those mechanisms which involve cable imperfections and those which involve connector imperfections. The technical basis for setting up formalized loss budgets for the connector does not yet exist. However, as additional data becomes available and as the program moves from a technology development phase into a full missile development phase, such loss budgeting will become necessary. Our purpose in pursuing this investigation thus far has been to identify the type of data required and to permit a preliminary assessment as to the magnitude of cable-related contributions to connector loss. For each of the six cable parameters which have been identified as influencing connector loss,

a first order model has been identified relating the parameter to loss. These mechanisms are as follows:

Fiber diameter fluctuations and fiber ellipticity influence the functioning of the connector alignment mechanism. Short term diameter fluctuations can permit lateral and angular misalignments in any direction while ellipticity can result in misalignments in or about a particular axis. The magnitudes of any misalignments resulting from fiber diameter fluctuations or ellipticity depend upon the detailed design of the connector. Substantial data exists in the literature on the effect of connector lateral and angular misalignments on loss.

The loss resulting from core diameter fluctuations has been evaluated based on the assumption of uniform power distribution across the core. If two cores are perfectly aligned at a connector with energy propagating from a larger core to the smaller core, part of the energy contained in the larger core will be coupled into the cladding of the second fiber and becomes lost. The ratio of transmitted power then is the ratio of the squares of the two diameters and the resulting loss due to core diameter fluctuations is

$$L_{d_c} = 10 \log \left(\frac{d_{c2}}{d_{c1}} \right)^2 \quad (5-6)$$

where d_{c2} and d_{c1} are the smaller and larger core diameters.

The loss due to core eccentricity has been evaluated based on the assumptions of uniform power distribution in the core and perfect alignment of the fibers. Core eccentricity can result in a lateral offset between cores; however, for a given eccentricity ϵ , in each cable, the magnitude of the lateral offset is statistically distributed between zero and 2ϵ as one cable is rotated relative to the other. Hence, for a given eccentricity, the magnitude of the resulting loss is random. Since the magnitude of ϵ is also statistically distributed, the evaluation of the mean and standard deviation of the expected offset is somewhat complex.

The mechanism for the loss due to core ellipticity is simple to visualize but somewhat more complex to evaluate. Again, for assumptions of perfect fiber alignment and uniform energy distribution in the core, the loss due to this mechanism has been evaluated. With two identical elliptically shaped cores whose centers are aligned, but whose major axes are misaligned, the transmission across the connector is proportional to the ratio of the area of overlap to the total area of the ellipse. Since the angle of misalignment between major axes of the ellipses is randomly distributed, a given ellipticity results in a random value of attenuation. Since both the magnitude of the ellipticity and the angular misalignment are random, the evaluation of the statistical properties of the attenuation due to core ellipticity is somewhat complicated. Using graphical integration techniques, the variation in area of overlap between two identical ellipses was evaluated as a function of the angle of misalignment for various ratios of major and minor axes. Equation 5-7 was found to provide a reasonably good fit of the data

$$a/a_{\text{tot}} = 1 - A \sin \theta \quad (5-7)$$

where A is a function of the ratio of the axes of the ellipse and θ is the angle of misalignment. Assuming a uniform distribution of θ , the mean and standard deviation for a/a_{tot} was computed.

The loss due to fluctuations in the numerical aperture of the fiber is quite simple to evaluate on the assumption of uniform distribution of the energy in the various modes and across the core. Since the maximum angle of propagation measured from the fiber axis in a fiber is

$$\theta_{\text{max}} = \sin^{-1} (\text{N.A.}) \quad (5-8)$$

where N.A. is the numerical aperture of the fiber, a mismatch of numerical apertures at a connector will result in a condition where guided high order modes in one fiber become radiated modes in the fiber across the junction with the lower N.A. By comparing the surface area of overlap on a unit sphere of the two circles subtended by the two maximum angles of propagation, we conclude that the loss due to variations in numerical aperture is

$$L_{N.A.} = 10 \log \left(\frac{N.A._2}{N.A._1} \right)^2 \quad (5-9)$$

where N.A.₂ and N.A.₁ are the smaller and larger values of numerical aperture for the two fibers.

Where available, data has been gathered on the magnitudes of the imperfections of the various cable characteristics which influence connector loss. This data is presented in table 5-III for both ITT and Hughes Research Laboratories manufactured cables. Since, during the program to date various sizes of cables have been examined, the data has been normalized by dividing the values of all data for a particular cable by the maximum value of that parameter for that cable. For example, for the data for fiber diameter fluctuations, usually diameter data is available for each end of the cable. In this case, the values for each of the two measurements would be divided by the larger value yielding normalized values of 1.0 and a number less than 1. If a cable had been divided into two lengths with measurement data available for each end, four normalized values would result with the largest of 1.0 and three values less than 1.

Table 5-III also contains an estimate of the connector loss directly attributable to the particular cable characteristic where such an evaluation could be made. For purposes of simplicity in most cases, the value of the loss corresponding to the mean value of cable parameters was computed. An examination of the resulting values for the loss contributors is somewhat encouraging in that there are no extremely large values which would preclude achieving the overall goal of 1.5 dB per connector pair. The value of 0.34 dB for core diameter fluctuations represents the largest value obtained; this value is sufficiently large to cause some concern but when combined with the other values which are substantially smaller, it is believed that no great difficulty should result from the cable characteristics as observable thus far.

TABLE 5-III. CABLE PARAMETERS INFLUENCING CONNECTOR LOSS

Parameter	Characteristic					
	ITT			HRL		
	Mean	σ	\bar{L}_{dB}	Mean	σ	\bar{L}_{dB}
Fiber Dia Fluctuations (d_i/d_{max})	.973	.023	*	-	-	-
Fiber Ellipticity (d_{min}/d_{max})	-	-	-	.997	.007	*
Core Dia Fluctuations ($d_{ci}/d_{c max}$)	.962	.038	.34	-	-	-
Core Eccentricity (ϵ/d_c)	-	-	-	.0082	.0065	.02
Core Ellipticity ($d_{c min}/d_{c max}$)	.94	.056	.13	.943	.029	.13
Numerical Aperture Fluctuations ($N.A._i/N.A._{max}$)	-	-	-	-	-	-
*Loss depends upon connector design.						

6.0 ROCKET SLED TEST INSTRUMENTATION

The rocket sled test instrumentation equipment is being designed and will be fabricated by ITT-EOPD on a subcontract to Hughes Aircraft Company. This instrumentation link consists of the fiber optic cable payout dispenser under development, an optical transmitter located on the rocket sled, and a receiver located in a ground station. This link will monitor the optical signal in an attempt to identify characteristics that could affect the ability of the dispenser to function as a control link in an operational environment. The transmitter and payout dispenser will be mounted within a simulated missile airframe which is attached to a rocket sled. The optical fiber developed in this program will interconnect the transmitter and receiver.

6.1 INSTRUMENTATION DESIGN

The instrumentation package consists of a fiber optic transmitter, figure 6-1, and a receiver, figure 6-2. This link provides the capability of transmitting a constant amplitude carrier; any variations of the amplitude can be monitored at the receiver. These amplitude fluctuations, if any exist, will be monitored at the receiver and are attributable to the payout dynamics. Using synchronization pulses derived from the 1 MHz carrier, the receiver has the capability of providing a standard television signal format to permit recording and viewing of the carrier one frame at a time or at various repetition rates up to the actual speed, through the use of a video recorder. In addition, the received data will be peak detected and recorded on the audio channel of the video recorder.

An optically stabilized laser, designed and built by ITT-Electro Optical Products Division, will transmit a pulse train of approximately 1 MHz at 0 dBm into the fiber. With a nominal receiver sensitivity of 0.2 μ w, this leaves a link loss budget of 67 dB. The receiver pre-amp consists of an RCA C30921F avalanche photo diode feeding a transimpedance front end followed by two fixed gain stages. The proposed system link budget is outlined in table 6-I.

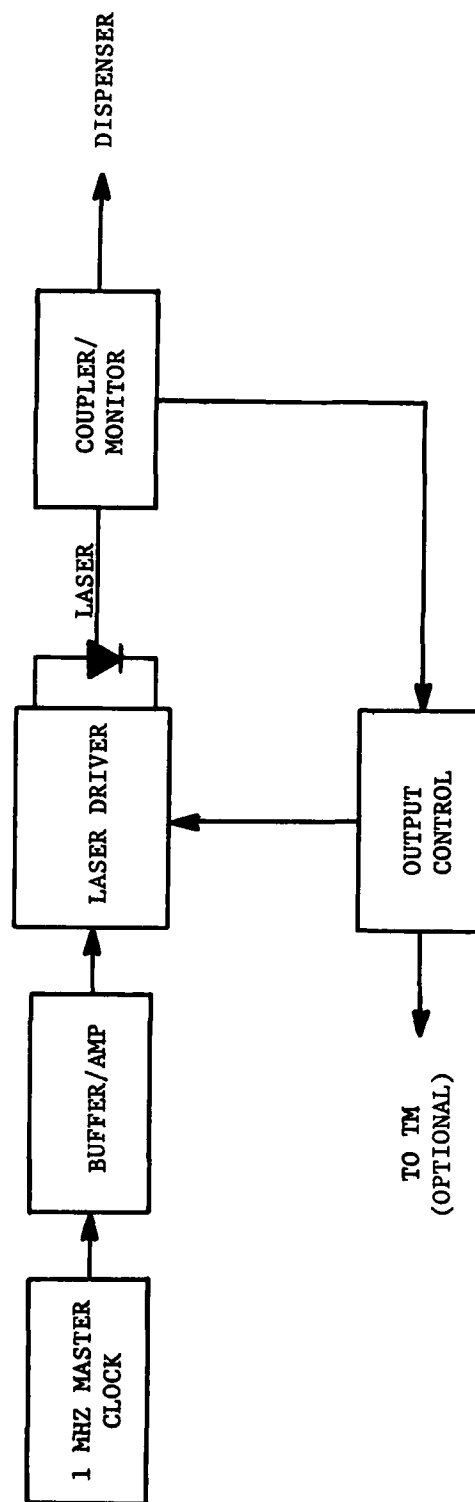


Figure 6-1. Downlink Transmitter Block Diagram

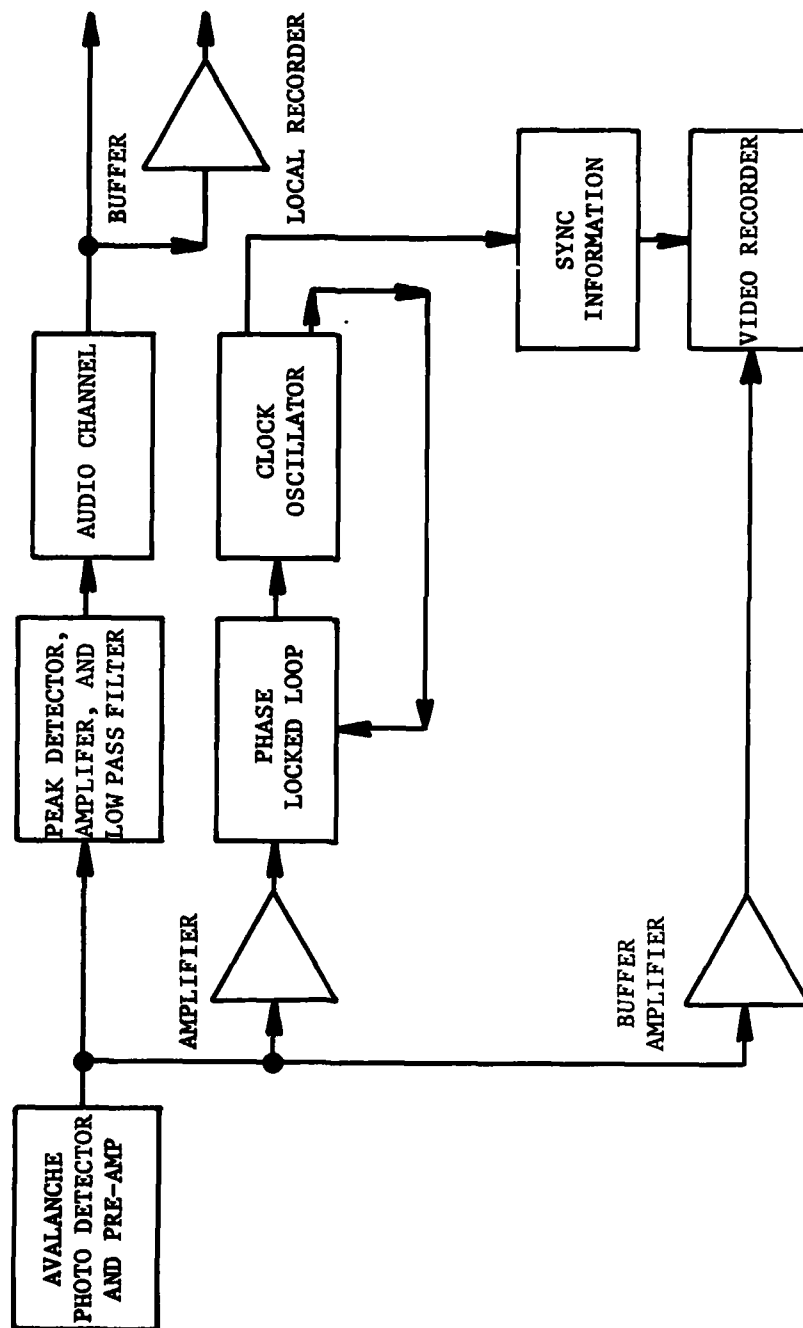


Figure 6-2. Ground Station Receiver Block Diagram

TABLE 6-I. LINK BUDGET

Laser Output (average)	0 dBm
Receiver Sensitivity (25 dB Signal (p-p)/Noise)	-67 dBm
Available Link Margin	67 dB
Beamsplitter Loss	1.0 dB
Splice Losses (at 0.5 dB)	1.0 dB
Cable (10 km at 6.0 dB/km)	60 dB
Excess Margin	5 dB

6.2 PACKAGING

The transmitter unit will be packaged to survive the operational environment during rocket sled payout tests. The receiver package is designed for mounting in a 19-inch rack. Preliminary vibration tests were performed on critical components within the transmitter unit. The coupled laser and coupled laser plus beamsplitter were sinusoidally vibrated between 5 to 2000 Hz at 5 g's for one hour. A constant signal output was monitored during the vibration test. No vibration-induced modulation occurred in either the coupled laser or coupled laser plus beamsplitter combinations. Care was taken to encapsulate the optical fiber to the mounting board for both configurations. This technique will be employed in the hardware to be delivered.

The ground station receiver unit consists of a fiber optic receiver circuit board, a synchronization circuit board, a power supply module, and a video recorder. The two circuit boards and the power supply module will be housed in a standard 19 inch rack-mount chassis. The chassis panel height is 3-1/2 inches. All outside connections will be made on the front panel with the exception of a power cord which will mount on the rear panel. The video recorder will sit on a rack mountable shelf.

The transmitter unit consists of an electronics/fiber optic circuit board, a vibration damper, a circuit board mounting plate, energy absorbing RTV, and a frame.

The circuit board is made from 1/8-inch copper-clad FR-4/G10 and has a natural frequency of approximately 2150 Hz. The fiber optic components will be bonded to the board and encapsulated with epoxy. The circuit card is backed with a Barry circuit board damper. This damper is a combination of viscoelastic material and a fiberglass restraining layer. The circuit board is attached to the circuit board mounting plate with machine screws and lock nuts. The damping material is sandwiched between the circuit board and the mounting plate. The circuit board mounting plate is made from 1/4 inch aluminum plate and has a natural frequency of approximately 2400 Hz. The mounting plate with circuit board and damping material attached is installed on the frame with machine screws. The frame is an open rectangle made from 3/4-inch aluminum plate. It has 1/4-20 tapped mounting holes and a natural frequency of approximately 2800 Hz.

7.0 CONCLUSIONS

The basic conclusions, which are indicated by the results to date, are reviewed in some detail in the previous sections. For convenience, a few key conclusions discussed in those sections are summarized here. It is important to recognize that these conclusions, although based on actual test results, must still be considered as tentative or qualified. The work to date is believed to have laid a good foundation for making the technical decisions necessary for program direction and for identifying key technical questions and approaches; however, there is still much work to be done. The technology associated with the high speed payout of optical fibers is at a very early stage; virtually every question that is answered raises new questions. Regardless of this situation, it is believed that the following conclusions may be reached with some confidence.

1. It is tentatively concluded that fiber optic cables can be fabricated to possess attenuation characteristics when spooled, and that spooled cables are suitable for use in lengths at least up to 10 km. This conclusion is based on test data obtained using test bobbins with short lengths (≈ 1 km) of cable plus analytical techniques which permit the prediction of the attenuation in long cable lengths when wound with geometry similar to that of the test bobbin. Since the long cable lengths are not yet available for confirmation, this conclusion must be qualified, but there is a definite indication that suitable fiber optic cables can be fabricated. It is significant that, in order to achieve suitable small diameter cables, it was necessary to alter some of the key optical parameters such as core diameter, and numerical aperture. In addition, the cable diameter was increased from the goal of 254 microns (0.010 inch) to 305 microns (0.012 inch). At this point, it cannot be concluded that a suitable 254-micron (0.010-inch) cable cannot be achieved. Because of the design sequence which was used, the revised optical parameters were not introduced until after the cable diameter had been increased to 305 microns (0.012 inch). When the

combination of 300-micron cable with revised optical parameters indicated suitable characteristics, there was insufficient time and resources remaining to prepare and evaluate cable with the revised optical parameters and a 254-micron (0.010-inch) diameter.

2. It is tentatively concluded that the basic cable configurations are suitable for high speed payout and that adequate strength can be achieved. At the time of this report, the maximum successful payout speed that has been achieved in this program is about 90 percent of the program goal of 183 m/s (600 ft/sec). The fact that substantial lengths (≈ 0.5 km) have been payed out at this speed indicates that these cables can withstand the bending and tensile loads to which they are exposed during high speed payout. Currently cables are being prooftested to a level of 200 kpsi based on the cross-sectional area of the glass fiber. It is believed that this level is quite adequate for payout at 100 percent of the contract goal.

3. The strong interaction between bobbin design and cable requirements has been demonstrated. This relationship was suspected at the outset of the program, but has now been illustrated. For example, the resulting attenuation levels of three substantially different bobbin configurations (which had been wound using identical cable samples) were significantly different, indicating the importance of this inter-relationship.

4. Although it is desirable to reach a favorable conclusion at this time regarding the long term storability of the wound bobbins as determined by static fatigue mechanism, such a conclusion cannot yet be made. There is some evidence to support that conclusion but the data is not yet definite. It appears that a suitable storage life for laboratory testing and flight test purposes is available. The question of storage lifetimes of 5, 10, or 15 years has not yet been answered, nor is it expected to be answered within this current program.

5. In summary, with the possible exception of the question of long-term storage life, it is tentatively concluded that the overall concept

involving the high speed payout of a fiber optic cable for a data link to a rapidly moving vehicle is feasible. To date, many questions have been examined with favorable results; although negative results have been experienced, such results have served to indicate that a certain solution was not suitable. At no time has there been a result which has tended to indicate that a particular function was infeasible. For this reason, it is believed that the basic concept is sound and that, even though much work remains to be done to design a functional system, a system with these capabilities can be designed.

DISTRIBUTION LIST

Defense Documentation Center
ATTN: DDC-TCA
Cameron Station (Building 5)
Alexandria, VA 22314
(12 copies)

Director
National Security Agency
ATTN: TDL
Fort George G. Meade, MD 20755

DCA Defense Comm Engrg Ctr
ATTN: Code R123, Tech Library
1860 Wiehle Ave
Reston, VA 22090

Defense Communications Agency
Technical Library Center
Code 205 (P. A. Tolovi)
Washington, DC 20305

Office of Naval Research
Code 427
Arlington, VA 22217

GIDEP Engineering & Support Dept
TE Section
PO Box 398
Norco, CA 91760

Director
Naval Research Laboratory
ATTN: Code 2627
Washington, DC 20375

Commander
Naval Electronics Laboratory Center
ATTN: Library
San Diego, CA 92152

Command, Control & Communications Div
Development Center
Marine Corps Development & Educ Cmd
Quantico, VA 22134

Naval Telecommunications Command
Technical Library, Code 91L
4401 Massachusetts Avenue, NW
Washington, DC 20390

Rome Air Development Center
ATTN: Documents Library (TILD)
Griffiss AFB, NY 13441

CDR, MIRCOM
Redstone Scientific Info Center
ATTN: Chief, Document Section
Redstone Arsenal, AL 35809

Commander
HQ Fort Huachuca
ATTN: Technical Reference Div
Fort Huachuca, AZ 85613

Commander
US Army Electronic Proving Ground
ATTN: STEEP-MT
Fort Huachuca, AZ 85613

Dir, US Army Air Mobility R&D Lab
ATTN: T. Gossett, Bldg 207-5
NASA Ames Research Center
Moffett Field, CA 94035

HQDA (DAMO-TCE)
Washington, DC 20310

Deputy for Science & Technology
Office, Assist Sec Army (R&D)
Washington, DC 20310

Director
US Army Materiel Systems Analysis Actv
ATTN: DRXSYP-MP
Aberdeen Proving Ground, MD 21005

HQDA (DAMA-ARP/Dr. F. D. Verderame)
Washington, DC 20310

Director
US Army Human Engineering Labs
Aberdeen Proving Ground, MD 21005

CDR, AVRADCOM
ATTN: DRSAY-E
PO Box 209
St. Louis, MO 63166

AFGL/SULL
S-29
Hanscom AFB, MA 01731

DISTRIBUTION LIST (Continued)

Director
Joint Comm Office (TRI-TAC)
ATTN: TT-AD (Tech Docu Cen)
Fort Monmouth, NJ 07703

Commander
US Army Satellite Communications Agcy
ATTN: DRCPM-SC-3
Fort Monmouth, NJ 07703

TRI-TAC Office
ATTN: TT-SE (Dr. Pritchard)
Fort Monmouth, NJ 07703

CDR, US Army Research Office
ATTN: DRXRO-IP
PO Box 12211
Research Triangle Park, NC 27709

Commander, DARCOM
ATTN: DRCDE
5001 Eisenhower Ave
Alexandria, VA 22333

CDR, US Army Signals Warfare Lab
ATTN: DELSW-OS
Vinthill Farms Station
Warrenton, VA 22186

CDR, US Army Signals Warfare Lab
ATTN: DELSW-AW
Vinthill Farms Station
Warrenton, VA 22186

Commander
US Army Logistics Center
ATTN: ATCL-MC
Fort Lee, VA 22801

Commander
US Army Training & Doctrine Command
ATTN: ATCD-TEC
Fort Monroe, VA 23651

Commander
US Army Training & Doctrine Command
ATTN: ATCD-TM
Fort Monroe, VA 23651

NASA Scientific & Tech Info Facility
Baltimore/Washington Intl Airport
PO Box 8757
Baltimore, MD 21240

Advisory Group on Electron Devices
201 Varick Street, 9th Floor
New York, NY 10014

Advisory Group on Electron Devices
ATTN: Secy, Working Group D (Lasers)
201 Varick Street
New York, NY 10014

TACTEC
Battelle Memorial Institute
505 King Avenue
Columbus, OH 43201

Ketron, Inc.
ATTN: Mr. Frederick Leuppert
1400 Wilson Blvd, Architect Bldg
Arlington, VA 22209

R. C. Hansen, Inc.
PO Box 215
Tarzana, CA 91356

CDR, US Army Avionics Lab
AVRADCOM
ATTN: DAVAA-D
Fort Monmouth, NJ 07703

Ballistic Missile Systems Defense
Command
ATTN: BMDSC-HD (Mr. C. D. Lucas)
PO Box 1500
Huntsville, AL 35807

Project Manager, ATACS
ATTN: DRCPM-ATC (Mr. J. Montgomery)
Fort Monmouth, NJ 07703

Commander
ERADCOM
ATTN: DELET-D (1 cy)
DELS-D-L-S (2 cys)
DELS-D-L (1 cy)
Fort Monmouth, NJ 07703

Commander
CORADCOM
ATTN: DRDCO-COM-D (1 cy)
DRDCO-SEI (1 cy)
DRDCO-COM-RM-1 (50 cys)
Fort Monmouth, NJ 07703

DISTRIBUTION LIST (Continued)

ITT Electro-Optical Prod Div
7635 Plantation Road
Roanoke, VA 24019

Corning Glass Works
Telecommunication Prod Dept
Corning, New York 14830

Galileo Electro-Optics Corp.
Galileo Park
Sturbridge, MA 01518

Times Fiber Comm Inc
358 Hall Avenue
Wallingford, CT 06492

Bell Norther Research
PO Box 3511, Station C
Ottawa, Canada K1Y 4H7

Valtec Corporation
Electro Fiber Optic Div
West Boylston, MA 01583

Hughes Research Laboratory
3011 Malibu Canyon Road
Malibu, CA 90265
ATTN: Dr. R. Abrams

Belden Corporation
Technical Research Center
2000 S. Batavia Avenue
Geneva, IL 60134
ATTN: Mr. J. McCarthy

Optelecom, Inc.
15940 Shady Grove Road
Gaithersburg, MD 20760

Bell Telephone Laboratories
Whippany Road
Whippany, NJ 07981
ATTN: Mr. G. A. Baker

Deutsch Co.
Elec Components Div
Municipal Airport
Banning, CA 92220

Xerox Electro-Optical Systems
ATTN: Mr. Ronald E. Purkis
300 North Halstead Street
Pasadena, CA 91107

US Army Missile R&D Command
ATTN: DRDMI-TDD (Mr. R. Powell)
Redstone Arsenal, AL 35809 (8 cys)

The Mitre Corporation
ATTN: J. A. Quarato
PO Box 208
Bedford, MA 01730

Electronics Group of TRW, Inc.
401 N. Broad Street
Philadelphia, PA 19108

Martin Mareitta Aerospace
ATTN: Dr. G. L. Harmon
Orlando Division
PO Box 5837 MP-3
Orlando, FL 32805

GTE Sylvania Inc.
Communications System Division
189 B Street
Needham Heights, MA 02194
ATTN: Mr. J. Concordia

Harris Electronics Systems Division
P.O. Box 37
Melbourne, FL 32901
ATTN: Mr. R. Stachouse
Fiber Optics Plant
Rodes Boulevard

ITT Defense Communications Division
492 River Road
Nutley, NJ 07110
ATTN: Dr. P. Steensma

General Cable Corporation
ATTN: Mr. M. Tenzer
160 Fieldcrest Avenue
Edison, NJ 08817

Naval Ocean System Center,
ATTN: Howard Rast Jr, Code 8115
271 Catalina Blvd.
San Diego, CA 92152

Booz-Allen & Hamilton
ATTN: B. D. DeMarinis
776 Shrewsbury Avenue
Tinton Falls, NJ 07724